

ÉCOLE DE TECHNOLOGIE SUPÉRIEURE
UNIVERSITÉ DU QUÉBEC

THÈSE PAR ARTICLES PRÉSENTÉE À
L'ÉCOLE DE TECHNOLOGIE SUPÉRIEURE

COMME EXIGENCE PARTIELLE
À L'OBTENTION D'UN
DOCTORAT EN GÉNIE
Ph. D.

PAR
Raouf FAREH

STRATÉGIE DE COMMANDE DISTRIBUÉE POUR LES MANIPULATEURS RIGIDES
ET FLEXIBLES ASSURANT LA STABILITÉ DES ERREURS DE SUIVI DE
TRAJECTOIRES

MONTRÉAL, LE 3 MAI 2013

©Tous droits réservés, Raouf Fareh, 2013

©Tous droits réservés

Cette licence signifie qu'il est interdit de reproduire, d'enregistrer ou de diffuser en tout ou en partie, le présent document. Le lecteur qui désire imprimer ou conserver sur un autre media une partie importante de ce document, doit obligatoirement en demander l'autorisation à l'auteur.

PRÉSENTATION DU JURY

CETTE THÈSE A ÉTÉ ÉVALUÉE
PAR UN JURY COMPOSÉ DE :

M. Maarouf Saad, directeur de thèse
Département de génie électrique à l'École de technologie supérieure

M. Mohamad Saad, codirecteur de thèse
École de génie à l'université du Québec en Abitibi-Témiscamingue

M. Pascal Bigras, président du jury
Département de génie de la production automatisée à l'École de technologie supérieure

M. Ilian Bonev, membre du jury
Département de génie de la production automatisée à l'École de technologie supérieure

M. Wael Suleiman, examinateur externe indépendant
Département de génie électrique et de génie informatique à l'Université de Sherbrooke.

IL A FAIT L'OBJET D'UNE SOUTENANCE DEVANT JURY ET PUBLIC

LE 1^{ER} MAI 2013

À L'ÉCOLE DE TECHNOLOGIE SUPÉRIEURE

REMERCIEMENTS

Mes premiers remerciements vont d'abord à mon directeur de thèse, le professeur Maarouf Saad, qui m'a accompagné et dirigé tout au long ce travail. Je lui suis reconnaissant pour sa disponibilité, ses généreux secours au cours de certains de mes moments difficiles, son enthousiasme et sa confiance.

Mes remerciements vont conjointement à mon co-directeur de thèse, le professeur Mohamad Saad de l'école de génie à Université du Québec en Abitibi-Témiscamingue, pour sa disponibilité, son suivi quotidien de mes travaux et ses précieux conseils. Je le remercie infiniment.

Je suis honoré par la présence de tous les membres de jury qui m'ont prodigué d'utiles conseils qui m'ont aidé à bien structurer mon étude durant le cursus de ma thèse : il s'agit de Monsieur Pascal Bigras et Monsieur Ilian Bonev, professeurs à l'École de technologie supérieure. Je remercie également Monsieur Wael Suleiman, professeur à Université de Sherbrooke, d'avoir accepté de participer à ce jury de thèse.

De plus, mes remerciements seraient incomplets, si je ne fais pas mention de ma femme, mes enfants, mes parents, mes beaux-parents et ma famille.

Enfin, mes remerciements à tous mes amis et mes collègues qui m'ont aidé, de près ou de loin, directement ou indirectement, à l'élaboration de ce travail.

STRATÉGIE DE COMMANDE DISTRIBUÉE POUR LES MANIPULATEURS RIGIDES ET FLEXIBLES ASSURANT LA STABILITÉ DES ERREURS DE SUIVI DE TRAJECTOIRES

Raouf FAREH

RÉSUMÉ

Cette thèse de doctorat propose et valide expérimentalement une nouvelle stratégie de commande distribuée pour les manipulateurs rigides et flexibles assurant le suivi de trajectoires dans l'espace articulaire et cartésien. Cette stratégie est développée, dans un premier temps, pour les manipulateurs rigides. Ensuite, elle est modifiée pour prendre en compte la flexibilité des bras au niveau des manipulateurs flexibles.

Dans le cas des manipulateurs rigides, cette stratégie est utilisée pour assurer un bon suivi de trajectoires dans l'espace de travail. Dans le cas où les paramètres du système sont parfaitement connus, une stratégie de commande distribuée est utilisée. Cette stratégie de commande décompose, dans un premier temps, la dynamique du manipulateur en plusieurs sous-systèmes non linéaires interconnectés. Chaque sous-système représente une articulation. Ensuite, la commande distribuée consiste à contrôler le manipulateur en commençant par la dernière articulation (sous-système) toute en supposant que le reste des articulations est stable. La même procédure est utilisée au rebours jusqu'à la première articulation. Dans le cas où les paramètres du système ne sont pas connus, une commande adaptative est développée. Dans ce contexte, la commande distribuée et adaptative peut être interprétée comme étant une commande hiérarchique. En effet, les paramètres inconnus, existant dans l'équation de mouvement du dernier sous-système, sont tout d'abord estimés et la loi de commande est ainsi déduite en fonction de ces paramètres. Puis, passant à l'avant-dernier sous-système, la loi de commande est développée en fonction de leurs propres paramètres estimés, existant dans l'équation de mouvement de l'avant-dernière articulation, et les paramètres estimés du sous-système de niveau supérieur. La même stratégie est utilisée à contresens jusqu'au premier sous-système. L'approche de Lyapunov est utilisée pour prouver la stabilité globale des erreurs de suivi. Les deux lois de commande sont validées expérimentalement sur un manipulateur rigide à 7 ddl et elles montrent un bon suivi dans l'espace articulaire et cartésien.

Dans le cas des manipulateurs flexibles, cette stratégie est modifiée et étendue pour assurer un bon suivi de trajectoires dans l'espace articulaire et, en même temps, minimiser les vibrations au niveau des bras flexibles. Donc, en plus de l'objectif de suivi de trajectoire utilisé dans le cas des manipulateurs flexibles, la stratégie de commande doit assurer la déformation bornée et minimiser les vibrations des bras flexibles. Au contraire des manipulateurs rigide, les manipulateurs flexibles sont des systèmes sous-actionnés, c'est-à-dire ils possèdent plus de degrés de liberté que d'entrées de commande. Dans ce cas, chaque sous-système est composé d'une articulation et le bras flexible associé. Dans le cas où les paramètres du manipulateur sont parfaitement connus, une commande distribuée est développée pour assurer la stabilité des erreurs de suivi dans l'espace articulaire et réduire les vibrations des bras flexibles. Cette stratégie consiste à commander et stabiliser la dernière

articulation ainsi que le dernier bras flexible en supposant que le reste des sous-systèmes sont stables. Puis, passons aux contrôle et stabilité de l'avant-dernier sous-système de la même façon. Cette démarche est suivie, au rebours, jusqu'au premier sous-système. Sa version adaptative, dite « hiérarchique », est également développée. La stabilité globale est prouvée en utilisant l'approche de Lyapunov. La validation expérimentale des deux lois de commande sur un manipulateur flexible à 2 ddl montre un bon suivi de trajectoires dans l'espace articulaire et des vibrations minimales au niveau des bras flexibles.

Dans le cas de suivi de trajectoires dans l'espace de travail des manipulateurs flexibles, la cinématique inverse, utilisée pour les manipulateurs rigides, n'est plus suffisante pour transformer les trajectoires désirées de l'espace de travail vers l'espace articulaire. En plus d'une relation cinématique, il existe une relation dynamique entre l'espace de travail et articulaire. Pour résoudre ce problème, un espace intermédiaire, nommé « virtuel » et la méthode quasi-statique sont utilisés. En effet, la cinématique inverse est utilisée pour transformer la trajectoire désirée de l'espace de travail vers l'espace virtuel tandis que l'approche quasi-statique est utilisée pour le passage de l'espace virtuel à l'espace articulaire. Lors du contrôle direct de l'extrémité, les manipulateurs flexibles deviennent des systèmes à non minimum de phase et la dynamique interne n'est plus bornée. Pour surmonter ce problème, la technique de la redéfinition de sortie est utilisée pour sélectionner une sortie la plus proche possible de l'extrémité assurant une dynamique interne bornée. Cette sortie est composée de la position angulaire plus une valeur pondérée de la déformation de l'extrémité du bras flexible. Une étude de stabilité de la dynamique interne (ou dynamique des zéros) en utilisant la passivité est utilisée pour déterminer la valeur critique du paramètre caractérisant cette sortie paramétrisée. Deux lois de commande sont développées pour un robot à deux bras flexibles. La première loi de commande basée sur l'approche de linéarisation par retour d'état assure juste la stabilité locale des erreurs de suivi. La deuxième loi de commande constitue une généralisation pour assurer la stabilité globale de la dynamique des erreurs de suivi. Ces deux algorithmes sont testés sur un robot à deux bras flexibles et montrent un bon suivi de trajectoires dans l'espace de travail.

Mots-clés: manipulateurs rigides, manipulateurs flexibles, commande distribuée, commande adaptative, stabilité, erreur de suivi, espace articulaire, espace de travail.

DISTRIBUTED CONTROL STRATEGY FOR RIGID AND FLEXIBLE LINK MANIPULATORS ENSURING THE STABILITY OF TRACKING ERRORS

Raouf FAREH

ABSTRACT

This thesis studies and proposes a distributed nonlinear control strategy for rigid and flexible manipulators ensuring the stability of the tracking errors in the joint space and workspace. First, this strategy is applied to rigid manipulators. Then, it is modified and extended to take into account the links' flexibility of flexible link manipulators.

For the rigid manipulators, the control strategy is used to ensure a good tracking in the workspace. When the system parameters are perfectly known, a distributed control strategy is developed. First, this control strategy decomposes the dynamical model into a set of nonlinear interconnected subsystems. Each subsystem has one joint. Then, this distributed control strategy consists of controlling the last joint while assuming that the remaining joints are stable. Then, going backward to the next to the last joint, the same strategy is applied and so on until the first joint. When, the system parameters are unknown, an adaptive version is developed. In this case, the distributed and adaptive control can be interpreted as an hierarchical control. Indeed, the unknown parameters existing in the equation of motion of last subsystem are first estimated and the control is developed using this estimated parameters. Then, going backward to the before last joint, the control law is developed using its own estimated parameters and the ones already estimated in the upper level subsystem. The adaptive control strategy consists to control one subsystem in each step starting from the last subsystem. The same procedure is used, backward to the first subsystem. Global stability of the error dynamics is proved using Lyapunov approach. The proposed approaches are implemented in real time on a 7 DOF ANAT robot. Experimental results show the effectiveness of the approach and good tracking performance in the workspace.

For the flexible manipulators, the above control strategies are modified and extended to solve the tracking control problem and minimizing vibrations of the flexible links. In this case, the control problem is twofold: in addition to motion objectives as in a rigid manipulator, it must also stabilize the vibrations that are naturally excited. The number of controlled variables for a flexible-link manipulator is strictly less than the number of mechanical degrees of freedom, i.e. it represents an under actuated system. For flexible link manipulators, each subsystem has a pair of one joint and one link. In the joint space, a distributed control strategy, based on the one proposed for the rigid manipulators, is developed when the flexible link manipulators parameters are known. An adaptive version or hierarchical control strategy is also deduced to track the desired trajectories and reducing vibrations of the links. These algorithms were tested on a two-flexible-link manipulator and gave effective results, a good tracking performance, and capability to eliminate the links' vibrations.

For the workspace tracking of flexible link manipulators, the inverse kinematics, used for rigid manipulators, is not sufficient to transform the desired trajectories from the workspace to the joint space. There exist two relationships between the workspace and joint: a

kinematics and dynamics relations. To overcome this problem, an intermediate space, called virtual space, and quasi-static approach are used. Indeed, the inverse kinematics is used to transform the desired trajectories from workspace to the virtual space and the quasi-static approach is used between the virtual space and the joint space. The flexible links manipulators are non-minimum phase system when controlling the position of the end-effector. To solve the non-minimum phase problem, an output redefinition technique is used. This output consists of the motor's angle augmented with a weighted value of the links extremity. The distributed control strategy consists in controlling the last link by assuming that the first link is stable and follows its desired trajectories. The control law is developed to stabilize the errors dynamics and to guarantee bounded internal dynamics such that the new output is as close as possible to the tip. The weighted parameter defining the non-collocated output is then selected. The same procedure is applied to control and stabilize the first link. The asymptotical stability is proved using Lyapunov theory. The control strategies are applied to a two-flexible-link manipulator in horizontal plane and simulations results showed a good tracking of the desired trajectory in the workspace.

Key Words: rigid manipulators, Flexible manipulators, distributed control, adaptive control, stability, tracking errors, joint space, workspace.

TABLE DES MATIÈRES

	Page
INTRODUCTION	1
CHAPITRE 1 CONSIDÉRATIONS GÉNÉRALES.....	9
1.1 Problématique et objectif de recherche.....	9
1.2 Revue de littérature	13
1.2.1 Commande des manipulateurs rigides	13
1.2.1.1 Dynamique vue comme un système MIMO	13
1.2.1.2 Dynamique vue comme des systèmes SISO interconnectés.....	15
1.2.2 Commande des manipulateurs flexibles	16
1.2.2.1 Commande dans l'espace articulaire	16
1.2.2.2 Commande dans l'espace cartésien	19
1.3 Méthodologie	22
1.4 Originalités des travaux	26
CHAPITRE 2 ARTICLE 1: WORKSPACE DISTRIBUTED REAL-TIME CONTROL OF RIGID MANIPULATORS	29
2.1 Introduction.....	30
2.2 Modeling of the ANAT Robot.....	32
2.3 Distributed Control Strategy	35
2.3.1 Control law.....	35
2.3.2 Global Stability Analysis	40
2.4 Experimental Results	42
2.5 Conclusion	48
2.6 Appendix.....	49
Proof of proposition 1:	49
CHAPITRE 3 ARTICLE 2: HIERARCHICAL ADAPTIVE CONTROL IN THE WORKSPACE OF RIGID MANIPULATORS	55
3.1 Introduction.....	56
3.2 Modeling	58
3.3 Hierarchical Control Strategy	62
3.4 Adaptive Hierarchical Control.....	67
3.5 Experimental Results	72
3.6 Conclusion	80
3.7 Appendix.....	81
CHAPITRE 4 ARTICLE 3: DISTRIBUTED CONTROL STRATEGY FOR FLEXIBLE LINK MANIPULATORS	85
4.1 Introduction.....	86
4.2 Modeling and problem formulation	88
4.3 Distributed control strategy.....	92
4.3.1 Control law development.....	92

4.3.2	Stability analysis	96
4.4	Application to two-flexible-link manipulator	99
4.4.1	System description	99
4.4.2	Distributed control law	101
4.4.3	Experimental results.....	104
4.5	Conclusion	111
4.6	Appendix.....	111
CHAPITRE 5	ARTICLE 4: ADAPTIVE CONTROL FOR FLEXIBLE LINK MANIPULATORS USING DISTRIBUTED CONTROL STRATEGY.....	115
Abstract:	115	
5.1	Introduction.....	116
5.2	Modeling and problem formulation	118
5.3	Adaptive distributed control strategy.....	122
5.4	Stability analysis	128
5.5	Experimental results.....	129
5.6	Conclusion	137
5.7	Appendix.....	138
CHAPITRE 6	ARTICLE 5: WORKSPACE TRAJECTORY TRACKING CONTROL FOR TWO-FLEXIBLE-LINK MANIPULATOR THROUGH OUTPUT REDEFINITION	143
6.1	Introduction.....	144
6.2	Modeling	146
6.3	Trajectory transformation	149
6.4	Control Strategy	151
6.4.1	Hierarchical control strategy for n flexible links	151
6.4.2	Application to two flexible links manipulator	153
6.4.2.1	Control and stability of the second link	155
6.4.2.2	Control and stability of the first link.....	158
6.5	Simulation results.....	160
CHAPITRE 7	ARTICLE 6: WORKSPACE TRAKING CONTROL OF TWO- FLEXIBLE-LINK MANIPULATOR USING DISTRIBUTED CONTROL STRATEGY	175
7.1	Introduction.....	176
7.2	Modeling	179
7.2.1	System description	179
7.2.2	Proprieties and problem formulation	180
7.3	Distributed control strategy.....	182
7.3.1	Inverse dynamics	182
7.4	Control strategy.....	184
7.5	Stability analysis	192
7.5.1	Stability of rigid part.....	192
7.5.2	Stability of the flexible part	195

7.6	Simulation results.....	197
7.7	Conclusion	204
7.8	Appendix.....	205
CONCLUSIONS ET RECOMMANDATION.....		211
LISTE DE RÉFÉRENCES BIBLIOGRAPHIQUES.....		217

LISTE DES TABLEAUX

	Page
Table 2.1 Denavit-Hartenberg parameters of ANAT robot	33
Table 3.1 Denavit-Hartenberg parameters of ANAT robot	72
Table 4.1 System physical parameters.....	105
Table 5.1 System parameters.....	131
Table 6.1 System parameters	160
Table 7.1 System parameters	198

LISTE DES FIGURES

	Page
Figure 2.1 ANAT robot and axes.....	33
Figure 2.2 The i-th control law.	39
Figure 2.3 Distributed control strategy.....	40
Figure 2.4 Real-time setup.....	43
Figure 2.5 Joint space tracking. (a) joint 2, (b) joint 3, (c) joint 4 and (d) joint 5.....	44
Figure 2.6 Joint space tracking errors. (a) joint 2, (b) joint 3, (c) joint 4 and (d) joint 5.....	45
Figure 2.7 Workspace tracking. (a) x-tracking, (b) y-tracking, (c) x-tracking error and (d) y- tracking error.	45
Figure 2.8 Workspace tracking	46
Figure 2.9 Workspace tracking with another initial point.	46
Figure 2.10 Tracking errors for the computed torque. (a) joint 2, (b) joint 3 (c) joint 4, (d) joint 5, (e) x-position and (f) y-position.....	47
Figure 3.1 ANAT robot.....	59
Figure 3.2 Control chart.....	61
Figure 3.3 i-th control law.	65
Figure 3.4 Hierarchical adaptive control strategy.....	68
Figure 3.5 Real-time setup.....	74
Figure 3.6 Hierarchical control: (a) Joint space tracking, (b) Tracking errors.	75
Figure 3.7 Hierarchical control: (a) Workspace tracking and (b) Workspace tracking error.	76
Figure 3.8 Hierarchical control: Workspace tracking.....	76
Figure 3.9 Hierarchical adaptive control: (a) Joint space tracking, (b)Tracking errors.....	77
Figure 3.10 Hierarchical adaptive control: (a) x and y position tracking, (b) tracking errors of x and y, (c) xyz workspace tracking.....	78
Figure 3.11 Tracking errors in joint space for the computed torque method.	79
Figure 4.1 Flexible-link manipulator.	89
Figure 4.2 The i-th control law.	96
Figure 4.3 Two-flexible-link manipulator.	99
Figure 4.4 Quanser two link flexible robot.....	104

Figure 4.5 Real-Time setup.....	106
Figure 4.6 Desired trajectories: (a)-(b) position, (c)-(d) velocity, (e)-(f) acceleration of rigid part	107
Figure 4.7 Distributed control: (a)-(b) joint tracking trajectories, (c)-(d) joint tracking errors.....	108
Figure 4.8 Distributed control: errors of flexible parts.....	108
Figure 4.9 Distributed control: input torque.....	109
Figure 4.10 PD control: (a)-(b) joint tracking trajectories, (c)-(d) joint tracking errors.....	109
Figure 4.11 PD control : errors of flexible parts.	110
Figure 4.12 PD control: input torques.....	110
Figure 5.1 Flexible-link manipulator.....	119
Figure 5.2 The i-th control law.	126
Figure 5.3 Distributed adaptive control strategy.....	127
Figure 5.4 Two-flexible-link manipulator	130
Figure 5.5 Quanser two-link flexible robot.....	131
Figure 5.6. Real time setup.	132
Figure 5.7. Desired trajectories: (a)-(b) position, (c)-(d) velocity, (e)-(f) acceleration of rigid part.	133
Figure 5.8 Adaptive control: (a)-(b) joints' tracking trajectories, (c)-(d) joints' tracking errors	134
Figure 5.9. Adaptive control: errors of flexible part.....	134
Figure 5.10 Adaptive control: control input.....	135
Figure 5.11 Distributed control: (a)-(b) joints' tracking trajectories, (c)-(d) joints' tracking errors.	135
Figure 5.12 Distributed control: errors of the flexible parts.....	136
Figure 5.13 Distributed control: control input.....	136
Figure 6.1 Two-flexible-link manipulator	148
Figure 6.2 Transformation of the desired trajectories.....	150
Figure 6.3 Virtual space.....	150
Figure 6.4 Control strategy.	153

Figure 6.5 Workspace desired trajectory: (a) Y_d vs X_d and (b) $x_d(t)$, $y_d(t)$	161
Figure 6.6 (a) Nyquist diagram, and (b) eigenvalues evolution.	162
Figure 6.7 Eigenvalues vs. α_1	162
Figure 6.8 Tracking of X-Y trajectory.....	163
Figure 6.9 (a)-(b) Position of virtual joints, (c)-(d) velocity of virtual joints, (e)-(f) acceleration of virtual joints.	163
Figure 6.10 (a)-(b) Flexible coordinates; (c)-(d) Rigid coordinates.	164
Figure 6.11 (a)-(b) Errors of joints 1 and 2; (c)-(d) errors of flexible coordinates 1, 2; (e)-(f) tracking errors of workspace trajectories $x(t)$ and $y(t)$	164
Figure 7.1 Two-flexible-link manipulator.	179
Figure 7.2 Virtual space.	183
Figure 7.3 Distributed control strategy.	191
Figure 7.4 X-Y desired workspace trajectory.....	198
Figure 7.5 Desired workspace trajectory: (a)-(b) position trajectory,	199
Figure 7.6 Desired virtual space trajectories: (a)-(b) position trajectories, (c)-(d) velocity trajectories and (e)-(f) acceleration trajectories.....	199
Figure 7.7 Desired joint space trajectories: (a)-(b) positiontrajectories of rigid coordinates, (c)-(d) velocity trajectories of rigidcoordinates, (e)-(f) acceleration trajectories of rigid coordinatesand (g)-(h) position trajectories of flexible coordinates... ..	200
Figure 7.8 Stbility of second link. (a) Nyquist diagram, and (b) eigenvalues evolution. ...	200
Figure 7.9 Stability of first link: Eigenvalues vs α_1	201
Figure 7.10 Tracking trajectories of non-collocated outputs.	201
Figure 7.11. Tracking errors in joint space. (a)-(b) tracking errors of non-collocated outputs and (c)-(d) tracking errors of the flexible coordinates.....	202
Figure 7.12. Tracking in the workspace. (a) x-position tracking and (b) y-position tracking.	202
Figure 7.13. Workspace tracking errors. (a) x-position tracking errors and (b) y-position tracking errors.....	203
Figure 7.14. X-Y workspace tracking.....	203

LISTE DES ABRÉVIATIONS, SIGLES ET ACRONYMES

- SISO : Seule-entrée, seule sortie.
- ddl : Degré de liberté.
- MIMO : Multi-entrées multi-sorties
- PD : Proportionnel-dérivée.
- PID : Proportionnel-dérivée-intégral.
- ANAT: Articulated nimble adaptable trunk.
- DOF: Degrees of freedom.
- LOG: Linear-Quadratic-Gaussian
- LQR: Linear Quadratic Regulator (LQR)

LISTE DES SYMBOLES ET UNITÉS DE MESURE

q	Coordonnée généralisée.
q_r	Coordonnée généralisée de la partie rigide.
q_f	Coordonnée généralisée de la partie flexible.
τ	Vecteur des couples.
M	Matrice de masse.
C	Matrice de Coriolis
G	Vecteur de gravité.
J	Matrice de jacobien.
s	Surface de glissement.
s_r	Surface de glissement de la partie rigide.
s_f	Surface de glissement de la partie flexible.
x	Vecteur d'état.
x_r	Vecteur d'état de la partie rigide.
x_f	Vecteur d'état de la partie flexible.
$v_i(x, t)$	Déformation di $i^{\text{ème}}$ bras flexible.
$\emptyset_{ij}(x)$	$j^{\text{ème}}$ fonction forme du $i^{\text{ème}}$ bras.
v_{Li}	Déformation de l'extrémité de $i^{\text{ème}}$ bras flexible.
V	Fonction de Lyapunov.
\cdot	Dérivée pa rapport au temps t.
\sim	Désigne l'erreur de suivi
$\hat{\cdot}$	Désigne l'estimation.
d	Désigne le désirée d'une valeur.

INTRODUCTION

La principale raison de la création des robots manipulateurs, au début des années soixante, est de libérer et décharger l'être humain de certaines tâches complexes, dangereuses, répétitives et/ou infaisables parfois. De plus, l'utilisation des robots manipulateurs offre d'autres avantages tels que la diminution des coûts de production, l'amélioration de la qualité et de la productivité, etc. Les progrès continus dans les domaines de l'électronique et de l'informatique ont poussé le domaine de la robotique à des évolutions assez importantes. Suite à cette progression, plusieurs domaines d'applications, telles que l'industrie automobile, les applications spatiales, forestières, etc., ont profité de cette progression continue pour améliorer leurs productivités. En milieu industriel, l'utilisation des manipulateurs est très répandue. En effet, ils réalisent des tâches répétitives à hautes vitesses dans un temps très limité. En plus, ils sont pratiquement autonomes et peuvent fonctionner sans l'aide de l'opérateur quand ils sont programmés et mis en place.

Généralement, les manipulateurs destinés à des applications industrielles sont extrêmement rigides, massifs. Avec l'évolution de la technologie, les applications industrielles deviennent de plus en plus complexes et exigent une mobilité et des vitesses de déplacement relativement grandes. Dans ce cas, la rigidité n'est plus un avantage et les robots utilisés dans ce genre d'applications doivent avoir un poids minimal et une grande flexibilité. Généralement, la diminution du poids d'un manipulateur réduit la puissance nécessaire de ses actionneurs ce qui amène à une économie d'énergie. Pour améliorer les performances des robots, les membrures doivent être plus légères et par conséquent, elles deviennent plus flexibles, la vitesse augmente, la consommation d'énergie diminue et le coût de production devient minimal.

La plupart des tâches sont définies dans l'espace de travail tel que la peinture, le soudage, l'assemblage, etc. ce qui rend la commande des manipulateurs dans l'espace cartésien très importante. Dans le cas des manipulateurs rigides, une étude de la cinématique, inverse et directe, est largement suffisantes pour assurer le passage de l'espace de travail vers l'espace

articulaire et vice versa. La connaissance de l'angle du moteur est suffisante pour déterminer directement la position de l'extrémité. Ce qui n'est pas le cas pour les manipulateurs flexibles dont la flexibilité des bras n'est plus un phénomène négligeable. Lors du contrôle direct de l'extrémité, le système devient à non-minimum de phase. Deux relations, une cinématique et une dynamique, sont utilisées pour basculer entre l'espace de travail et l'espace articulaire pour ce type de robots. Par la suite, les méthodes de commande utilisées pour les manipulateurs rigides ne peuvent pas être directement appliquées pour les manipulateurs flexibles.

Plusieurs travaux de recherches ont mis l'accent sur les méthodes de commande assurant le suivi de trajectoires dans l'espace articulaire et de travail. Dans ce cas, la dynamique des manipulateurs est vue sous forme de deux configurations: 1) un seul système MIMO où une seule commande est produite pour contrôler toutes les articulations du robot, 2) un ensemble de sous-systèmes interconnectés qui sont contrôlés chacun par une commande indépendante.

Le but de la présente thèse est de proposer et valider expérimentalement une stratégie de commande distribuée pour les manipulateurs rigides et flexibles assurant la stabilité des erreurs de suivi. Cette stratégie sera développée, dans un premier temps, pour les manipulateurs rigides pour assurer le suivi de trajectoires dans l'espace de travail. Puis, elle sera modifiée pour prendre en compte la flexibilité des bras au niveau des manipulateurs flexibles.

L'organisation de la présente thèse est donnée comme suit. Chapitre 1 présente la problématique de recherche, les objectifs, la revue de littérature, la méthodologie suivie pour atteindre les objectifs ainsi que l'originalité du travail. Par la suite, les chapitres 2, 3, 4, 5, 6 et 7 présenteront les résultats des travaux sous forme d'articles, soient soumis pour publication (chapitres 3, 4, 5 et 6) ou acceptés et publiés (chapitres 2 et 7). Le Chapitre 2 présentera l'étude théorique et expérimentale de la stratégie de commande distribuée appliquée à un robot rigide à 7 ddl. Une version adaptative de la stratégie de commande présentée dans le Chapitre 2 sera présentée et appliquée au même robot rigide à 7 ddl dans le

Chapitre 3. Le Chapitre 4 présente une commande distribuée appliquée aux manipulateurs flexibles pour assurer la stabilité des erreurs de suivi dans l'espace articulaire tout en minimisant les vibrations au niveau des bras flexibles. Cette stratégie de commande a été appliquée à un manipulateur à deux bras flexibles. La version adaptative de cette stratégie a été présentée dans le chapitre 5 et appliquée au même système à deux ddl. Dans l'espace de travail, la stratégie de commande distribuée est présentée dans les chapitres 6 et 7 avec des lois de commande différentes pour assurer la stabilité locale et globale des erreurs de suivi.

Dans la suite de cette partie, nous présentons un résumé de chaque article :

L'article du chapitre 2 présente une nouvelle stratégie de commande distribuée pour les manipulateurs rigides afin de suivre une trajectoire désirée dans l'espace de travail. Trois étapes sont utilisées pour assurer le suivi. La première étape consiste à utiliser la cinématique inverse pour transformer la trajectoire désirée de l'espace de travail vers l'espace articulaire. Puis, une loi de commande distribuée est développée, dans la deuxième étape, pour contrôler les articulations du manipulateur. Enfin, la trajectoire obtenue dans l'espace articulaire est transformée vers l'espace de travail via la cinématique directe. Pour faciliter le développement de la loi de commande, la dynamique du manipulateur est mise sous forme d'un ensemble de sous-systèmes interconnectés. Chaque sous-système représente une articulation. La stratégie de commande distribuée consiste à commander un sous-système à chaque étape en commençant par le dernier. En effet, le dernier sous-système est commandé tout en supposant que le reste des sous-systèmes sont stables et suivent leurs trajectoires désirées. Puis, passons à l'avant-dernier sous-système, l'articulation associée est commandée en utilisant la même démarche, c'est-à-dire, le reste des articulations sont supposées stables. La même procédure est utilisée à rebours jusqu'au premier sous-système. Cette stratégie de commande distribuée assure la stabilité globale de la dynamique des erreurs de suivi. Cette stabilité globale est prouvée par l'approche de Lyapunov. L'implémentation en temps-réel de cette approche sur un robot modulaire (Hyper Redundant Articulate Nimble Adaptable Trunk (ANAT) montre un bon suivi de trajectoire dans l'espace de travail. Les résultats

expérimentaux ont été comparés avec ceux obtenus par la méthode du couple pré-calculé pour montrer l'efficacité et l'apport de cette stratégie de commande distribuée.

L'article présent dans le chapitre 3 propose deux stratégies de commande pour assurer le suivi de trajectoire désirée dans l'espace de travail des manipulateurs rigides. En plus de la stratégie de commande distribuée, présentée dans le chapitre 2, la version adaptative ou dite « hiérarchique » est proposée dans cet article. Dans ce cas, les paramètres du système sont supposés inconnus et la loi de commande contient un processus d'adaptation pour estimer ces paramètres. La cinématique inverse est utilisée pour transformer la trajectoire désirée de l'espace de travail vers l'espace articulaire et la cinématique directe est utilisée dans le sens inverse. La dynamique du manipulateur est mise sous forme d'un ensemble de sous-systèmes interconnectés dont chacun représente une articulation. Cette stratégie de commande exploite la forme hiérarchique des manipulateurs. La commande hiérarchique est appliquée aux manipulateurs rigides en commençant par le dernier sous-système (articulation) jusqu'au premier. Chaque articulation est commandée en supposant que le reste des articulations est stable. L'équation de mouvement du dernier sous-système contient uniquement les paramètres inconnus du dernier sous-système. La loi de commande de ce dernier sous-système est ainsi déduite en fonction de ces paramètres estimés. Puis, passons à l'avant-dernier sous-système, l'équation de mouvement contient les paramètres de ce sous-système et celles du dernier sous-système. La loi de commande est ainsi développée en utilisant les paramètres estimés de ce sous-système et celles déjà estimées dans l'étape précédente. La même stratégie est suivie au rebours jusqu'au premier sous-système. En effet, la loi de commande du premier sous-système est développée en fonction des paramètres estimés de ce sous-système est de tous les paramètres estimés correspondant aux sous-systèmes de niveau supérieur. La stabilité globale est assurée en utilisant la théorie de Lyapunov. L'implémentation en temps réel sur un robot rigide à 7 ddl (ANAT) est présentée dans cet article pour montrer l'efficacité de ces lois de commande.

L'article du chapitre 4 présente une stratégie de commande distribuée pour les manipulateurs flexibles pour assurer le suivi de trajectoire dans l'espace articulaire et minimiser les vibrations au niveau des bras flexibles. La première étape consiste à réorganiser la

dynamique du manipulateur pour prendre la forme d'un ensemble de sous-systèmes interconnectés afin de l'exploiter pour le développement de la loi de commande. Chaque sous-système contient une articulation et le bras flexible associé. La stratégie de commande distribuée consiste à contrôler un seul sous-système à chaque étape tout en commençant du dernier jusqu'au premier sous-système. Chaque sous-système est contrôlé pour que l'articulation suive une trajectoire désirée et, en même temps, les vibrations du bras flexible associé soient minimales. En commençant par le dernier sous-système, une loi de commande est développée en supposant que le reste des sous-systèmes sont stables. Puis, passons à l'avant-dernier sous-système pour développer une loi de commande assurant un suivi de trajectoire de l'articulation et minimisant les vibrations du bras. La même procédure est suivie au rebours jusqu'au premier sous-système. La loi de commande de chaque sous-système est développée en utilisant la surface de glissement. Cette stratégie de commande distribuée assure la stabilité globale de la dynamique des erreurs de suivi. L'implémentation en temps réel de cette stratégie sur le robot à deux bras flexibles est présentée pour montrer l'efficacité et la simplicité de cette approche. Une comparaison avec la commande PD montre les avantages de cette approche lors de l'implémentation en temps réel.

Pour le chapitre 5, l'article présente une stratégie de commande adaptative distribuée pour les manipulateurs flexibles assurant la stabilité de la dynamique des erreurs de suivi dans l'espace articulaire en minimisant les vibrations des bras flexibles. Pour une bonne exploitation dans le développement de cette stratégie de commande, la dynamique du manipulateur est réorganisée pour prendre la forme d'un ensemble de sous-systèmes interconnectés dont chacun représente une articulation et le bras flexible associé. À chaque étape un seul contrôleur est fourni pour chaque sous-système. Par exemple, pour le $i^{\text{ème}}$ sous-système, la loi de commande est déduite en utilisant ses propres paramètres estimés et ceux déjà estimés pour chaque sous-système de niveau supérieur. La stabilité globale de la dynamique des erreurs de suivi est assurée par cette stratégie de commande en utilisant l'approche de Lyapunov. Cette stratégie de commande adaptative est appliquée et validée expérimentalement sur un robot à deux bras flexibles. Les résultats expérimentaux montrent que cette stratégie de commande assure un bon suivi de trajectoire dans l'espace articulaire et

réduit les vibrations au niveau des bras flexibles. La comparaison avec la version non-adaptative montre bien l'apport et la performance de cette stratégie.

Dans le chapitre 6, l'article propose une commande distribuée pour assurer un suivi de trajectoire dans l'espace de travail pour un manipulateur à deux bras flexibles. Lors de la commande directe de l'extrémité, les manipulateurs flexibles deviennent des systèmes à non-minimum de phase et la dynamique interne n'est plus bornée. La technique de redéfinition de la sortie est utilisée pour sélectionner une sortie la plus proche possible de l'extrémité. En plus de la relation cinématique utilisée pour les manipulateurs rigides, il existe une relation dynamique entre l'espace de travail et articulaire. La cinématique inverse et l'approche quasi statique sont utilisées pour transformer la trajectoire désirée de l'espace de travail vers l'espace articulaire. La stratégie de commande consiste à commander et stabiliser le dernier sous-système, constitué de la deuxième articulation et bras flexible associé, en supposant que le premier sous-système est stable. Cette démarche est suivie, au rebours, pour le premier couple articulation-bras. À chaque étape, l'approche de linéarisation par retour d'état est utilisée pour développer la loi commande. La sortie la plus proche de l'extrémité est sélectionnée de telle sorte que la dynamique interne devienne bornée. La valeur critique du paramètre caractérisant cette sortie paramétrisée est déterminée suite à une étude de stabilité de la dynamique interne (ou dynamique des zéros) en utilisant la passivité. Cette loi de commande assure la stabilité locale du système. Cette commande a été appliquée à un robot à deux bras flexibles et les résultats de simulation montrent un bon suivi de trajectoire dans l'espace de travail sous forme triangulaire.

L'article présent dans le chapitre 7 propose une stratégie de commande distribuée assurant la stabilité globale de la dynamique des erreurs de suivi d'un manipulateur à deux bras flexibles. La cinématique inverse n'est pas suffisante pour transformer la trajectoire désirée de l'espace de travail vers l'espace articulaire. Le problème de l'inversion de la dynamique est résolu en utilisant un espace intermédiaire nommée espace virtuel. Ce dernier est créé de telle sorte qu'il soit lié avec l'espace de travail par une simple relation cinématique (comme dans le cas des manipulateurs rigides) et lié avec l'espace articulaire par une relation dynamique qui peut être résolue par l'approche quasi-statique. Le problème de non-minimum

de phase pour les manipulateurs flexibles est résolu en utilisant la technique de redéfinition de sortie. La commande distribuée consiste à commencer par le contrôle et la stabilisation du deuxième sous-système, représenté par le deuxième couple articulation-bras, en supposant que le premier est stable. La dynamique des erreurs de suivi de la partie rigide est prouvée en utilisant la théorie de Lyapunov. Pour la partie flexible, la stabilité de la dynamique des erreurs de suivi et la sélection de la valeur critique du paramètre caractérisant cette sortie paramétrisée sont étudiées en utilisant la passivité. Les résultats de simulation de cette stratégie de commande sur un robot à deux bras flexibles montrent un bon suivi de trajectoires dans l'espace de travail sous forme d'un losange.

CHAPITRE 1

CONSIDÉRATIONS GÉNÉRALES

1.1 Problématique et objectif de recherche

Les manipulateurs rigides sont des systèmes non linéaires et vu l'importance de leur contrôle, plusieurs méthodes de commande ont été développées pour différents objectifs de commande à savoir, régulation, suivi dans l'espace articulaire ou le suivi dans l'espace de travail. Jusqu'à présent, le problème de suivi de trajectoire dans l'espace de travail est beaucoup moins couvert que celui dans l'espace d'articulations. Il existe moins de solutions (par rapport au suivi dans l'espace articulaire) pour le problème de suivi de trajectoire dans l'espace opérationnel bien que le suivi de trajectoire dans ce dernier est très important puisque la plupart des tâches sont définies dans cet espace, telles que la peinture, la soudure, l'assemblage, l'ébavurage, etc. Dans le cas des manipulateurs rigides, une relation cinématique est suffisante pour passer de l'espace de travail vers l'espace articulaire. En effet, pour transformer les trajectoires désirées de l'espace de travail vers l'espace articulaire, la cinématique inverse est utilisée. Par contre, la cinématique directe est utilisée pour transformer les trajectoires de l'espace articulaire vers l'espace de travail.

Dans le cas des manipulateurs flexibles, la situation est plus complexe puisqu'ils sont des systèmes fortement non linéaires à cause de la présence des équations de couplage dynamique entre les variables rigides et flexibles. Contrairement à un robot rigide, un robot flexible est un système sous actionné : il existe plus de sorties à contrôler (variables rigides et flexibles) que d'entrées de commande (couples articulaires). Dans le cas des robots rigides, la mission est de concevoir une loi de commande pour suivre une trajectoire désirée. Tandis que pour les robots flexibles, une condition supplémentaire doit être rajoutée, c'est que les vibrations des bras flexibles doivent être minimales. Dans ce cas, la cinématique inverse n'est plus suffisante pour transformer les trajectoires désirées de l'espace de travail vers l'espace articulaire des robots flexibles. En effet, ces deux espaces sont liés par une relation

cinématique et dynamique. Pour surmonter ce problème, l'espace virtuel et l'approche quasi-statique sont utilisés. De plus, un robot flexible est un système à non minimum de phase lorsque la sortie à contrôler représente l'extrémité du robot. Cette caractéristique augmente la complexité du contrôle direct de l'extrémité d'un robot flexible. Pour résoudre ce problème, la technique de redéfinition de sortie est utilisée. Cette nouvelle sortie est constituée de la position angulaire plus une valeur pondérée de la déformation de l'extrémité.

Plusieurs méthodes de commande basées sur une seule commande pour toutes les articulations ont été couvertes dans la littérature. Dans ce cas, la dynamique des manipulateurs est vue comme étant un seul système MIMO. Malheureusement, l'implémentation en temps réel de ce type des contrôleurs dans l'industrie n'est pas facile à cause de la complexité de la structure de commande et le coût élevé de calcul. Pour surmonter ce problème, la dynamique du manipulateur peut être vue comme un ensemble de sous-systèmes interconnectés dont chacun représente une articulation (dans le cas des manipulateurs rigides) ou une articulation et un bras flexible dans le cas des manipulateurs flexibles. Cette structure offre un certain nombre d'avantages à savoir : la simplicité des lois de commande et de leur implémentation en temps réel, la minimisation du taux d'information traité par les unités de commande, la réduction de l'effort de calcul, la tolérance aux pannes, etc. Avec cette configuration, chaque sous-système est commandé indépendamment des autres.

Dans le cas où le système est vu comme étant un ensemble de sous-systèmes interconnectés, le niveau de performance des lois de commande est mis en question en fonction du choix des sous-systèmes. Par exemple, si les interactions entre les sous-systèmes choisis ne sont pas prises en considération les blocs de sous-systèmes voisins peuvent être déstabilisés. Souvent l'étude de la stabilité globale représente un grand défi pour les méthodes utilisant l'idée de colocalisation. En effet, les sous-systèmes sont généralement commandés localement et la vérification de la stabilité globale n'est pas évidente. Vu que les systèmes complexes demandent un niveau de performance extrêmement élevé, on comprend assez facilement l'intérêt que présente la stabilité globale pour ces systèmes. Pour les manipulateurs rigides ou

flexibles, une stratégie de commande distribuée peut offrir une solution en contrôlant le manipulateur à partir de son dernier sous-système (une articulation pour les robots rigides et une articulation et un bras pour les robots flexibles) jusqu'au premier. En effet, le dernier sous-système est généralement la moins couplée des autres sous-systèmes, donc il est le plus facile à le contrôler et à stabiliser. Puis, en utilisant la même stratégie, nous passons au contrôle et la stabilisation de l'avant-dernier sous-système, qui sera le moins couplé du reste et le plus facile à commander. Ainsi de suite, les autres articulations seront contrôlées de la même façon au rebours jusqu'à la première.

Dans la plupart des manipulateurs industriels, la commande utilisée est basée sur le fait que le système robotique est considéré comme étant un système linéaire. Une commande de type PID à des gains constants est utilisée pour chaque articulation. La commande linéaire est satisfaisante juste autour des points de fonctionnement bien déterminés, mais en dehors de ces plages, le contrôleur n'est plus valable et peut déstabiliser le système. Étant donné que les manipulateurs sont des systèmes non-linéaires (fortement non linéaire dans le cas des manipulateurs flexibles), cette méthode de commande linéaire est limitée à des vitesses faibles. Dans ce cas, une technique de commande non-linéaire est indispensable pour une meilleure représentation du comportement non-linéaire des manipulateurs rigides ou flexibles.

Pour remédier aux problèmes présentés précédemment, cette thèse vise le développement d'une nouvelle stratégie de commande distribuée non linéaire pour les manipulateurs rigides et flexibles assurant la stabilité des erreurs de suivi. Cette stratégie de commande exploite la forme des manipulateurs rigides et flexibles. Premièrement, elle consiste à organiser la dynamique du manipulateur pour prendre la forme d'un ensemble de sous-systèmes interconnectés. Pour les manipulateurs rigides, chaque articulation représente un sous-système et dans le cas des manipulateurs flexibles, chaque sous-système est composé d'une articulation et du bras flexible correspondant. Deuxièmement, en commençant par le dernier sous-système, la loi de commande est développée en supposant que le reste des sous-

systèmes sont stables. Puis, la même stratégie est utilisée au rebours jusqu'au premier sous-système.

Suite à cette stratégie globale, on propose la stratégie détaillée suivante:

1. Recenser les travaux en relation avec la commande des manipulateurs rigides et flexibles par une revue de littérature ;
2. Développer une nouvelle stratégie de commande distribuée non linéaire des manipulateurs rigides assurant la stabilité globale de l'erreur de suivi de trajectoire dans l'espace opérationnel et la valider expérimentalement sur un robot rigide à 7 ddl (Chapitre 2) ;
3. Assurer la robustesse de la loi de commande développée dans (2) en développant sa version adaptative pour assurer la stabilité globale des erreurs de suivi dans l'espace de travail des robots rigides. Valider expérimentalement cette version adaptative sur le robot rigide à 7 ddl (Chapitre 3) ;
4. Modifier la stratégie de commande distribuée développée dans (2) pour prendre en compte la flexibilité présente dans les manipulateurs flexibles. L'objectif est d'assurer la stabilité des erreurs de suivi dans l'espace articulaire et minimiser les vibrations au niveau des bras flexibles. Valider expérimentalement cette stratégie sur un robot à deux bras flexibles (Chapitre 4) ;
5. Développer la version adaptative de la commande développée dans (4) pour assurer la robustesse de la loi de commande et la valider expérimentalement sur un robot à deux bras flexibles (Chapitre 5) ;
6. Développer une stratégie de commande distribuée pour les manipulateurs flexibles pour assurer le suivi de trajectoire dans l'espace de travail. Pour le problème de l'inversion dynamique, l'espace virtuel et l'approche quasi-statique sont utilisés. La technique de redéfinition de sortie est utilisée pour le problème de déphasage non-minimal. L'approche

de linéarisation par retour d'état est utilisée pour développer la loi de commande qui assure la stabilité locale des erreurs de suivi dans l'espace de travail. (Chapitre 6) ;

7. Généraliser la loi de commande développée dans (7) pour les robots flexibles pour assurer la stabilité globale des erreurs de suivi dans l'espace de travail des robots flexibles (Chapitre 7).

1.2 Revue de littérature

1.2.1 Commande des manipulateurs rigides

Dans ce travail, le robot est considéré comme étant un système automatique qui a comme variable d'entrée les couples appliqués aux articulations et comme sortie les positions articulaires et leurs dérivées, c'est-à-dire que la partie mécanique n'est pas prise en compte. Deux configurations possibles sur lesquelles les méthodes de commande sont basées : 1) la dynamique du robot est considérée comme étant un seul système multi-variables (MIMO), 2) la dynamique est considérée comme étant un ensemble des sous-systèmes mono-variable (SISO) interconnectés. Dans la suite de cette section, nous détaillerons les différentes techniques utilisées dans la littérature pour ces deux configurations.

1.2.1.1 Dynamique vue comme un système MIMO

Plusieurs méthodes de commande utilisées dans la littérature considèrent le système à commander comme étant un seul système multi-variables. La méthode de commande par linéarisation par retour d'état (Feedback Linearization), au sens entrée-état ou bien au sens entrée-sortie (Slotine et Li, 1991), représente l'une des approches les plus répandues et les plus connues. Dans le domaine de la robotique, la méthode de découplage non linéaire (Khalil et Dombre, 1999; Slotine et Li, 1991) (Computed Torque Method), basée sur la méthode de linéarisation par retour d'état, a connu beaucoup de succès. Son principe est de découpler l'équation dynamique du robot pour calculer les couples appliqués aux

articulations. En effet, les non linéarités de la dynamique sont compensées par la loi de commande et un système linéaire découplé est obtenu. Dans le cas où les paramètres du système ne sont pas parfaitement connus, la méthode de linéarisation par retour d'état n'est pas directement appliquée. L'ajout d'un processus adaptatif est ainsi nécessaire pour corriger les déficiences de la méthode de découplage non linéaire et stabiliser le système d'une façon robuste. On parle dans ce cas de la commande adaptative (Hung, 2008; Middleton, 1988; Ortega, 1989; Zhenhua et Xiongxiong, 2011). En effet, les paramètres du système utilisés pour la conception de la loi de commande sont estimés et ajustés en ligne. Le calcul complexe nécessaire pour développer la commande constitue l'inconvénient principal de cette approche.

On trouve aussi la commande à structure variable ou commande par mode de glissement appliquée aux systèmes robotiques (Harashima, Hashimoto et Kondo, 1985; Hashimoto et al., 1986; Slotine et Li, 1991). Cette approche se base sur une surface de glissement qui représente la réponse temporelle d'un système linéaire du premier ordre. L'objectif est de commander les variables du système pour qu'elles atteignent le régime glissant et le système suive une dynamique bien définie. Cette approche a connu beaucoup de succès dès son apparition, surtout au niveau de sa robustesse vis-à-vis des perturbations et des incertitudes du modèle, mais son inconvénient majeur est le problème de commutation. En effet, la dynamique négligée du système peut être excitée par des signaux à haute fréquence et la discontinuité de la commande peut conduire à un effet néfaste sur les actionneurs. Pour remédier ce problème, une fonction de saturation a été considérée dans la commande pour remplacer la fonction de commutation (Slotine et Li, 1991). Une autre méthode qui permet d'augmenter l'ordre du système (Second-Order Sliding Mode Control) a été établi par (Bartolini, Ferrara et Usani, 1998) puis par (Parra-Vega et Hirzinger, 2001) pour résoudre le problème de commutation en utilisant une commande virtuelle. Dernièrement (Fallaha et al., 2011) a introduit des termes exponentiels dans les composantes discontinues pour réduire les commutations hautes fréquences. Cette approche a été testée expérimentalement avec succès sur un robot manipulateur et a été comparée à d'autres approches de mode glissant pour montrer son apport.

La commande par « Backstepping » a été récemment utilisée pour les manipulateurs rigides (Chen et Lin, 2004; Irani et Talebi, 2011; Yang et al., 2004). Le principe de cette méthode de commande est d'utiliser des fonctions de Lyapunov, dépendantes des erreurs de poursuite, d'une façon progressive pour assurer la convergence du système vers le comportement désiré. Cette méthode est très répandue dans le cas des systèmes à structure triangulaire quand le calcul des lois de commande est très compliqué en augmentant l'ordre du système.

Quand le robot est considéré comme étant un système qui dissipe l'énergie (passif), la commande utilisée est dite passive (Sciavicco et Siciliano, 2000). Dans ce cas, un bloc non linéaire passif est utilisé dans la boucle de retour pour minimiser l'énergie du système en utilisant le formalisme de Hamilton. La commande passive est plus robuste que celle de découplage non linéaire quand on n'a pas besoin d'annuler les non linéarités existantes dans le modèle dynamique.

1.2.1.2 Dynamique vue comme des systèmes SISO interconnectés

Malgré que les méthodes de commande citées dans la section précédente ont été bien appliquées théoriquement, elles sont moins répandues dans le domaine industriel et leur implémentation en temps réel n'est pas toujours facile. La plupart des contrôleurs industriels utilisent l'idée de colocalisation. En effet, chaque système complexe est décomposé en un ensemble de sous-systèmes interconnectés et chacun d'eux est muni de son propre capteur et actionneur et en plus il est commandé séparément et indépendamment. Plusieurs avantages sont offerts par ce type de configuration à savoir, la simplicité de la synthèse et de la mise en œuvre en temps réel des lois de commande, la réduction de l'effort de calcul et la réduction de l'ordre de complexité (chaque sous-système est d'ordre moins élevé que le système au complet). Plusieurs techniques ont été utilisées dans le cas où le système est vu comme étant un ensemble de sous-systèmes interconnectés. Une méthode de commande basée sur le contrôle des joints indépendant (Hsia, Lasky et Guo, 1991; Seraji, 1988; Spong et Vidyasagar, 1989) est très utilisée pour les robots industriels. Son principe est de contrôler chaque joint comme étant un système SISO. Un contrôleur de type PID classique est utilisé

pour chaque joint (Spong et Vidyasagar, 1989). Chaque sous-système est traité comme étant un système linéaire et les effets de couplage sont traités comme des perturbations. Cette méthode contient des limites dans le cas du suivi à vitesse élevée.

La commande décentralisée est aussi utilisée pour le contrôle des systèmes robotiques quand la dynamique est vue comme étant des sous-systèmes interconnectés (Colbaugh et Glass, 1996; Colbaugh, Seraji et Glass, 1994; Indrawanto, Swevers et Van Brussel, 1998; Katic et Vukobratovic, 1994). Deux lois de commande décentralisées adaptatives ont été appliquées aux robots manipulateurs (Colbaugh et Glass, 1996): la première est utilisée pour le problème de suivi et le deuxième est utilisé pour le problème de régulation de la position. La convergence semi-globale des erreurs est uniquement assurée quand la commande adaptive est utilisée en absence des perturbations externes.

La commande distribuée est également utilisée pour ce type de configuration (Fareh, Saad et Saad, 2012b; 2012 ; Fareh, Saad et Saad, 2012c; Fareh et al., 2011). Cette stratégie de commande a été développée pour un robot rigide à 7 ddl. Elle consiste à contrôler une seule articulation à chaque étape en commençant de la dernière articulation jusqu'à la première. Une commande adaptive indirecte dite hiérarchique a été déduite dans (Fareh, Saad et Saad, 2012). La loi de commande de la $i^{\text{ème}}$ articulation est développée en fonction de ses propres paramètres estimés et des paramètres estimés et de toutes les articulations de niveau supérieur (de $n^{\text{ème}}$ jusqu'à $(i-1)^{\text{ème}}$). Juste la stabilité locale a été prouvée en utilisant l'approche de Lyapuov. Donc, il est intéressant de développer des lois de commande assurant la stabilité globale.

1.2.2 Commande des manipulateurs flexibles

1.2.2.1 Commande dans l'espace articulaire

Régulation

L'objectif est de développer une loi de commande capable d'amener le système à un point désiré. Dans le cas des manipulateurs flexibles, plusieurs algorithmes de commande ont été proposés dans la littérature afin de résoudre le problème de régulation dans l'espace articulaire. La commande proportionnelle dérivée (PD) est très utilisée pour résoudre ce type de problème. Dans (Canudas de Wit, Siciliano et Bastin, 1996; De Luca et Siciliano, 1993), les auteurs ont utilisé la commande PD avec compensation de l'effet de gravité pour un robot à plusieurs bras flexibles. En utilisant la théorie de Lyapunov, ils ont prouvé que cette commande assure la stabilisation globale de la position articulaire. La théorie de passivité a été utilisée dans (Lanari, 1992; Wang, 1992) pour stabiliser la position articulaire d'un système à un bras flexible par un régulateur PD. La passivité entre la vitesse articulaire et le couple de commande a été démontrée pour un robot à un bras flexible.

Une contrainte supplémentaire peut être prise en compte dans le problème de régulation tel que le temps de mouvement articulaire qui sera un paramètre fixe. Cette méthode a été utilisée pour un modèle masse-ressort dans (Meckl, 1994). Le signal de commande a été décomposé en deux fonctions : sinusoïdale et linéaire afin de minimiser l'énergie de commande pendant le début à la fin du mouvement désiré. Dans (Chan, 1995), les auteurs ont proposé une méthode basée sur la planification des consignes rigides. Dans le cas d'un robot à deux bras dont le dernier est flexible, la position articulaire finale est atteinte sans avoir des oscillations en utilisant une méthode basée sur la planification de mouvements articulaires dans (De Luca et Di Giovanni, 2001).

Il faut noter que la régulation (dans l'espace articulaire) est très limitée, car elle n'assure même pas un suivi de trajectoire au niveau articulaire et par conséquent ne peut pas assurer un suivi dans l'espace cartésien.

Suivi de trajectoire dans l'espace articulaire

Pour ce problème, l'objectif est de suivre des trajectoires articulaires temporelles tout en annulant ou minimisant les vibrations au niveau du bras flexible à la fin du mouvement désiré.

Plusieurs approches ont été proposées pour résoudre ce problème tel que la linéarisation entrée-sortie, les perturbations singulières et la commande adaptative.

La linéarisation entrée-sortie a connu un grand succès dans le cas des robots rigides. Cette approche consiste à linéariser la dynamique du système par une rétroaction de la partie non linéaire. Plusieurs travaux ont utilisé cette approche pour les manipulateurs flexibles (Aoustin, 1994; Siciliano et Book, 1988; Truckenbrodt, 1982). Dans (Siciliano et Book, 1988) , une linéarisation au sens entrée-sortie a été appliquée pour un système à bras flexible tournant dans le plan horizontal. Le suivi de trajectoires désirées dans l'espace articulaire est assuré, mais un sous-système non observable est apparu. Cette dynamique non observable est stable et elle est associée à la déformation. Malheureusement, cette méthode ne peut pas être appliquée pour assurer le suivi de trajectoires dans l'espace de travail à cause du déphasage non minimal.

La technique des perturbations singulières a été aussi appliquée pour la commande des manipulateurs flexibles (Salehi et Vossoughi, 2008; Siciliano et Book, 1988; Subudhi, 2005). Cette technique consiste à séparer les variables évoluant dans des échelles de temps différents. En effet, la dynamique non linéaire des manipulateurs flexibles est divisée en deux parties : une partie lente qui correspond aux coordonnées généralisées rigides et une partie rapide correspondant aux coordonnées généralisées flexibles. En profitant de la différence entre les deux constantes de temps de la partie lente et rapide, un couple pré calculé pour contrôler la partie rigide et une commande linéaire pour la partie flexible ont été appliqués à un système à un bras flexible (Siciliano et Book, 1988). L'avantage de cette technique a été prouvé après une comparaison avec une commande linéaire. Pour que le premier mode reste dominant, ce dernier doit être inclus dans le sous-système lent. Cette conclusion est vraie si la première fréquence naturelle est proche de zéro. Cette méthode peut être appliquée à un système à plusieurs bras flexibles.

La commande adaptative a été également utilisée pour résoudre le problème de suivi de trajectoire dans l'espace d'articulations (Abiko et Yoshida, 2005; Fareh, Saad et Saad, 2009; Lih-Chang et Sy-Lin, 1996). Dans (Fareh, Saad et Saad, 2009), les auteurs ont appliqué une

commande adaptative robuste pour un robot à un bras flexible tournant dans le plan horizontal pour suivre une trajectoire désirée dans l'espace d'articulations. Ils ont défini une surface de glissement composée des erreurs de suivi de vitesse plus une valeur pondérée de la dynamique des erreurs de suivi de position. Un couple pré-calculé a été appliqué dans un premier temps puis une version adaptative a été développée et appliquée. Un bon suivi de trajectoire a été obtenu. La stabilité de la dynamique des erreurs de suivi a été prouvée en utilisant la théorie de Lyapunov. La passivité est utilisée dans (Cheong, Chung et Youm, 2000) pour proposer une commande qui assure le suivi de trajectoire dans l'espace articulaire. Un compromis entre l'annulation des vibrations et la précision du suivi articulaire a été présent dans les résultats trouvés.

1.2.2.2 Commande dans l'espace cartésien

La propriété de déphasage non-minimal, qui caractérise les modèles des manipulateurs flexibles lorsque les sorties sont définies dans l'espace de travail, rend le problème de la commande plus complexe par rapport aux problèmes annoncés précédemment. Pour trouver une solution à ce problème, le premier obstacle à résoudre est l'inversion de la dynamique des manipulateurs flexibles. Une fois la dynamique est inversée, la conception d'une commande permettant d'assurer la stabilité des erreurs de suivi est possible.

L'espace de travail et articulaire sont liés par deux relations : une relation cinématique et une relation dynamique. La cinématique inverse, utilisée pour les manipulateurs rigides, n'est plus suffisante pour transformer les trajectoires désirées de l'espace de travail vers l'espace articulaire. Pour résoudre ce problème, l'idée de définition d'un espace intermédiaire entre l'espace de travail et celui des articulations a été utilisée dans la littérature (Christoforou, 2000; Saad, 2004; Talebi, Khorasani et Patel, 1999; Wang, 1991; Yang, Krishnan et Ang Jr, 1999). Cet espace est lié avec l'espace de travail par une relation cinématique comme le cas des manipulateurs rigides. La transformation de trajectoires désirées de cet espace intermédiaire à l'espace articulaire nécessite une résolution d'une équation différentielle non linéaire. Dans ce contexte, la méthode quasi-statique (Pfeiffer et Gebler, 1988) est utilisée

pour assurer la transformation des trajectoires désirées vers l'espace articulaire. Cette approche néglige la vitesse et l'accélération des coordonnées généralisées flexibles. Une méthode itérative, basée sur l'intégration causal-anticausale, a été également développée dans (Bigras, 2003) pour résoudre le problème de l'inversion de la dynamique. Le théorème de contraction a été utilisé pour démontrer les conditions de convergence.

Contrairement aux manipulateurs rigides, les actionneurs et les capteurs utilisés pour mesurer la déformation, dans les manipulateurs flexibles, ne sont pas localisés aux mêmes endroits. Par conséquent, les techniques d'inversion de la dynamique utilisées pour les robots rigides ne sont plus applicables à cause de l'instabilité de la dynamique des zéros. Pour contourner ce problème, plusieurs solutions ont été proposées dans la littérature telle que la technique basée sur la redéfinition de la sortie non localisée. Le principe de cette technique est la redéfinition des sorties à commander de façon à ce que la nouvelle dynamique soit à minimum de phase. Un système est dit à minimum de phase si, dans le cas des systèmes linéaires, tous les zéros de la fonction de transfert sont dans le demi-plan gauche et dans le cas des systèmes non linéaires, la dynamique des zéros est stable. Dans (Saad, Saydy et Akhrif, 2000b), l'auteur a utilisé la méthode de redéfinition de la sortie pour contrôler l'extrémité d'un système à un bras flexible tournant dans le plan vertical. Il a utilisé la passivité pour sélectionner la sortie la plus proche de l'extrémité du bras pour laquelle la dynamique interne soit bornée. La sortie trouvée est paramétrisée par un paramètre réel. Après l'inversion de la dynamique, il a utilisé un contrôleur strictement passif pour assurer un suivi de trajectoire dans l'espace de travail. Cette méthode a été bien appliquée à un système à un seul bras flexible, mais il est intéressant de voir sa performance pour des manipulateurs à plusieurs bras flexibles. La technique de redéfinition de sorties est également utilisée pour définir une sortie non colocalisée pour un système à un bras flexible dans (Wang, 1991). Le système devient passif avec la nouvelle sortie si l'inertie concentrée du moteur est assez importante. Cette nouvelle sortie est définie comme étant la différence entre la position articulaire multipliée par la longueur du bras et la déformation à l'extrémité.

Une fois le problème de l'inversion dynamique résolu, les stratégies de commande peuvent être utilisées pour assurer un bon suivi de trajectoires dans l'espace de travail. Pour une classe des manipulateurs dont le dernier bras est flexible, une stratégie de commande qui assure la stabilité des erreurs de suivi de trajectoire dans l'espace virtuel a été proposée dans (Bigras, 2003). Cette stratégie de commande est composée d'une loi de commande linéarisante par rapport aux articulations ainsi que deux retours d'état linéaire. Les gains des contrôleurs, qui assurent la stabilité exponentielle des erreurs de suivi, sont calculés en utilisant le théorème de passivité, l'étude de la stabilité des systèmes hiérarchiques et l'inégalité matricielle linéaire des systèmes (Bigras, 1997). Plusieurs hypothèses ont été supposées dans ce travail. Cette méthode n'est pas applicable directement à un système à plusieurs bras flexibles et elle n'a pas été validée expérimentalement.

La commande adaptative, appliquée pour les robots rigides (Slotine et Weiping, 1987), a été modifiée dans (Fareh, Saad et Saad, 2009; Kelkar et Joshi, 2004; Lih-Chang et Sy-Lin, 1996) pour prendre en considération la flexibilité au niveau des manipulateurs flexibles. Une sortie non localisée la plus proche de l'extrémité a été sélectionnée dans (Saad, Saydy et Akhrif, 2000a; Saad, Saydy et Akhril, 2000; Saad, Saydy et Akhrif, 2000b) pour assurer un bon suivi dans l'espace de travail et une dynamique interne stable. Les auteurs ont étudié la robustesse de la loi de commande face aux variations de la charge et de l'inertie du moteur pour un système à un bras flexible. Dans (Wang et Vidyasagar, 1991), les auteurs ont utilisé un observateur non linéaire pour estimer les variables d'état de la déformation. Pour réduire les vibrations résiduelles, une commande optimale, basée sur un filtre de Kalman, a été utilisée dans (Kwon, 2006). La robustesse par rapport à la variation des paramètres est assurée dans ce cas.

Dans (Moallem, Patel et Khorasani, 2001a), les auteurs ont utilisé la méthode des perturbations singulières pour développer une commande basée sur la dynamique inverse tout en assurant le suivi de l'extrémité d'un robot à un bras flexible. Une faible erreur de suivi est obtenue et la performance robuste est assurée. Dans (Wang et al., 1996), les auteurs ont développé, dans un premier temps, la dynamique d'un manipulateur à deux bras flexibles. Des

nouvelles sorties sont définies pour remplacer les coordonnées généralisées rigides dans le modèle dynamique. Ces sorties représentent les angles formés par les extrémités des deux bras. Par la suite, ils ont utilisé une linéarisation entrée-sortie pour linéariser partiellement le modèle dynamique. Une commande non linéaire par retour d'état a été développée pour stabiliser la dynamique interne du nouveau système. Cette loi de commande peut être appliquée à un système à plusieurs bras flexibles.

Une stratégie de commande distribuée a été développée dans (Fareh, Saad et Saad, 2013b) pour un manipulateur à deux bras flexibles. Cette stratégie consiste à mettre le modèle dynamique sous forme de deux sous-systèmes interconnectés. Le premier sous-système contient le deuxième bras flexible ainsi que l'articulation associée. Le deuxième sous-système contient la première paire articulation-bras flexible. La loi de commande du deuxième sous-système est tout d'abord développée en supposant que le premier sous-système est stable. Puis, en utilisant la même procédure, la loi de commande du premier sous-système est déduite. Juste la stabilité locale a été prouvée en utilisant l'approche de Lyapunov.

1.3 Méthodologie

La stratégie de commande distribuée que nous proposons concerne les manipulateurs rigides et flexibles. La phase de modélisation est nécessaire pour déterminer le modèle mathématique des manipulateurs et, par la suite, déduire certaines propriétés qui seront utiles pour la conception des lois de commande.

Pour développer une nouvelle stratégie de commande pour les manipulateurs rigides et flexibles, il est intéressant de commencer le développement et l'application à des manipulateurs rigides, qui représentent la majorité des manipulateurs utilisés dans l'industrie. De plus, la commande de ce type de manipulateurs est beaucoup moins compliqué par rapport des manipulateurs flexibles. En effet, les manipulateurs rigides sont totalement actionnés et à minimum de phase lors du contrôle de l'extrémité. Pour la validation, deux approches sont testées sur un robot à 7 ddl assurant la poursuite dans l'espace de travail: une commande

distribuée et sa version adaptative. Puis, en augmentant le niveau de complexité, cette stratégie de commande est développée et appliquée aux systèmes sous-actionnés (manipulateurs flexibles) pour suivre les trajectoires désirées dans l'espace articulaire et minimiser les vibrations au niveau des bras flexibles. Deux versions de commande sont développées et implémentées en temps réel sur un robot à deux bras flexibles: une commande distribuée et sa version adaptative. Après avoir appliqué l'idée principale sur les manipulateurs rigides et les manipulateurs flexibles dans l'espace articulaire, nous passons à l'application aux manipulateurs flexibles dans l'espace de travail qui présente la tâche la plus compliquée. Deux approches sont développées dans ce cas, la première assurant la stabilité locale et la deuxième est plus générale qui assure la stabilité globale. D'une façon plus détaillée, les étapes suivies sont présentées ci-dessous :

La première étape consiste à développer une stratégie de commande distribuée pour les manipulateurs rigides assurant la stabilité des erreurs de suivi dans l'espace de travail. Premièrement, la dynamique du manipulateur est mise sous forme d'un ensemble des sous-systèmes interconnectés. Chaque articulation représente un sous-système. Cette stratégie de commande utilise, dans un premier temps, la cinématique inverse pour transformer les trajectoires désirées de l'espace de travail vers l'espace articulaire. Ensuite, une commande distribuée est développée pour assurer le suivi de trajectoires dans l'espace articulaire. Cette stratégie de commande consiste à commander et stabiliser le dernier sous-système tout en supposant que le reste des articulations est stable. Puis, nous passons à la commande et la stabilisation de l'avant-dernier sous-système jusqu'à la première articulation en utilisant la même stratégie. La transformation de trajectoire de l'espace articulaire à l'espace de travail est assurée par la cinématique directe. L'étude expérimentale et l'implémentation en temps réel sur un robot rigide à 7 ddl sont nécessaires pour valider cette nouvelle approche.

Dans la deuxième étape, les paramètres du manipulateur rigide sont supposés inconnus et la loi de commande distribuée développée pour les robots rigides dans la première étape doit contenir un processus d'adaptation pour estimer ces paramètres. Une commande adaptative est ainsi proposée. En effet, en commençant par le dernier sous-système (articulation) tout en

supposant que le reste des articulations est stable, on estime les paramètres du système existant dans l'équation du mouvement du dernier sous-système et la loi de commande est ainsi développée en fonction de ces paramètres estimés. En reculant vers l'arrière (avant dernière articulation), on suppose que le reste des articulations est stable et on estime les paramètres du système existant dans l'équation du mouvement de cette articulation. La loi de commande est déduite en fonction des anciens paramètres estimés pour l'articulation précédente et les nouveaux paramètres estimés pour la présente articulation. La même procédure est utilisée, au rebours, pour estimer les paramètres et développer les lois de commande adaptative. La validation expérimentale sur un manipulateur rigide à 7 ddl est présente pour montrer l'apport et la performance de cet algorithme.

En augmentant le degré de difficulté, la troisième étape consiste à modifier et étendre la stratégie de commande distribuée pour l'appliquer aux systèmes sous-actionnés à savoir les manipulateurs flexibles. De plus pour le suivi de trajectoires, cette stratégie de commande doit minimiser les vibrations des bras flexibles. Pour atteindre cet objectif, le modèle dynamique des manipulateurs flexibles est réorganisé, dans un premier temps, pour prendre la forme d'un ensemble de sous-systèmes interconnectés. Chaque sous-système contient une articulation et son bras flexible associé. Puis, la loi de commande de chaque sous-système est développée en supposant que le reste de sous-systèmes est stable. Cette stratégie est appliquée à partir du dernier sous-système jusqu'au premier. La stabilité globale de tout le système est assurée par l'approche de Lyapunov. L'implémentation en temps-réel sur un robot à deux bras flexibles est présente pour montrer le niveau de performance de cette loi de commande.

La quatrième étape consiste à modifier la stratégie de commande distribuée développée pour les manipulateurs flexibles pour être applicable dans le cas où les paramètres sont inconnus. L'objectif est de développer la version adaptative de la commande distribuée assurant le suivi de trajectoires dans l'espace articulaire et minimisant les vibrations. Pour le $i^{\text{ème}}$ sous-système, constitué de la $i^{\text{ème}}$ articulation et le bras flexible associé, la loi de commande est développée en fonction de ses propres paramètres estimés ainsi que tous les paramètres déjà estimés pour

les sous-systèmes de niveau supérieur. La stabilité globale est assurée par l'approche de Lyapunov. La validation expérimentale est présente pour un robot à deux bras flexibles.

Jusqu'à présent, une stratégie de commande distribuée pour les manipulateurs rigides assurant la poursuite dans l'espace de travail a été développée. Puis, elle a été modifiée pour l'appliquer sur les manipulateurs flexibles assurant la poursuite dans l'espace articulaire et la minimisation des vibrations des bras flexibles. Il sera intéressant de pousser le niveau de difficulté et essayer cette stratégie de commande aux systèmes à déphasage non minimal tel que le suivi de trajectoires dans l'espace de travail pour les manipulateurs flexibles. Pour l'inversion de la dynamique, un espace intermédiaire nommé espace virtuel, entre l'espace de travail et l'espace articulaire, est utilisé pour transformer la trajectoire désirée de l'espace cartésien vers l'espace articulaire. L'approche quasi-statique est utilisée pour le passage de l'espace virtuel à l'espace articulaire. Pour surmonter le problème de déphasage non-minimal, la technique de redéfinition de la sortie est utilisée pour sélectionner une sortie la plus proche possible de l'extrémité assurant une dynamique interne bornée. Une étude de stabilité de la dynamique interne (ou dynamique des zéros) en se basant sur la passivité est utilisée pour déterminer la valeur critique du paramètre caractérisant cette sortie paramétrisée. Une loi de commande basée sur l'approche de linéarisation par retour d'état est proposée pour assurer la stabilité locale des erreurs de suivi.

La sixième étape consiste à étudier la stabilité globale des erreurs de suivi dans l'espace de travail d'un manipulateur à deux bras flexibles en utilisant la loi de commande des robots rigides modifiée. La transformation des trajectoires désirées de l'espace de travail vers l'espace articulaire est assurée par l'espace virtuel et l'approche quasi-statique. La technique de redéfinition de la sortie est utilisée pour résoudre le problème de non-minimum de phase. La loi de commande assurant la stabilité globale est développée en généralisant celle développée dans la deuxième étape.

1.4 Originalités des travaux

Cette recherche porte sur le développement des lois de commande non linéaire permettant d'assurer la stabilité de la dynamique des erreurs de suivi pour des manipulateurs rigides et flexibles.

Suite à la revue de littérature, malgré que plusieurs travaux portent sur la commande des manipulateurs, peu d'entre eux portent un regard précis sur le suivi de trajectoire dans l'espace de travail tout en assurant la stabilité globale de la dynamique de l'erreur. De plus, parmi les méthodes de commande assurant le suivi dans l'espace de travail, très peu d'entre elles profitent de la structure spécifique des manipulateurs pour la conception des lois de commande distribuées. Souvent, les méthodes de commande utilisées pour les manipulateurs offrent une seule loi de commande pour toutes les articulations et la dynamique des manipulateurs est vue comme étant un seul système MIMO ce qui complique l'implémentation en temps-réel.

Par contre, dans le cas des applications industrielles, les contrôleurs se basent sur l'idée de colocalisation et chaque articulation est commandée par son propre contrôleur et la dynamique est regardée comme un ensemble de sous-systèmes interconnectés. Pour le suivi de trajectoires dans l'espace de travail, la commande des manipulateurs flexibles est différente à celles des manipulateurs rigides, car, dans ce cas, le système devient à non minimum de phase et sous actionné.

À la meilleure de la connaissance de l'auteur, cette recherche a donné lieu aux contributions suivantes :

1. Conception d'une nouvelle stratégie de commande distribuée pour les manipulateurs rigides assurant la stabilité globale des erreurs de suivi dans l'espace de travail. Une validation expérimentale de cette stratégie, sur un robot rigide à 7 DDL, est présentée dans le chapitre 2 pour montrer la performance de cette stratégie;

2. Modification de la loi de commande proposée dans le premier point pour assurer la robustesse de la loi de commande distribuée en développant la version adaptative assurant la stabilité globale de la dynamique des erreurs de suivi. Pour montrer l'efficacité de cette approche, l'implémentation en temps-réel est présentée dans le chapitre 3;
3. Conception d'une stratégie de commande distribuée pour les manipulateurs à bras flexibles pour assurer le suivi de trajectoire dans l'espace articulaire et minimiser les vibrations des bras flexibles. La validation expérimentale sur un robot à deux bras flexibles est présente dans le chapitre 4;
4. Développement de la version adaptative de la loi de commande proposée dans (3) pour assurer la dynamique des erreurs de suivi dans l'espace articulaire et minimiser les vibrations des bras flexibles. L'implémentation de cet algorithme sur un robot à deux bras flexibles est présente dans le chapitre 5;
5. Conception d'une commande distribuée pour un manipulateur à deux bras flexibles assurant le suivi de trajectoire dans l'espace de travail. l'espace virtuel et l'approche quasi-statique sont utilisés pour le problème de l'inversion de la dynamique. Pour le problème de déphasage non-minimal, la technique de redéfinition de sortie est utilisée. Un contrôleur strictement passif, assurant la stabilité locale, est également utilisé dans le chapitre 6;
6. Généralisation de la stratégie de commande proposée dans (1) pour assurer la stabilité globale de la dynamique des erreurs de suivi d'un robot à deux bras flexibles. Les résultats de simulation sur un robot à deux bras flexibles montrant un bon suivi dans l'espace de travail sont présentés dans le chapitre 7.

CHAPITRE 2

ARTICLE 1: WORKSPACE DISTRIBUTED REAL-TIME CONTROL OF RIGID MANIPULATORS

Fareh Raouf¹ Saad Mohamad² and Saad Maarouf¹

¹Electrical Engineering Department, Université du Québec, École de technologie supérieure,
1100, rue Notre-Dame ouest, Montréal (Québec), H3C 1K3, Canada

²School of Engineering, Université du Québec en Abitibi-Témiscamingue, 445, boul. de
l'Université, Rouyn-Noranda (Québec), J9X 5E4

Article publié à la revue « Journal of Vibration and Control » en Novembre 2012.

Abstract

This paper proposes a novel distributed nonlinear controller for a hyper redundant articulated nimble adaptable trunk (ANAT) robot to track a desired trajectory in the robot's workspace. The distributed control strategy consists in controlling the last joint by assuming that the remaining joints are stable and follow their desired trajectories. Then, going backward to the (n-1)-th joint, the same strategy is applied, and so on until the first joint. The proposed control law guarantees the global asymptotical stability of the tracking errors. This global stability is proved using Lyapunov theory. The proposed approach is implemented in real time on a 7 DOF ANAT robot. Experimental results and the comparison with the computed torque approach show the effectiveness of the approach and good tracking performance in the workspace.

Key Words: Distributed control, ANAT robot, workspace tracking, stability analysis.

2.1 Introduction

In the past few decades, many authors have considered the tracking control problem in the workspace of manipulators because the tasks, defined in the workspace (painting, assembly ...), are usually performed by the end effectors. Robot manipulators, with their nonlinear dynamics, present a challenging control problem and have been the focus of attention of the control community in the literature. Indeed, multi-link manipulators can be regarded as: 1) one MIMO system and a single controller designed to control all joints of the manipulator or 2) interconnected subsystems (joints) with constraints on information flow between these subsystems.

In the case of a one MIMO system, many control strategies were proposed for robot manipulators to solve the tracking control problem in the joint space or in the workspace. The computed torque method (Dawson, Grabbe et Lewis, 1991; Krstic, 2004; Li, Tso et Poo, 1998; Yim et Singh, 1993) is widely used and very successful in controlling robot manipulators. The nonlinearity of the dynamical systems is cancelled using the systems' mathematical model. However, due to the requirement of precise knowledge of the system structure and parameters, the computational task is very extensive. Sliding mode control (Asada et Slotine, 1986; Man et al., 2011; Mu, 2011) is also widely used for controlling robot manipulators. This approach is based on switching surface in order to drive the system state variables of tracking error to the origin. When the system state intersects with the sliding surface, it becomes more sensitive to variations of parameters. Exact knowledge of the system parameters is not required for this method; it only requires the upper bound of uncertainty. This method is applied in (Asada et Slotine, 1986) and oscillations of the control activity (chattering problem) appeared. To reduce the chattering level of the control input, a sliding surface with a new reaching law that contains an exponential term is used in (Fallaha et al., 2011). For n degrees-of-freedom robot manipulators, the backstepping approach and passivity theory were used in (Lotfazar et Eghtesad, 2007b) to solve a tracking problem in the presence of disturbance friction and parameter uncertainty.

In the previous nonlinear control schemes, the robot manipulators are controlled by a single controller as one MIMO system. Unfortunately, the real-time implementation of these controllers in industrial control systems is not easy (Fu, Gonzalez et Lee, 1987) due to the complexity of the control structures. To overcome this problem, the dynamics of robot manipulators can be viewed as interconnected subsystems (joints) and most industrial control systems can be solved using independent controllers for each joint. There exist many advantages of this control strategy, such as simplicity of implementation, fault tolerance, reduction of computational effort, etc.

Many control schemes were used in this context. A distributed control was used in (Fareh, Saad et Saad, 2012b; 2012 ; 2012 ; Fareh et al., 2011) to solve the tracking control problem. This distributed control strategy consists in controlling the n joints of the manipulator starting from the last joint, then going backward until the first joint. At each step, the corresponding joint is controlled assuming that the remaining joints are stable and follow their desired trajectories. In (Fareh, Saad et Saad, 2012 ; Fareh et al., 2011), the system parameters are assumed to be perfectly known and the control law is based on feedback linearization and sliding mode approaches, respectively. A good tracking of workspace trajectory was obtained for a 5 DOF ANAT robot. An adaptive version was presented in (Fareh, Saad et Saad, 2012) to track a desired trajectory in the joint space for a 3 DOF ANAT robot. In these studies, local stability is guaranteed. However, the global stability is not proved. Decentralized control was also used in (Hsu et Fu, 2003; Jian-Qi et Wend, 1999; Osman et Roberts, 1994; Sadati et Elhamifar, 2005; Vukobratovic et Karan, 1996). In (Osman et Roberts, 1994) the authors applied a decentralized control to solve robots' tracking control problem. They only considered a particular class of manipulators where joints' inputs don't have a control coupling. An Independent Joint Control where each joint is controlled by a PID controller is proposed in (Spong et Vidyasagar, 1989). Each subsystem is treated as a linear system and the nonlinear coupling effects are considered as disturbances to be rejected by the controller. This approach has a low performance for tracking purposes at high velocities.

In this work, we propose a novel nonlinear distributed controller to solve the tracking control problem in the workspace for a 7-DOF ANAT robot. The tracking in the workspace is first transformed into the joint space using inverse kinematics. The inverse kinematics problem is then solved using the pseudo-inverse of the Jacobian. The distributed control strategy consists of controlling the last joint while assuming that the remaining joints are stable and follow their desired trajectories. Then, going backward to the $(n-1)$ -th joint, the same strategy is applied, i.e. the $(n-1)$ -th joint is controlled while assuming the remaining joints follow their desired trajectories, and so on until the first joint. The global asymptotical stability is proved using Lyapunov theory. The distributed strategy is tested on the ANAT robot.

The paper is organized as follows. Section 2.2 presents the model of the ANAT robot and describes its features. Section 2.3 proposes the distributed control strategy and presents global stability analysis. Experimental results are presented in Section 2.4. Finally, a conclusion is given in Section 2.5.

2.2 Modeling of the ANAT Robot

The system considered in this work is shown in Figure 2.1. It is a hyper redundant articulated nimble adaptable trunk (ANAT) robot. It has seven degrees of freedom: the first joint is prismatic, followed by three redundant rotary joints (joints 2, 3, and 4), and an end effector that consists of three rotary joints (joints 5, 6, and 7).

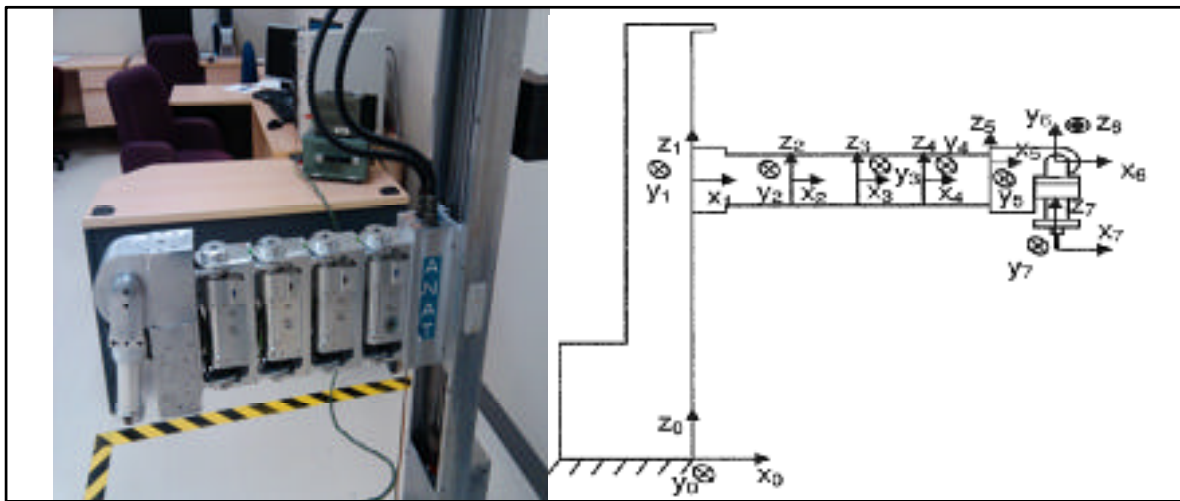


Figure 2.1 ANAT robot and axes.

The Denavit-Hartenberg parameters of the ANAT robot are given in Table 2.1.

Table 2.1 Denavit-Hartenberg parameters of ANAT robot
Tiré de (Le Boudec, Saad et Nergizian, 2006)

Joints	α_{i-1}	a_{i-1}	d_i	q_i
1	0	0	d_1	0
2	0	L_1	0	q_2
3	0	L	0	q_3
4	0	L	0	q_4
5	0	L	L_2	q_5
6	$\pi/2$	L_3	0	q_6
7	$-\pi/2$	0	$-L_4$	q_7

For a redundant robot, assuming a collision-free space, the velocities in the workspace and the joint space are linked by the generalized inverse Jacobian matrix as follows:

$$\dot{q} = J^T (JJ^T)^{-1} v \quad (2.1)$$

where J is the Jacobian matrix, \dot{q} is the joint space velocity vector and v is the Cartesian velocity vector. The position in the joint space q is given from \dot{q} using an integrator. The position of the tool relative to the base reference is calculated using the homogeneous transformation matrices (Le Boudec, Saad et Nerguizian, 2006) and is given by:

$$\begin{bmatrix} x \\ y \\ z \end{bmatrix} = \begin{bmatrix} L_4 c_{2345} s_6 + L_3 c_{2345} + L[c_{234} + c_{23} + c_2] + L_1 \\ L_4 s_{2345} s_6 + L_3 s_{2345} + L[s_{234} + s_{23} + s_2] \\ -L_4 c_6 + L_2 + q_1 \end{bmatrix} \quad (2.2)$$

where $s_i = \sin(q_i)$, $c_i = \cos(q_i)$, $s_{ij} = \sin(q_i + q_j)$, $c_{ij} = \cos(q_i + q_j)$ and L_i are given in Table 1.

Using Lagrange equations, the manipulator's equation of motion is given by:

$$M(q)\ddot{q} + C(q, \dot{q})\dot{q} + G(q) = \tau \quad (2.3)$$

where $q \in \mathcal{R}^n$ denotes the vector of the generalized positions in the joint space, $M(q) \in \mathcal{R}^{n \times n}$ is a symmetric positive definite inertia and mass matrix, $C(q, \dot{q})\dot{q}$ is the Coriolis and centrifugal forces vector, $G(q) \in \mathcal{R}^n$ is a vector of gravity terms, $\tau \in \mathcal{R}^n$ is the joint input torque vector, and finally \dot{q} and \ddot{q} are the joints' velocity and acceleration vectors respectively.

The model has the following properties that will be used in the stability analysis of the developed control law:

P1. Since the inertia and mass matrix $M(q)$ is a symmetric positive definite matrix then we can deduce that the diagonal elements are positive:

$$M_{ii}(q) > 0; \text{ for } i = 1 \dots n \quad (2.4)$$

P2. $\dot{M}(q) - 2C(q, \dot{q})$ is a skew symmetric matrix. Then, this property is preserved for the diagonal elements of $M(q)$ and $C(q, \dot{q})$ and we can write,

$$\dot{M}_{ii}(q) - 2C_{ii}(q, \dot{q}) = 0; \text{ for } i = 1 \dots n \quad (2.5)$$

The objective of this work is to track a desired trajectory defined in the workspace of the ANAT robot. Three steps are considered to achieve this objective. The inverse kinematics of the redundant robot is used, in the first step, to transform the desired trajectory from the workspace to the joint space. In the second step, a distributed control law, is developed to ensure tracking of the desired trajectory in the joint space obtained in the first step. In the third step, the direct kinematics is used to transform trajectories from the joint space to the workspace.

2.3 Distributed Control Strategy

The strategy of the distributed control consists in controlling the last joint by assuming that the remaining joints are stable and follow their desired trajectories. Then, going backward to the (n-1)-th joint, we assume that the remaining joints (1, ..., n-2, n) follow their desired values. By following the same strategy, the control laws of the remaining joints are developed. At each step, the control law is developed. The control law of the n joints and the stability analysis are developed in this section.

2.3.1 Control law

The dynamical model of the ANAT robot (2.3) can be written as follows:

$$\begin{bmatrix} M_1^T(q) \\ \vdots \\ M_n^T(q) \end{bmatrix} \begin{bmatrix} \ddot{q}_1 \\ \vdots \\ \ddot{q}_n \end{bmatrix} + \begin{bmatrix} C_1^T(q, \dot{q}) \\ \vdots \\ C_n^T(q, \dot{q}) \end{bmatrix} \begin{bmatrix} \dot{q}_1 \\ \vdots \\ \dot{q}_n \end{bmatrix} + \begin{bmatrix} G_1(q) \\ \vdots \\ G_n(q) \end{bmatrix} = \begin{bmatrix} \tau_1 \\ \vdots \\ \tau_n \end{bmatrix} \quad (2.6)$$

where $M_i^T(q) = [M_{i1} \dots M_{in}]$, and $C_i^T(q, \dot{q}) = [C_{i1} \dots C_{in}]$.

When controlling the i-th joint, we assume that the remaining joints follow their desired trajectories. New generalized coordinates are then defined where the i-th coordinate is controlled and the remaining coordinates follow their desired trajectories such that:

$$\begin{cases} Q_{ij} = q_j; \dot{Q}_{ij} = \dot{q}_j; \ddot{Q}_{ij} = \ddot{q}_j & \text{for } j = i \\ Q_{ij} = q_{jd}; \dot{Q}_{ij} = \dot{q}_{jd}; \ddot{Q}_j = \ddot{q}_{jd} & \text{for } j \neq i \end{cases} \quad (2.7)$$

To control the last joint, the remaining joints (1, ..., n-1) are assumed to be stable and follow their desired trajectories. The equation of movement of the n-th joint becomes:

$$M_n^T(Q_n)\ddot{Q}_n + C_n^T(Q_n, \dot{Q}_n)\dot{Q}_n + G_n(Q_n) = \tau_n \quad (2.8)$$

where:

$$M_n^T(Q_n) = [M_{n1}(Q_n) \dots M_{ni}(Q_n) \dots M_{nn}(Q_n)] \quad (2.9)$$

$$C_n^T(Q_n, \dot{Q}_n) = [C_{n1}(Q_n, \dot{Q}_n) \dots C_{ni}(Q_n, \dot{Q}_n) \dots C_{nn}(Q_n, \dot{Q}_n)]$$

and the position, the velocity, and the acceleration are given by:

$$Q_n = [q_{1d} \dots q_{(n-1)d} q_n]^T \quad (2.10)$$

$$\dot{Q}_n = [\dot{q}_{1d} \dots \dot{q}_{(n-1)d} \dot{q}_n]^T \quad (2.11)$$

$$\ddot{Q}_n = [\ddot{q}_{1d} \dots \ddot{q}_{(n-1)d} \ddot{q}_n]^T \quad (2.12)$$

Note that the first (n-1) coordinates are the desired ones, and the n-th coordinate is the controlled one.

The control law for the n-th joint is proposed as follows:

$$\tau_n = K_{pn}\tilde{q}_n + K_{dn}\dot{\tilde{q}}_n + M_n^T(Q_n)\ddot{Q}_n^* + C_n^T(Q_n, \dot{Q}_n)\dot{Q}_{nd} + G_n(Q_n) - \delta\tau_n \quad (2.13)$$

where K_{pn} and K_{dn} are positive gains, $\ddot{Q}_n^* = \ddot{Q}_{nd} + \gamma_n \dot{\tilde{Q}}_n$, $\dot{Q}_{nd} = [\dot{q}_{1d} \dots \dot{q}_{(n-1)d} \dot{q}_{nd}]^T$, \ddot{Q}_{nd} is its time derivative, $\tilde{Q}_n = Q_{nd} - Q_n = [0 \dots 0 \tilde{q}_n]^T$, and $\gamma_n = \frac{K_{pn}}{K_{dn}}$. The last element of the proposed control law is defined using the Taylor series as:

$$\delta\tau_n = \sum_{j=1}^{n-1} \delta M_{nj} \ddot{q}_{jd} + \sum_{j=1}^n \delta C_{nj} \dot{q}_{jd} + \delta G_n + \delta M_{nn} \ddot{q}_n^* \quad (2.14)$$

where $\ddot{q}_n^* = \ddot{q}_{nd} + \gamma_n \dot{\tilde{q}}_n$,

$$\delta M_{nj} = \sum_{j=1}^{n-1} \frac{\partial M_{nj}(q)}{\partial q_j} \Big|_{q_{jd}} \tilde{q}_j + R_{M_{nj}}(\tilde{q}_j) \quad (2.15)$$

$$\delta M_{nn} = \sum_{j=1}^{n-1} \frac{\partial M_{nn}(q)}{\partial q_j} \Big|_{q_{jd}} \tilde{q}_j + R_{M_{nn}}(\tilde{q}_j)$$

$$\delta C_{nj} = \sum_{j=1}^{n-1} \frac{\partial C_{nj}(q, \dot{q})}{\partial q_j} \Big|_{q_{jd}} \tilde{q}_j + \sum_{j=1}^{n-1} \frac{\partial C_{nj}(q, \dot{q})}{\partial \dot{q}_j} \Big|_{q_{jd}} \dot{\tilde{q}}_j + R_{C_{nj}}(\tilde{q}_j, \dot{\tilde{q}}_j) \quad (2.16)$$

$$\delta G_n = \sum_{j=1}^{n-1} \frac{\partial G_n(q)}{\partial q_j} \Big|_{q_{jd}} \tilde{q}_j + R_{G_n}(\tilde{q}_j) \quad (2.17)$$

$R_{M_{nj}}$, $R_{C_{nj}}$, and R_{G_n} are the high order terms given in Appendix of the Taylor series for $M_{nj}(q)$, $C_{nj}(q)$, and $G_n(q)$, respectively (Bartle et Sherbert, 2000) (See Appendix for more detail).

Then, we apply the same strategy by going backward from the (n-1)-th joint until the first joint. Taking for example the i-th joint, the equation of movement is given by the following expression:

$$M_i^T(Q_i) \ddot{Q}_i + C_i^T(Q_i, \dot{Q}_i) \dot{Q}_i + G_i(Q_i) = \tau_i \quad (2.18)$$

where:

$$M_i^T(Q_i) = [M_{i1}(Q_i) \dots M_{ii}(Q_i) \dots M_{in}(Q_i)] \quad (2.19)$$

$$C_i^T(Q_i, \dot{Q}_i) = [C_{i1}(Q_i, \dot{Q}_i) \dots C_{ii}(Q_i, \dot{Q}_i) \dots C_{in}(Q_i, \dot{Q}_i)]$$

and the new generalized coordinate is given by:

$$Q_i = [q_{1d} \dots q_{(i-1)d} \ q_i \ q_{(i+1)d} \dots q_{nd}]^T \quad (2.20)$$

$$\dot{Q}_i = [\dot{q}_{1d} \dots \dot{q}_{(i-1)d} \ \dot{q}_i \ \dot{q}_{(i+1)d} \dots \dot{q}_{nd}]^T \quad (2.21)$$

$$\ddot{Q}_i = [\ddot{q}_{1d} \dots \ddot{q}_{(i-1)d} \ \ddot{q}_i \ \ddot{q}_{(i+1)d} \dots \ddot{q}_{nd}]^T \quad (2.22)$$

Note also that the i-th element is the controlled coordinate and the remaining ones are the desired coordinates. Then, we propose the following control law:

$$\tau_i = K_{pi}\tilde{q}_i + K_{di}\dot{\tilde{q}}_i + M_i^T(Q_i)\ddot{Q}_i^* + C_i^T(Q_i, \dot{Q}_i)\dot{Q}_{id} + G_i(Q_i) - \delta\tau_i \quad (2.23)$$

where K_{pi} , K_{di} and $\gamma_i = \frac{K_{pi}}{K_{di}}$ are positive gains,

$\ddot{Q}_i^* = \ddot{Q}_{id} + \gamma_i\dot{\tilde{Q}}_i = [\ddot{q}_{1d} \dots \ddot{q}_{(i-1)d} \ \ddot{q}_i^* \ \ddot{q}_{(i+1)d} \dots \ddot{q}_{nd}]^T_{n \times 1}$ has the desired accelerations of the n joints and the desired velocity of the i-th joint, $\ddot{q}_i^* = \ddot{q}_{id} + \gamma_i\dot{\tilde{q}}_i$,

$$\delta\tau_i = \sum_{\substack{j=1 \\ j \neq i}}^n \delta M_{ij} \ddot{q}_{jd} + \sum_{\substack{j=1 \\ j \neq i}}^n \delta C_{ij} \dot{q}_{jd} + \delta G_i + \delta M_{ii} \ddot{q}_i^* \quad (2.24)$$

and

$$\delta M_{ij} = \sum_{\substack{j=1 \\ j \neq i}}^n \frac{\partial M_{ij}(q)}{\partial q_j} \Big|_{q_{jd}} \tilde{q}_j + R_{M_{ij}}(\tilde{q}_j) \quad (2.25)$$

$$\delta C_{ij} = \sum_{\substack{j=1 \\ j \neq i}}^n \frac{\partial C_{ij}(q, \dot{q})}{\partial q_j} \Big|_{q_{jd}} \tilde{q}_j + \sum_{\substack{j=1 \\ j \neq i}}^n \frac{\partial C_{ij}(q, \dot{q})}{\partial \dot{q}_j} \Big|_{q_{jd}} \dot{\tilde{q}}_j + R_{C_{ij}}(\tilde{q}_j, \dot{\tilde{q}}_j) \quad (2.26)$$

$$\delta G_i = \sum_{\substack{j=1 \\ j \neq i}}^n \frac{\partial G_i(q)}{\partial q_j} \Big|_{q_{ja}} \tilde{q}_j + R_{G_i}(\tilde{q}_j) \quad (2.27)$$

$R_{M_{ij}}$, $R_{C_{ij}}$, and R_{G_i} are the high order terms of the Taylor series.

The i -th control law is shown in Figure 2.2, where

$$Z_i(Q_i, \dot{Q}_i) = M_i^T(Q_i)\ddot{Q}_i^* + C_i^T(Q_i, \dot{Q}_i)\dot{Q}_{id} + G_i(Q_i) \quad (2.28)$$

$$\begin{aligned} \bar{q}_{id} &= [q_{1d} \dots q_{(i-1)d} \ 0 \ q_{(i+1)d} \dots q_{nd}]^T \\ \bar{q}_i &= [0 \dots 0 \ q_i \ 0 \dots 0]^T \end{aligned} \quad (2.29)$$

Then, $Q_i = \bar{q}_i + \bar{q}_{id}$.

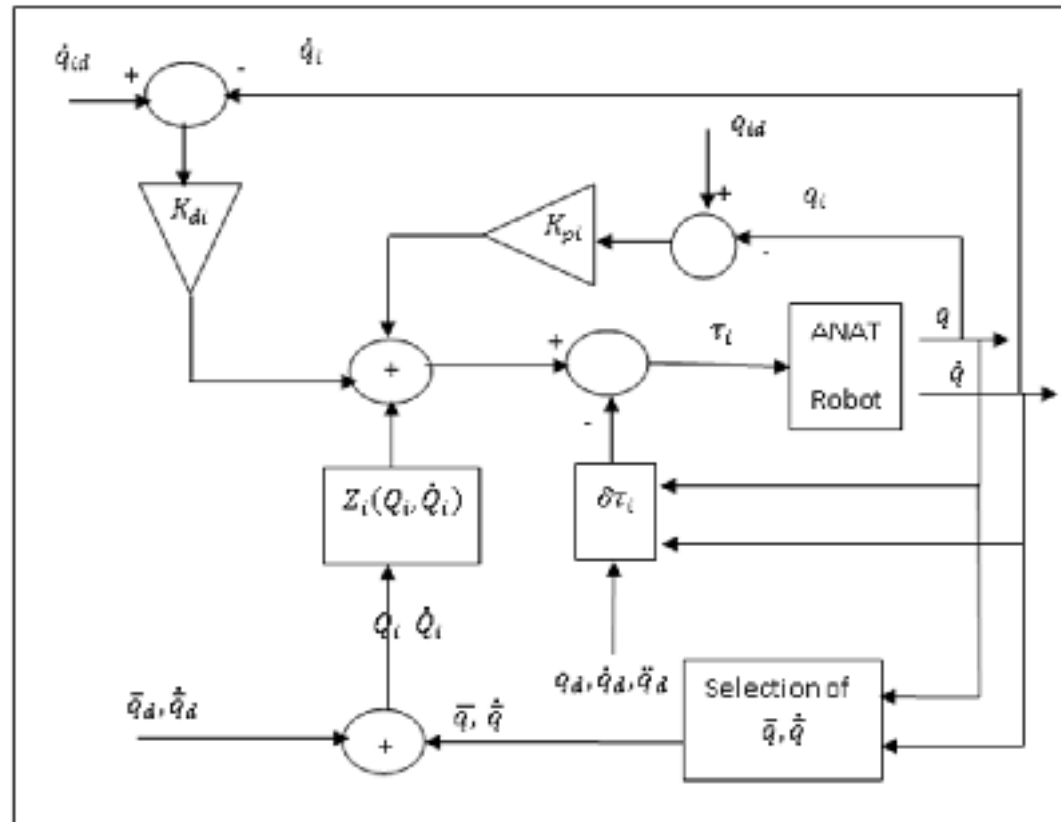


Figure 2.2 The i -th control law.

The distributed control strategy can be presented in Figure 2.3

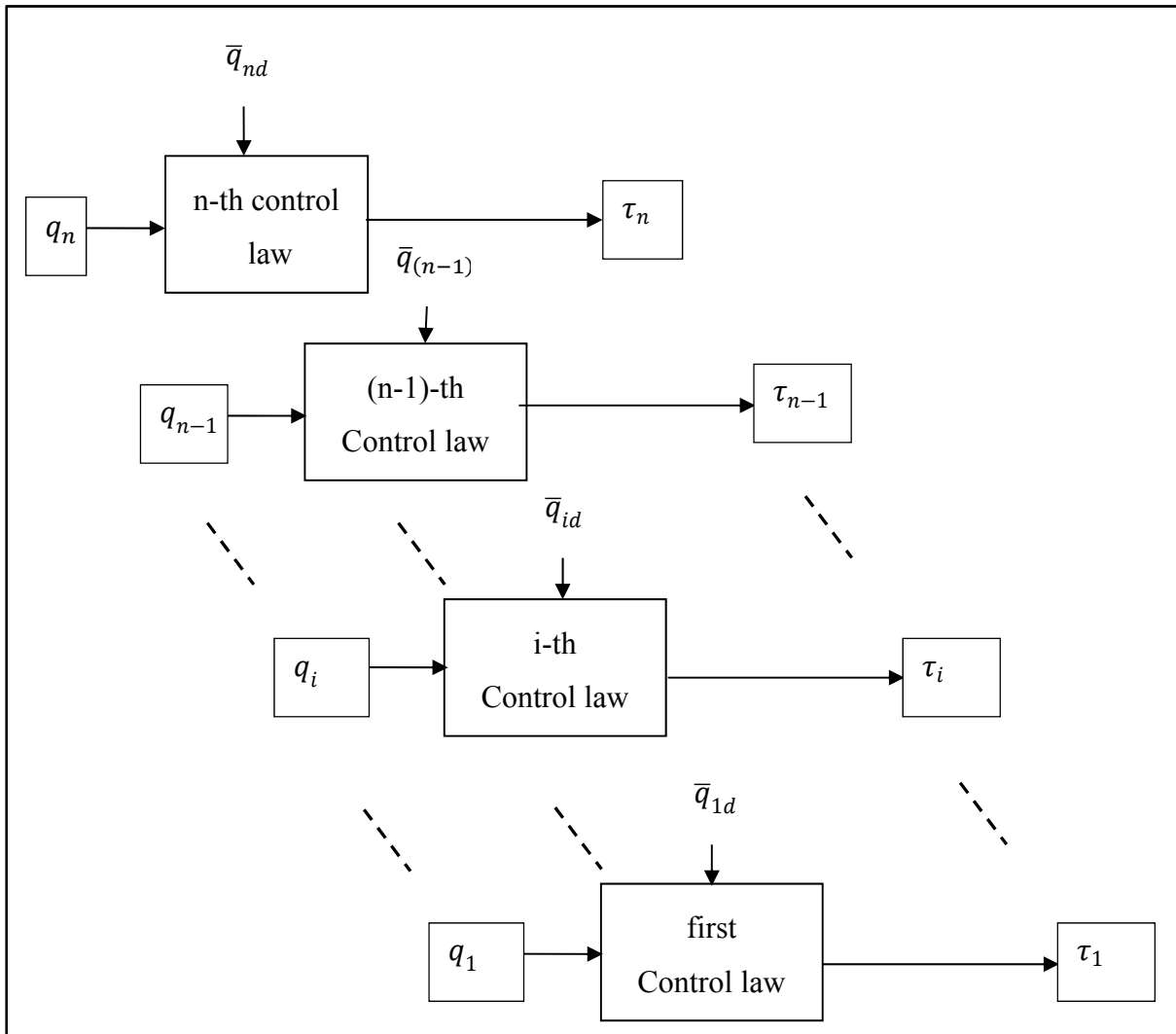


Figure 2.3 Distributed control strategy.

2.3.2 Global Stability Analysis

In this section, the global stability of the feedback system is presented. In a compact form, the n control laws (2.23) can be written as follows:

$$\tau = K_p \tilde{q} + K_d \dot{\tilde{q}} + \overline{M}(Q) \ddot{Q}^* + \overline{C}(Q, \dot{Q}) \dot{Q}_d + G(Q) - \delta \tau \quad (2.30)$$

where $Q = [Q_1^T \dots Q_n^T]^T_{n^2 \times 1}$; $\ddot{Q}^* = [\ddot{Q}_1^{*T} \dots \ddot{Q}_n^{*T}]^T_{n^2 \times 1}$; Q_i , \ddot{Q}_i^* and \ddot{q}_i^* are given in (2.23).

$$K_p = \text{diag}(K_{pi})_{n \times n}; K_d = \text{diag}(K_{di})_{n \times n}; \gamma = \text{diag}(\gamma_i)_{n \times n}$$

$$\overline{M}(Q) = \text{diag}(M_i^T(Q_i))_{n \times n^2}; \overline{C}(Q, \dot{Q}) = \text{diag}(C_i^T(Q_i, \dot{Q}_i))_{n \times n^2};$$

$$G(Q) = [G_1(Q_1) \dots G_n(Q_n)]^T_{n \times 1};$$

$$\delta\tau = \delta M_{diag} \ddot{q}^* + \delta C \dot{q}_d + \delta M_{ndiag} \ddot{q}_d + \delta G \quad (2.31)$$

$\ddot{q}^* = [\ddot{q}_1^* \dots \ddot{q}_n^*]^T_{n \times 1}$; δM_{diag} is the diagonal matrix of δM ; δM_{ndiag} is the non-diagonal matrix of δM . Then $\delta M_{diag} + \delta M_{ndiag} = \delta M$. δM_{ij} , δC_{ij} and δG_i are given in (25-27).

Substituting the control law (2.30) in the dynamical system (2.3), the error dynamics of the system can be written as follows:

$$K_p \tilde{q} + K_d \dot{\tilde{q}} + (\overline{M}(Q) \ddot{Q}^* - M(q) \ddot{q}) + (\overline{C}(Q, \dot{Q}) \dot{Q}_d - C(q, \dot{q}) \dot{q}) + (G(Q) - G(q)) - \delta\tau = 0 \quad (2.32)$$

Proposition 1

The error dynamics (2.32) is equivalent to the following equation:

$$M(q) \ddot{\tilde{q}} + C(q, \dot{q}) \dot{\tilde{q}} + K_d \dot{\tilde{q}} + \gamma(M_{diag}(q) \dot{q} + K_d \tilde{q}) = 0 \quad (2.33)$$

Proof: see Appendix.

Proposition 2

The dynamical system (2.3) with the feedback control (2.30) is globally asymptotically stable.

To prove the asymptotical stability, the following Lyapunov function is proposed:

$$V = \frac{1}{2} \tilde{q}^T M(q) \tilde{q} + \frac{1}{2} \tilde{q}^T \gamma K_d \tilde{q} \quad (2.34)$$

Taking the time derivative of $V(t)$, we get

$$\begin{aligned} \dot{V}(t) &= \tilde{q}^T M(q) \ddot{\tilde{q}} + \frac{1}{2} \tilde{q}^T \dot{M}(q) \tilde{q} + \tilde{q}^T \gamma K_d \tilde{q} \\ &= \tilde{q}^T \left(-C(q, \dot{q}) \tilde{q} - K_d \tilde{q} - \gamma (M_{diag}(q) \tilde{q} + K_d \tilde{q}) \right) + \frac{1}{2} \tilde{q}^T \dot{M}(q) \tilde{q} + \frac{1}{2} \tilde{q}^T \gamma K_d \tilde{q} \end{aligned}$$

Using property P2 given in Section 2.2, we can write:

$$-\tilde{q}^T C(q, \dot{q}) \tilde{q} + \frac{1}{2} \tilde{q}^T \dot{M}(q) \tilde{q} = \tilde{q}^T \left(\dot{M}(q) - 2C(q, \dot{q}) \right) \tilde{q} = 0$$

Then, we can conclude that:

$$\dot{V}(t) = -\tilde{q}^T \left(K_d + \gamma M_{diag}(q) \right) \tilde{q} \quad (2.35)$$

Because K_d , γ and $M_{diag}(q)$ are positive definite diagonal matrices, then $\dot{V}(t)$ is negative. Using Barbalat lemma (Spong et Vidyasagar, 1989) the error dynamics is globally asymptotically stable.

2.4 Experimental Results

In this section, the controllers presented in the previous sections are tested on the ANAT robot (Figure 1). Simulink with Real-Time Workshop (RTW) of Mathworks® is used for the implementation of the proposed controllers. The national Instruments PCI 6024E digital card is chosen for the real-time target. The ATMEGA 16 microcontrollers are used to translate the information to serial peripheral interface.

Using Matlab/Simulink, the trajectory in the workspace is first defined. The inverse kinematics is used to transform the desired trajectory from the workspace to the joint space. Then, using the desired trajectory of the joints and their real values from the

microcontrollers, the control algorithm executes and sends the torques to the microcontrollers. The microcontrollers translate the control signal into a pulse width modulation (PWM) signal. The latter is applied to the H-bridge drive of the actuators of the ANAT robot. The current of each actuator is measured by a current sensor located in the H-bridge drive. The microcontrollers process the digital information of the actuators' encoders and send the angles' positions to Simulink. The real-time setup is given in Figure 2.4.

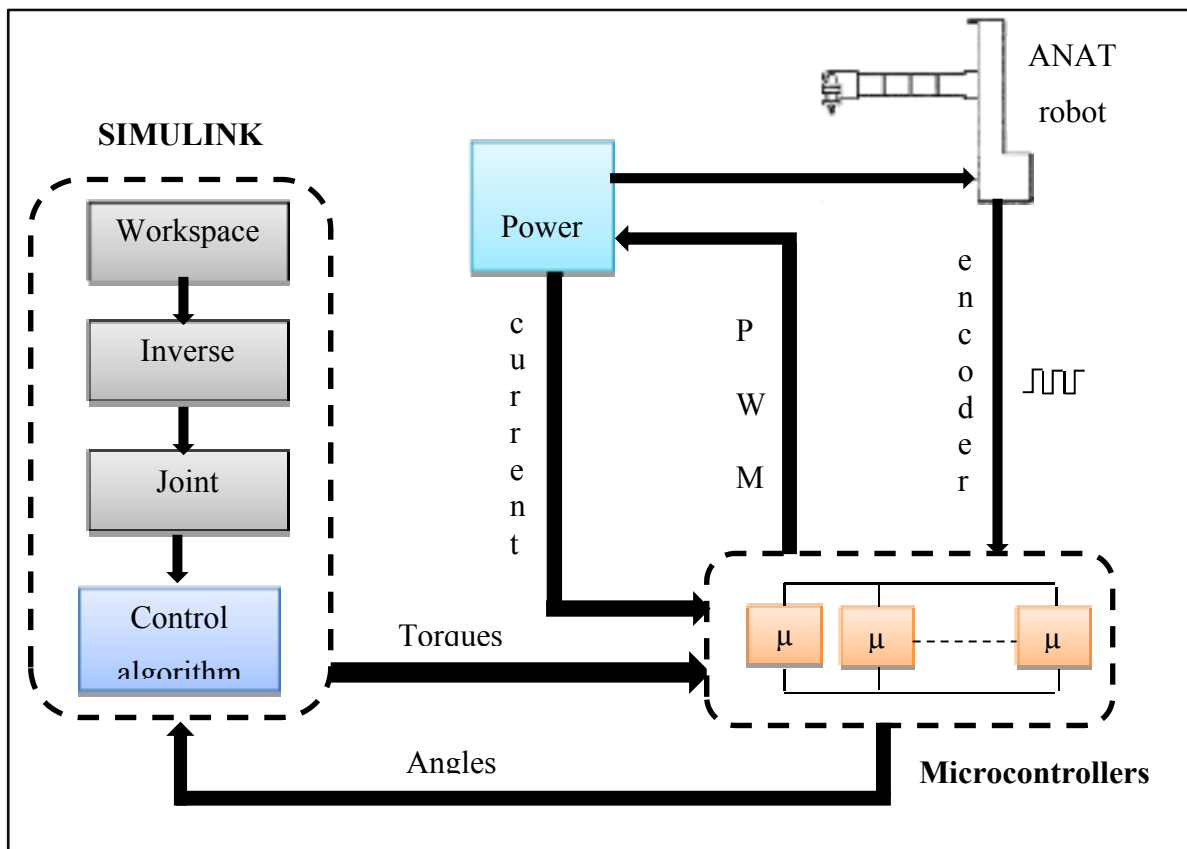


Figure 2.4 Real-time setup.

The ANAT robot is used to test the control strategy performance. Joints 2, 3, 4, and 5 are used but first, the sixth and seventh joints are locked. The controllers' gains are chosen as: $K_{p2} = 25, K_{p3} = 20, K_{p4} = 10, K_{p5} = 10; K_{d2} = 1.85, K_{d3} = 2, K_{d4} = 10, K_{d5} = 10$.

In the section 3, the theoretical development of the control law that ensures the global stability is given in the general case i.e. for any higher order. In the real-time implementation, a finite order of Taylor series is fixed. In this section, and for simplicity, the Taylor series is limited to the first order. Then, $R_{M_{nj}} = R_{C_{nj}} = R_{G_n} = 0$.

The experimental results are shown in Figure 2.5-2.10.

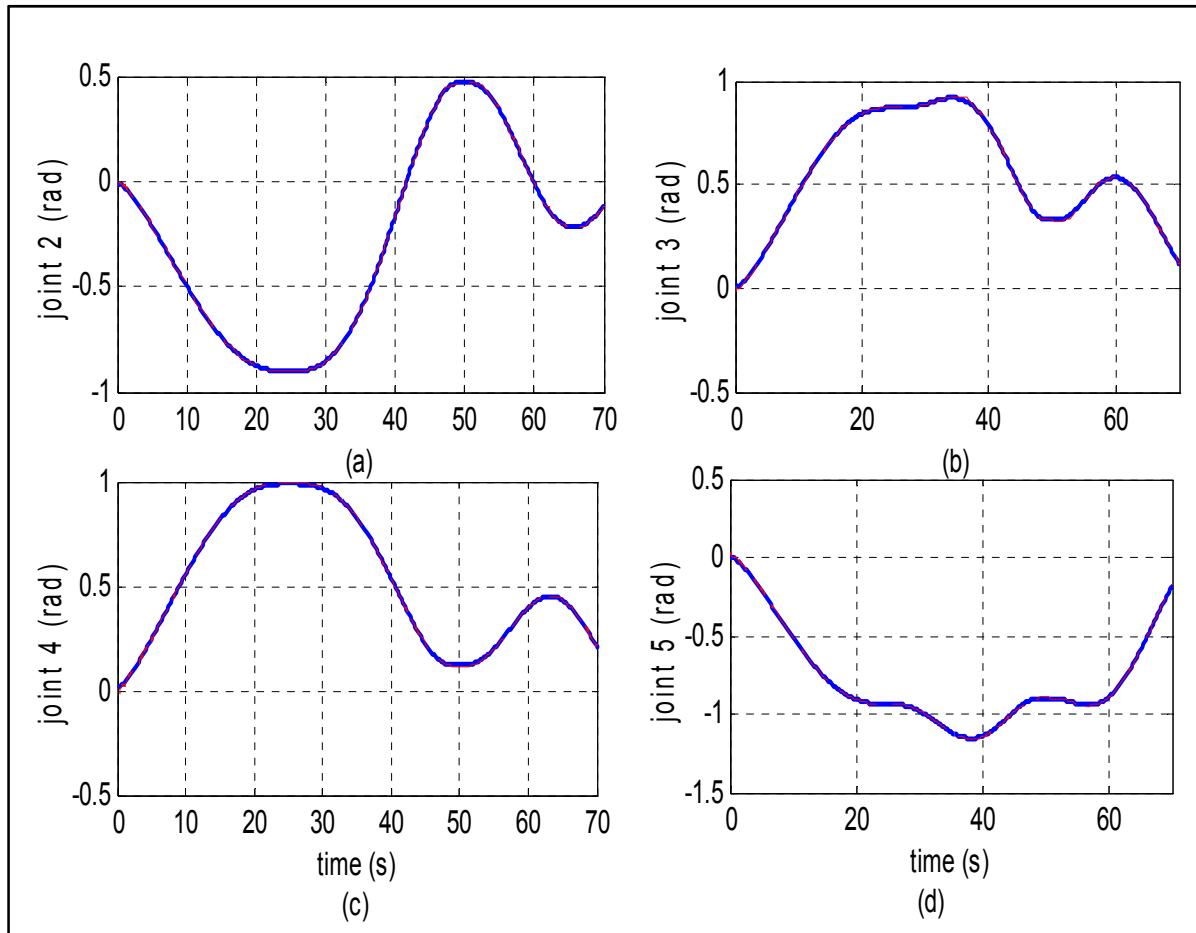


Figure 2.5 Joint space tracking. (a) joint 2, (b) joint 3, (c) joint 4 and (d) joint 5.

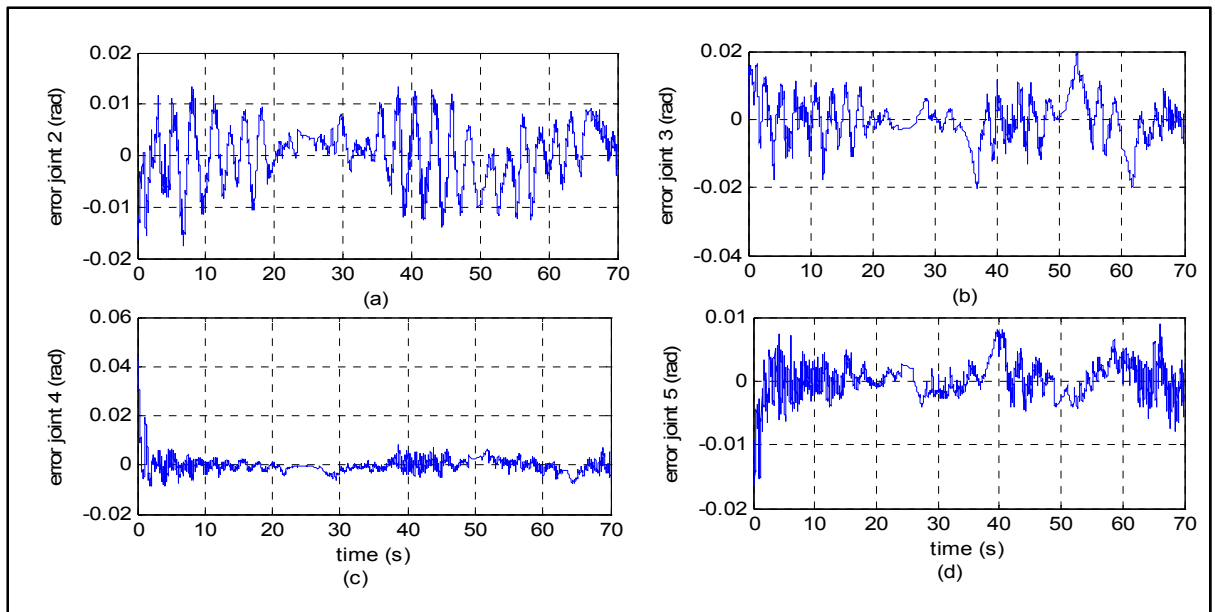


Figure 2.6 Joint space tracking errors. (a) joint 2, (b) joint 3, (c) joint 4 and (d) joint 5.

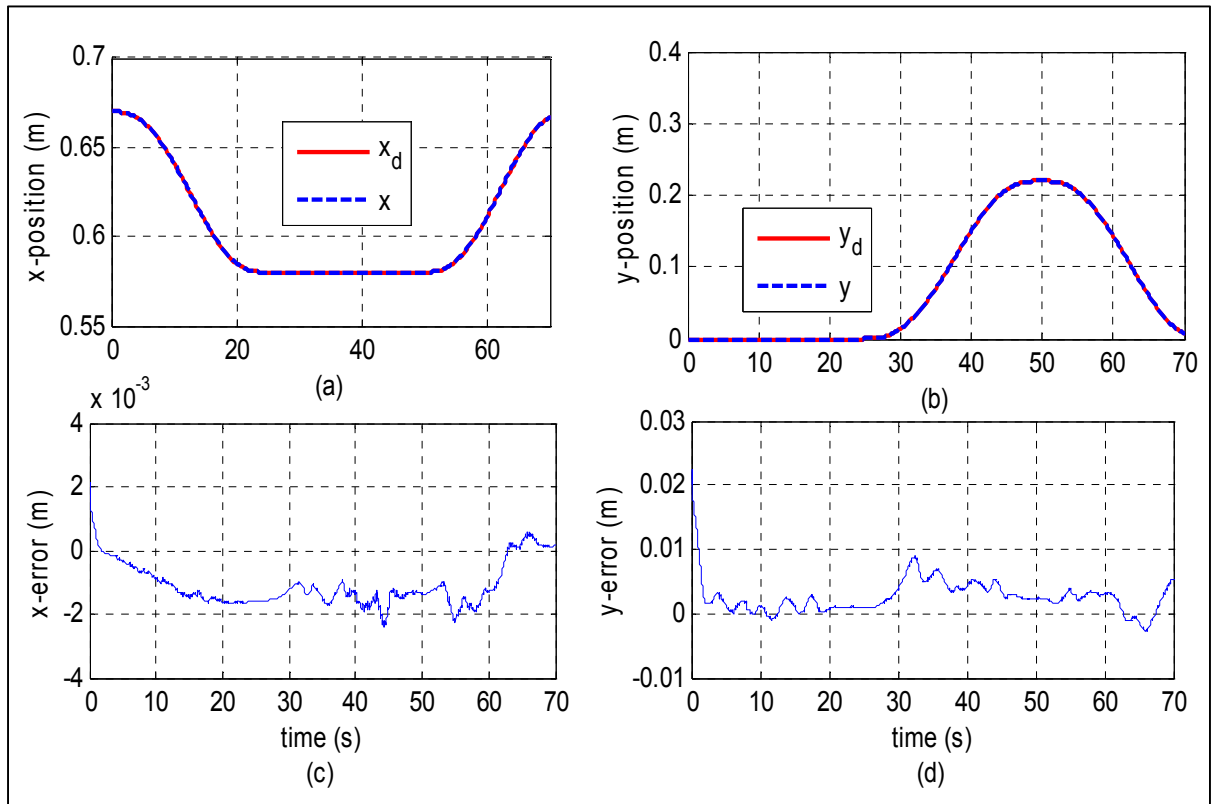


Figure 2.7 Workspace tracking. (a) x-tracking, (b) y-tracking, (c) x-tracking error and (d) y- tracking error.

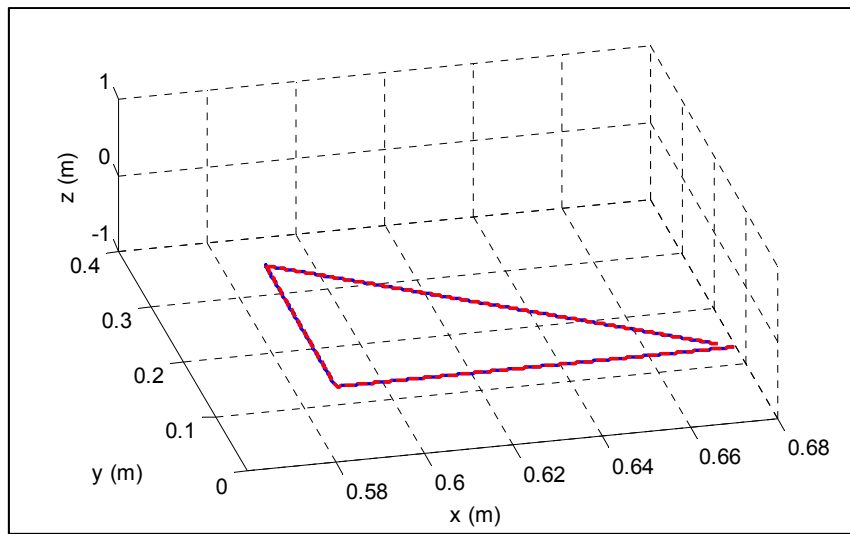


Figure 2.8 Workspace tracking.

When the initial tracking error is different to zero, the workspace tracking and the tracking error in the workspace are given in Figure 2.9.

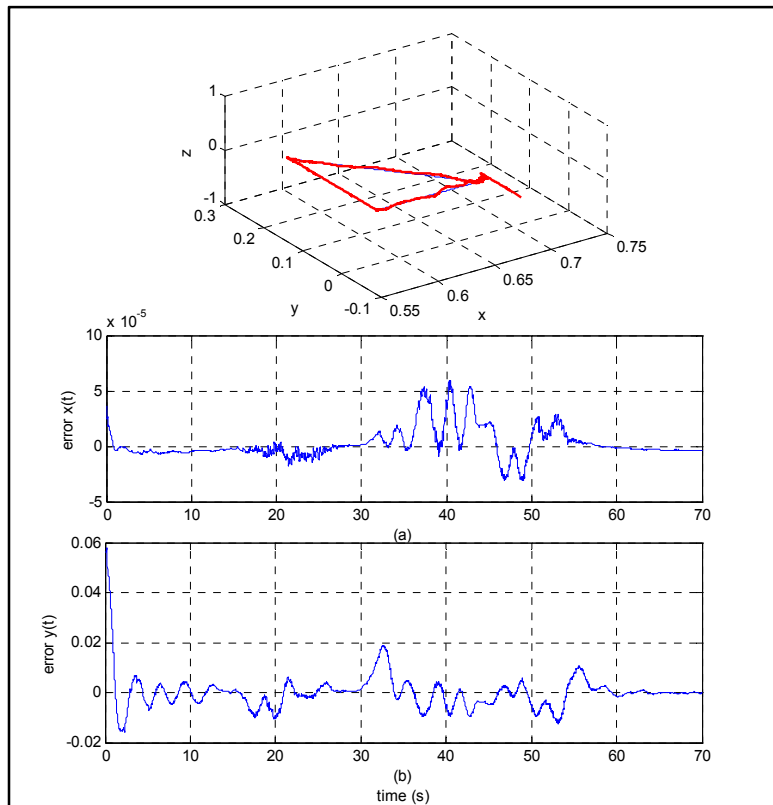


Figure 2.9 Workspace tracking with another initial point.

To show the effectiveness of the previous control strategy, the computed torque approach (Slotine et Li, 1991) is used for the ANAT robot. Figure 2.10 shows the experimental results for the computed torque approach using the same desired trajectory.

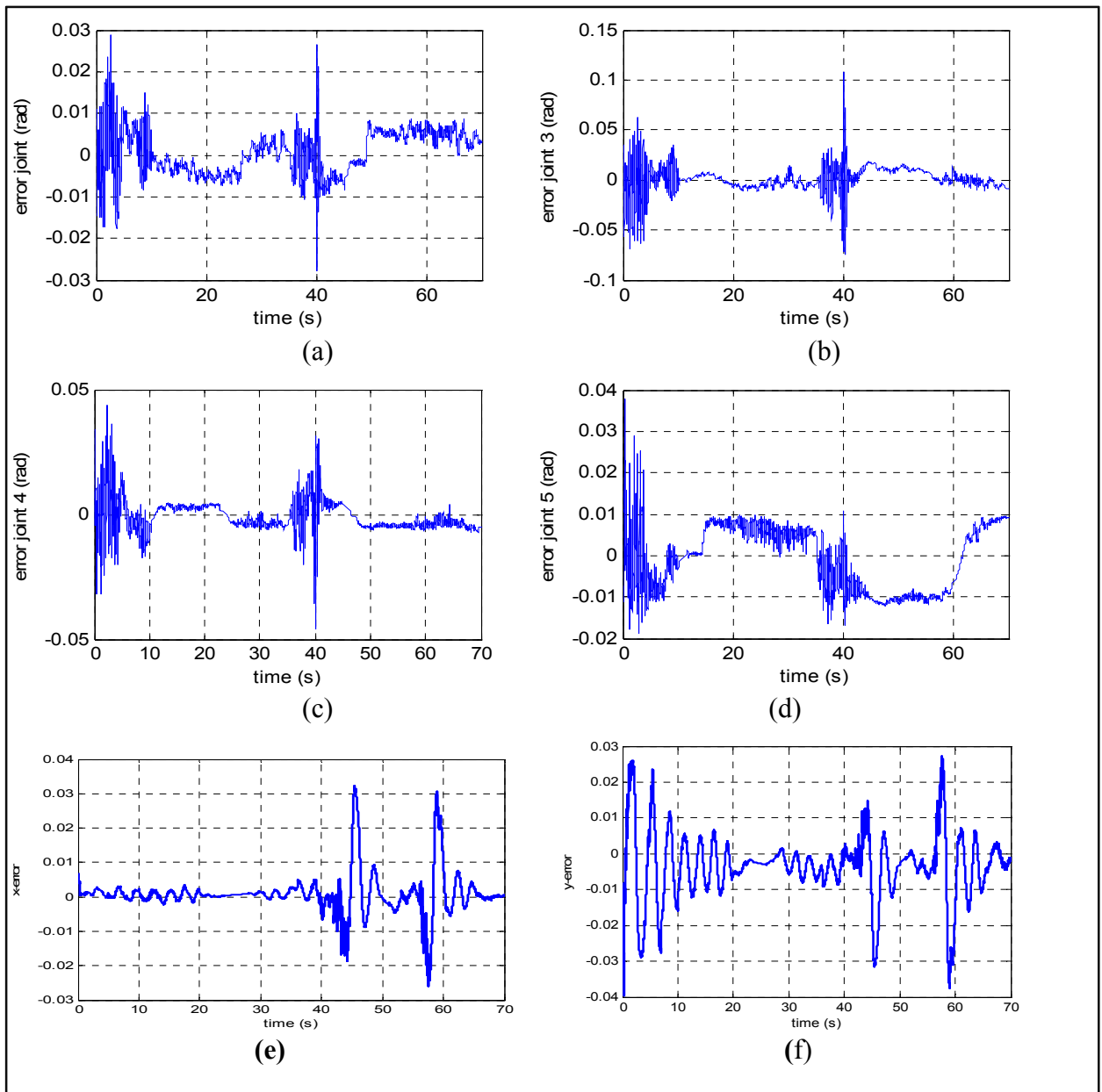


Figure 2.10 Tracking errors for the computed torque. (a) joint 2, (b) joint 3
(c) joint 4, (d) joint 5, (e) x-position and (f) y-position.

For the distributed control strategy, the tracking trajectories of the second, third, fourth and fifth joints are shown in Figure 2.5. Good tracking is obtained in the joint space. This good tracking is confirmed in Figure 2.6, which shows the tracking errors in the joint space. However, the objective of this work is the tracking in the workspace. Using the direct kinematics, good tracking of $x(t)$ and $y(t)$ trajectories in the workspace is shown in Figure 2.7. The tracking errors presented in Figure 2.7 show a small error in the workspace, less than 2mm for $x(t)$ and 10 mm for $y(t)$. Finally, Figure 2.8 shows good tracking in x-y-z workspace. Using the computed torque approach and the same desired trajectory, Figure 2.10 shows the tracking errors in the joint space. A good tracking in workspace is also obtained in Figure 2.9 by changing the initial point. According to the experimental results for the four joints affected by the workspace trajectory, the resulting tracking error of the computed torque method is greater than that found in the distributed approach. This illustrates the effectiveness of the proposed approach.

2.5 Conclusion

In this paper, a novel nonlinear distributed control strategy is proposed for rigid manipulators to track a desired trajectory in the workspace. The distributed control strategy consists in starting by controlling the last joint while assuming that the remaining joints are stable. Then, we follow the same strategy backward until the first joint. Lyapunov theory is used for global stability analysis of the feedback system. The controller is tested on a 7-DOF hyper redundant articulated nimble adaptable trunk (ANAT) robot to track a desired trajectory in the workspace. The experimental results were compared with the well-known computed torque method and showed good tracking in the workspace, which demonstrates the effectiveness of the proposed distributed control strategy.

Funding

This research was supported by the Natural Sciences and Engineering Research Council (NSERC) of Canada under the Discovery Grants Program.

2.6 Appendix

Proof of proposition 1:

In this section, we study the error dynamics given by (2.33). In the first step, we investigate the following elements of the error dynamics: $(\bar{M}(Q)\ddot{Q}^* - M(q)\ddot{q})$, $(\bar{C}(Q, \dot{Q})\dot{Q}_d - C(q, \dot{q})\dot{q})$ and $(G(Q) - G(q))$.

For the first element, we can write:

$$\begin{aligned} \bar{M}(Q)\ddot{Q}^* - M(q)\ddot{q} &= \begin{bmatrix} M_1^T(Q_1) & 0 & \cdots & 0 \\ 0 & \ddots & & \vdots \\ \vdots & & \ddots & 0 \\ 0 & \cdots 0 & M_n^T(Q_n) \end{bmatrix} \begin{bmatrix} \ddot{Q}_1^* \\ \vdots \\ \ddot{Q}_n^* \end{bmatrix} - \\ &\quad \begin{bmatrix} M_{11}(q) & \cdots & M_{1n}(q) \\ \vdots & \ddots & \vdots \\ M_{n1}(q) & \cdots & M_{nn}(q) \end{bmatrix} \begin{bmatrix} \ddot{q}_1 \\ \vdots \\ \ddot{q}_n \end{bmatrix} = \begin{bmatrix} M_1^T(Q_1)\ddot{Q}_1^* - M_1^T(q)\ddot{q} \\ \vdots \\ M_n^T(Q_n)\ddot{Q}_n^* - M_n^T(q)\ddot{q} \end{bmatrix} \end{aligned} \quad (2.36)$$

where M_i^T and \ddot{Q}_i^* are given in (2.6) and (2.23). Taking for example the i-th term, we get:

$$M_i^T(Q_i)\ddot{Q}_i^* - M_i^T(q)\ddot{q} = M_{ii}(Q_i)\ddot{q}_i^* - M_{ii}(q)\ddot{q}_i + \sum_{\substack{j=1 \\ j \neq i}}^n (M_{ij}(Q_i)\ddot{q}_{jd} - M_{ij}(q)\ddot{q}_j) \quad (2.37)$$

Using Taylor series, we can write:

$$M_{ij}(q) = M_{ij}(Q_i) + DM_{ij}(Q_i)^T(q - Q_i) + \frac{1}{2!}(q - Q_i)^T\{D^2M_{ij}(Q_i)\}(q - Q_i) + \cdots$$

where $DM_{ij}(Q_i)$ is the gradient of M_{ij} evaluated at $q = Q_i$ and $D^2M_{ij}(Q_i)$ is a Hessian matrix. Then, we can write:

$$\begin{aligned}
M_{ij}(q) &= M_{ij}(Q_i) + \frac{\partial M_{ij}(q)}{\partial [q_1 \dots q_{i-1} q_{i+1} \dots q_n]} \left| \begin{array}{c} q_{1d} \\ \vdots \\ q_{(i-1)d} \\ q_{(i+1)d} \\ \vdots \\ q_{nd} \end{array} \right| \begin{bmatrix} q_1 - q_{1d} \\ \vdots \\ q_{i-1} - q_{(i-1)d} \\ q_{i+1} - q_{(i+1)d} \\ \vdots \\ q_n - q_{nd} \end{bmatrix} + R_{M_{ij}}(\tilde{q}_j) \\
&= M_{ij}(Q_i) - \sum_{\substack{j=1 \\ j \neq i}}^n \frac{\partial M_{ij}(q)}{\partial q_j} \Big|_{q_{jd}} \tilde{q}_j + R_{M_{ij}}(\tilde{q}_j) \\
&= M_{ij}(Q_i) - \delta M_{ij}
\end{aligned}$$

where $\delta M_{ij} = \sum_{j=1}^n \frac{\partial M_{ij}(q)}{\partial q_j} \Big|_{q_{jd}} \tilde{q}_j - R_{M_{ij}}(\tilde{q}_j)$ and $R_{M_{ij}}$ is the remaining terms given as

$$\text{follows: } R_{M_{ij}}(\tilde{q}_j) = M_{ij}(q) - M_{ij}(Q_i) + \sum_{\substack{j=1 \\ j \neq i}}^n \frac{\partial M_{ij}(q)}{\partial q_j} \Big|_{q_{jd}} \tilde{q}_j$$

Using the same strategy of Taylor series for M_{ii} we can write:

$$\begin{aligned}
M_{ii}(q) &= M_{ii}(Q_i) - \sum_{\substack{j=1 \\ j \neq i}}^n \frac{\partial M_{ii}(q)}{\partial q_j} \Big|_{q_{jd}} \tilde{q}_j + R_{M_{ii}}(\tilde{q}_j) \\
&= M_{ii}(Q_i) - \delta M_{ii}.
\end{aligned}$$

where $\delta M_{ii} = \sum_{j=1}^n \frac{\partial M_{ii}(q)}{\partial q_j} \Big|_{q_{jd}} \tilde{q}_j + R_{M_{ii}}(\tilde{q}_j)$. $R_{M_{ii}}$ and $R_{M_{ii}}$ are the high order terms of the

Taylor series for $M_{ii}(q)$. Then,

$$\begin{aligned}
M_{ij}(Q_i) &= M_{ij}(q) + \delta M_{ij} \\
(2.38)
\end{aligned}$$

$$M_{ii}(Q_i) = M_{ii}(q) + \delta M_{ii}$$

Inserting (2.38) into (2.37), we get:

$$\begin{aligned}
M_{ii}(Q_i)\ddot{q}_i^* - M_{ii}(q)\ddot{q}_i + \sum_{\substack{j=1 \\ j \neq i}}^n (M_{ij}(Q_i)\ddot{q}_{jd} - M_{ij}(q)\ddot{q}_j) = \\
M_{ii}(q)\ddot{q}_i^* - M_{ii}(q)\ddot{q}_i + \delta M_{ii}\ddot{q}_i^* + \sum_{\substack{j=1 \\ j \neq i}}^n (M_{ij}(q)\ddot{q}_{jd} - M_{ij}(q)\ddot{q}_j + \delta M_{ij}\ddot{q}_{jd}) \quad (2.39) \\
= M_{ii}(q)\dot{S}_i + \delta M_{ii}\ddot{q}_i^* + \sum_{\substack{j=1 \\ j \neq i}}^n (M_{ij}(q)\ddot{\tilde{q}}_j + \delta M_{ij}\ddot{q}_{jd})
\end{aligned}$$

where $\dot{S}_i = \ddot{\tilde{q}}_i + \gamma_n \dot{\tilde{q}}_i = \ddot{q}_i^* - \ddot{q}_i$; \ddot{q}_i^* is given in (2.23). Using (2.39), (2.36) is rewriting as:

$$\begin{aligned}
\overline{M}(Q)\ddot{Q}^* - M(q)\ddot{q} = & \begin{bmatrix} M_{11}(q)\dot{S}_1 \\ \vdots \\ M_{nn}(q)\dot{S}_n \end{bmatrix} + \begin{bmatrix} \sum_{\substack{j=1 \\ j \neq 1}}^n \delta M_{1j}\ddot{q}_{jd} \\ \vdots \\ \sum_{\substack{j=1 \\ j \neq n}}^n \delta M_{nj}\ddot{q}_{jd} \end{bmatrix} + \begin{bmatrix} \sum_{\substack{j=1 \\ j \neq 1}}^n M_{1j}(q)\ddot{\tilde{q}}_j \\ \vdots \\ \sum_{\substack{j=1 \\ j \neq n}}^n M_{nj}(q)\ddot{\tilde{q}}_j \end{bmatrix} + \begin{bmatrix} \delta M_{11}\ddot{q}_1^* \\ \vdots \\ \delta M_{nn}\ddot{q}_n^* \end{bmatrix} + \\
& \begin{bmatrix} \sum_{\substack{j=1 \\ j \neq 1}}^n \delta M_{1j}\ddot{q}_{jd} \\ \vdots \\ \sum_{\substack{j=1 \\ j \neq n}}^n \delta M_{nj}\ddot{q}_{jd} \end{bmatrix}
\end{aligned}$$

In a compact form:

$$\overline{M}(Q)\ddot{Q}^* - M(q)\ddot{q} = M_{diag}(q)\dot{S} + M_{ndiag}(q)\ddot{\tilde{q}} + \delta M_{diag}\ddot{q}^* + \delta M_{ndiag}\ddot{q}_d \quad (2.40)$$

where M_{diag} and δM_{diag} are the diagonal matrices of M and δM ; M_{ndiag} and δM_{ndiag} are the non-diagonal matrices of M and δM , respectively. Then $M_{diag} + M_{ndiag} = M$ and $\delta M_{diag} + \delta M_{ndiag} = \delta M$.

Using the same strategy, the second term is:

$$\begin{aligned}\bar{C}(Q, \dot{Q})\dot{Q}_d - C(q, \dot{q})\dot{q} &= \begin{bmatrix} C_1^T(Q_1, \dot{Q}_1)\dot{Q}_{1d} - C_1^T(q, \dot{q})\dot{q} \\ \vdots \\ C_n^T(Q_n, \dot{Q}_n)\dot{Q}_{nd} - C_n^T(q, \dot{q})\dot{q} \end{bmatrix} \\ &= \begin{bmatrix} C_{11}(q, \dot{q}) & \cdots & C_{1n}(q, \dot{q}) \\ \vdots & \ddots & \vdots \\ C_{n1}(q, \dot{q}) & \cdots & C_{nn}(q, \dot{q}) \end{bmatrix} \begin{bmatrix} \dot{\tilde{q}}_1 \\ \vdots \\ \dot{\tilde{q}}_n \end{bmatrix} + \begin{bmatrix} \delta C_{11} & \cdots & \delta C_{1n} \\ \vdots & \ddots & \vdots \\ \delta C_{n1} & \cdots & \delta C_{nn} \end{bmatrix} \begin{bmatrix} \dot{q}_{1d} \\ \vdots \\ \dot{q}_{nd} \end{bmatrix}\end{aligned}$$

where $\dot{Q}_d = [\dot{q}_{1d} \ \cdots \ \dot{q}_{nd}]$.

$$\bar{C}(Q, \dot{Q})\dot{Q}_d - C(q, \dot{q})\dot{q} = C(q, \dot{q})\dot{\tilde{q}} + \delta C\dot{q}_d \quad (2.41)$$

By following the same strategy, the third term is given as follows:

$$G(Q) - G(q) = \delta G \quad (2.42)$$

Then, the error dynamics (2.32) can be written as:

$$\begin{aligned}K_p\tilde{q} + K_d\dot{\tilde{q}} + (M_{diag}(q)\dot{S} + M_{ndiag}(q)\ddot{\tilde{q}} + \delta M_{diag}\ddot{q}^* + \delta M_{ndiag}\ddot{q}_d) \\ + (C(q, \dot{q})\dot{\tilde{q}} + \delta C\dot{q}_d) + \delta G - \delta\tau = 0\end{aligned} \quad (2.43)$$

Using (2.31), the error dynamics becomes:

$$K_p\tilde{q} + K_d\dot{\tilde{q}} + M_{diag}(q)\dot{S} + M_{ndiag}(q)\ddot{\tilde{q}} + C(q, \dot{q})\dot{\tilde{q}} = 0 \quad (2.44)$$

Using $\dot{S} = \ddot{\tilde{q}} + \gamma \dot{\tilde{q}}$, $M_{diag} + M_{ndiag} = M$, and $K_p \tilde{q} + K_d \dot{\tilde{q}} = K_d \dot{\tilde{q}} + \gamma K_d \tilde{q}$, the error dynamics becomes:

$$M(q)\ddot{\tilde{q}} + C(q, \dot{q})\dot{\tilde{q}} + K_d \dot{\tilde{q}} + \gamma(M_{diag}(q)\dot{\tilde{q}} + K_d \tilde{q}) = 0 \quad (2.45)$$

CHAPITRE 3

ARTICLE 2: HIERARCHICAL ADAPTIVE CONTROL IN THE WORKSPACE OF RIGID MANIPULATORS

Fareh Raouf¹ Saad Mohamad² and Saad Maarouf¹

¹Electrical Engineering Department, Université du Québec, École de technologie supérieure,
1100, rue Notre-Dame ouest, Montréal (Québec), H3C 1K3, Canada

²School of Engineering, Université du Québec en Abitibi-Témiscamingue, 445, boul. de
l'Université, Rouyn-Noranda (Québec), J9X 5E4

Article soumis à la revue « IEEE Transactions on Control Systems Technology » en Octobre
2012.

Abstract

This paper presents two hierarchical nonlinear controller strategies for rigid manipulators to track a desired trajectory in the robot's workspace. For serial link manipulators, the hierarchical control strategy consists in controlling the last joint by assuming that the remaining joints are stable and follow their desired trajectories. Then we follow the same strategy backward from the (n-1)th joint until the first joint. First, the model parameters are perfectly known and a hierarchical control strategy is developed. Second, an adaptive version of the hierarchical nonlinear controller is proposed. The asymptotical stability is proved using Lyapunov theory. These algorithms are experimented on a 7 DOF hyper redundant articulated nimble adaptable trunk ANAT robot and compared with the computed torque approach. Good tracking in the workspace is obtained and effectiveness of the results is shown.

Key Words : ANAT robot, hierarchical control, adaptive control, workspace tracking, stability.

3.1 Introduction

Robot manipulators are characterized by a set of nonlinear-coupled equations. Their nonlinear dynamics present a challenging control problem. In the workspace, the control problem is very important because the tasks are usually performed in the Cartesian space such as: painting, assembly, etc. Two configurations characterize manipulators' dynamics. In the first, the dynamics of manipulators are considered as a MIMO system. In this case, a single controller is used for all joints. In the second configuration, the dynamical system is regarded as a set of interconnected subsystems (joints) with constraints on information flow between these subsystems.

For the MIMO case, many control strategies were successfully applied. The computed torque method which cancels the nonlinearity of the dynamical system by using the mathematical model was applied in (Fei et Wu, 2005; Isidori, 1995; Krstic, 2004; Yim et Singh, 1993). The sliding mode method, which utilizes discontinuous feedback control law to drive the state of the system into switching surface and keep this state on the manifold surface, was used in (Khalil, 2002; Slotine et Coetsee, 1986; Utkin, 1993). The backstepping approach can be used when the control design of manipulators is built systematically. In this approach the cancellation of “useful nonlinearities” is avoided. For rigid-link robot manipulators, an application of the integrator backstepping method is used in (Lotfazar et Eghtesad, 2007a) to track a joint space's desired trajectory.

Usually, the load and the friction torque of manipulators vary during the execution of a particular task or are unknown in advance, which causes the dynamical equations of manipulators to contain uncertain parameters. In this case, adaptive control (Arnautovic et Koivo, 1990; Colbaugh et Glass, 1995; Galicki, 2006; Tatlicioglu et al., 2009; Xu, Wu et Liang, 2000) is used to take into account the effect of these uncertainties in the controller design.

The previous nonlinear methods use a single controller for all manipulator's joints. Unfortunately, due to the complexity of the control structures, the real-time implementation of these controllers in industrial control systems is very difficult (Fu, Gonzalez et Lee, 1987). Most industrial control are solved this problem by using an independent controller for each joint where the dynamics of robot manipulators is viewed as interconnected subsystems (joints). This control strategy has many advantages, such as simplicity of implementation, fault tolerance, reduction of computational effort, etc.

Decentralized adaptive control was used in (Colbaugh et Glass, 1996; Colbaugh, Seraji et Glass, 1994; Indrawanto, Swevers et Van Brussel, 1998; Katic et Vukobratovic, 1994) to solve the manipulators' control problem. In (Colbaugh et Glass, 1996), the authors propose two decentralized adaptive controls for an electricaly-driven manipulator: one for tracking problems and one for position regulation. However, the adaptive control used for position regulation ensures only the semiglobal convergence of the error in the absence of any external disturbances.

An Independent Joint Control was used in (Hsia, Lasky et Guo, 1991; Seraji, 1988; Spong et Vidyasagar, 1989) for robot manipulators control. A PID controller is used for each joint in (Spong et Vidyasagar, 1989) for the tracking control problem. In this approch, each subsystem (joint) is treated as a linear system and the nonlinear coupling effects are considered as disturbances. This approach has low performance for tracking purposes at high velocities.

A hierarchical and distributed control were also used in (Fareh, Saad et Saad, 2012a; 2012b; 2012 ; 2012 ; Fareh et al., 2011) to solve the tracking control problem. The hierarchical control strategy takes advantage of the configuration of n serial-link manipulators. It consists in controlling the manipulator starting from the last joint, then going backward until the first joint. At each step, the corresponding joint is controlled by assuming that the remaining joints are stable and follow their desired trajectories. In (Fareh, Saad et Saad, 2012b; 2012 ; Fareh et al., 2011), the system parameters are supposed perfectly known and the control law

is based on feedback linearization and sliding mode approaches. Good tracking of the workspace trajectory was obtained for a 5 DOF ANAT robot. An adaptive version is presented in (Fareh, Saad et Saad, 2012) to track a desired trajectory in the joint space of a 3 DOF ANAT robot. In these studies, only local stability is guaranteed. The global stability is proved in (Fareh, Saad et Saad, 2012a) for a workspace tracking trajectory of 5-DOF ANAT robot.

In this work, we extend the previous works and we propose two nonlinear control strategies based on a hierarchical form for workspace tracking control of (ANAT) rigid manipulators. In the first case, the system parameters are perfectly known and a hierarchical control strategy is used to track a desired trajectory in the workspace. In the second case, the system parameters are assumed to be unknown and a hierarchical adaptive version is developed. In both cases, the global asymptotical stability is proved using the well-known Lyapunov theory. The controllers are tested on the ANAT robot.

The paper is organized as follows: section 3.2 presents the model of the ANAT robot and presents its features and properties. Section 3.3 proposes the hierarchical control strategy. Section 3.4 presents the adaptive version of the previous controller. Experimental results are presented in section 3.5. Finally, a conclusion is given in section 3.6.

3.2 Modeling

The system considered in this work is a hyper redundant articulated nimble adaptable trunk (ANAT) robot shown in Figure 3.1. This robot has seven degrees of freedom: one prismatic (joint 1), followed by three redundant rotary joints (joints 2, 3, and 4) and finally three rotary joints (joints 5, 6, and 7) that describe the end effector.

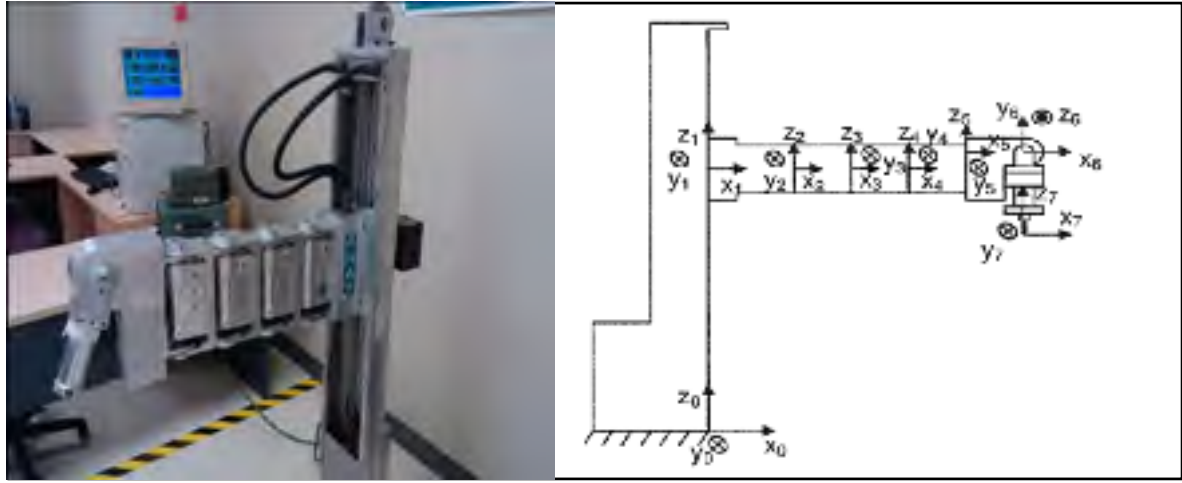


Figure 3.1 ANAT robot.

Using Lagrange equations, the dynamical model is given by:

$$M(q)\ddot{q} + C(q, \dot{q})\dot{q} + G(q) = \tau \quad (3.1)$$

where $M(q) \in \mathcal{R}^{n \times n}$ is an inertia and mass matrix, $C(q, \dot{q})\dot{q}$ is the Coriolis vector, $G(q) \in \mathcal{R}^n$ is a vector of gravity terms, $\tau \in \mathcal{R}^n$ is the joint input torque vector. $q \in \mathcal{R}^n$ denotes the vector of the generalized positions in the joint space, \dot{q} and \ddot{q} are the joints' velocity and acceleration vectors, respectively.

The model has the following properties that will be used for the control law:

P1. The inertia and mass matrix $M(q)$ is symmetric positive definite.

P2. From **P1**, we can deduce that the diagonal elements are positive (Bhatia, 2007):

$$M_{ii}(q) > 0; \text{ for } i = 1 \dots n \quad (3.2)$$

P3: The inertia-mass matrix $M(q)$ and the Coriolis matrix $C(q, \dot{q})$ satisfy the following skew-symmetric property:

$$X^T (\dot{M}(q, \dot{q}) - 2C(q, \dot{q})) X = 0 \quad \forall X \in \mathcal{R}^n \quad (3.3)$$

P4. Property **P3** is preserved for the diagonal elements of $M(q)$ and $C(q, \dot{q})$. Then, we can write:

$$\dot{M}_{ii}(q) - 2C_{ii}(q, \dot{q}) = 0; \text{ for } i = 1 \dots n \quad (3.4)$$

When controlling the i -th joint, we assume that the remaining joints follow their desired trajectories. Then, we can introduce the following assumption:

A1. For the i -th joint, the new generalized coordinates Q_i and their time derivatives are defined such that the i -th coordinate is the controlled one and the remaining coordinates follow their desired trajectories such that:

$$\begin{aligned} Q_i &= [q_{1d} \quad \dots \quad q_{(i-1)d} \quad q_i \quad q_{(i+1)d} \quad \dots \quad q_{nd}]^T \\ \dot{Q}_i &= [\dot{q}_{1d} \quad \dots \quad \dot{q}_{(i-1)d} \quad \dot{q}_i \quad \dot{q}_{(i+1)d} \quad \dots \quad \dot{q}_{nd}]^T \\ \ddot{Q}_i &= [\ddot{q}_{1d} \quad \dots \quad \ddot{q}_{(i-1)d} \quad \ddot{q}_i \quad \ddot{q}_{(i+1)d} \quad \dots \quad \ddot{q}_{nd}]^T \end{aligned} \quad (3.5)$$

The objective of this work is to track a desired trajectory defined in the workspace of rigid manipulators using hierarchical control. To achieve this objective, three steps are considered.

1) The first step consists in transforming the desired trajectory from the workspace to the joint space using pseudo-inverse kinematics. 2) In the second step, the control law is developed to ensure tracking of the desired trajectory in the joint space. 3) The third step consists in transforming trajectories from the joint space to the workspace using direct kinematics. These steps are presented in Figure 3.2.

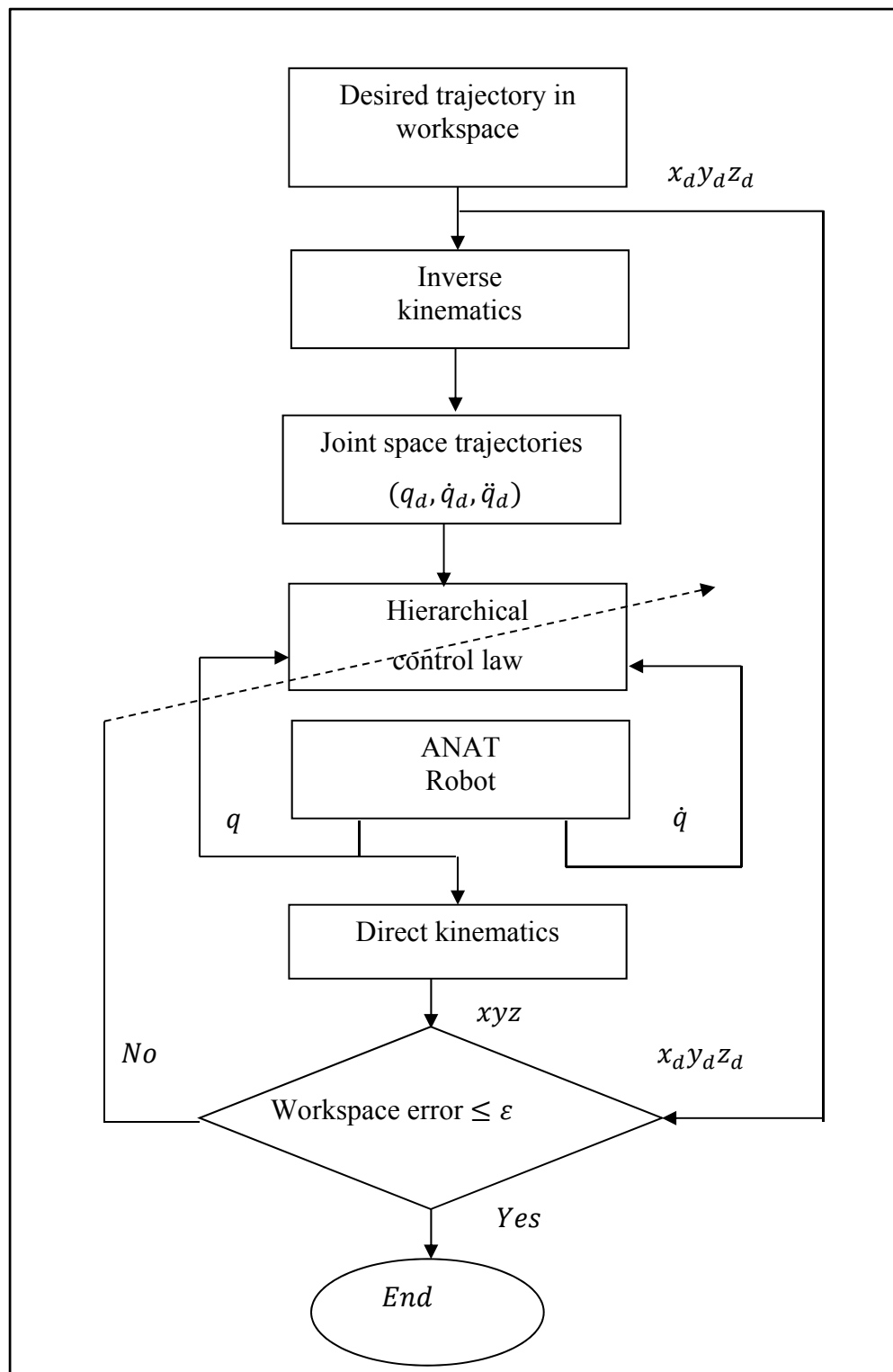


Figure 3.2 Control chart.

3.3 Hierarchical Control Strategy

The control strategy uses a hierarchical structure starting with the last joint and proceeding backward to the first joint. To control the last joint, we assume that the remaining joints are stable and follow their desired trajectories. Then, going backward to the before last joint, we assume that the remaining joints (1, ..., n-2, n) are stable. The control laws of the remaining joints are developed using the same strategy.

To clarify the hierarchical control strategy, the control law of the last joint and of an i-th joint is developed in this section. The dynamical model (3.1) is equivalent to:

$$\begin{bmatrix} M_1^T(q) \\ \vdots \\ M_n^T(q) \end{bmatrix} \begin{bmatrix} \ddot{q}_1 \\ \vdots \\ \ddot{q}_n \end{bmatrix} + \begin{bmatrix} C_1^T(q, \dot{q}) \\ \vdots \\ C_n^T(q, \dot{q}) \end{bmatrix} \begin{bmatrix} \dot{q}_1 \\ \vdots \\ \dot{q}_n \end{bmatrix} + \begin{bmatrix} G_1(q) \\ \vdots \\ G_n(q) \end{bmatrix} = \begin{bmatrix} \tau_1 \\ \vdots \\ \tau_n \end{bmatrix} \quad (3.6)$$

where $M_i^T(q) = [M_{i1} \quad \dots \quad M_{in}]$, and $C_i^T(q, \dot{q}) = [C_{i1} \quad \dots \quad C_{in}]$.

To control the last joint, the remaining joints (1, ..., n-1) are assumed to be stable and follow their desired trajectories. Then, the new generalized coordinate is given as follows:

$$Q_n = [q_{1d} \quad \dots \quad q_{(n-1)d} \quad q_n]^T \quad (3.7)$$

Note that the first (n-1) coordinates are the desired ones, and the n-th coordinate is the controlled one. The velocity \dot{Q}_n is the time derivative of Q_n and the acceleration \ddot{Q}_n is the time derivative of \dot{Q}_n .

The equation of movement of the n-th joint becomes:

$$M_n^T(Q_n)\ddot{Q}_n + C_n^T(Q_n, \dot{Q}_n)\dot{Q}_n + G_n(Q_n) = \tau_n \quad (3.8)$$

where

$$M_n^T(Q_n) = [M_{n1}(Q_n) \quad \dots \quad M_{ni}(Q_n) \quad \dots \quad M_{nn}(Q_n)] \quad (3.9)$$

$$C_n^T(Q_n, \dot{Q}_n) = [C_{n1}(Q_n, \dot{Q}_n) \dots \ C_{ni}(Q_n, \dot{Q}_n) \dots \ C_{nn}(Q_n, \dot{Q}_n)]$$

The following control law is proposed for the n-th joint:

$$\tau_n = K_{pn}\tilde{q}_n + K_{dn}\tilde{\dot{q}}_n + M_n^T(Q_n)\ddot{Q}_n^* + C_n^T(Q_n, \dot{Q}_n)\dot{Q}_{nd} + G_n(Q_n) - \delta\tau_n \quad (3.10)$$

where K_{pn} and K_{dn} are positive gains, $\dot{Q}_{nd} = [\dot{q}_{1d} \dots \dot{q}_{(n-1)d} \ \dot{q}_{nd}]^T$, \ddot{Q}_{nd} is its time derivative, $\tilde{Q}_n = Q_{nd} - Q_n = [0 \ \dots \ 0 \ \tilde{q}_n]^T$, and $\gamma_n = \frac{K_{pn}}{K_{dn}}$.

$$\ddot{Q}_n^* = \ddot{Q}_{nd} + \gamma_n \dot{\tilde{Q}}_n = [\ddot{q}_{1d} \dots \ddot{q}_{(n-1)d} \ \ddot{q}_n^*]^T \quad (3.11)$$

where $\ddot{q}_n^* = \ddot{q}_{nd} + \gamma_n \dot{\tilde{q}}_n$. $\delta\tau_n$ is defined using the Taylor series as:

$$\delta\tau_n = \sum_{j=1}^{n-1} \delta M_{nj} \ddot{q}_{jd} + \sum_{j=1}^n \delta C_{nj} \dot{q}_{jd} + \delta G_n + \delta M_{nn} \ddot{q}_n^* \quad (3.12)$$

$$\delta M_{nj} = \sum_{j=1}^{n-1} \frac{\partial M_{nj}(q)}{\partial q_j} \Big|_{q_{jd}} \tilde{q}_j + R_{M_{nj}}(\tilde{q}_j); \quad \delta M_{nn} = \sum_{j=1}^{n-1} \frac{\partial M_{nn}(q)}{\partial q_j} \Big|_{q_{jd}} \tilde{q}_j + R_{M_{nn}}(\tilde{q}_j) \quad (3.13)$$

$$\delta C_{nj} = \sum_{j=1}^{n-1} \frac{\partial C_{nj}(q, \dot{q})}{\partial q_j} \Big|_{q_{jd}} \tilde{q}_j + \sum_{j=1}^{n-1} \frac{\partial C_{nj}(q, \dot{q})}{\partial \dot{q}_j} \Big|_{q_{jd}} \dot{\tilde{q}}_j + R_{C_{nj}}(\tilde{q}_j, \dot{\tilde{q}}_j) \quad (3.14)$$

$$\delta G_n = \sum_{j=1}^{n-1} \frac{\partial G_n(q)}{\partial q_j} \Big|_{q_{jd}} \tilde{q}_j + R_{G_n}(\tilde{q}_j) \quad (3.15)$$

where $R_{M_{nj}}$, $R_{C_{nj}}$, and R_{G_n} are the high order terms of the Taylor series for $M_{nj}(q)$, $C_{nj}(q)$, and $G_n(q)$, respectively (Bartle et Sherbert, 2000) (See Appendix for more detail).

The same strategy is applied by going backward from the (n-1)-th joint until the first joint. Taking for example the i-th joint, the equation of motion is:

$$M_i^T(Q_i)\ddot{Q}_i + C_i^T(Q_i, \dot{Q}_i)\dot{Q}_i + G_i(Q_i) = \tau_i \quad (3.16)$$

where

$$\begin{aligned} M_i^T(Q_i) &= [M_{i1}(Q_i) \dots \ M_{ii}(Q_i) \ \dots \ M_{in}(Q_i)] \\ C_i^T(Q_i, \dot{Q}_i) &= [C_{i1}(Q_i, \dot{Q}_i) \dots \ C_{ii}(Q_i, \dot{Q}_i) \ \dots \ C_{in}(Q_i, \dot{Q}_i)] \end{aligned} \quad (3.17)$$

and the new generalized coordinate is given by:

$$Q_i = [q_{1d} \ \dots \ q_{(i-1)d} \ q_i \ q_{(i+1)d} \ \dots \ q_{nd}]^T \quad (3.18)$$

The control law for the i-th joint is given as follows:

$$\tau_i = K_{pi}\tilde{q}_i + K_{di}\dot{\tilde{q}}_i + M_i^T(Q_i)\ddot{Q}_i^* + C_i^T(Q_i, \dot{Q}_i)\dot{Q}_{id} + G_i(Q_i) - \delta\tau_i \quad (3.19)$$

where K_{pi} and K_{di} , $\gamma_i = \frac{K_{pi}}{K_{di}}$ are positive gains, $\ddot{q}_i^* = \ddot{q}_{id} + \gamma_i\dot{\tilde{q}}_i$, and:

$$\ddot{Q}_i^* = \ddot{Q}_{id} + \gamma_i\dot{\tilde{Q}}_i = [\ddot{q}_{1d} \ \dots \ \ddot{q}_{(i-1)d} \ \ddot{q}_i^* \ \ddot{q}_{(i+1)d} \ \dots \ \ddot{q}_{nd}]^T_{n \times 1} \quad (3.20)$$

$$\delta\tau_i = \sum_{\substack{j=1 \\ j \neq i}}^n \delta M_{ij} \ddot{q}_{jd} + \sum_{j=1}^n \delta C_{ij} \dot{q}_{jd} + \delta G_i + \delta M_{ii} \ddot{q}_i^* \quad (3.21)$$

$$\delta M_{ij} = \sum_{\substack{j=1 \\ j \neq i}}^n \left. \frac{\partial M_{ij}(q)}{\partial q_j} \right|_{q_{jd}} \tilde{q}_j + R_{M_{ij}}(\tilde{q}_j) \quad (3.22)$$

$$\delta C_{ij} = \sum_{\substack{j=1 \\ j \neq i}}^n \left. \frac{\partial C_{ij}(q, \dot{q})}{\partial q_j} \right|_{q_{jd}} \tilde{q}_j + \sum_{\substack{j=1 \\ j \neq i}}^n \left. \frac{\partial C_{ij}(q, \dot{q})}{\partial \dot{q}_j} \right|_{q_{jd}} \dot{\tilde{q}}_j + R_{C_{ij}}(\tilde{q}_j, \dot{\tilde{q}}_j) \quad (3.23)$$

$$\delta G_i = \sum_{\substack{j=1 \\ j \neq i}}^n \frac{\partial G_i(q)}{\partial q_j} \Big|_{q_{jd}} \tilde{q}_j + R_{G_i}(\tilde{q}_j) \quad (3.24)$$

Note that \ddot{Q}_i^* has the desired accelerations of the n joints and the desired velocity of the i-th joint. The i-th control law is presented in Figure 3.3, where $Z_i(Q_i, \dot{Q}_i) = M_i^T(Q_i)\ddot{Q}_i^* + C_i^T(Q_i, \dot{Q}_i)\dot{Q}_{id} + G_i(Q_i) - \delta\tau_i$, $\bar{q}_{id} = [q_{1d} \dots q_{(i-1)d} \ 0 \ q_{(i+1)d} \dots \ q_{nd}]^T$, and $\bar{q}_i = [0 \ \dots \ 0 \ q_i \ 0 \ \dots \ 0]^T$. Then, $Q_i = \bar{q}_i + \bar{q}_{id}$.

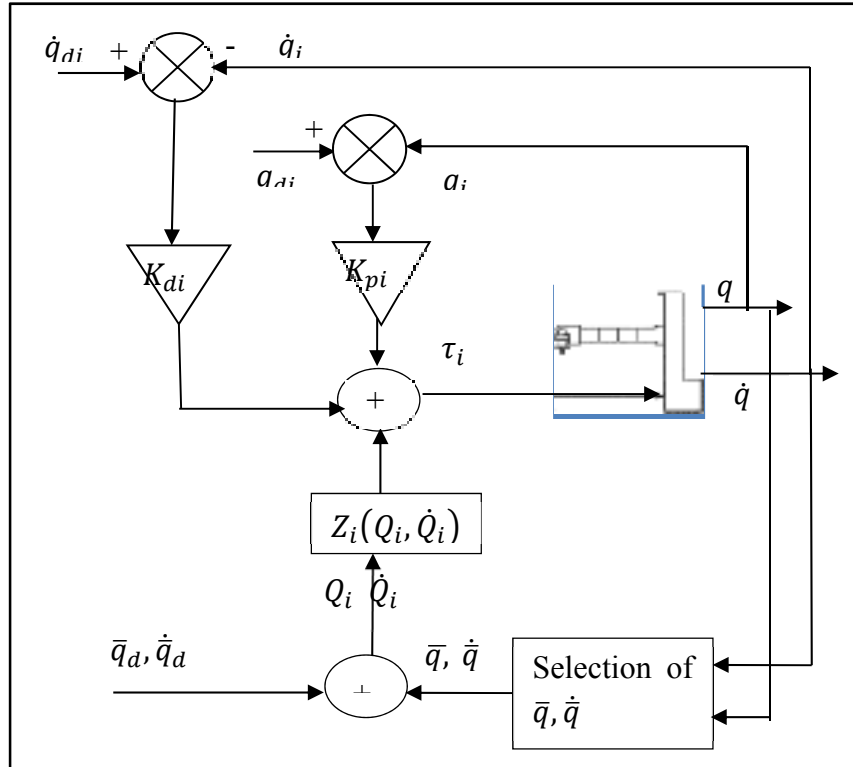


Figure 3.3 i-th control law.

In a compact form, the n control laws (3.19) can be written as follows:

$$\tau = K_p \tilde{q} + K_d \dot{\tilde{q}} + \overline{M}(Q) \ddot{Q}^* + \overline{C}(Q, \dot{Q}) \dot{Q}_d + G(Q) - \delta \tau \quad (3.25)$$

where

$Q = [Q_1^T \dots Q_n^T]^T_{n^2 \times 1}$; $\ddot{Q}^* = [\ddot{Q}_1^{*T} \dots \ddot{Q}_n^{*T}]^T_{n^2 \times 1}$; Q_i, \ddot{Q}_i^* are given in (3.18) and (3.20).

$$\begin{aligned}
K_p &= \text{diag}(K_{pi})_{n \times n}; K_d = \text{diag}(K_{di})_{n \times n}; \gamma = \text{diag}(\gamma_i)_{n \times n} \\
\bar{M}(Q) &= \text{diag}(M_i^T(Q_i))_{n \times n^2}; \bar{C}(Q, \dot{Q}) = \text{diag}(C_i^T(Q_i, \dot{Q}_i))_{n \times n^2}; \\
G(Q) &= [G_1(Q) \dots G_n(Q)]^T_{n \times 1}; \ddot{q}^* = [\ddot{q}_1^* \dots \ddot{q}_n^*]^T_{n \times 1}; \ddot{q}_i^* \text{ is given in (3.19).}
\end{aligned}$$

$$\delta\tau = \delta M_{diag}\ddot{q}^* + \delta C\dot{q}_d + \delta M_{ndiag}\ddot{q}_d + \delta G \quad (3.26)$$

The error dynamics of the system is given by substituting the control law (3.25) in the dynamical system (3.1) as follows:

$$\begin{aligned}
&K_p\tilde{q} + K_d\tilde{\dot{q}} + (\bar{M}(Q)\ddot{Q}^* - M(q)\ddot{q}) + (\bar{C}(Q, \dot{Q})\dot{Q}_d - C(q, \dot{q})\dot{q}) + (G(Q) - G(q)) \\
&\quad - \delta\tau = 0
\end{aligned} \quad (3.27)$$

Proposition 3.1

The error dynamics (3.27) is equivalent to the following equation:

$$M(q)\ddot{\tilde{q}} + C(q, \dot{q})\dot{\tilde{q}} + K_d\tilde{\dot{q}} + \gamma M_{diag}(q)\tilde{q} + K_p\tilde{q} = 0 \quad (3.28)$$

Proof: see Appendix.

The previous error dynamics (3.27) is global asymptotically stable. Then, to prove the global asymptotical stability, we propose the following Lyapunov function:

$$V = \frac{1}{2}\tilde{q}^T M(q)\tilde{q} + \frac{1}{2}\tilde{q}^T K_p\tilde{q} \quad (3.29)$$

Taking the time derivative of $V(t)$, we get:

$$\dot{V}(t) = \tilde{q}^T M(q)\ddot{\tilde{q}} + \frac{1}{2}\tilde{q}^T \dot{M}(q)\tilde{q} + \tilde{q}^T K_p\dot{\tilde{q}}$$

$$= \tilde{q}^T (-C(q, \dot{q})\tilde{q} - K_d\tilde{q} - \gamma M_{diag}(q)\tilde{q} - K_p\tilde{q}) + \frac{1}{2}\tilde{q}^T \dot{M}(q)\tilde{q} + \tilde{q}^T K_p\tilde{q}$$

Then, using the properties given in Section 3.2, we can conclude that:

$$\dot{V}(t) = -\tilde{q}^T (K_d + \gamma M_{diag}(q))\tilde{q} \quad (3.30)$$

Since K_d , γ and $M_{diag}(q)$ are positive definite diagonal matrices. Using Barbalat lemma, the error dynamics is globally asymptotically stable.

3.4 Adaptive Hierarchical Control

In this section, an adaptive version of the previous control strategy is developed to cope with the parameter's uncertainty. As in the previous section, the control strategy consists in starting with the last joint and going backward until the first joint. Using the uncertain parameters of the n-th equation of motion, the control law that ensures the asymptotical stability of the corresponding error dynamics is then developed. First, the uncertain parameters existing in the equation of motion of the last joint are estimated and secondly, the control law is developed by using these estimated parameters. After that, we go backward to the (n-1)-th joint and apply the same strategy. Note that the parameters of the (n-1)-th joint depend on both the n-th and the (n-1)-th joints. Therefore, these uncertain parameters are decomposed into two parts: the first part has the uncertain parameters which were estimated in the previous step, and the second part has the new parameters that depend only on the (n-1)-th joint. The control law is then derived using the previous estimated parameters (n-th joint) and the new ones ((n-1)-th joint). The control of the remaining joints is developed using the same hierarchical strategy. This strategy is presented in Figure 3.4.

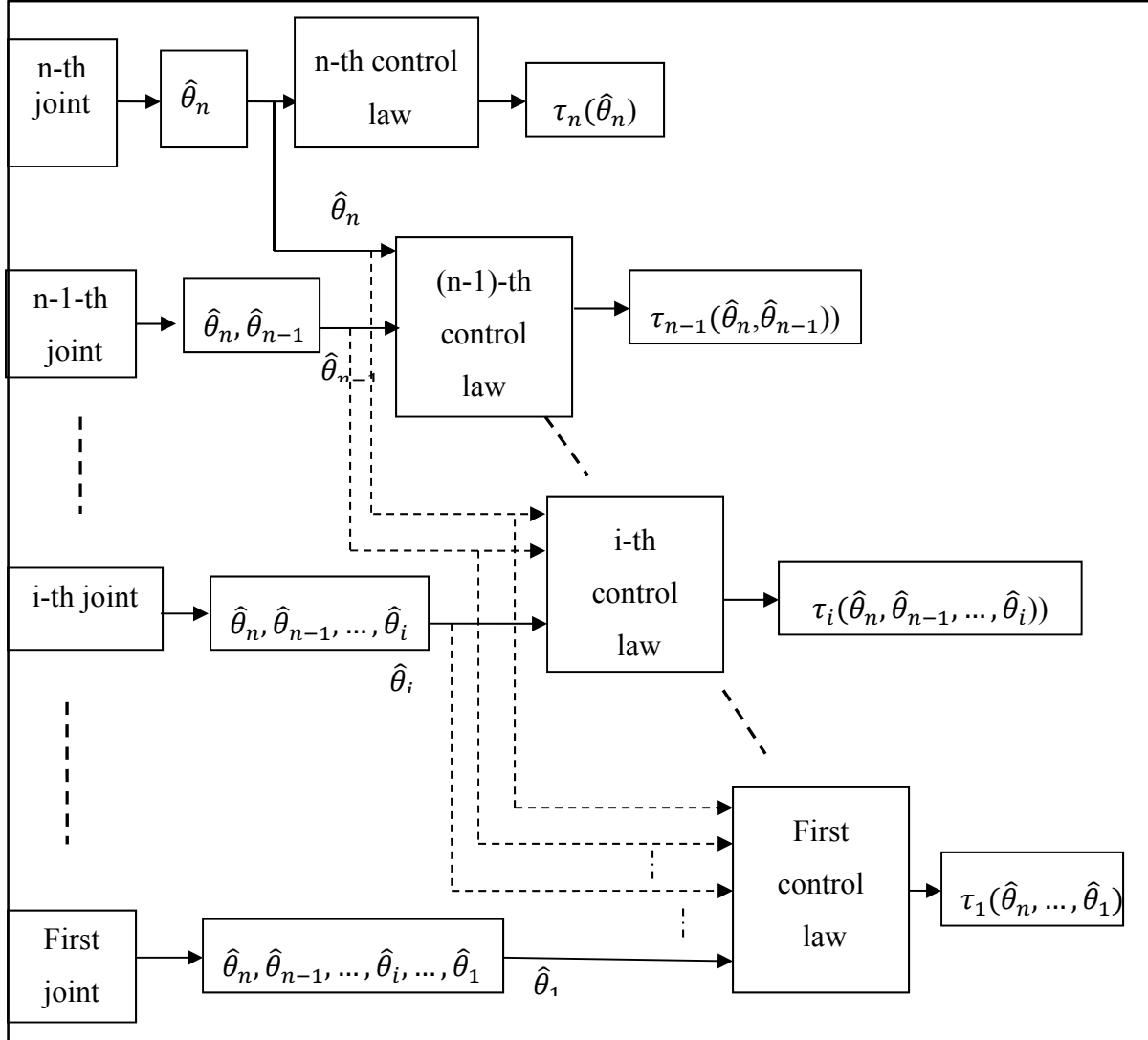


Figure 3.4 Hierarchical adaptive control strategy.

For the n -th joint, the equation of motion is given by (3.8). There exists a vector $\theta_n \in \mathcal{R}^{r_n}$ with components depending on the manipulator's parameters (masses, moments of inertia, etc.), such as:

$$\phi_n(Q_n, \dot{Q}_n, \ddot{Q}_n^*)\theta_n = M_n^T(Q_n)\ddot{Q}_n^* + C_n^T(Q_n, \dot{Q}_n)\dot{Q}_{nd} + G_n(Q_n) \quad (3.31)$$

where $\phi_n(1 \times r_n)$ is a regression matrix which contains all known functions.

The adaptive control law is proposed as follows:

$$\tau_n = K_{pn}\tilde{q}_n + K_{dn}\dot{\tilde{q}}_n + \emptyset_n(Q_n, \dot{Q}_n, \ddot{Q}_n^*)\hat{\alpha}_n - \delta\tau_n \quad (3.32)$$

where K_{pn}, K_{dn} are positive gains, $\gamma_n = \frac{K_{pn}}{K_{dn}}$, and $\hat{\alpha}_n = \hat{\theta}_n$. $\delta\tau_n$ is given in (3.12).

The adaptive law is given by:

$$\dot{\hat{\alpha}}_n = \mu_n \emptyset_n^T(Q_n, \dot{Q}_n, \ddot{Q}_n^*) \cdot \dot{\tilde{q}}_n \quad (3.33)$$

The error of the parameters vector is given by:

$$\tilde{\alpha}_n = \hat{\alpha}_n - \alpha_n \quad (3.34)$$

Using (3.31) and (3.34), we can write:

$$\emptyset_n \hat{\alpha}_n = \emptyset_n \tilde{\alpha}_n + M_n^T(Q_n) \ddot{Q}_n^* + C_n^T(Q_n, \dot{Q}_n) \dot{Q}_{nd} + G_n(Q_n) \quad (3.35)$$

The same strategy is applied backward from the (n-1)-th joint until the first joint. For the i-th joint, for which the equation of motion is given by (3.17), there exists a vector of uncertain parameters $\theta_i \in \mathcal{R}^{r_i}$ and a regression matrix $\emptyset_i(Q_i, \dot{Q}_i, \ddot{Q}_i^*) \in \mathcal{R}^{r_i}$ such as:

$$\emptyset_i(Q_i, \dot{Q}_i, \ddot{Q}_i^*)\theta_i = M_i(Q_i) \ddot{Q}_i^* + C_i(Q_i, \dot{Q}_i) \dot{Q}_{id} + G_i(Q_i) \quad (3.36)$$

The i-th control law is given by:

$$\tau_i = K_{pi}\tilde{q}_i + K_{di}\dot{\tilde{q}}_i + \emptyset_i(Q_i, \dot{Q}_i, \ddot{Q}_i^*)\hat{\alpha}_i - \delta\tau_i \quad (3.37)$$

where $\hat{\alpha}_i = [\hat{\theta}_i \quad \hat{\alpha}_{i+1}]^T$; $\hat{\alpha}_{i-1} = [\hat{\theta}_{i-1} \quad \hat{\alpha}_i]^T$, etc...

The adaptive law is:

$$\dot{\hat{\alpha}}_i = \mu_i \phi_i^T(Q_i, \dot{Q}_i, \ddot{Q}_i^*) \tilde{q}_i \quad (3.38)$$

To prove the global asymptotical stability, we use the n control laws (3.37) and the equation of motion (3.1). The n control laws can be written as follows:

$$\tau = K_p \tilde{q} + K_d \dot{\tilde{q}} + \phi(Q, \dot{Q}, \ddot{Q}^*) \hat{\alpha} - \delta \tau \quad (3.39)$$

where

$$Q = [Q_1^T \dots Q_n^T]^T_{n^2 \times 1}; \ddot{Q}^* = [\ddot{Q}_1^* \dots \ddot{Q}_n^*]^T_{n^2 \times 1}; Q_i, \ddot{Q}_i^* \text{ and } \ddot{q}_i^* \text{ are given in (3.18-3.20).}$$

$$K_p = \text{diag}(K_{pi})_{n \times n}; K_d = \text{diag}(K_{di})_{n \times n}; \gamma = \text{diag}(\gamma_i)_{n \times n}$$

$$\phi = \begin{bmatrix} (\phi_1)_{1 \times r_1} & 0_{1 \times \sum_{j=2}^n r_j} \\ 0_{1 \times r_1} & (\phi_2)_{1 \times r_2} 0_{1 \times \sum_{j=3}^n r_j} \\ \vdots & \vdots \\ 0_{1 \times \sum_{j=1}^{i-1} r_j} & (\phi_i)_{1 \times r_i} 0_{1 \times \sum_{j=i+1}^n r_j} \\ \vdots & \vdots \\ 0_{1 \times \sum_{j=1}^{n-1} r_j} & (\phi_n)_{1 \times r_n} \end{bmatrix}_{n \times r} = \text{diag}(\phi_1, \phi_2, \dots, \phi_n); \alpha = \begin{bmatrix} \alpha_1 \\ \alpha_2 \\ \vdots \\ \alpha_i \\ \vdots \\ \alpha_n \end{bmatrix}_{r \times 1}; r = \sum_{j=1}^n r_j$$

To study the global asymptotical stability we insert (3.39) in (3.1). Then, the error dynamics is given as follows:

$$K_p \tilde{q} + K_d \dot{\tilde{q}} - M(q) \ddot{q} - C(q, \dot{q}) \dot{q} - G(q) + \phi(Q, \dot{Q}, \ddot{Q}^*) \hat{\alpha} - \delta \tau = 0 \quad (3.40)$$

where

$$\dot{\hat{\alpha}} = \mu \phi^T(Q, \dot{Q}, \ddot{Q}^*) \tilde{q} \quad (3.41)$$

$\mu = \text{diag}(\mu_i)_{r \times r}$ is a positive definite matrix.

The parameters error vector is given by:

$$\tilde{\alpha} = \hat{\alpha} - \alpha \quad (3.42)$$

Then, we can write:

$$\emptyset\hat{\alpha} = \emptyset\tilde{\alpha} + M(Q)\ddot{Q}^* + C(Q, \dot{Q})\dot{Q}_d + G(Q) \quad (3.43)$$

Using (3.43), the error dynamics can be written as follows:

$$\begin{aligned} K_p\tilde{q} + K_d\tilde{\dot{q}} + (M(Q)\ddot{Q}^* - M(q)\ddot{q}) + (C(Q, \dot{Q})\dot{Q}_d - C(q, \dot{q})\dot{q}) + (G(Q) - G(q)) \\ - \delta\tau + \emptyset\tilde{\alpha} = 0 \end{aligned} \quad (3.44)$$

Using Proposition 3.1, the error dynamics can be simplified as follows:

$$M(q)\ddot{\tilde{q}} + C(q, \dot{q})\dot{\tilde{q}} + K_d\tilde{\dot{q}} + \gamma M_{diag}(q)\tilde{q} + K_p\tilde{q} + \emptyset\tilde{\alpha} = 0 \quad (3.45)$$

Proposition 3.2

Using the control law (3.39), the error dynamics (3.45) is globally asymptotically stable.

To prove the above proposition, we propose the following Lyapunov function:

$$V = \frac{1}{2}\tilde{q}^T M(q)\tilde{q} + \frac{1}{2}\tilde{q}^T K_p\tilde{q} + \frac{1}{2}\tilde{\alpha}^T \mu^{-1}\tilde{\alpha} \quad (3.46)$$

Taking the time derivative of $V(t)$, we get

$$\begin{aligned} \dot{V}(t) &= \dot{\tilde{q}}^T M(q)\tilde{q} + \frac{1}{2}\dot{\tilde{q}}^T M(q)\dot{\tilde{q}} + \tilde{q}^T \gamma K_d\tilde{\dot{q}} + \tilde{\alpha}^T \mu^{-1}\dot{\tilde{\alpha}} \\ &= \dot{\tilde{q}}^T (-C(q, \dot{q})\tilde{q} - K_d\tilde{\dot{q}} - \gamma(M_{diag}(q)\tilde{q} + K_d\tilde{q}) - \emptyset\tilde{\alpha}) + \frac{1}{2}\dot{\tilde{q}}^T M(q)\dot{\tilde{q}} + \tilde{q}^T \gamma K_d\tilde{\dot{q}} + \\ &\quad \dot{\tilde{\alpha}}^T \mu^{-1}\tilde{\alpha} = -\dot{\tilde{q}}^T (K_d + \gamma M_{diag}(q))\tilde{\dot{q}} + (\dot{\tilde{\alpha}}^T \mu^{-1}\tilde{\alpha} - \dot{\tilde{q}}^T \emptyset\tilde{\alpha}) \end{aligned}$$

Using (3.41), the time derivative of $V(t)$ is:

$$\dot{V}(t) = -\dot{\tilde{q}}^T (K_d + \gamma M_{diag}(q))\tilde{\dot{q}} + ((\mu\emptyset^T \dot{\tilde{q}})^T \mu^{-1} - \dot{\tilde{q}}^T \emptyset)\tilde{\alpha}$$

Then,

$$\dot{V}(t) = -\dot{\tilde{q}}^T \left(K_d + \gamma M_{diag}(q) \right) \dot{\tilde{q}} \quad (3.47)$$

K_d, γ and $M_{diag}(q)$ are positive definite diagonal matrices. Then using Barbalat lemma, the error dynamics is globally asymptotically stable.

3.5 Experimental Results

In this section, the control strategies presented in the previous sections are tested on the ANAT robot (Figure 3.1). The Denavit-Hartenberg parameters of the ANAT robot are given in Table 3.1.

Table 3.1 Denavit-Hartenberg parameters of ANAT robot
Tiré de (Le Boudec, Saad et Nerguizian, 2006)

Joint	α_{i-1}	a_{i-1}	d_i	q_i
1	0	0	d_1	0
2	0	L_1	0	θ_2
3	0	L	0	θ_3
4	0	L	0	θ_4
5	0	L	L_2	θ_5
6	$\pi/2$	L_3	0	θ_6
7	$-\pi/2$	0	$-L_4$	θ_7

For a redundant robot, the velocities in the workspace and the joint space are linked by generalized inverse Jacobean:

$$\dot{q} = J^T (JJ^T)^{-1} v \quad (3.48)$$

where J is the Jacobean matrix, \dot{q} is the joint space velocity vector and v is the workspace velocity vector. The position q is obtained by a simple integrator.

The relation between the position of the tool and the base reference is given in (Le Boudec, Saad et Nerguizian, 2006) as follows:

$$\begin{bmatrix} x \\ y \\ z \end{bmatrix} = \begin{bmatrix} L_4 c_{2345} s_6 + L_3 c_{2345} + L[c_{234} + c_{23} + c_2] + L_1 \\ L_4 s_{2345} s_6 + L_3 s_{2345} + L[s_{234} + s_{23} + s_2] \\ -L_4 c_6 + L_2 + q_1 \end{bmatrix} \quad (3.49)$$

where $s_i = \sin(q_i)$, $c_i = \cos(q_i)$, $s_{ij} = \sin(q_i + q_j)$, and $c_{ij} = \cos(q_i + q_j)$.

For real-time implementation of the proposed controllers, Simulink with Real-Time Workshop (RTW) of Mathworks® is used. The real-time setup is given in Figure 3.5. The National Instruments PCI 6024E digital card and ATMEGA 16 microcontrollers are chosen for the real-time target and the translation of information to serial peripheral interface (SPI). In the first step, the workspace desired trajectory is transformed to joint space using inverse kinematics. Then, the hierarchical control algorithm is derived from the joint space's desired trajectory and their real values given by the microcontrollers. The torque input provided by the control algorithm is sent to the microcontrollers which translates the control signal into a pulse width modulation (PWM) signal. The latter is applied to the H-bridge drive of the actuators of the ANAT robot. A current sensor located in the H-bridge drive measures the current of each actuator. After receipt of the digital information of the actuators' encoders, the microcontrollers send the angles' positions to Simulink.

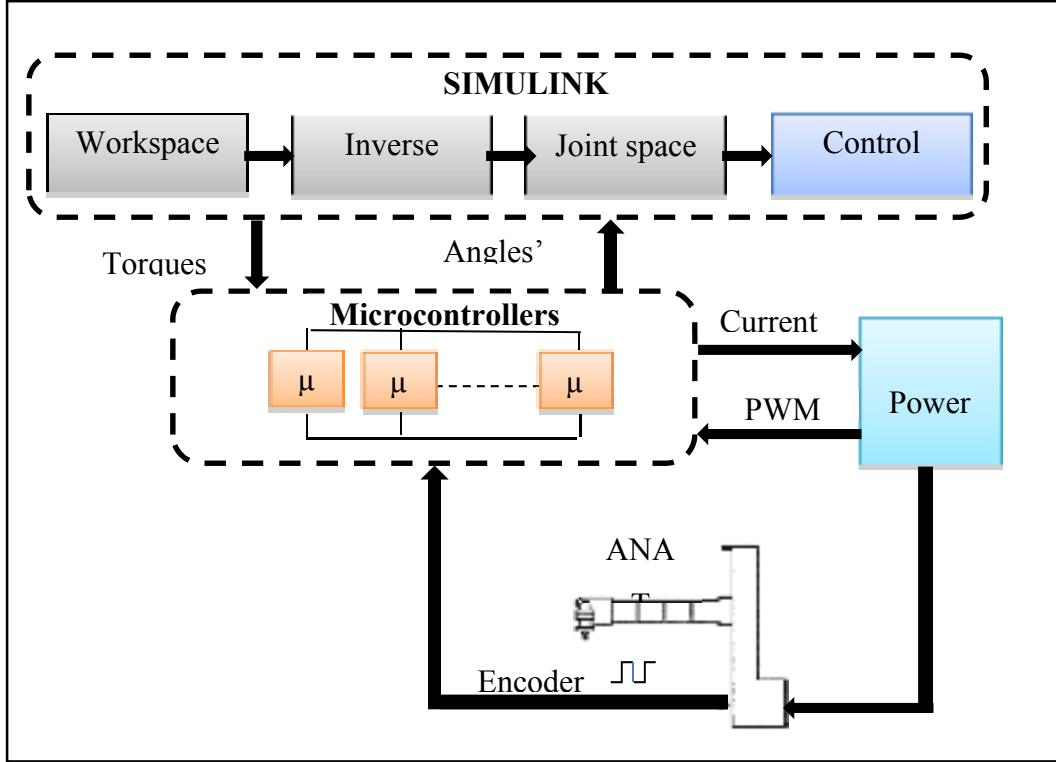


Figure 3.5 Real-time setup.

For this implementation, the first, sixth and seventh joints are locked and joints 2, 3, 4, and 5 are used. The controller's gains are chosen using a trial and error method as follows:

For the non-adaptive hierarchical control strategy, the selected gains are: $K_{p2} = 25, K_{p3} = 20, K_{p4} = 10, K_{p5} = 10; K_{d2} = 1.85, K_{d3} = 2, K_{d4} = 10, K_{d5} = 10$. For the adaptive hierarchical control strategy, the selected gains are: $K_{p2} = 30, K_{p3} = 25, K_{p4} = 12, K_{p5} = 12; K_{d2} = 2.5, K_{d3} = 2.5, K_{d4} = 12, K_{d5} = 12$. $\mu_i = \text{diag}(10), i=2 \dots 5$.

For an i -th joint, the previous theoretical development of the control law is given in the general case. For simplicity of real-time implementation, a finite order of Taylor series is fixed. In this section, and, the the Taylor series is limited to the first order. Then, $R_{M_{nj}} = R_{C_{nj}} = R_{G_n} = 0$.

For the adaptive hierarchical control; the uncertain parameters are chosen as follows:

For last joint: $\alpha_5 = \theta_5 = [m_5 L^2 \quad I_{z5}]^T$; τ_5 is developed using $\hat{\theta}_5$.

For the fourth joint: $\alpha_4 = [\theta_4 \quad \alpha_5]^T$; $\theta_4 = [m_4L^2 \quad I_{z4}]^T$; τ_4 is developed using $\hat{\theta}_5$ and $\hat{\theta}_4$.

For the third joint: $\alpha_3 = [\theta_3 \quad \alpha_4]^T$; $\theta_3 = [m_3L^2 \quad I_{z3}]^T$; τ_3 is developed by using $\hat{\theta}_5, \hat{\theta}_4$ and $\hat{\theta}_3$.

For the second joint: $\alpha_2 = [\theta_2 \quad \alpha_3]^T$; $\theta_2 = [m_2L^2 \quad I_{z2}]^T$; τ_2 is developed by using $\hat{\theta}_5, \hat{\theta}_4, \hat{\theta}_3$ and $\hat{\theta}_2$.

The experimental results for the non-adaptive hierarchical control are shown in Figures 3.6-3.8.

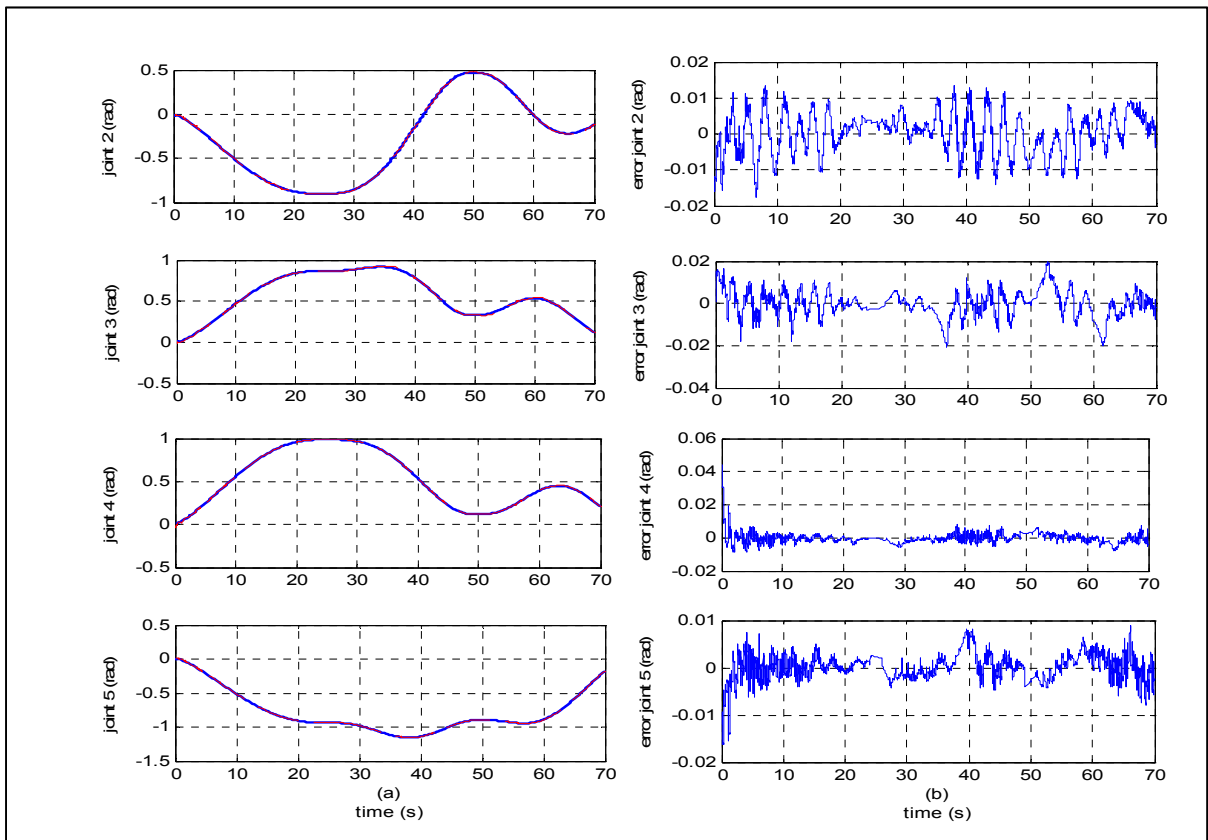


Figure 3.6 Hierarchical control: (a) Joint space tracking, (b) Tracking errors.

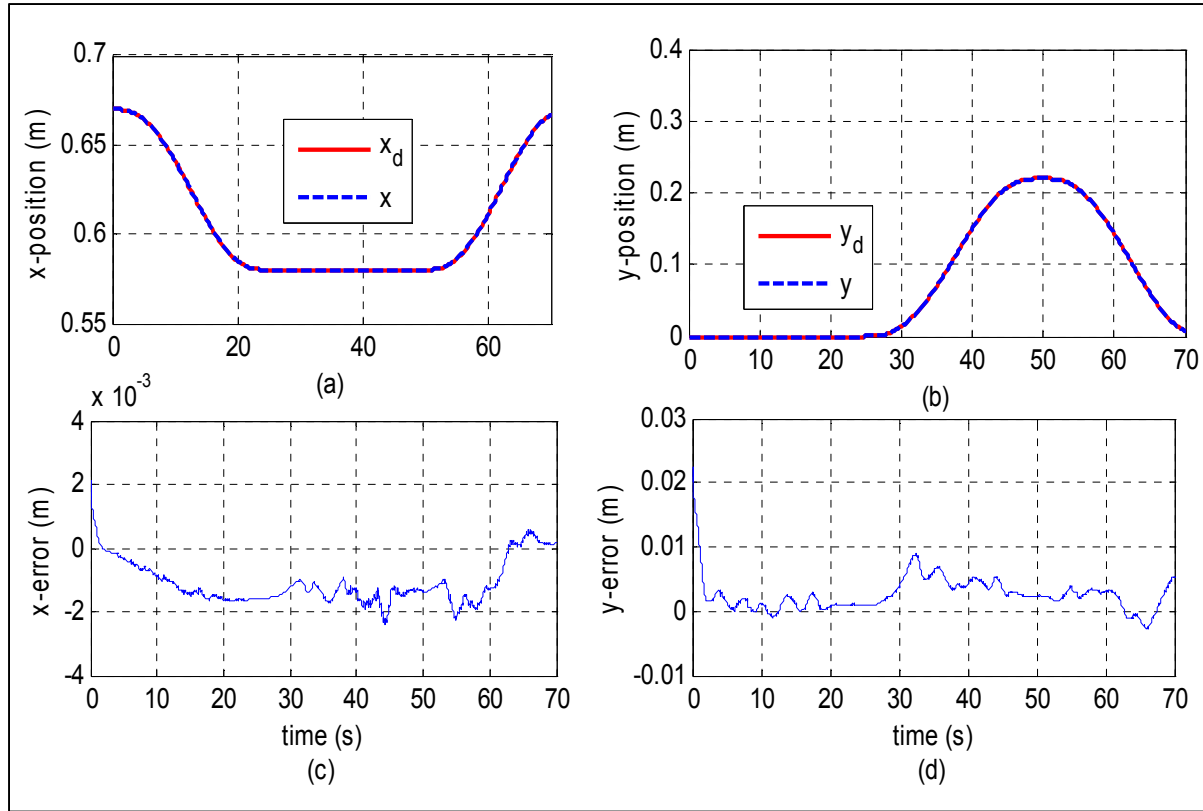


Figure 3.7 Hierarchical control: (a) Workspace tracking and
(b) Workspace tracking error.

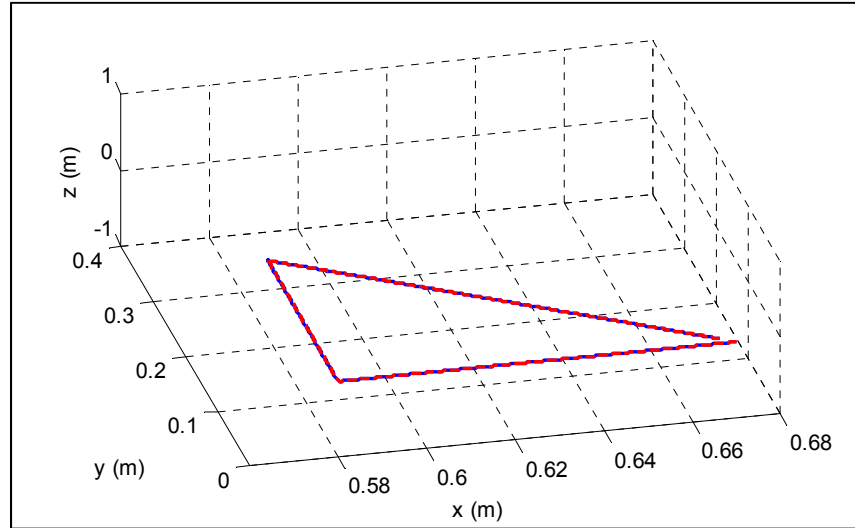


Figure 3.8 Hierarchical control: Workspace tracking.

For the adaptive hierarchical control, the experimental results are given in Figures 9-10.

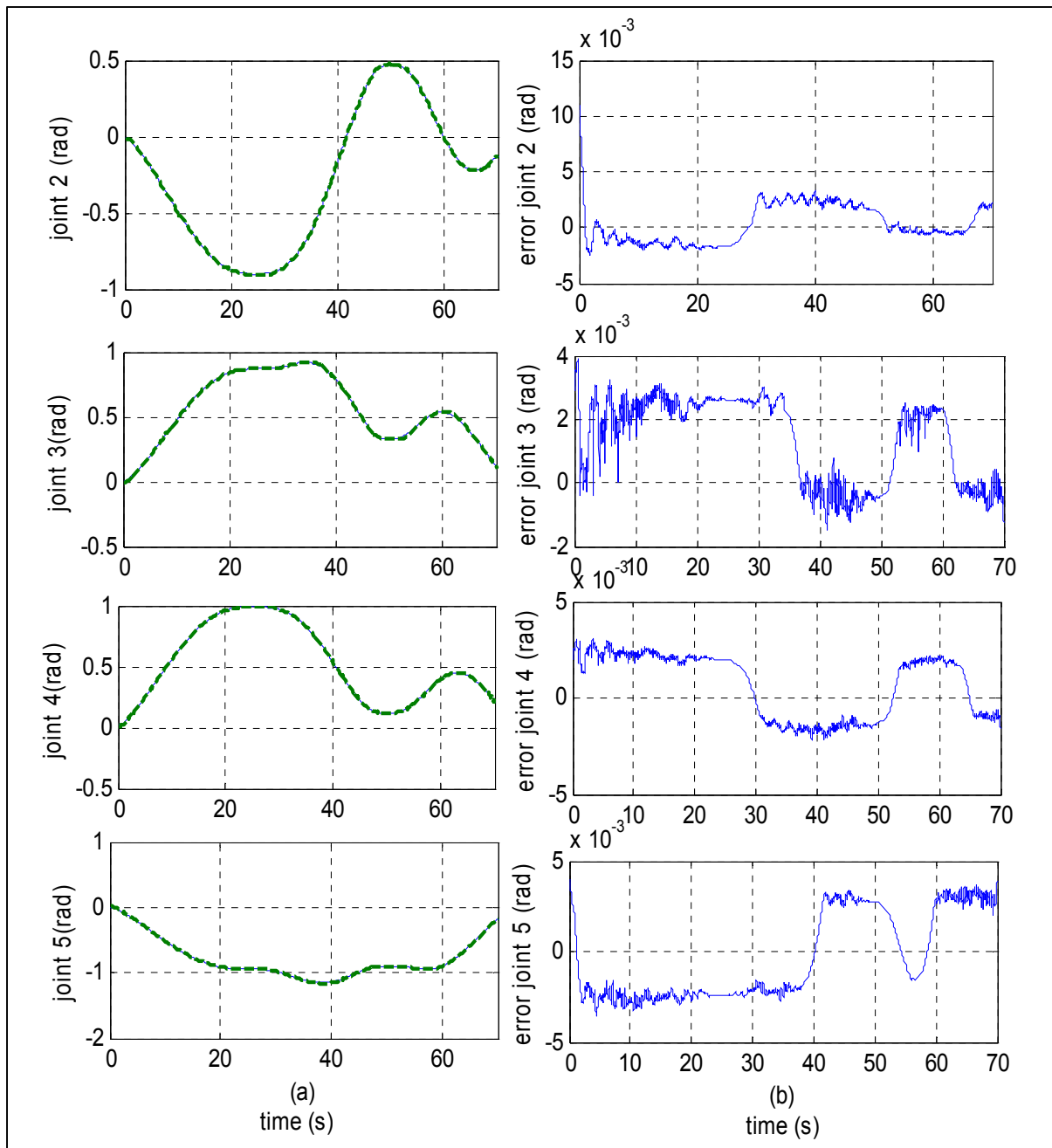


Figure 3.9 Hierarchical adaptive control: (a) Joint space tracking, (b) Tracking errors.

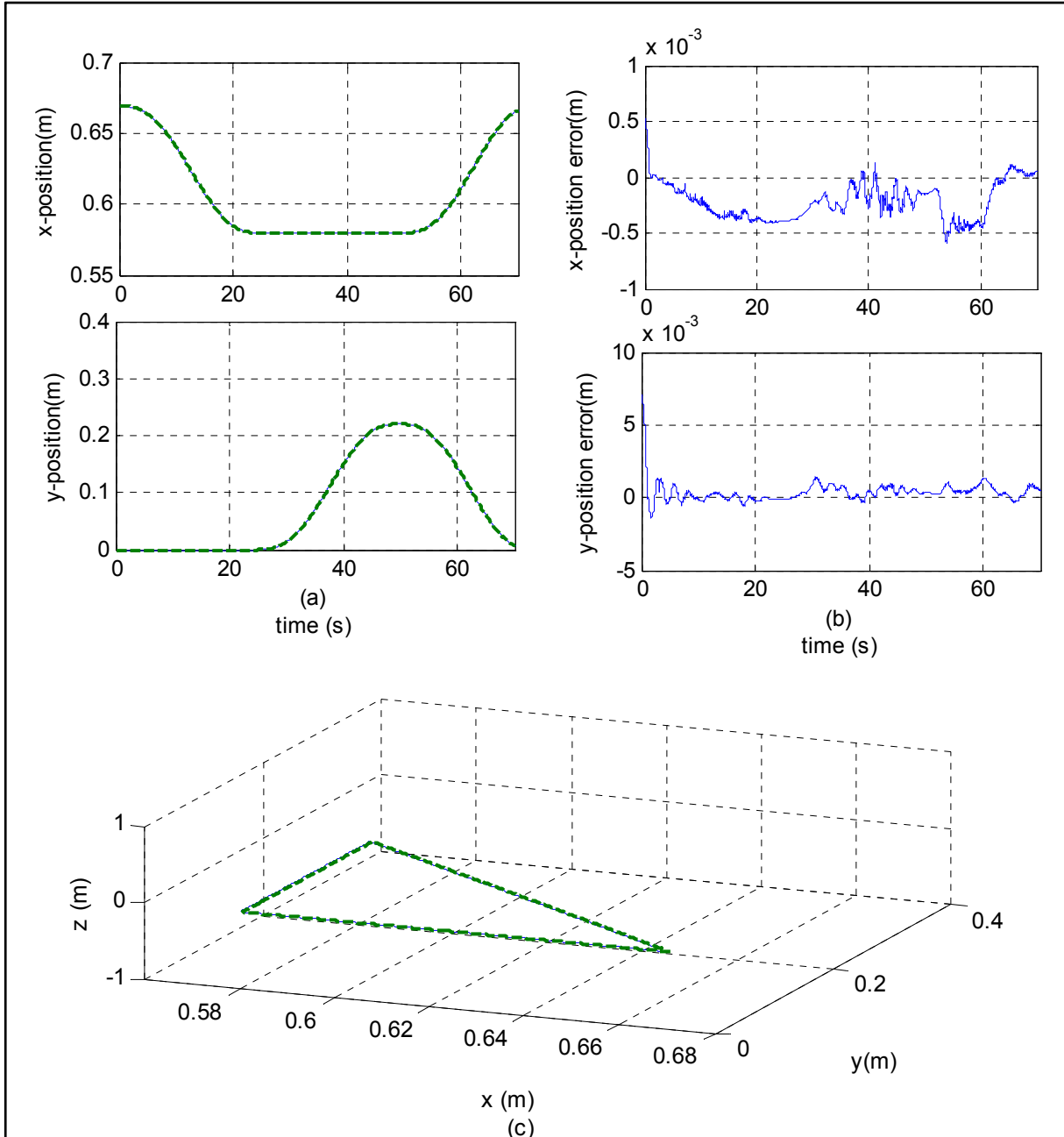


Figure 3.10 Hierarchical adaptive control: (a) x and y position tracking,
 (b) tracking errors of x and y, (c) xyz workspace tracking.

The computed torque approach (Slotine et Li, 1991) is used for the ANAT robot for comparison with the previous controllers. Using the same desired trajectory, the experimental results for the computed torque approach are shown in Figure 3.11.

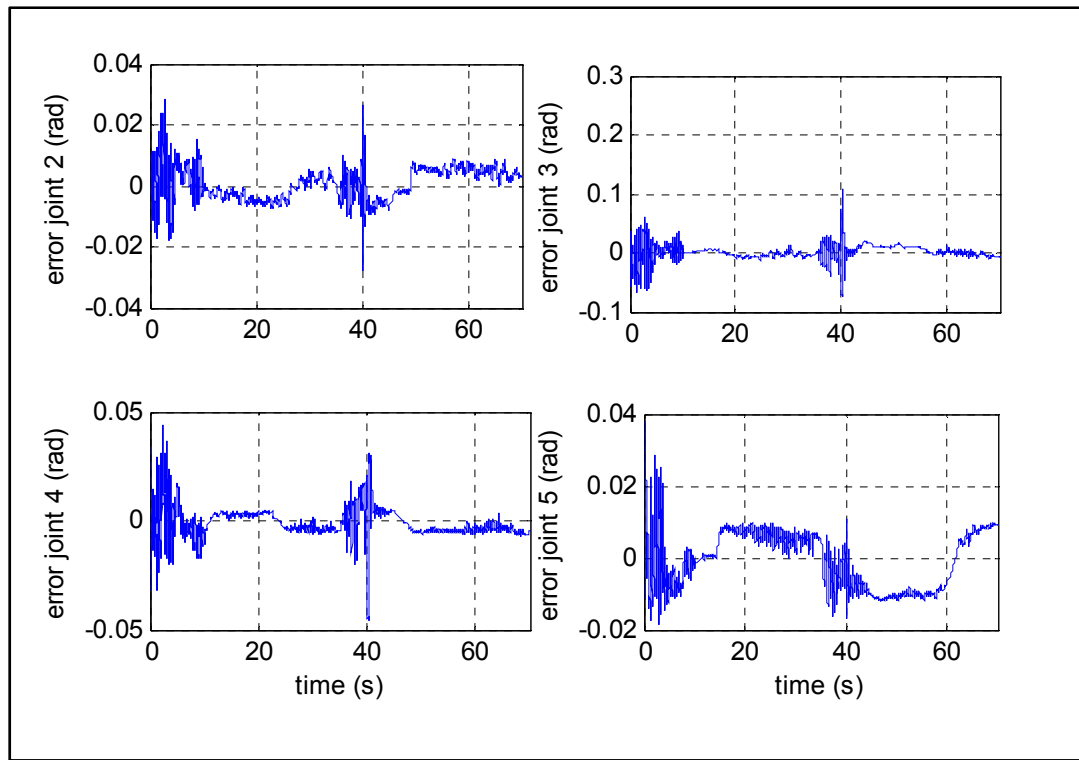


Figure 3.11 Tracking errors in joint space for the computed torque method.

For the hierarchical control strategy, Figure 3.6-(a) presents the tracking trajectories of the second, third, fourth and fifth joints. Good tracking is obtained in the joint space and is confirmed in Figure 3.6-(b), which shows the tracking errors in the joint space. However, the objective of this work is the tracking in the workspace. Using direct kinematics, good tracking of $x(t)$ and $y(t)$ trajectories in the workspace is shown in Figure 3.7. The tracking errors presented in Figures 3.6-3.7 show a small error in the joint space and workspace. Finally, Figure 3.8 shows good tracking in x-y-z workspace.

For the hierarchical adaptive control, using the inverse kinematics, the workspace desired trajectory is transformed to the joint space. The tracking trajectory and the tracking error in the joint space are shown in Figure 3.9. Using direct kinematics, the tracking trajectory and the error of the tracking are shown in Figure 3.10. Good tracking is obtained in the joint space (less than 0.02 rad) and the workspace (less than 5mm for $x(t)$ and 10 mm for $y(t)$).

For the same desired trajectory, the computed torque approach is used and the tracking error in the joint space is shown in Figure 3.11. According to the experimental results the resulting tracking errors of the hierarchical approach (non-adaptive and adaptive controller) are smaller than those found in the computed torque method. This illustrates the effectiveness of the proposed approaches.

3.6 Conclusion

In this paper, a novel hierarchical adaptive control strategy is proposed for rigid manipulators to track a desired trajectory in the workspace. Two nonlinear control strategies are presented. In the first, the system parameters are perfectly known and a hierarchical control is derived. The hierarchical control strategy consists in starting by controlling the last joint while assuming that the remaining joints are stable. Then, we follow the same strategy backward until the first joint. The second control strategy presents the adaptive version of the hierarchical control strategy. Lyapunov theory is used for global stability analysis of the feedback system. These controllers are tested and compared with the computed torque approach on a 7-DOF hyper redundant articulated nimble adaptable trunk (ANAT) robot to track a desired trajectory in the workspace. The effectiveness of the proposed hierarchical control strategy is shown by the experimental results, which demonstrate good tracking in the workspace.

3.7 Appendix

Proof of proposition 3.1:

To prove proposition 3.1, we need to investigate the following elements of the error dynamics (3.27): $(\bar{M}(Q)\ddot{Q}^* - M(q)\ddot{q})$, $(\bar{C}(Q, \dot{Q})\dot{Q}_d - C(q, \dot{q})\dot{q})$ and $(G(Q) - G(q))$.

The first element can be written as follows:

$$\bar{M}(Q)\ddot{Q}^* - M(q)\ddot{q} = \begin{bmatrix} M_1^T(Q_1)\ddot{Q}_1^* - M_1^T(q)\ddot{q} \\ \vdots \\ M_n^T(Q_n)\ddot{Q}_n^* - M_n^T(q)\ddot{q} \end{bmatrix} \quad (3.50)$$

where M_i^T and \ddot{Q}_i^* are given in (3.17) and (3.20).

The i-th term of (3.50) can be written as:

$$M_i^T(Q_i)\ddot{Q}_i^* - M_i^T(q)\ddot{q} = M_{ii}(Q_i)\ddot{q}_i^* - M_{ii}(q)\ddot{q}_i + \sum_{\substack{j=1 \\ j \neq i}}^n (M_{ij}(Q_i)\ddot{q}_{jd} - M_{ij}(q)\ddot{q}_j) \quad (3.51)$$

Using Taylor series, we can write:

$$M_{ij}(q) = M_{ij}(Q_i) + DM_{ij}(Q_i)^T(q - Q_i) + \frac{1}{2!}(q - Q_i)^T\{D^2M_{ij}(Q_i)\}(q - Q_i) + \dots$$

where $DM_{ij}(Q_i)$ is the gradient of M_{ij} evaluated at $q = Q_i$. Then, we can write:

$$\begin{aligned} M_{ij}(q) &= M_{ij}(Q_i) + \frac{\partial M_{ij}(q)}{\partial [q_1 \dots q_{i-1} q_{i+1} \dots q_n]} \begin{bmatrix} q_1 - q_{1d} \\ \vdots \\ q_{i-1} - q_{(i-1)d} \\ q_{i+1} - q_{(i+1)d} \\ \vdots \\ q_n - q_{nd} \end{bmatrix} + R_{M_{ij}}(\tilde{q}_j) \\ &= M_{ij}(Q_i) - \sum_{\substack{j=1 \\ j \neq i}}^n \frac{\partial M_{ij}(q)}{\partial q_j} \Big|_{q_{jd}} \tilde{q}_j + R_{M_{ij}}(\tilde{q}_j) \end{aligned}$$

$$= M_{ij}(Q_i) - \delta M_{ij}$$

where $\delta M_{ij} = \sum_{j=1}^n \frac{\partial M_{ij}(q)}{\partial q_j} \Big|_{q_{jd}} \tilde{q}_j - R_{M_{ij}}(\tilde{q}_j)$ and $R_{M_{ij}}$ is the remaining terms. Then,

$$M_{ij}(Q_i) = M_{ij}(q) + \delta M_{ij} \quad (3.52)$$

Inserting (3.52) into (3.51), we get:

$$\begin{aligned} M_{ii}(Q_i)\ddot{q}_i^* - M_{ii}(q)\ddot{q}_i + \sum_{\substack{j=1 \\ j \neq i}}^n (M_{ij}(Q_i)\ddot{q}_{jd} - M_{ij}(q)\ddot{q}_j) &= \\ M_{ii}(q)\ddot{q}_i^* - M_{ii}(q)\ddot{q}_i + \delta M_{ii}\ddot{q}_i^* + \sum_{\substack{j=1 \\ j \neq i}}^n (M_{ij}(q)\ddot{q}_{jd} - M_{ij}(q)\ddot{q}_j + \delta M_{ij}\ddot{q}_{jd}) & \quad (3.53) \\ &= M_{ii}(q)\dot{S}_i + \delta M_{ii}\ddot{q}_i^* + \sum_{\substack{j=1 \\ j \neq i}}^n (M_{ij}(q)\ddot{q}_j + \delta M_{ij}\ddot{q}_{jd}) \end{aligned}$$

where $\dot{S}_i = \ddot{q}_i + \gamma_n \tilde{q}_i = \ddot{q}_i^* - \ddot{q}_i$; \ddot{q}_i^* is given under (3.19).

Using (3.53), (3.50) is rewritten as:

$$\begin{aligned} \overline{M}(Q)\ddot{Q}^* - M(q)\ddot{q} &= \begin{bmatrix} M_{11}(q) & 0 & \cdots & 0 \\ 0 & M_{ii}(q) & & \vdots \\ \vdots & & 0 & \\ 0 & \cdots & 0 & M_{nn}(q) \end{bmatrix} \begin{bmatrix} \dot{S}_1 \\ \vdots \\ \dot{S}_n \end{bmatrix} + \\ \begin{bmatrix} 0 & M_{12}(q) \cdots & M_{1n}(q) \\ M_{21}(q) & 0 & \vdots \\ \vdots & & M_{(n-1)n}(q) \\ M_{n1}(q) & \cdots & M_{n(n-1)}(q) \end{bmatrix} \begin{bmatrix} \ddot{q}_1 \\ \vdots \\ \ddot{q}_n \end{bmatrix} + \begin{bmatrix} \delta M_{11}\ddot{q}_1^* \\ \vdots \\ \delta M_{nn}\ddot{q}_n^* \end{bmatrix} + \begin{bmatrix} \sum_{j=1}^n \delta M_{1j}\ddot{q}_{jd} \\ \vdots \\ \sum_{j=1}^n \delta M_{nj}\ddot{q}_{jd} \end{bmatrix} \end{aligned}$$

In a compact form:

$$\bar{M}(Q)\ddot{Q}^* - M(q)\ddot{q} = M_{diag}(q)\dot{S} + M_{ndiag}(q)\ddot{\tilde{q}} + \delta M_{diag}\ddot{q}^* + \delta M_{ndiag}\ddot{q}_d \quad (3.54)$$

where M_{diag} and δM_{diag} are the diagonal matrices of M and δM ; M_{ndiag} and δM_{ndiag} are the non-diagonal matrices of M and δM , respectively. Then $M_{diag} + M_{ndiag} = M$ and $\delta M_{diag} + \delta M_{ndiag} = \delta M$.

Using the same strategy, the second term is:

$$\begin{aligned} \bar{C}(Q, \dot{Q})\dot{Q}_d - C(q, \dot{q})\dot{q} &= \begin{bmatrix} C_1^T(Q_1, \dot{Q}_1)\dot{Q}_{1d} - C_1^T(q, \dot{q})\dot{q} \\ \vdots \\ C_n^T(Q_n, \dot{Q}_n)\dot{Q}_{nd} - C_n^T(q, \dot{q})\dot{q} \end{bmatrix} \\ &= \begin{bmatrix} C_{11}(q, \dot{q}) & \cdots & C_{1n}(q, \dot{q}) \\ \vdots & \ddots & \vdots \\ C_{n1}(q, \dot{q}) & \cdots & C_{nn}(q, \dot{q}) \end{bmatrix} \begin{bmatrix} \dot{\tilde{q}}_1 \\ \vdots \\ \dot{\tilde{q}}_n \end{bmatrix} + \begin{bmatrix} \delta C_{11} & \cdots & \delta C_{1n} \\ \vdots & \ddots & \vdots \\ \delta C_{n1} & \cdots & \delta C_{nn} \end{bmatrix} \begin{bmatrix} \dot{q}_{1d} \\ \vdots \\ \dot{q}_{nd} \end{bmatrix} \end{aligned}$$

where $\dot{Q}_d = [\dot{q}_{1d} \cdots \dot{q}_{nd}]$.

$$\bar{C}(Q, \dot{Q})\dot{Q}_d - C(q, \dot{q})\dot{q} = C(q, \dot{q})\dot{\tilde{q}} + \delta C\dot{q}_d \quad (3.55)$$

By following the same strategy, the third term is given as follows:

$$G(Q) - G(q) = \delta G \quad (3.56)$$

Then, the error dynamics (3.27) can be written as:

$$\begin{aligned} K_p\tilde{q} + K_d\dot{\tilde{q}} + (M_{diag}(q)\dot{S} + M_{ndiag}(q)\ddot{\tilde{q}} + \delta M_{diag}\ddot{q}^* + \delta M_{ndiag}\ddot{q}_d) \\ + (C(q, \dot{q})\dot{\tilde{q}} + \delta C\dot{q}_d) + \delta G - \delta \tau = 0 \end{aligned} \quad (3.57)$$

Using (3.26), the error dynamics is:

$$K_p \tilde{q} + K_d \dot{\tilde{q}} + M_{diag}(q) \dot{S} + M_{ndiag}(q) \ddot{\tilde{q}} + C(q, \dot{q}) \dot{\tilde{q}} = 0 \quad (3.59)$$

Using $\dot{S} = \ddot{\tilde{q}} + \gamma \dot{\tilde{q}}$, $M_{diag} + M_{ndiag} = M$, the error dynamics becomes:

$$M(q) \ddot{\tilde{q}} + C(q, \dot{q}) \dot{\tilde{q}} + K_d \dot{\tilde{q}} + \gamma M_{diag}(q) \dot{\tilde{q}} + K_p \tilde{q} = 0 \quad (3.60)$$

CHAPITRE 4

ARTICLE 3: DISTRIBUTED CONTROL STRATEGY FOR FLEXIBLE LINK MANIPULATORS

Fareh Raouf¹ Saad Mohamad² and Saad Maarouf¹

¹Electrical Engineering Department, Université du Québec, École de technologie supérieure,
1100, rue Notre-Dame ouest, Montréal (Québec), H3C 1K3, Canada

²School of Engineering, Université du Québec en Abitibi-Témiscamingue, 445, boul. de
l'Université, Rouyn-Noranda (Québec), J9X 5E4

Article soumis à la revue « Robotica » en Février 2013.

Abstract

This paper presents a nonlinear distributed control strategy for flexible-link manipulators to solve the tracking control problem in the joint space and cancel vibrations of the links. First, the dynamic of an n-flexible-link manipulator is decomposed into n subsystems. Each subsystem has a pair of one joint and one link. The distributed control strategy is applied to each subsystem starting from the last subsystem. The strategy of control consists in controlling the n^{th} joint and stabilizing the n^{th} link by assuming that the remaining subsystems are stable. Then, going backward to the $(n-1)^{\text{th}}$ subsystem, the same control strategy is applied to each corresponding joint-link subsystem until the first. Sliding mode technique is used to develop the control law of each subsystem and the global stability of the resulting tracking errors is proved using Lyapunov technique. This algorithm was tested on a two-flexible-link manipulator and gave effective results, a good tracking performance, and capability to eliminate the links' vibrations.

Key Words: Distributed control, flexible-link manipulators, sliding mode, stability, tracking trajectories.

4.1 Introduction

There are many advantages of using manipulators with thin and lightweight links in contrast to traditional rigid manipulators. Indeed, flexible-link manipulators have faster response time, lower energy consumption, lower overall mass, low-rated actuators, and, in general, lower overall cost. Due to links' flexibility, the dynamical model of flexible-link manipulators is much more complicated than that of rigid manipulators. As a result of this complicated dynamic model, several challenges in the design and implementation of controllers were motivated. Indeed, the number of controlled variables for a flexible-link manipulator is strictly less than the number of mechanical degrees of freedom, i.e. it represents an underactuated system. In this case, the control problem is twofold: in addition to motion objectives as in a rigid manipulator, it must also stabilize the vibrations that are naturally excited. Two possible configurations can describe the dynamical model of flexible manipulators. First, the dynamical model can be regarded as one multi-input and multi-output (MIMO) system; one controller is used in this case for all joints and links. Second, the dynamical model can be viewed as interconnected subsystems. Each subsystem has a pair of one joint and one link and is controlled with one controller.

Many control strategies are based on the MIMO representation of the dynamical model of flexible manipulators. In the linear case, Linear-Quadratic-Gaussian (LQG) approach and the stable factorization technique were used in [1, 2]. A comparative study of a State-Feedback controller and a Linear Quadratic Regulator (LQR) using the tip deflection feedback measured by a strain gauge were proposed in [3] to minimize the link vibrations of a single link flexible manipulator. The generalization of the computed-torque method is used in [4, 5] for the tracking control of nonlinear flexible-link manipulators. The objectives were to track desired trajectories in the joint space and vibration suppression in the links. Adaptive control is used in [6, 7] where the system parameters are considered unknown. The reinforcement learning (RL) technique is used in [6] for developing a real-time adaptive control of a two-link flexible manipulator. The controller consists of a proportional derivative (PD) tracking loop and an adaptive bloc based on RL loop used for tip trajectory control and cancelling the

deflection of a two-link flexible manipulator. Intelligent control strategies were also applied to flexible link manipulators in [8-10]. Several works used sliding mode to control the flexible link manipulators [11, 12]. Sliding mode technique based on a partial feedback linearization controller was used in [12] to achieve set point precision positioning control for a single flexible link manipulator with payload. For a two-flexible-link manipulator, a high-order nonsingular terminal sliding mode optimal control scheme is used in [11] to solve the non-minimum phase and chattering problems.

All the previous control schemes use one controller for all joints and links. Unfortunately, when using the dynamical model as one MIMO system, the real-time implementation of these controllers is not easy due to the complexity of their structures [13]. To overcome this problem, the dynamical model of flexible manipulators can be considered as n interconnected subsystems. Each subsystem consists of one joint and the corresponding flexible link. Several control schemes used this configuration. Decentralized control is used in [14, 15] for flexible links manipulators. In [14], the authors used the decentralized control strategy featuring a proportional derivative (PD) controller for the joint, and a linear quadratic regulator (LQR) for the link to control two-flexible-link manipulators. A decentralized control strategy composed of a PD controller for the joint, and a linear velocity feedback controller for the flexible link was proposed in [15]. Independent joint control is used in [16] for the endpoint position control problem of a two-flexible-link mechanism with very flexible links. The drawback of this method is that the authors used acceleration sensing for acceleration measurement, which is not always available. Using the nonlinear model of flexible manipulators, a hierarchical control strategy to track desired trajectories in the workspace of a two-flexible-link manipulator was developed in [17]. A feedback linearization approach is used for each subsystem (a pair of joint and link) to develop control laws. To simplify the real-time implementation we present in this paper, a distributed control strategy is proposed for multi-link flexible manipulators to track desired trajectories in the joint space and to remove link vibration. The control strategy consists to rewrite, in the first time, the dynamical model of n-flexible-links manipulator as n subsystems. Each subsystem contains a pair of one joint and one link. Secondly, the control strategy consists to start by controlling

the last subsystem while considering the remaining subsystems stable. Then, going backward to the (n-1)-th subsystem, the same strategy is applied, and so on, until the first subsystem. The control laws are developed using sliding mode technique. Lyapunov theory is used to prove the global stability of the error dynamics. This control strategy is implemented on a two-flexible-link manipulator.

This paper is organized as follows: section 4.2 presents the description and the modeling of the n-flexible-link manipulator. The distributed control strategy of multi-flexible link and stability analysis of the error dynamics are presented in section 4.3. Section 4.4 presents the experimental results of the proposed control strategy of a two-flexible-link manipulator. Finally, conclusions are given in section 4.5.

4.2 Modeling and problem formulation

The n-flexible-link manipulator is shown in Figure 4.1. The links are presented in a cascade form and actuated by individual motors. An inertial payload is attached to the end effectors. The motion of each link is assumed to be in the horizontal plane and has a very small deflection. Using Lagrange equations, the dynamical model of an n DOF flexible manipulator is given by (De Luca et Siciliano, 1991):

$$M(\mathbf{q})\ddot{\mathbf{q}} + C(\mathbf{q}, \dot{\mathbf{q}})\dot{\mathbf{q}} + D\dot{\mathbf{q}} + K\mathbf{q} = L\boldsymbol{\tau} \quad (4.1)$$

where M is the inertia and mass matrix, $C(\mathbf{q}, \dot{\mathbf{q}})\dot{\mathbf{q}}$ is the Coriolis and centrifugal forces vector, D is the friction matrix and K is the rigidity matrix. \mathbf{q} represents the vector of the generalized coordinates and $\boldsymbol{\tau}$ is the vector of the applied torques.

Note: in the rest of paper, the scalar is written in lower case, the vector in **lower case bold** and the matrix is in upper case.

For the n rigid coordinates and n flexible links, the deformation of the i^{th} flexible link is given by the following equation:

$$v_i(x, t) = \sum_{j=1}^{z_i} \phi_{ij}(x) q_{fij}(t) \quad i = 1, \dots, n \quad (4.2)$$

where q_{fij} is the j^{th} generalized flexible coordinate, $\phi_{ij}(x)$ is its j^{th} shape function and z_i is the number of retained flexible modes of the i^{th} flexible link. Note that the total number of flexible modes is $z = \sum_{i=1}^n z_i$ and the number of rigid modes is n .

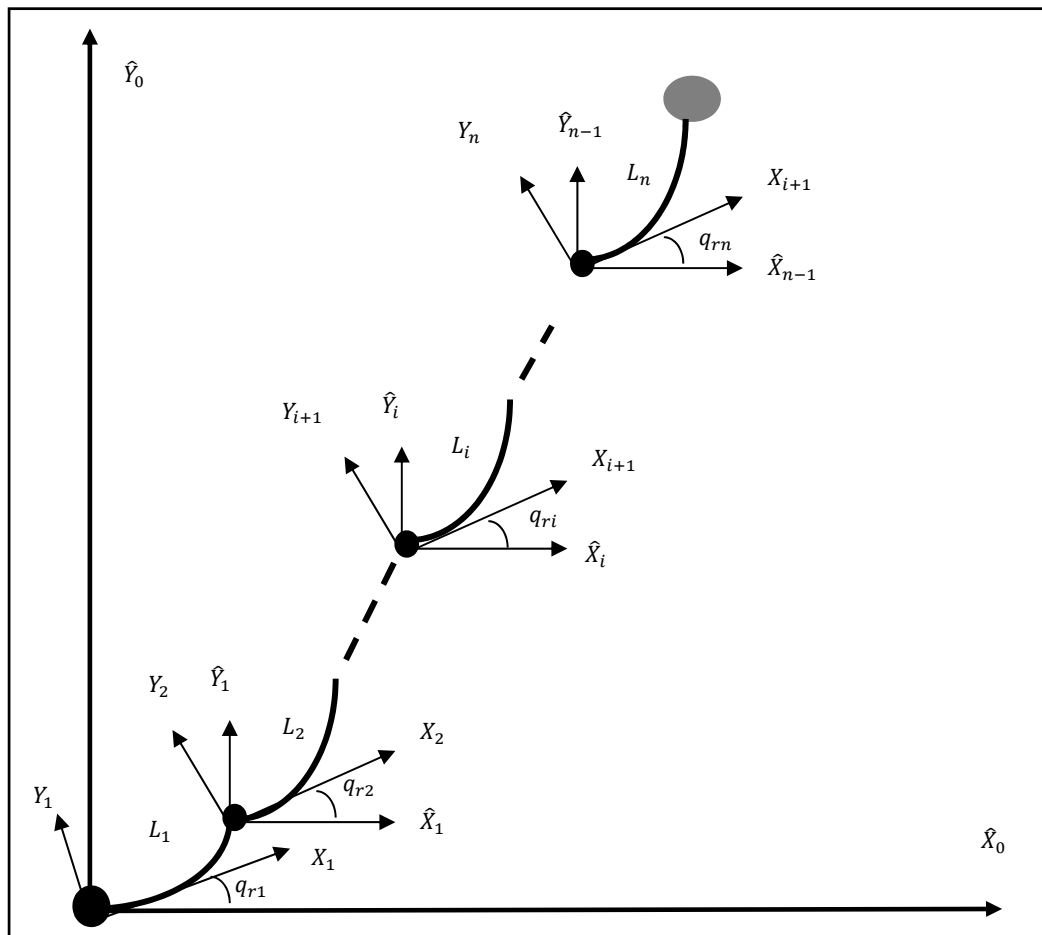


Figure 4.1 Flexible-link manipulator.

The dynamical model (4.1) can be written as follows:

$$\begin{aligned}
& \begin{bmatrix} [M_r]_{n \times n} & [M_{rf}]_{n \times z} \\ [M_{rf}^T]_{z \times n} & [M_f]_{z \times z} \end{bmatrix}_{(n+z) \times (n+z)} \begin{bmatrix} \ddot{\mathbf{q}}_r \\ \ddot{\mathbf{q}}_f \end{bmatrix} + \begin{bmatrix} [C_r]_{n \times n} & [C_{rf}]_{n \times z} \\ [C_{rf}^T]_{z \times n} & [C_f]_{z \times z} \end{bmatrix} \begin{bmatrix} \dot{\mathbf{q}}_r \\ \dot{\mathbf{q}}_f \end{bmatrix} \\
& + \begin{bmatrix} 0 & 0 \\ 0 & [D_f]_{z \times z} \end{bmatrix} \begin{bmatrix} \dot{\mathbf{q}}_r \\ \dot{\mathbf{q}}_f \end{bmatrix} + \begin{bmatrix} 0_{n \times n} & 0_{n \times z} \\ 0_{z \times n} & [K_f]_{z \times z} \end{bmatrix} \begin{bmatrix} \mathbf{q}_r \\ \mathbf{q}_f \end{bmatrix} = \begin{bmatrix} I_{n \times n} \\ 0_{z \times n} \end{bmatrix} \boldsymbol{\tau}_{n \times 1}
\end{aligned} \tag{4.3}$$

where M_r and M_f are the mass and inertia matrices for the rigid and the flexible parts respectively. M_{rf} is a coupled element. The subscripts r and f denote the rigid and flexible modes. In this work we consider only the first flexible mode of each link, then $z=n$.

There exists a non-singular matrix of transformation T_r such as:

$$\bar{\mathbf{q}} = T_r \mathbf{q} \tag{4.4}$$

where $\mathbf{q} = [\mathbf{q}_r \quad \mathbf{q}_f]^T = [q_{r1} \quad \dots \quad q_{rn} \quad q_{f1} \quad \dots \quad q_{fn}]^T$ is the original generalized coordinate, $\bar{\mathbf{q}} = [\mathbf{q}_1 \quad \dots \quad \mathbf{q}_i \quad \dots \quad \mathbf{q}_n]^T = [q_{r1} \quad q_{f1} \quad \dots \quad q_{ri} \quad q_{fi} \quad \dots \quad q_{rn} \quad q_{fn}]^T$ is the transformed one, $\mathbf{q}_i = [q_{ri} \quad q_{fi}]^T$ is the generalized coordinate associated with the i^{th} subsystem (i^{th} joint and link) and the matrix of transformation T_r is given by:

$$T_r = \begin{bmatrix} 1 & & & & & & & & \\ & \overbrace{1 \ 2 \ \dots \ i \ \dots \ n} & & & & \overbrace{n+1 \ \dots \ n+i} & & & 2n \\ & \begin{bmatrix} 1 & 0 & \dots & 0 & 0 & 0 & \dots & 0 & 0 & 0 \\ 0 & 0 & \dots & 0 & 0 & 0 & \dots & 0 & 0 & 0 \end{bmatrix} & & & & \begin{bmatrix} 0 & 0 & \dots & 0 & 0 & 0 & \dots & 0 & 0 & 0 \\ 1 & 0 & \dots & 0 & 0 & 0 & \dots & 0 & 0 & 0 \end{bmatrix} & & & \begin{bmatrix} 0 & 0 & \dots & 0 & 0 & 0 & \dots & 0 & 0 & 0 \\ 0 & 0 & \dots & 0 & 0 & 0 & \dots & 0 & 0 & 0 \end{bmatrix} \\ & & & & & \vdots & & & \\ & & & & & & \begin{bmatrix} 0 & 0 & \dots & 0 & 1 & 0 & \dots & 0 & 0 & 0 \\ 0 & 0 & \dots & 0 & 0 & 0 & \dots & 0 & 0 & 0 \end{bmatrix} & & & & \begin{bmatrix} 0 & 0 & \dots & 0 & 0 & 0 & \dots & 0 & 0 & 0 \\ 0 & 0 & \dots & 0 & 0 & 0 & \dots & 0 & 1 & 0 \end{bmatrix} & & & \begin{bmatrix} 0 & 0 & \dots & 0 & 0 & 0 & \dots & 0 & 0 & 0 \\ 0 & 0 & \dots & 0 & 0 & 0 & \dots & 0 & 0 & 0 \end{bmatrix} \\ & & & & & & \vdots & & & \\ & & & & & & & \begin{bmatrix} 0 & 0 & \dots & 0 & 0 & 0 & \dots & 0 & 0 & 1 \\ 0 & 0 & \dots & 0 & 0 & 0 & \dots & 0 & 0 & 0 \end{bmatrix} & & & & & \begin{bmatrix} 0 & 0 & \dots & 0 & 0 & 0 & \dots & 0 & 0 & 0 \\ 0 & 0 & \dots & 0 & 0 & 0 & \dots & 0 & 0 & 0 \end{bmatrix} \\ & & & & & & & & \vdots & & \\ & & & & & & & & & \begin{bmatrix} 0 & 0 & \dots & 0 & 0 & 0 & \dots & 0 & 0 & 1 \\ 0 & 0 & \dots & 0 & 0 & 0 & \dots & 0 & 0 & 0 \end{bmatrix} & & & & & \end{bmatrix} \tag{4.5}$$

Using the previous transformation, the dynamical model (4.1) can be written as follows:

$$M(\mathbf{q})T_r^{-1}\ddot{\bar{\mathbf{q}}} + C(\mathbf{q}, \dot{\mathbf{q}})T_r^{-1}\dot{\bar{\mathbf{q}}} + DT_r^{-1}\bar{\mathbf{q}} + KT_r^{-1}\bar{\mathbf{q}} = L\boldsymbol{\tau} \tag{4.6}$$

where $\ddot{\bar{\mathbf{q}}} = T_r \ddot{\mathbf{q}}$ and $\dot{\bar{\mathbf{q}}} = T_r \dot{\mathbf{q}}$, note that the vectors \mathbf{q} and $\bar{\mathbf{q}}$ have the same elements but in different order, then : $\bar{M}(\mathbf{q}) = \bar{M}(\bar{\mathbf{q}})$ and $\bar{C}(\mathbf{q}, \dot{\mathbf{q}}) = \bar{C}(\bar{\mathbf{q}}, \dot{\bar{\mathbf{q}}})$.

Equation (4.6) is equivalent to the following expression:

$$\bar{M}(\mathbf{q})\ddot{\bar{\mathbf{q}}} + \bar{C}(\mathbf{q}, \dot{\mathbf{q}})\dot{\bar{\mathbf{q}}} + \bar{D}\dot{\bar{\mathbf{q}}} + \bar{K}\bar{\mathbf{q}} = \bar{L}\tau \quad (4.7)$$

where $\bar{M}(\mathbf{q})_{2n \times 2n} = T_r M(\mathbf{q}) T_r^{-1}$; $\bar{C}(\mathbf{q}, \dot{\mathbf{q}})_{2n \times 2n} = T_r C(\mathbf{q}, \dot{\mathbf{q}}) T_r^{-1}$; $\bar{D}_{2n \times 2n} = T_r D T_r^{-1}$; $\bar{K}_{2n \times 2n} = T_r K T_r^{-1}$, $\bar{L}_{2n \times n} = T_r L$.

The dynamical model (4.7) can be written as follows:

$$\begin{bmatrix} \bar{M}_1^T(\mathbf{q}) \\ \vdots \\ \bar{M}_n^T(\mathbf{q}) \end{bmatrix} \begin{bmatrix} \ddot{\bar{\mathbf{q}}}_1 \\ \vdots \\ \ddot{\bar{\mathbf{q}}}_n \end{bmatrix} + \begin{bmatrix} \bar{C}_1^T(q, \dot{q}) \\ \vdots \\ \bar{C}_n^T(q, \dot{q}) \end{bmatrix} \begin{bmatrix} \dot{\bar{\mathbf{q}}}_1 \\ \vdots \\ \dot{\bar{\mathbf{q}}}_n \end{bmatrix} + \begin{bmatrix} \bar{D}_1^T \\ \vdots \\ \bar{D}_n^T \end{bmatrix} \begin{bmatrix} \dot{\bar{\mathbf{q}}}_1 \\ \vdots \\ \dot{\bar{\mathbf{q}}}_n \end{bmatrix} + \begin{bmatrix} \bar{K}_1^T \\ \vdots \\ \bar{K}_n^T \end{bmatrix} \begin{bmatrix} \bar{\mathbf{q}}_1 \\ \vdots \\ \bar{\mathbf{q}}_n \end{bmatrix} = \begin{bmatrix} \bar{L}_1 \\ \vdots \\ \bar{L}_n \end{bmatrix} \tau \quad (4.8)$$

where $\mathbf{q}_i = [q_{ri} \ q_{fi}]^T$; $\bar{M}_i^T = [\bar{M}_{i1} \ \dots \ \bar{M}_{ii} \ \dots \ \bar{M}_{in}]$; $\bar{C}_i^T = [\bar{C}_{i1} \ \dots \ \bar{C}_{ii} \ \dots \ \bar{C}_{in}]$
 $\bar{D}_i^T = [0_{2 \times 2} \ \dots \ 0_{2 \times 2} \ \bar{D}_{ii} \ 0_{2 \times 2} \ \dots \ 0_{2 \times 2}]$; $\bar{K}_i^T = [0_{2 \times 2} \ \dots \ 0_{2 \times 2} \ \bar{K}_{ii} \ 0_{2 \times 2} \ \dots \ 0_{2 \times 2}]$,
 $\bar{M}_{ii} = \begin{bmatrix} M_{ri} & M_{rfi} \\ M_{rfi} & M_{fi} \end{bmatrix}$; $\bar{C}_{ii} = \begin{bmatrix} C_{ri} & C_{rfi} \\ C_{rfi} & C_{fi} \end{bmatrix}$; $\bar{D}_{ii} = \begin{bmatrix} 0 & 0 \\ 0 & D_{fi} \end{bmatrix}$; $\bar{K}_{ii} = \begin{bmatrix} 0 & 0 \\ 0 & K_{fi} \end{bmatrix}$.

The properties that will be used in the control law development can be deduced from the dynamical model of the flexible link manipulator and are given as follows:

P1: $M, M_{rr}, M_{ff}, D_{ff}$ and K_{ff} are symmetric positive definite matrices (De Luca et Siciliano, 1991).

P2: The inertia-mass matrix $M(\mathbf{q})$ and the Coriolis matrix $C(\mathbf{q}, \dot{\mathbf{q}})$ satisfy the following skew-symmetric property:

$$\mathbf{x}^T (\dot{M}(\mathbf{q}, \dot{\mathbf{q}}) - 2C(\mathbf{q}, \dot{\mathbf{q}})) \mathbf{x} = 0 \quad \forall \mathbf{x} \in \mathbb{R}^{n+z} \quad (4.9)$$

Let the desired trajectory associated to the rigid part of the i^{th} subsystem, its first and second-order derivatives be $q_{ird}(t)$, $\dot{q}_{ird}(t)$ and $\ddot{q}_{ird}(t)$ respectively, and $q_{ifd}(t)$, $\dot{q}_{ifd}(t)$ and $\ddot{q}_{ifd}(t)$ are those associated to the flexible part of this subsystem. The objective is to track

desired trajectories in the joint space and cancel vibration of the links. The desired positions of the flexible modes are then set to zero. Therefore, the desired trajectories must be carefully chosen so as to satisfy the control objective:

$$(q_{ir}, q_{if}) = (q_{ird}, 0) \quad (4.10)$$

4.3 Distributed control strategy

In this section, we present a distributed control strategy for n-flexible-link manipulator to track desired trajectories in the joint space while eliminating links' vibrations. The n-flexible-link system can be viewed as n interconnected subsystems. Each subsystem has a pair of a joint and a flexible link. The distributed control strategy consists in controlling the nth subsystem while assuming that the remaining subsystems are stable. Then, the same strategy is applied backward to the (n-1)th subsystem and so on until the first subsystem.

4.3.1 Control law development

As mentioned, the control strategy consists to begin by controlling the last subsystem. The equation of motion of the nth subsystem is given from (4.8) as follows:

$$\bar{M}_n^T(\boldsymbol{q})\ddot{\boldsymbol{q}} + \bar{C}_n^T(\boldsymbol{q}, \dot{\boldsymbol{q}})\dot{\boldsymbol{q}} + \bar{D}_n^T\dot{\boldsymbol{q}} + \bar{K}_n^T\bar{\boldsymbol{q}} = \bar{L}_n\boldsymbol{\tau} \quad (4.11)$$

where $\bar{M}_n^T = [\bar{M}_{n1} \dots \bar{M}_{ni} \dots \bar{M}_{nn}]_{2 \times 2n}$; $\bar{C}_n^T = [\bar{C}_{n1} \dots \bar{C}_{ni} \dots \bar{C}_{nn}]_{2 \times 2n}$;

$\bar{D}_n^T = [0_{2 \times 2} \dots 0_{2 \times 2} \bar{D}_{nn}]_{2 \times 2n}$; $\bar{K}_n^T = [0_{2 \times 2} \dots 0_{2 \times 2} \bar{K}_{nn}]_{2 \times 2n}$ and $\bar{L}_n = \begin{bmatrix} 0 & 0 & \dots & 1 \\ 0 & 0 & \dots & 0 \end{bmatrix}_{2 \times n}$.

The nth subsystem is controlled by assuming that the remaining subsystems are stable. Then we can define a generalized coordinate as follows:

$$\bar{\boldsymbol{q}}_n = [\boldsymbol{q}_{d1} \dots \boldsymbol{q}_{d(n-1)} \boldsymbol{q}_n]^T \quad (4.12)$$

where $\boldsymbol{q}_{di} = [q_{rai} \ q_{fai}]$ for i=1 ... n-1. Note that the rigid and flexible coordinates of the nth subsystem are the controlled ones and the rigid and flexible coordinates of the remaining

subsystems are the desired ones. The velocity $\dot{\bar{q}}_n$ is the time derivative of \bar{q}_n and the acceleration $\ddot{\bar{q}}_n$ is the time derivative of $\dot{\bar{q}}_n$. Using the new coordinate, the corresponding equation of motion is given as follows:

$$\bar{M}_n^T(\bar{q}_n)\ddot{\bar{q}}_n + \bar{C}_n^T(\bar{q}_n, \dot{\bar{q}}_n)\dot{\bar{q}}_n + \bar{D}_n^T\dot{\bar{q}}_n + \bar{K}_n^T\bar{q}_n = \bar{L}_n\tau \quad (4.13)$$

In other form, (4.13) can be written as:

$$\bar{M}_{nn}(\bar{q}_n)\ddot{\bar{q}}_n + \bar{C}_{nn}(\bar{q}_n, \dot{\bar{q}}_n)\dot{\bar{q}}_n + \bar{D}_{nn}\dot{\bar{q}}_n + \bar{K}_{nn}\bar{q}_n + \sum_{j=1}^{n-1} \bar{M}_{nj}\ddot{\bar{q}}_{dj} + \bar{C}_{nj}\dot{\bar{q}}_{dj} = \begin{bmatrix} \tau_n \\ 0 \end{bmatrix} \quad (4.14)$$

Define the sliding surface of n^{th} subsystem as follows:

$$s_n = \begin{bmatrix} S_{rn} \\ S_{fn} \end{bmatrix} = \begin{bmatrix} \dot{e}_{rn} + \lambda_{rn}e_{rn} \\ \dot{e}_{fn} + \lambda_{fn}e_{fn} \end{bmatrix} = \begin{bmatrix} \dot{q}_{rdn} - \dot{q}_{rn} + \lambda_{rn}e_{rn} \\ \dot{q}_{fdn} - \dot{q}_{fn} + \lambda_{fn}e_{fn} \end{bmatrix} \quad (4.15)$$

where $e_{rn} = q_{rdn} - q_{rn}$, and $e_{fn} = q_{fdn} - q_{fn}$ are the error signals and $\lambda_{rn}, \lambda_{fn}$ are positive constants.

The previous sliding surface can be written as follows:

$$s_n = \begin{bmatrix} S_{rn} \\ S_{fn} \end{bmatrix} = \begin{bmatrix} \dot{u}_{rn} - \dot{q}_{rn} \\ \dot{u}_{fn} - \dot{q}_{fn} \end{bmatrix} = \dot{u}_n - \dot{q}_n \quad (4.16)$$

where $\dot{u}_{rn} = \dot{q}_{rdn} + \lambda_{rn}e_{rn}$ and $\dot{u}_{fn} = \dot{q}_{fdn} + \lambda_{fn}e_{fn}$.

To control the n^{th} subsystem, we propose the following control law:

$$\tau_n = T_n + v_{rn} - \delta\tau_{rn} \quad (4.17)$$

where

$$T_n = \begin{cases} \frac{s_{fn}(v_{fn} + \delta\tau_{fn})}{s_{rn}} & ; s_{rn} \neq 0 \\ 0 & ; s_{rn} = 0 \end{cases} \quad (4.18)$$

$$\boldsymbol{v}_n = \begin{bmatrix} v_{rn} \\ v_{fn} \end{bmatrix} = \bar{M}_n^T(\bar{\Psi}_n) \ddot{\boldsymbol{u}} + \bar{C}_n^T(\bar{\Psi}_n, \dot{\bar{\Psi}}_n) \dot{\boldsymbol{u}} + \bar{D}_n^T \ddot{\boldsymbol{u}} + \bar{K}_n^T \bar{\boldsymbol{q}} + \bar{K}_{dn}^T \bar{\boldsymbol{s}} \quad (4.19)$$

$$\boldsymbol{\delta\tau}_n = \begin{bmatrix} \delta\tau_{rn} \\ \delta\tau_{fn} \end{bmatrix} = \delta\bar{M}_n^T \ddot{\boldsymbol{u}} - \delta\bar{C}_n^T \dot{\boldsymbol{u}} \quad (4.20)$$

where $K_{dn} \in \mathcal{R}^{2 \times 2}$ is a diagonal positive matrix, $\delta\bar{M}_n^T = [\delta\bar{M}_{n1} \ \dots \ \delta\bar{M}_{ni} \ \dots \ \delta\bar{M}_{nn}]_{2 \times 2n}$; $\delta\bar{C}_n^T = [\delta\bar{C}_{n1} \ \dots \ \delta\bar{C}_{ni} \ \dots \ \delta\bar{C}_{nn}]_{2 \times 2n}$ $\bar{K}_{dn}^T \bar{\boldsymbol{s}} = \text{diag}(K_{drn} s_{rn}, K_{dfn} s_{fn})$ and,

$$\bar{\boldsymbol{u}} = [\boldsymbol{u}_1 \ \dots \ \boldsymbol{u}_i \ \dots \ \boldsymbol{u}_n]^T = [u_{r1} \ u_{f1} \ \dots \ u_{ri} \ u_{fi} \ \dots \ u_{rn} \ u_{fn}]^T \quad (4.21)$$

$$= T_r \boldsymbol{u}$$

$$\delta\bar{M}_{nj} = \sum_{j=1}^{n-1} \left. \frac{\partial \bar{M}_{nj}(\boldsymbol{q})}{\partial \boldsymbol{q}_j} \right|_{q_{jd}} \tilde{\boldsymbol{q}}_j + R_{\bar{M}_{nj}}(\tilde{\boldsymbol{q}}_j) \quad (4.22)$$

$$\delta\bar{C}_{nj} = \sum_{j=1}^{n-1} \left. \frac{\partial \bar{C}_{nj}(\boldsymbol{q}, \dot{\boldsymbol{q}})}{\partial \boldsymbol{q}_j} \right|_{q_{jd}} \tilde{\boldsymbol{q}}_j + \sum_{j=1}^{n-1} \left. \frac{\partial \bar{C}_{nj}(\boldsymbol{q}, \dot{\boldsymbol{q}})}{\partial \dot{\boldsymbol{q}}_j} \right|_{q_{jd}} \dot{\tilde{\boldsymbol{q}}}_j + R_{\bar{C}_{nj}}(\tilde{\boldsymbol{q}}_j, \dot{\tilde{\boldsymbol{q}}}_j) \quad (4.23)$$

$R_{\bar{M}_{nj}}$ and $R_{\bar{C}_{nj}}$ are the high order terms of the Taylor series for $\bar{M}_{nj}(\boldsymbol{q})$ and $\bar{C}_{nj}(\boldsymbol{q})$, respectively (Bartle et Sherbert, 2000) (see Appendix for more detail). This control strategy is used backward for the remaining subsystems. Taking for example the i^{th} subsystem, the corresponding generalized coordinate can be written as follows:

$$\bar{\Psi}_i = [\boldsymbol{q}_{d1} \ \dots \ \boldsymbol{q}_{d(i-1)} \ \boldsymbol{q}_i \ \boldsymbol{q}_{d(i+1)} \ \dots \ \boldsymbol{q}_{dn}]^T \quad (4.24)$$

where $\boldsymbol{q}_{dj} = [q_{rdj} \ q_{fdj}]^T, j = 1, \dots, n$ and $j \neq i$, and $\boldsymbol{q}_i = [q_{ri} \ q_{fi}]^T$.

The new equation of motion is given as follows:

$$\bar{M}_i^T(\bar{\mathbf{q}}_i)\ddot{\bar{\mathbf{q}}}_i + \bar{C}_i^T(\bar{\mathbf{q}}_i, \dot{\bar{\mathbf{q}}}_i)\dot{\bar{\mathbf{q}}}_i + \bar{D}_i^T\dot{\bar{\mathbf{q}}}_i + \bar{K}_i^T\bar{\mathbf{q}}_i = \bar{L}_i\tau_i \quad (4.25)$$

where $\bar{M}_i^T = [\bar{M}_{i1} \ \dots \ \bar{M}_{ii} \ \dots \ \bar{M}_{in}]^T$; $\bar{C}_i^T = [\bar{C}_{i1} \ \dots \ \bar{C}_{ii} \ \dots \ \bar{C}_{in}]^T$;
 $\bar{L}_i = \begin{bmatrix} 0 & \dots & 010 & \dots & 0 \\ 0 & \dots & 000 & \dots & 0 \end{bmatrix}_{2 \times n}$; $\bar{D}_i^T = [\bar{D}_{i1} \ \dots \ \bar{D}_{ii} \ \dots \ \bar{D}_{in}]^T$; $\bar{K}_i^T = [\bar{K}_{i1} \ \dots \ \bar{K}_{ii} \ \dots \ \bar{K}_{in}]^T$;
 $\bar{M}_{ii} = \begin{bmatrix} M_{ri} & M_{rfi} \\ M_{rfi} & M_{fi} \end{bmatrix}$; $\bar{C}_{ii} = \begin{bmatrix} C_{ri} & C_{rfi} \\ C_{rfi} & C_{fi} \end{bmatrix}$; $\bar{D}_{ii} = \begin{bmatrix} 0 & 0 \\ 0 & D_{fi} \end{bmatrix}$; $\bar{K}_{ii} = \begin{bmatrix} 0 & 0 \\ 0 & K_{fi} \end{bmatrix}$.

The previous equation of motion is equivalent to:

$$\begin{aligned} \bar{M}_{ii}(\bar{\mathbf{q}}_i)\ddot{\bar{\mathbf{q}}}_i + \bar{C}_{ii}(\bar{\mathbf{q}}_i, \dot{\bar{\mathbf{q}}}_i)\dot{\bar{\mathbf{q}}}_i + \bar{D}_{ii}\dot{\bar{\mathbf{q}}}_i + \bar{K}_{ii}\bar{\mathbf{q}}_i + \sum_{j=1}^n \bar{M}_{ij}(\bar{\mathbf{q}}_i)\ddot{\bar{\mathbf{q}}}_j + \bar{C}_{ij}(\bar{\mathbf{q}}_i, \dot{\bar{\mathbf{q}}}_j)\dot{\bar{\mathbf{q}}}_j \\ = \begin{bmatrix} \tau_i \\ 0 \end{bmatrix} \end{aligned} \quad (4.26)$$

The sliding surface of i^{th} subsystem is given as follows:

$$\mathbf{s}_i = \begin{bmatrix} s_{ri} \\ s_{fi} \end{bmatrix} = \begin{bmatrix} \dot{u}_{ri} - \dot{q}_{ri} \\ \dot{u}_{fi} - \dot{q}_{fi} \end{bmatrix} = \dot{\mathbf{u}}_i - \dot{\mathbf{q}}_i \quad (4.27)$$

where $\dot{u}_{ri} = \dot{q}_{rdi} + \lambda_{ri}e_{ri}$ and $\dot{u}_{fi} = \dot{q}_{fdi} + \lambda_{fi}e_{fi}$. $e_{ri} = q_{rdi} - q_{ri}$, and $e_{fi} = q_{fdi} - q_{fi}$ are the error signals and $\lambda_{ri}, \lambda_{fi}$ are positive constants.

The proposed control law of the i^{th} subsystem is:

$$\tau_i = T_i + v_{ri} - \delta\tau_{ri} \quad (4.28)$$

where

$$T_i = \begin{cases} \frac{s_{fi}(v_{fi} + \delta\tau_{fi})}{s_{ri}} & ; s_{ri} \neq 0 \\ 0 & ; s_{ri} = 0 \end{cases} \quad (4.29)$$

$$\boldsymbol{v}_i = \begin{bmatrix} v_{ri} \\ v_{fi} \end{bmatrix} = \bar{M}_i^T(\bar{\boldsymbol{q}}_i) \ddot{\boldsymbol{u}} + \bar{C}_i^T(\bar{\boldsymbol{q}}_i, \dot{\bar{\boldsymbol{q}}}_i) \dot{\boldsymbol{u}} + \bar{D}_i^T \dot{\boldsymbol{u}} + \bar{K}_i^T \bar{\boldsymbol{q}} + \bar{K}_{di}^T \bar{\boldsymbol{s}} \quad (4.30)$$

$$\boldsymbol{\delta\tau}_i = \begin{bmatrix} \delta\tau_{ri} \\ \delta\tau_{fi} \end{bmatrix} = \delta\bar{M}_i^T \ddot{\boldsymbol{u}} - \delta\bar{C}_i^T \dot{\boldsymbol{u}} \quad (4.31)$$

where $K_{di} \in \mathcal{R}^{2 \times 2}$ is a diagonal positive matrix, $\delta\bar{M}_i^T = [\delta\bar{M}_{i1} \ \dots \ \delta\bar{M}_{ii} \ \dots \ \delta\bar{M}_{in}]_{2 \times 2n}$; $\delta\bar{C}_i^T = [\delta\bar{C}_{i1} \ \dots \ \delta\bar{C}_{ii} \ \dots \ \delta\bar{C}_{in}]_{2 \times 2n}$ and:

$$\delta\bar{M}_{ij} = \sum_{j=1}^n \left. \frac{\partial \bar{M}_{ij}(\boldsymbol{q})}{\partial \boldsymbol{q}_j} \right|_{\boldsymbol{q}_{jd}} \tilde{\boldsymbol{q}}_j + R_{\bar{M}_{ij}}(\tilde{\boldsymbol{q}}_j) \quad (4.32)$$

$$\delta\bar{C}_{ij} = \sum_{\substack{j=1 \\ j \neq i}}^n \left. \frac{\partial \bar{C}_{ij}(\boldsymbol{q}, \dot{\boldsymbol{q}})}{\partial \boldsymbol{q}_j} \right|_{\boldsymbol{q}_{jd}} \tilde{\boldsymbol{q}}_j + \sum_{\substack{j=1 \\ j \neq i}}^n \left. \frac{\partial \bar{C}_{ij}(\boldsymbol{q}, \dot{\boldsymbol{q}})}{\partial \dot{\boldsymbol{q}}_j} \right|_{\boldsymbol{q}_{jd}} \dot{\tilde{\boldsymbol{q}}}_j + R_{\bar{C}_{ij}}(\tilde{\boldsymbol{q}}_j, \dot{\tilde{\boldsymbol{q}}}_j) \quad (4.33)$$

$R_{\bar{M}_{ij}}$, and $R_{\bar{C}_{ij}}$ are the high order terms of the Taylor series.

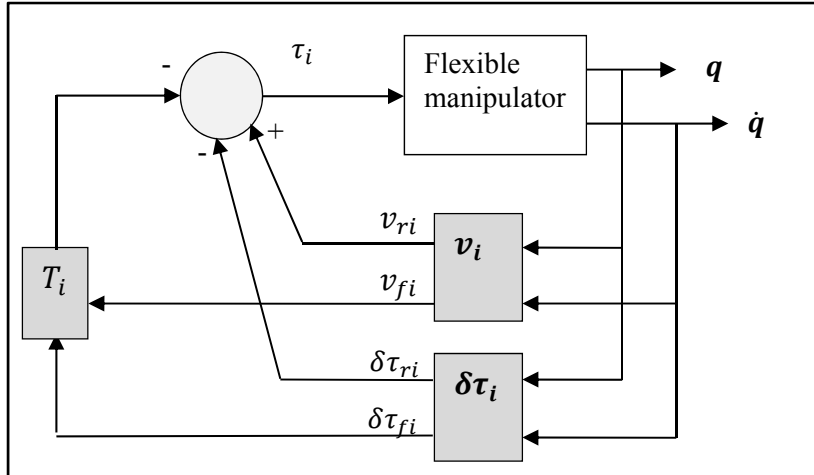


Figure 4.2 The i -th control law.

4.3.2 Stability analysis

This section presents the stability analysis of the error dynamics for all subsystems. The n control laws (4.28) can be written as follows:

$$\boldsymbol{\tau} = \mathbf{T} + \boldsymbol{v}_r - \boldsymbol{\delta\tau}_r \quad (4.34)$$

where $\boldsymbol{v}_r \in \Re^n$ is the first n elements of the vector \boldsymbol{v} , given in (4.30), while \boldsymbol{v}_f are the remaining elements of \boldsymbol{v} . $\mathbf{T} \in \Re^n$ has T_i , given in (4.29), in the ith element.

The sliding surface for all subsystems can be written as follows;

$$\mathbf{s} = \begin{bmatrix} s_r \\ s_f \end{bmatrix} = \begin{bmatrix} \dot{e}_r + \lambda_r e_r \\ \dot{e}_f + \lambda_f e_f \end{bmatrix} = \begin{bmatrix} \dot{q}_{ra} - \dot{q}_r + \lambda_r e_r \\ \dot{q}_{fa} - \dot{q}_f + \lambda_f e_f \end{bmatrix} = \begin{bmatrix} \dot{u}_r - \dot{q}_r \\ \dot{u}_f - \dot{q}_f \end{bmatrix} = \dot{\mathbf{u}} - \dot{\mathbf{q}} \quad (4.35)$$

Using (4.35), the dynamical model (4.1) is given as follows:

$$M(\mathbf{q})(\ddot{\mathbf{u}} - \dot{\mathbf{s}}) + C(\mathbf{q}, \dot{\mathbf{q}})(\dot{\mathbf{u}} - \mathbf{s}) + D(\dot{\mathbf{u}} - \mathbf{s}) + K\mathbf{q} = L\boldsymbol{\tau} \quad (4.36)$$

The error dynamics can be deduced as follows:

$$M(\mathbf{q})\dot{\mathbf{s}} + C(\mathbf{q}, \dot{\mathbf{q}})\mathbf{s} + D\mathbf{s} + K_d\mathbf{s} = M(\mathbf{q})\ddot{\mathbf{u}} + C(\mathbf{q}, \dot{\mathbf{q}})\dot{\mathbf{u}} + D\dot{\mathbf{u}} + K_d\mathbf{s} + K\mathbf{q} - L\boldsymbol{\tau} \quad (4.37)$$

Proposition 1: The error dynamics (4.37) is equivalent to the following expression:

$$M(\mathbf{q})\dot{\mathbf{s}} + C(\mathbf{q}, \dot{\mathbf{q}})\mathbf{s} + D\mathbf{s} + K_d\mathbf{s} = \begin{bmatrix} -T \\ \boldsymbol{v}_f + \boldsymbol{\delta\tau}_f \end{bmatrix} \quad (4.38)$$

Proof: see Appendix.

For the stability analysis, let us define the following positive Lyapunov function:

$$V = \frac{1}{2}\mathbf{s}^T M(\mathbf{q})\mathbf{s} \quad (4.39)$$

Take the time derivative of $V(t)$ to get

$$\dot{V}(t) = \mathbf{s}^T M \dot{\mathbf{s}} + \frac{1}{2} \mathbf{s}^T \dot{M} \mathbf{s} \quad (4.40)$$

Using (4.38), $\dot{V}(t)$ becomes:

$$\begin{aligned} \dot{V}(t) &= \mathbf{s}^T \left(-C(\mathbf{q}, \dot{\mathbf{q}})\mathbf{s} - D\mathbf{s} - K_d\mathbf{s} + \begin{bmatrix} -T \\ \boldsymbol{v}_f + \boldsymbol{\delta\tau}_f \end{bmatrix} \right) + \frac{1}{2} \mathbf{s}^T \dot{M} \mathbf{s} \\ &= -\mathbf{s}^T (D + K_d)\mathbf{s} + \mathbf{s}^T \begin{bmatrix} -T \\ \boldsymbol{v}_f + \boldsymbol{\delta\tau}_f \end{bmatrix} \end{aligned}$$

Using the transformation matrix T_r , we can write:

$$\mathbf{s}^T \begin{bmatrix} -\mathbf{T} \\ \mathbf{v}_f + \boldsymbol{\delta}\tau_f \end{bmatrix} = \bar{\mathbf{s}}^T \bar{\boldsymbol{\tau}}_s \quad (4.41)$$

where $\mathbf{s}_i = \begin{bmatrix} s_{ri} \\ s_{fi} \end{bmatrix}$ and $\bar{\boldsymbol{\tau}}_{si} = \begin{bmatrix} -T_i \\ v_{fi} + \delta\tau_{fi} \end{bmatrix}; i = 1 \dots n.$

$$\bar{\mathbf{s}}_i^T \bar{\boldsymbol{\tau}}_{si} = [s_{ri} \ s_{fi}] \begin{bmatrix} -T_i \\ v_{fi} + \delta\tau_{fi} \end{bmatrix} = -s_{ri} T_i + s_{fi} (v_{fi} + \delta\tau_{fi}) \quad (4.42)$$

Using (4.29), we can write:

$$\bar{\mathbf{s}}_i^T \bar{\boldsymbol{\tau}}_{si} = 0 \quad (4.43)$$

Using the transformation matrix T_r :

$$\mathbf{s}_i^T \boldsymbol{\tau}_{si} = 0 \quad (4.44)$$

Then,

$$\mathbf{s}^T \begin{bmatrix} -\mathbf{T} \\ \mathbf{v}_f + \boldsymbol{\delta}\tau_f \end{bmatrix} = \sum_{i=1}^n \mathbf{s}_i^T \boldsymbol{\tau}_{si} = 0 \quad (4.45)$$

Then, the time derivative of $V(t)$ becomes:

$$\dot{V}(t) = -\mathbf{s}^T (D + K_d) \mathbf{s} \quad (4.46)$$

Because D and K_d are positive definite diagonal matrices, then $\dot{V}(t)$ is negative. Using LaSalle theorem (Spong et Vidyasagar, 1989), the error dynamics is globally asymptotically stable.

4.4 Application to two-flexible-link manipulator

4.4.1 System description

The system considered in this section is a two-flexible-link manipulator shown in Fig.4.1. It consists of two motors, two flexible links, and a payload. It moves in the horizontal plane and is connected by rigid revolute joints. The system is actuated by two torques generated by the motors. The i-th motor has an angle q_{ri} and the i-th flexible link, supposed uniform, has a mass m_i and length L_i , linear density ρ_i , and rigidity EI_i . m_p is the mass of the payload. The second link is attached to the rotor of the second motor and the first link is attached to the first motor. Axes (X_1, Y_1) for link 1 and (X_2, Y_2) for link 2, move with the corresponding links. (\hat{X}_0, \hat{Y}_0) is the fixed reference frame. The deformations of the links are assumed to be small and the flexible links are modeled as Euler-Bernoulli beams.

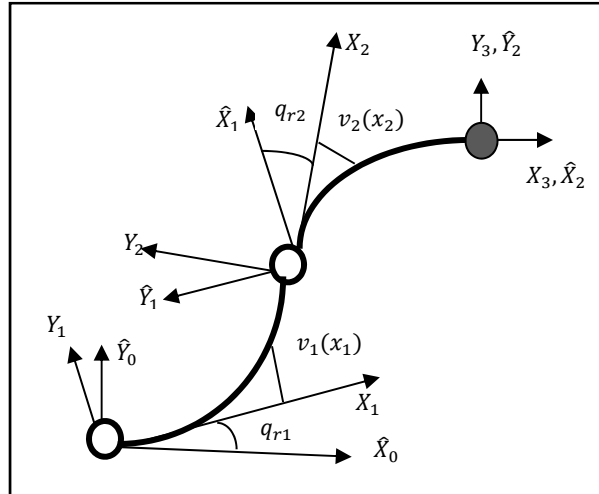


Figure 4.3 Two-flexible-link manipulator.

In this section, the two-flexible-link model given in (De Luca et Siciliano, 1991) is modified by only considering the first flexible mode of each link (see Appendix). Then, we have $n = 2$, $z = 2$ and $z_1 = z_2 = 1$.

The dynamical model of the two-flexible-link manipulator is given by:

$$M(q)\ddot{\mathbf{q}} + C(q, \dot{\mathbf{q}})\dot{\mathbf{q}} + D\dot{\mathbf{q}} + K\mathbf{q} = L\boldsymbol{\tau} \quad (4.47)$$

where

$$M = \begin{bmatrix} M_{11} & M_{12} & M_{13} & M_{14} \\ M_{21} & M_{22} & M_{23} & M_{24} \\ M_{31} & M_{32} & M_{33} & M_{34} \\ M_{41} & M_{42} & M_{43} & M_{44} \end{bmatrix}; C = \begin{bmatrix} C_{11} & C_{12} & C_{13} & C_{14} \\ C_{21} & C_{22} & C_{23} & C_{24} \\ C_{31} & C_{32} & C_{33} & C_{34} \\ C_{41} & C_{42} & C_{43} & C_{44} \end{bmatrix}; D = \begin{bmatrix} 0 & 0 & 0 & 0 \\ 0 & 0 & 0 & 0 \\ 0 & 0 & D_{f1} & 0 \\ 0 & 0 & 0 & D_{f2} \end{bmatrix};$$

$$K = \begin{bmatrix} 0 & 0 & 0 & 0 \\ 0 & 0 & 0 & 0 \\ 0 & 0 & K_{f1} & 0 \\ 0 & 0 & 0 & K_{f2} \end{bmatrix}, q = \begin{bmatrix} q_{r1} \\ q_{r2} \\ q_{f1} \\ q_{f2} \end{bmatrix}, L = \begin{bmatrix} 1 & 0 \\ 0 & 1 \\ 0 & 0 \\ 0 & 0 \end{bmatrix} \text{ and } \boldsymbol{\tau} = \begin{bmatrix} \tau_1 \\ \tau_2 \end{bmatrix}.$$

As in (4.3), we can write:

$$M_r = \begin{bmatrix} M_{11} & M_{12} \\ M_{21} & M_{22} \end{bmatrix}; M_{rf} = \begin{bmatrix} M_{13} & M_{14} \\ M_{23} & M_{24} \end{bmatrix}; M_f = \begin{bmatrix} M_{33} & M_{34} \\ M_{43} & M_{44} \end{bmatrix}; C_{rr} = \begin{bmatrix} C_{11} & C_{12} \\ C_{21} & C_{22} \end{bmatrix}; C_{rf} = \begin{bmatrix} C_{13} & C_{14} \\ C_{23} & C_{24} \end{bmatrix}; C_{ff} = \begin{bmatrix} C_{33} & C_{34} \\ C_{43} & C_{44} \end{bmatrix}; D_f = \begin{bmatrix} D_{f1} & 0 \\ 0 & D_{f2} \end{bmatrix} \text{ and } K_f = \begin{bmatrix} K_{f1} & 0 \\ 0 & K_{f2} \end{bmatrix}.$$

For two flexible links, the corresponding transformation matrix (4.5) becomes,

$$T_r = \begin{bmatrix} 1 & 0 & 0 & 0 \\ 0 & 0 & 1 & 0 \\ 0 & 1 & 0 & 0 \\ 0 & 0 & 0 & 1 \end{bmatrix} \quad (4.48)$$

Using the matrix of transformation (4.48), the dynamical model (4.47) is equivalent to the following equation:

$$\bar{M}(\mathbf{q})\ddot{\bar{\mathbf{q}}} + \bar{C}(\mathbf{q}, \dot{\mathbf{q}})\dot{\bar{\mathbf{q}}} + \bar{D}\dot{\bar{\mathbf{q}}} + \bar{K}\bar{\mathbf{q}} = \bar{L}\boldsymbol{\tau} \quad (4.49)$$

where

$$\bar{M} = \begin{bmatrix} M_{11} & M_{13} & M_{12} & M_{14} \\ M_{31} & M_{33} & M_{32} & M_{34} \\ M_{21} & M_{23} & M_{22} & M_{24} \\ M_{41} & M_{43} & M_{42} & M_{44} \end{bmatrix}; \bar{C} = \begin{bmatrix} C_{11} & C_{13} & C_{12} & C_{14} \\ C_{31} & C_{33} & C_{32} & C_{34} \\ C_{21} & C_{23} & C_{22} & C_{24} \\ C_{41} & C_{43} & C_{42} & C_{44} \end{bmatrix}; \bar{D} = \begin{bmatrix} 0 & 0 & 0 & 0 \\ 0 & D_{f1} & 0 & 0 \\ 0 & 0 & 0 & 0 \\ 0 & 0 & 0 & D_{f2} \end{bmatrix};$$

$$\bar{K} = \begin{bmatrix} 0 & 0 & 0 & 0 \\ 0 & K_{f1} & 0 & 0 \\ 0 & 0 & 0 & 0 \\ 0 & 0 & 0 & K_{f2} \end{bmatrix}; \bar{\mathbf{q}} = \begin{bmatrix} q_{r1} \\ q_{f1} \\ q_{r2} \\ q_{f2} \end{bmatrix}; \bar{L} = \begin{bmatrix} 1 & 0 \\ 0 & 0 \\ 0 & 1 \\ 0 & 0 \end{bmatrix} \text{ and } \boldsymbol{\tau} = \begin{bmatrix} \tau_1 \\ \tau_2 \end{bmatrix}$$

In the two subsystems form, (4.49) can be written as:

$$\begin{aligned} & \begin{bmatrix} \bar{M}_{11} & \bar{M}_{12} \\ \bar{M}_{21} & \bar{M}_{22} \end{bmatrix} \begin{bmatrix} \ddot{\mathbf{q}}_1 \\ \ddot{\mathbf{q}}_2 \end{bmatrix} + \begin{bmatrix} \bar{C}_{11} & \bar{C}_{12} \\ \bar{C}_{21} & \bar{C}_{22} \end{bmatrix} \begin{bmatrix} \dot{\mathbf{q}}_1 \\ \dot{\mathbf{q}}_2 \end{bmatrix} + \begin{bmatrix} \bar{D}_{11} & \bar{D}_{12} \\ \bar{D}_{21} & \bar{D}_{22} \end{bmatrix} \begin{bmatrix} \dot{\mathbf{q}}_1 \\ \dot{\mathbf{q}}_2 \end{bmatrix} + \begin{bmatrix} \bar{K}_{11} & \bar{K}_{12} \\ \bar{K}_{21} & \bar{K}_{22} \end{bmatrix} \begin{bmatrix} \mathbf{q}_1 \\ \mathbf{q}_2 \end{bmatrix} \\ &= \begin{bmatrix} \bar{L}_1 \boldsymbol{\tau} \\ \bar{L}_2 \boldsymbol{\tau} \end{bmatrix} \end{aligned} \quad (4.50)$$

$$\begin{aligned} \text{where } \bar{M}_{11} &= \begin{bmatrix} M_{11} & M_{13} \\ M_{31} & M_{33} \end{bmatrix}; \bar{M}_{12} = \begin{bmatrix} M_{12} & M_{14} \\ M_{32} & M_{34} \end{bmatrix}; \bar{C}_{11} = \begin{bmatrix} C_{11} & C_{13} \\ C_{31} & C_{33} \end{bmatrix}; \bar{C}_{12} = \begin{bmatrix} C_{12} & C_{14} \\ C_{32} & C_{34} \end{bmatrix}, \\ \bar{D}_{11} &= \begin{bmatrix} 0 & 0 \\ 0 & D_{f1} \end{bmatrix}; \bar{D}_{12} = \begin{bmatrix} 0 & 0 \\ 0 & 0 \end{bmatrix}; \bar{K}_{11} = \begin{bmatrix} 0 & 0 \\ 0 & K_{f1} \end{bmatrix}; \bar{K}_{12} = \begin{bmatrix} 0 & 0 \\ 0 & 0 \end{bmatrix}; \bar{M}_{21} = \begin{bmatrix} M_{21} & M_{23} \\ M_{41} & M_{43} \end{bmatrix}, \\ \bar{M}_{22} &= \begin{bmatrix} M_{22} & M_{24} \\ M_{42} & M_{44} \end{bmatrix}; \bar{C}_{21} = \begin{bmatrix} C_{21} & C_{23} \\ C_{41} & C_{43} \end{bmatrix}; \bar{C}_{22} = \begin{bmatrix} C_{22} & C_{24} \\ C_{42} & C_{44} \end{bmatrix}; \bar{D}_{21} = \begin{bmatrix} 0 & 0 \\ 0 & 0 \end{bmatrix}; \bar{D}_{22} = \\ & \begin{bmatrix} 0 & 0 \\ 0 & D_{f2} \end{bmatrix}; \bar{K}_{21} = \begin{bmatrix} 0 & 0 \\ 0 & 0 \end{bmatrix}; \bar{K}_{22} = \begin{bmatrix} 0 & 0 \\ 0 & K_{f2} \end{bmatrix}; \mathbf{q}_1 = \begin{bmatrix} q_{r1} \\ q_{f1} \end{bmatrix}; \mathbf{q}_2 = \begin{bmatrix} q_{r2} \\ q_{f2} \end{bmatrix}; \bar{L}_1 = \begin{bmatrix} 1 & 0 \\ 0 & 0 \end{bmatrix}; \\ \bar{L}_2 &= \begin{bmatrix} 0 & 1 \\ 0 & 0 \end{bmatrix}. \end{aligned}$$

Equation (4.50) can be written in the following form that will be used for the control law:

$$\begin{bmatrix} \bar{M}_1^T \\ \bar{M}_2^T \end{bmatrix} \ddot{\bar{\mathbf{q}}} + \begin{bmatrix} \bar{C}_1^T \\ \bar{C}_2^T \end{bmatrix} \dot{\bar{\mathbf{q}}} + \begin{bmatrix} \bar{D}_1^T \\ \bar{D}_2^T \end{bmatrix} \dot{\bar{\mathbf{q}}} + \begin{bmatrix} \bar{K}_1^T \\ \bar{K}_2^T \end{bmatrix} \bar{\mathbf{q}} = \begin{bmatrix} \bar{L}_1 \tau_1 \\ \bar{L}_2 \tau_2 \end{bmatrix} \quad (4.51)$$

$$\begin{aligned} \text{where } \bar{M}_1^T &= [\bar{M}_{11} \quad \bar{M}_{12}]; \bar{C}_1^T = [\bar{C}_{11} \quad \bar{C}_{12}]; \bar{D}_1^T = [\bar{D}_{11} \quad \bar{D}_{12}]; \bar{K}_1^T = [\bar{K}_{11} \quad \bar{K}_{12}]; \bar{M}_2^T = \\ & [\bar{M}_{21} \quad \bar{M}_{22}]; \bar{C}_2^T = [\bar{C}_{21} \quad \bar{C}_{22}]; \bar{D}_2^T = [\bar{D}_{21} \quad \bar{D}_{22}]; \bar{K}_2^T = [\bar{K}_{21} \quad \bar{K}_{22}]. \end{aligned}$$

4.4.2 Distributed control law

For a two-flexible-link manipulator, the control law is developed in two steps. The first consists of developing the control law for the second subsystem (second joint and link) by

assuming that the first subsystem is stable. In the second step, we develop the control law for the first subsystem using the same strategy.

Starting now by the last subsystem, the generalized rigid and flexible coordinates are given by:

$$\bar{\Psi}_2 = [\mathbf{q}_{d1} \quad \mathbf{q}_2]^T = [q_{rd1} \quad q_{fd1} \quad q_{r2} \quad q_{f2}]^T \quad (4.52)$$

Note that, for the first subsystem, the rigid and flexible coordinates are the desired coordinates and for the second subsystem they are the controlled ones.

According to dynamical model (4.51), the equation of motion of the second link is given by:

$$\bar{M}_2^T(\bar{\Psi}_2)\ddot{\bar{\Psi}}_2 + \bar{C}_2^T(\bar{\Psi}_2, \dot{\bar{\Psi}}_2)\dot{\bar{\Psi}}_2 + \bar{D}_2^T\dot{\bar{\Psi}}_2 + \bar{K}_2^T\bar{\Psi}_2 = \bar{L}_2\boldsymbol{\tau} = \begin{bmatrix} \tau_2 \\ 0 \end{bmatrix} \quad (4.53)$$

The control law proposed for the second subsystem is given by the following equation:

$$\tau_2 = T_2 + v_{r2} - \delta\tau_{r2} \quad (4.54)$$

where

$$T_2 = \begin{cases} \frac{s_{f2}(v_{f2} + \delta\tau_{f2})}{s_{r2}} & ; s_{r2} \neq 0 \\ 0 & ; s_{r2} = 0 \end{cases} \quad (4.55)$$

$$\mathbf{v}_2 = \begin{bmatrix} v_{r2} \\ v_{f2} \end{bmatrix} = \bar{M}_2^T(\bar{\Psi}_2)\ddot{\bar{\mathbf{u}}} + \bar{C}_2^T(\bar{\Psi}_2, \dot{\bar{\Psi}}_2)\dot{\bar{\mathbf{u}}} + \bar{D}_2^T\dot{\bar{\mathbf{u}}} + \bar{K}_2^T\bar{\mathbf{q}} + \bar{K}_{d2}^T\bar{\mathbf{s}} \quad (4.56)$$

$$\boldsymbol{\delta\tau}_2 = \begin{bmatrix} \delta\tau_{r2} \\ \delta\tau_{f2} \end{bmatrix} = \delta M_2^T \ddot{\bar{\mathbf{u}}} - \delta C_2^T \dot{\bar{\mathbf{u}}} \quad (4.57)$$

where $\bar{K}_2^T = \begin{bmatrix} 0 & 0 & K_{d2r} & 0 \\ 0 & 0 & 0 & K_{d2f} \end{bmatrix}$; K_{d2r} and K_{d2f} are positive constants.

$$\dot{\bar{\mathbf{u}}} = [\dot{\mathbf{u}}_1 \quad \dot{\mathbf{u}}_2]^T = [\dot{u}_{1r} \quad \dot{u}_{1f} \quad \dot{u}_{2r} \quad \dot{u}_{2f}]^T = T_r \dot{\mathbf{u}}; \quad \mathbf{u} = [\dot{u}_{1r} \quad \dot{u}_{2r} \quad \dot{u}_{1f} \quad \dot{u}_{2f}]^T;$$

$$\bar{\mathbf{s}} = [\mathbf{s}_1 \quad \mathbf{s}_2]^T = [s_{1r} \quad s_{1f} \quad s_{2r} \quad s_{2f}]^T = T_r \mathbf{s}; \quad \mathbf{s} = [s_{1r} \quad s_{2r} \quad s_{1f} \quad s_{2f}]^T$$

$$\delta \bar{M}_2^T = [\delta \bar{M}_{21} \quad \delta \bar{M}_{22}]; \quad \delta \bar{C}_2^T = [\delta \bar{C}_{21} \quad \delta \bar{C}_{22}]$$

$$\delta M_{ij} = \left. \frac{\partial M_{ij}(\mathbf{q})}{\partial q_1} \right|_{\mathbf{q}_{1d}} \tilde{\mathbf{q}}_1 + R_{M_{ij}}(\tilde{\mathbf{q}}_1); \quad \delta C_{ij} = \left. \frac{\partial C_{ij}(\mathbf{q}, \dot{\mathbf{q}})}{\partial \mathbf{q}_1} \right|_{\mathbf{q}_{1d}} \tilde{\mathbf{q}}_1 + \left. \frac{\partial C_{ij}(\mathbf{q}, \dot{\mathbf{q}})}{\partial \dot{\mathbf{q}}_1} \right|_{\mathbf{q}_{1d}} \dot{\tilde{\mathbf{q}}}_1 + R_{C_{ij}}(\tilde{\mathbf{q}}_1)$$

$R_{M_{ij}}$ and $R_{C_{ij}}$ are the high order terms of the Taylor series for $M_{ij}(\mathbf{q})$ and $C_{ij}(\mathbf{q}, \dot{\mathbf{q}})$, respectively.

Proceeding to the first subsystem and developing the control law assuming that the second subsystem is stable, the equation of motion of the first subsystem is given by:

$$\bar{M}_1^T(\bar{\mathbf{q}}_1) \ddot{\bar{\mathbf{q}}}_1 + \bar{C}_1^T(\bar{\mathbf{q}}_1, \dot{\bar{\mathbf{q}}}_1) \dot{\bar{\mathbf{q}}}_1 + \bar{D}_1^T \bar{\mathbf{q}}_1 + \bar{K}_1^T \bar{\mathbf{q}}_1 = \bar{L}_1 \boldsymbol{\tau} = \begin{bmatrix} \tau_1 \\ 0 \end{bmatrix} \quad (4.58)$$

where

$$\bar{\mathbf{q}}_1 = [\mathbf{q}_1 \quad \mathbf{q}_{d2}]^T = [q_{r1} \quad q_{f1} \quad q_{rd2} \quad q_{fd2}]^T \quad (4.59)$$

The control law is given by :

$$\tau_1 = T_1 + v_{r1} - \delta \tau_{r1} \quad (4.60)$$

where

$$T_1 = \begin{cases} \frac{s_{f1}(v_{f1} + \delta \tau_{f1})}{s_{r1}} & ; s_{r1} \neq 0 \\ 0 & ; s_{r1} = 0 \end{cases} \quad (4.61)$$

$$\boldsymbol{\nu}_1 = \begin{bmatrix} v_{r1} \\ v_{f1} \end{bmatrix} = \bar{M}_1^T(\bar{\mathbf{q}}_1) \ddot{\bar{\mathbf{u}}} + \bar{C}_1^T(\bar{\mathbf{q}}_1, \dot{\bar{\mathbf{q}}}_1) \dot{\bar{\mathbf{u}}} + \bar{D}_1^T \dot{\bar{\mathbf{u}}} + \bar{K}_1^T \bar{\mathbf{q}} + \bar{K}_{d1}^T \bar{\mathbf{s}} \quad (4.62)$$

$$\boldsymbol{\delta\tau_1} = \begin{bmatrix} \delta\tau_{r1} \\ \delta\tau_{f1} \end{bmatrix} = \delta M_1^T \ddot{\bar{\mathbf{u}}} - \delta C_1^T \dot{\bar{\mathbf{u}}} \quad (4.63)$$

where $K_{d1} = \begin{bmatrix} 0 & 0 & K_{d1r} & 0 \\ 0 & 0 & 0 & K_{d1f} \end{bmatrix}$; K_{d1r} and K_{d1f} are positive constants,

$$\delta \bar{M}_1^T = [\delta \bar{M}_{11} \ \delta \bar{M}_{12}]_{2 \times 4}; \delta \bar{C}_1^T = [\delta \bar{C}_{11} \ \delta \bar{C}_{12}]_{2 \times 4}.$$

$$\delta M_{ij} = \left. \frac{\partial M_{ij}(\mathbf{q})}{\partial \mathbf{q}_2} \right|_{q_{2d}} \tilde{\mathbf{q}}_2 + R_{M_{ij}}(\tilde{\mathbf{q}}_2); \delta C_{ij} = \left. \frac{\partial C_{ij}(\mathbf{q}, \dot{\mathbf{q}})}{\partial \mathbf{q}_2} \right|_{q_{2d}} \tilde{\mathbf{q}}_2 + \left. \frac{\partial C_{ij}(\mathbf{q}, \dot{\mathbf{q}})}{\partial \dot{\mathbf{q}}_2} \right|_{q_{2d}} \dot{\tilde{\mathbf{q}}}_2 + R_{C_{ij}}(\tilde{\mathbf{q}}_2)$$

$R_{\bar{M}_{1j}}$ and $R_{\bar{C}_{1j}}$ are the high order terms of the Taylor series for $\bar{M}_{2j}(\mathbf{q})$ and $\bar{C}_{2j}(\mathbf{q}, \dot{\mathbf{q}})$, respectively.

4.4.3 Experimental results

In this section, the control strategies presented in the previous sections are tested on the two-degree-of-freedom (dof) Serial Flexible Link robot (Figure 4.33) manufactured by Quanser. The system parameters are given in Table 4.1. The system consists of two motors, two serial flexible links actuated by dc motors, and two strain gauges clamped at the base of each flexible beam, used for measurement of tips deflection.



Figure 4.4 Quanser two link flexible robot.

Table 4.1 System physical parameters

Parameter	Link 1	Link 2
Link length (L_i)	0.202 m	0.2 m
Elasticity	$2.068 \cdot 10^{11} \text{ N/m}^2$	$2.068 \cdot 10^{11} \text{ N/m}^2$
Link moment of inertia	0.17 kg.m^2	$0.0064 \cdot 10^{-6} \text{ kg.m}^2$
Gear ratio	100	50
Rotor moment of inertia	$6.28 \cdot 10^{-6} \text{ kg.m}^2$	$1.03 \cdot 10^{-6} \text{ kg.m}^2$
Drive moment of inertia	$7.63 \cdot 10^{-4} \text{ kg.m}^2$	$44.55 \cdot 10^{-6} \text{ kg.m}^2$
Drive Torque constant	0.119 Nm/A	0.0234 N.m/A
Maximum Rotation	+/- 90 deg	+/- 90 deg

The experimental setup of the two link serial flexible manipulator robot is shown in Figure 4. The main components of the setup are: a linear amplifier, Q8 terminal board, DAQ system, sensors such as strain gauges, encoder and limit switches. The interface between the computer and the setup is the Quanser Q8 data acquisition board. Simulink with Real-Time Workshop (RTW) of Mathworks® is used for real-time implementation of the proposed controllers. Q8 software is used to transform the data from the computer to the system, which allows the SIMULINK models to run in real-time target. The torque input provided by the control algorithm is sent to the robot through Q8 data acquisition and the linear current amplifier. A current sensor measures the current of each actuator.

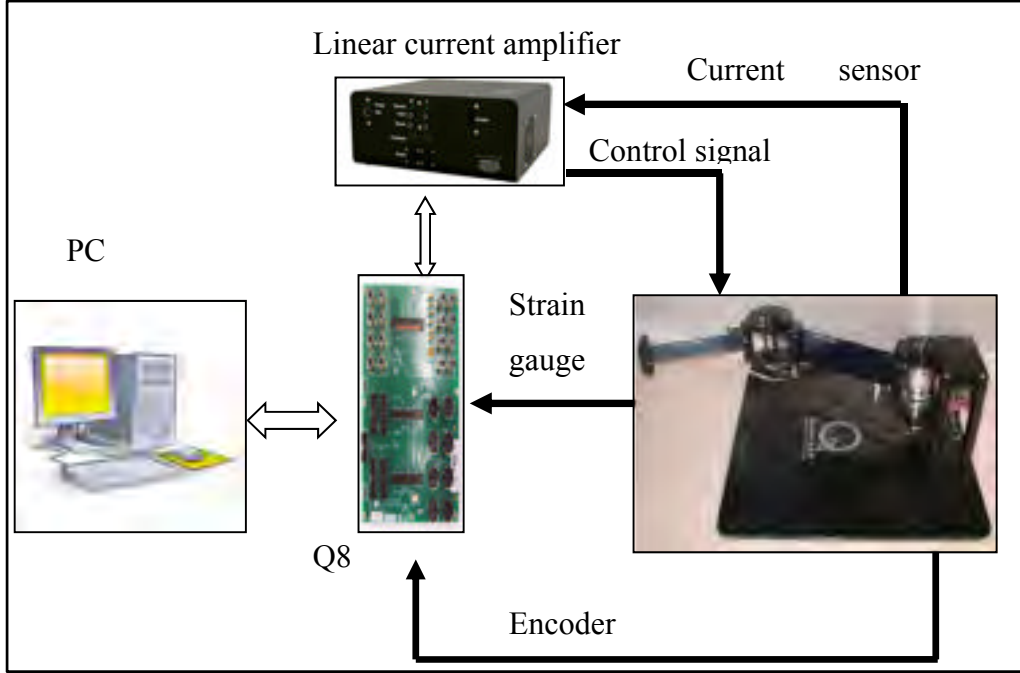


Figure 4.5 Real-Time setup.

The desired trajectory of the joint takes up a polynomial function given by the following expressions (Craig, 2005):

$$q_{rd1}(t) = a_{10} + a_{11}t + a_{12}t^2 + a_{13}t^3 + a_{14}t^4 + a_{15}t^5 \quad (4.64)$$

$$q_{rd2}(t) = a_{20} + a_{21}t + a_{22}t^2 + a_{23}t^3 + a_{24}t^4 + a_{25}t^5 \quad (4.65)$$

$$q_{fd1}(t) = q_{fd2}(t) = 0$$

for $0 \leq t \leq T_f = 5s$. For $t \geq T_f$, $q_{rd1}(t) = \frac{\pi}{4}$ and $q_{rd2}(t) = \frac{\pi}{8}$.

The desired trajectories are given in Figure 4.6.

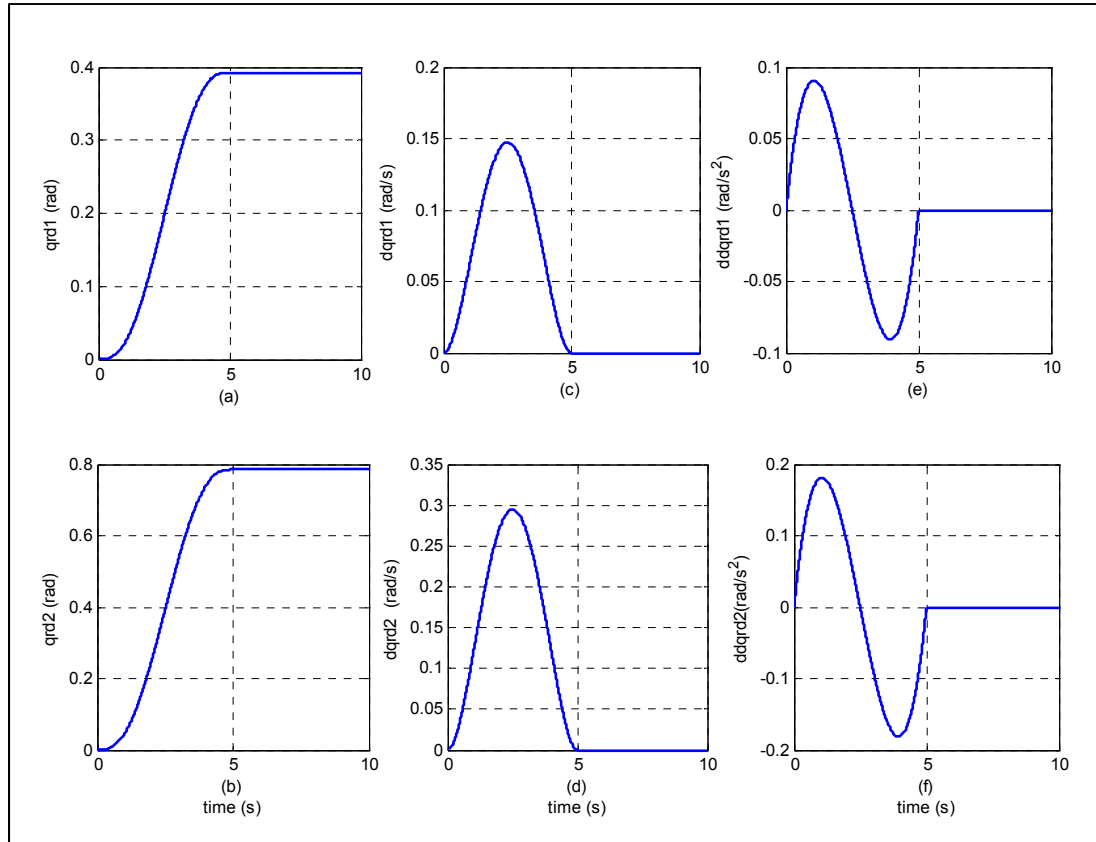


Figure 4.6 Desired trajectories: (a)-(b) position, (c)-(d) velocity, (e)-(f) acceleration of rigid part.

The controller's gains are chosen using a trial and error method as follows: For the distributed control strategy, the selected gains are: $K_{d1r} = 15$; $K_{d1f} = 10$, $K_{d2r} = 25$ and $K_{d2f} = 10$.

The previous theoretical development of the control law that ensures the global stability is given in the general case, i.e. for any high order in the Taylor series. In the real-time implementation, a finite order is fixed. In this section, and for simplicity, the Taylor series is limited to the first order. Then, $R_{M_{ij}} = R_{C_{ij}} = 0$.

The experimental results for the distributed control are shown in Figures 4.7-4.9.

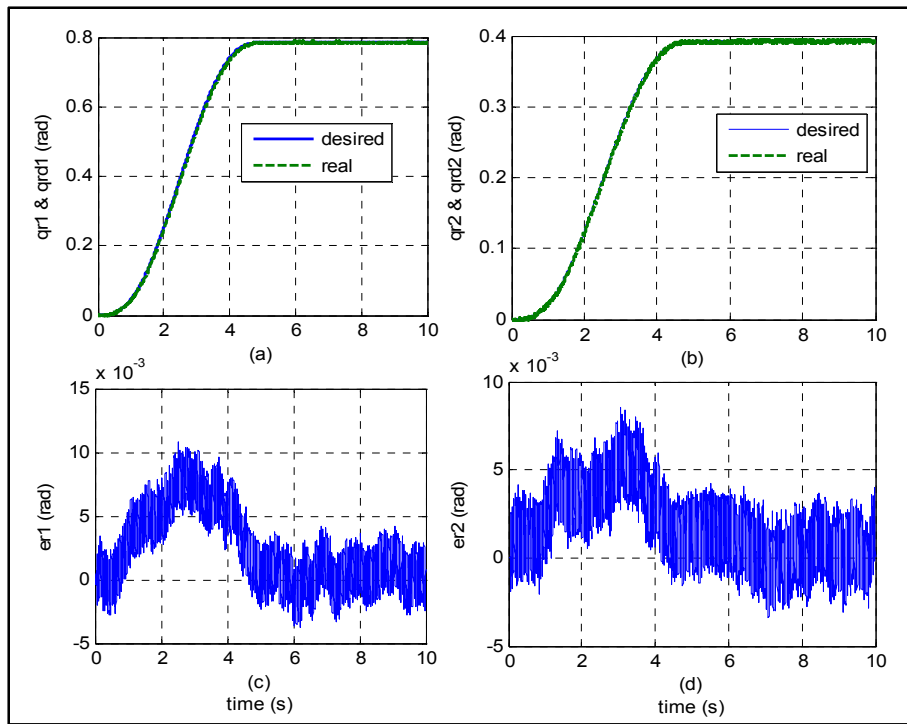


Figure 4.7 Distributed control: (a)-(b) joint tracking trajectories,
(c)-(d) joint tracking errors.

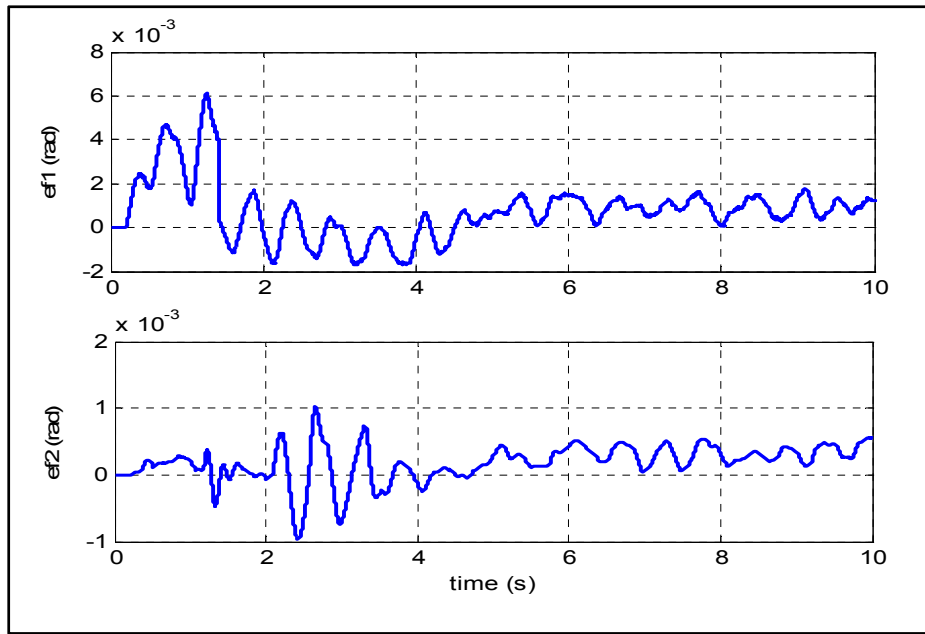


Figure 4.8 Distributed control: errors of flexible parts.

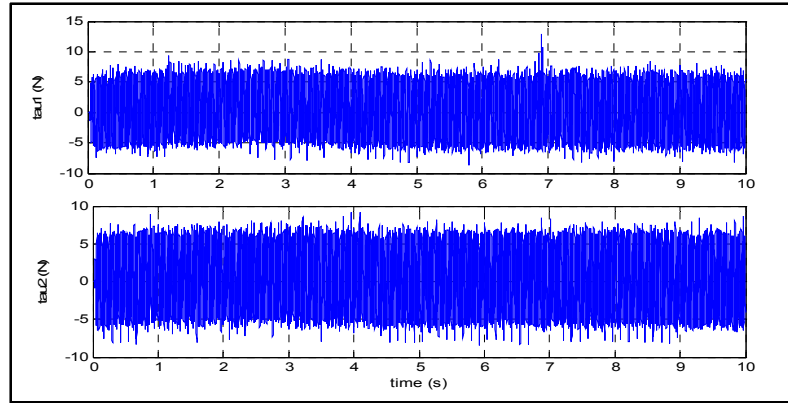


Figure 4.9 Distributed control: input torque.

The results of the developed distributed control method were compared with a PD type control to show the contribution of this proposed control strategy using the same desired trajectories. The PD control law can be written as follows:

$$\tau = K_p(q - q_d) + K_d(\dot{q} - \dot{q}_d) \quad (4.66)$$

where K_p and K_d are constant gain matrices. $Kp = diag(10,10,10,10)$ and $Kd = diag(8,8,8,8)$

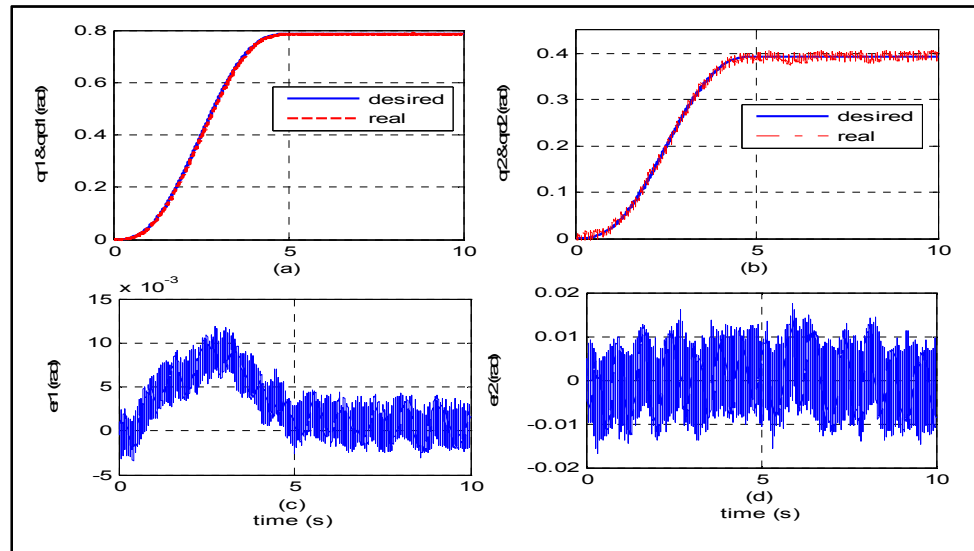


Figure 4.10 PD control: (a)-(b) joint tracking trajectories, (c)-(d) joint tracking errors.

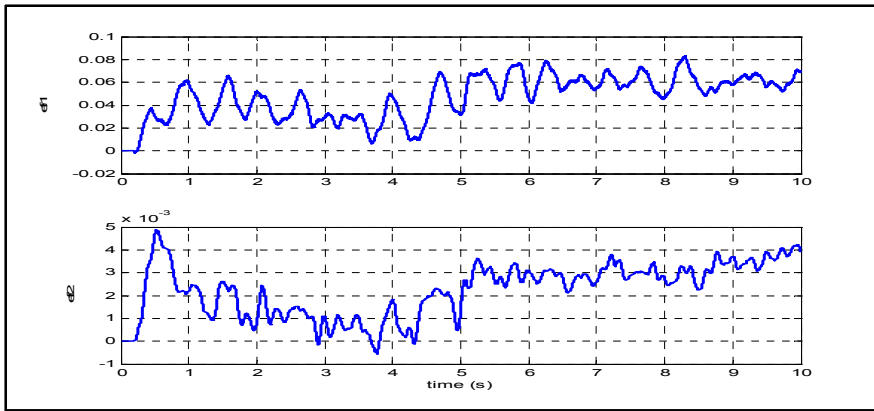


Figure 4.11 PD control : errors of flexible parts.

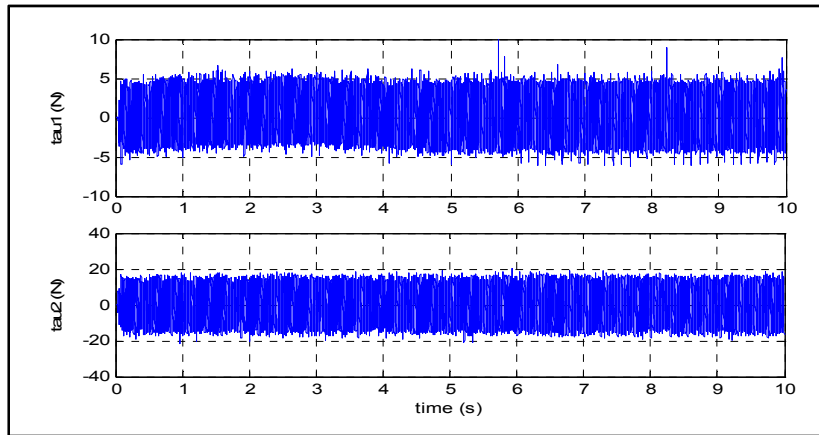


Figure 4.12 PD control: input torques.

According to the experimental results, for the distributed control strategy, a good tracking in the joint space is shown in Figure 4.7. This good tracking is confirmed by the very small tracking errors, less than 0.01 rad for the first joint and 0.008 rad for the second joint. For the flexible coordinates, a small error was obtained not exceeding 0.006 rad as shown in Figure 4.8. The input torque is shown in Figure 4.9. The errors obtained explain the ability of the distributed control strategy to cancel vibration in the links. The results of the distributed control strategy were compared with the PD controller results (Figures 4.10-4.12). For the distributed control method, the tracking errors of the joints and the links' vibrations are smaller than those resulting from the PD controller. Finally, we can conclude that the

distributed control strategy eliminates vibration and gives good tracking of the desired trajectories.

4.5 Conclusion

This paper presents a distributed control strategy for flexible-link manipulators. This strategy consists to start by controlling the last subsystem composed of the n^{th} joint and link by assuming that the remaining subsystems are stable. Then, working backward one subsystem at a time toward the first subsystem, we use the same strategy. The global stability is proven using Lyapunov approach. Experimental results, compared with a PD control, show that the distributed control strategy gives good tracking and cancels the links' vibration.

4.6 Appendix

Proof of proposition 4.1

Let us define the second term of the error dynamics (4.37) as follows:

$$\boldsymbol{\tau}_s = M(\boldsymbol{q})\ddot{\boldsymbol{u}} + C(\boldsymbol{q}, \dot{\boldsymbol{q}})\dot{\boldsymbol{u}} + D\dot{\boldsymbol{u}} + K_d\boldsymbol{s} + K\boldsymbol{q} - L\boldsymbol{\tau} \quad (4.67)$$

Using the transformation (4.6), the previous error dynamics is equivalent to :

$$\bar{\boldsymbol{\tau}}_s = \bar{M}(\boldsymbol{q})\ddot{\bar{\boldsymbol{u}}} + \bar{C}(\boldsymbol{q}, \dot{\boldsymbol{q}})\dot{\bar{\boldsymbol{u}}} + \bar{D}\dot{\bar{\boldsymbol{u}}} + \bar{K}_d\bar{\boldsymbol{s}} + \bar{K}\bar{\boldsymbol{q}} - \bar{L}\boldsymbol{\tau} \quad (4.68)$$

where $\bar{M}(\boldsymbol{q}) = T_r M(\boldsymbol{q}) T_r^{-1}$; $\bar{C}(\boldsymbol{q}, \dot{\boldsymbol{q}}) = T_r C(\boldsymbol{q}, \dot{\boldsymbol{q}}) T_r^{-1}$; $\bar{D} = T_r D T_r^{-1}$; $\bar{K} = T_r K T_r^{-1}$; $\bar{L} = T_r L$; $\dot{\bar{\boldsymbol{u}}} = T_r \dot{\boldsymbol{u}}$, $\bar{\boldsymbol{s}} = T_r \boldsymbol{s}$ and $\bar{\boldsymbol{\tau}}_s = T_r \boldsymbol{\tau}_s$

For the i^{th} subsystem $\boldsymbol{\tau}_{si}$ is given as:

$$\boldsymbol{\tau}_{si} = \bar{M}_i^T(\boldsymbol{q})\ddot{\bar{\boldsymbol{u}}} + \bar{C}_i^T(\boldsymbol{q}, \dot{\boldsymbol{q}})\dot{\bar{\boldsymbol{u}}} + \bar{D}_i^T\dot{\bar{\boldsymbol{u}}} + \bar{K}_i^T\bar{\boldsymbol{q}} + \bar{K}_{di}^T\bar{\boldsymbol{s}} - \bar{L}_i\boldsymbol{\tau}_i \quad (4.69)$$

where $\bar{M}_i^T(\boldsymbol{q}) = [\bar{M}_{i1} \dots \bar{M}_{in}]^T$; $\bar{C}_i^T(\boldsymbol{q}, \dot{\boldsymbol{q}}) = [\bar{C}_{i1} \dots \bar{C}_{in}]^T$; $\bar{K}_i^T = [\bar{K}_{i1} \dots \bar{K}_{in}]^T$; $\bar{D}_i^T = [\bar{D}_{i1} \dots \bar{D}_{in}]^T$; $\bar{K}_{di}^T = [\bar{K}_{di1} \dots \bar{K}_{din}]^T$ and $\bar{L}_i = \begin{bmatrix} 0 & \dots & 010 & \dots & 0 \\ 0 & \dots & 000 & \dots & 0 \end{bmatrix}_{2 \times n}$.

Using Taylor series, we can write:

$$\begin{aligned}\bar{M}_{ij}(\mathbf{q}) &= \bar{M}_{ij}(\bar{\mathbf{q}}) = \bar{M}_{ij}(\bar{\mathbf{q}}_i) + D\bar{M}_{ij}(\bar{\mathbf{q}}_i)^T(\bar{\mathbf{q}} - \bar{\mathbf{q}}_i) + \\ &\quad \frac{1}{2!}(\bar{\mathbf{q}} - \bar{\mathbf{q}}_i)^T\{D^2\bar{M}_{ij}(\bar{\mathbf{q}}_i)\}(\bar{\mathbf{q}} - \bar{\mathbf{q}}_i) + \dots\end{aligned}$$

where $D\bar{M}_{ij}(\bar{\mathbf{q}}_i)$ is the gradient of \bar{M}_{ij} evaluated at $\bar{\mathbf{q}} = \bar{\mathbf{q}}_i$ and $D^2\bar{M}_{ij}(\bar{\mathbf{q}}_i)$ is a Hessian matrix. Then, we can write:

$$\begin{aligned}\bar{M}_{ij}(\mathbf{q}) &= \bar{M}_{ij}(\bar{\mathbf{q}}_i) + \frac{\partial \bar{M}_{ij}(\mathbf{q})}{\partial [\mathbf{q}_1 \dots \mathbf{q}_{i-1} \mathbf{q}_{i+1} \dots \mathbf{q}_n]} \left| \begin{array}{c} \mathbf{q}_{1d} \\ \vdots \\ \mathbf{q}_{id} \\ \vdots \\ \mathbf{q}_{(i-1)d} \\ \mathbf{q}_{(i+1)d} \\ \vdots \\ \mathbf{q}_{nd} \end{array} \right| \left[\begin{array}{c} \mathbf{q}_1 - \mathbf{q}_{1d} \\ \vdots \\ \mathbf{q}_{i-1} - \mathbf{q}_{(i-1)d} \\ \mathbf{q}_{i+1} - \mathbf{q}_{(i+1)d} \\ \vdots \\ \mathbf{q}_n - \mathbf{q}_{nd} \end{array} \right] + R_{M_{ij}}(\tilde{\mathbf{q}}_j) \\ &= \bar{M}_{ij}(\bar{\mathbf{q}}_i) - \sum_{\substack{j=1 \\ j \neq i}}^n \frac{\partial \bar{M}_{ij}(\mathbf{q})}{\partial \mathbf{q}_j} \Big|_{\mathbf{q}_{jd}} \tilde{\mathbf{q}}_j + R_{M_{ij}}(\tilde{\mathbf{q}}_j) \\ &= \bar{M}_{ij}(\bar{\mathbf{q}}_i) - \delta \bar{M}_{ij}\end{aligned}$$

where $\delta \bar{M}_{ij} = \sum_{j=1}^n \frac{\partial \bar{M}_{ij}(\mathbf{q})}{\partial \mathbf{q}_j} \Big|_{\mathbf{q}_{jd}}$ $\tilde{\mathbf{q}}_j - R_{M_{ij}}(\tilde{\mathbf{q}}_j)$ and $R_{M_{ij}}$ is the remaining terms given as

$$\text{follows: } R_{M_{ij}}(\tilde{\mathbf{q}}_j) = \bar{M}_{ij}(\mathbf{q}) - \bar{M}_{ij}(\bar{\mathbf{q}}_i) + \sum_{\substack{j=1 \\ j \neq i}}^n \frac{\partial \bar{M}_{ij}(\mathbf{q})}{\partial \mathbf{q}_j} \Big|_{\mathbf{q}_{jd}} \tilde{\mathbf{q}}_j$$

Using the same strategy of Taylor series for M_{ii} we can write:

$$\begin{aligned}\bar{M}_{ii}(\mathbf{q}) &= \bar{M}_{ii}(\bar{\mathbf{q}}) = \bar{M}_{ii}(\bar{\mathbf{q}}_i) - \sum_{\substack{j=1 \\ j \neq i}}^n \frac{\partial \bar{M}_{ii}(\mathbf{q})}{\partial \mathbf{q}_j} \Big|_{\mathbf{q}_{jd}} \tilde{\mathbf{q}}_j + R_{M_{ii}}(\tilde{\mathbf{q}}_j) \\ &= \bar{M}_{ii}(\bar{\mathbf{q}}_i) - \delta \bar{M}_{ii}.\end{aligned}$$

where $\delta \bar{M}_{ii} = \sum_{j=1}^n \frac{\partial \bar{M}_{ii}(\mathbf{q})}{\partial \mathbf{q}_j} \Big|_{\mathbf{q}_{jd}}$ $\tilde{\mathbf{q}}_j + R_{M_{ii}}(\tilde{\mathbf{q}}_j)$. $R_{M_{ii}}$ and $R_{M_{ii}}$ are the high order terms of the

Taylor series for $\bar{M}_{ii}(\mathbf{q})$. Then, we can write:

$$\begin{aligned}\bar{M}_i^T(\boldsymbol{q}) &= \bar{M}_i^T(\bar{\boldsymbol{q}}) = \bar{M}_i^T(\bar{\boldsymbol{q}}_i) - \delta \bar{M}_i^T \\ \bar{C}_i^T(\boldsymbol{q}, \dot{\boldsymbol{q}}) &= \bar{C}_i^T(\bar{\boldsymbol{q}}, \dot{\bar{\boldsymbol{q}}}) = \bar{C}_i^T(\bar{\boldsymbol{q}}_i, \dot{\bar{\boldsymbol{q}}}_i) - \delta \bar{C}_i^T\end{aligned}\quad (4.70)$$

and

$$\bar{\tau}_{si} = \bar{M}_i^T(\bar{\boldsymbol{q}}_i)\ddot{\boldsymbol{u}} + \bar{C}_i^T(\bar{\boldsymbol{q}}_i, \dot{\bar{\boldsymbol{q}}}_i)\dot{\bar{\boldsymbol{u}}} - \delta \bar{M}_i^T \ddot{\boldsymbol{u}} - \delta \bar{C}_i^T \dot{\bar{\boldsymbol{u}}} + \bar{D}_i^T \dot{\bar{\boldsymbol{u}}} + \bar{K}_i^T \bar{\boldsymbol{q}} + \bar{K}_{di}^T \bar{\boldsymbol{s}} - \bar{L}_i \tau_i \quad (4.71)$$

Using (4.30) and (4.31), the equation (4.71) can be written as follows:

$$\bar{\tau}_{si} = \begin{bmatrix} v_{ri}(\bar{\boldsymbol{q}}_i) - \delta \tau_{ri} - \tau_i \\ v_{fi}(\bar{\boldsymbol{q}}_i) + \delta \tau_{fi} \end{bmatrix} \quad (4.72)$$

Using (4.29), we can deduce:

$$\bar{\tau}_{si} = \begin{bmatrix} -T_i \\ v_{fi}(\bar{\boldsymbol{q}}_i) + \delta \tau_{fi} \end{bmatrix} \quad (4.73)$$

Then,

$$M(\boldsymbol{q})\dot{\boldsymbol{s}} + C(\boldsymbol{q}, \dot{\boldsymbol{q}})\boldsymbol{s} + D\boldsymbol{s} + K_d\boldsymbol{s} = \begin{bmatrix} -\boldsymbol{T} \\ v_f + \boldsymbol{\delta\tau}_f \end{bmatrix} \quad (4.74)$$

CHAPITRE 5

ARTICLE 4: ADAPTIVE CONTROL FOR FLEXIBLE LINK MANIPULATORS USING DISTRIBUTED CONTROL STRATEGY

Fareh Raouf¹ Saad Mohamad² and Saad Maarouf¹

¹Electrical Engineering Department, Université du Québec, École de technologie supérieure,
1100, rue Notre-Dame ouest, Montréal (Québec), H3C 1K3, Canada

²School of Engineering, Université du Québec en Abitibi-Témiscamingue, 445, boul. de
l'Université, Rouyn-Noranda (Québec), J9X 5E4

Article soumis à la revue «Robotics and Autonomous Systems » en Février 2013.

Abstract: This paper presents an adaptive distributed control strategy for n-serial-flexible-link manipulators. The proposed adaptive controller is used for flexible-link-manipulators 1) to solve the tracking control problem in the joint space and 2) to cancel vibrations of the links. The dynamical model of flexible link manipulators is reorganized to take the form of n interconnected subsystems. Each subsystem has a pair of one joint and one link. The system parameters are supposed unknown. The adaptive distributed strategy controls one subsystem in each step starting from the last subsystem. The nth subsystem is controlled by assuming that the remaining subsystems are stable. Then, proceeding backward to (n-1)th system, the same strategy is applied, and so one until the first subsystem is reached. The gradient-based estimator is used to estimate the parameters of each subsystem. The control law of the ith subsystem uses its own estimated parameters and the estimated parameters of all upper-level subsystems. Global stability of error dynamics is proved using the Lyapunov approach. This algorithm was implemented in real time on a two-flexible-link-manipulator and a comparison with the non-adaptive version shows the effectiveness of this approach.

Key Words: Hierarchical control, adaptive control, flexible-link manipulators, stability, identification.

5.1 Introduction

Flexible link manipulators present some inherent advantages over conventional rigid robots such as lower energy consumption, faster response, relatively smaller actuators, higher payload-to-weight ratio and less overall cost. They can be found in a large diversity of applications such as: nuclear maintenance, microsurgery, space robots, contouring control, collision control, pattern recognition, and many others. Due to all these advantages and applications, the control of flexible link manipulators has received considerable attention in the literature [1, 2]. Flexible link manipulators are multivariable systems and their dynamics are strongly coupled and highly nonlinear. The dynamical model of flexible manipulators can be considered as one multi-input and multi-output (MIMO) system and one controller is considered for all links and joints. Many control strategies are proposed in the literature using this configuration. When the system parameters are known, linear control [3-5], feedback control [6-8], and sliding-mode control [9-12] have been proposed for flexible link manipulators' control problems. A proportional, integral, derivative (PID) controller was used in [4] to control the flexible manipulator. The controller is presented as a general second order linear regulator and its parameters were systematically chosen by pole placement. A feedback control using conventional motor with a gear actuator affected by non-linear friction torque is presented in [8] to solve the tracking problem in joint space of a flexible manipulator. A sliding mode controller is proposed in [10] for a two-link flexible manipulator to control the end-point position. An inverse dynamics terminal sliding mode control strategy is proposed. Adaptive control is used when the system parameters are unknown [13-16]. Non-adaptive and adaptive controllers were proposed in [16] for a one flexible link manipulator to track desired trajectories in the joint space. The asymptotical stability of the error dynamics is proved using Lyapunov theory.

When using the dynamical model as one MIMO system, all joints and links are controlled by a single controller. In this case, the control structure becomes more complex and the real time implementation in industrial applications is not easy [17]. To overcome this problem, the dynamical model of a flexible manipulator can be viewed as an interconnection of multiple

subsystems where each subsystem is controlled using one controller. In this case, many advantages are offered, such as simplicity of implementation, fault tolerance, reduction of computational effort, etc. Using this configuration, decentralized control was proposed in [18-20] for flexible link manipulators. An indirect adaptive decentralized control for a class of two time scale interconnected systems is proposed in [18]. The dynamics of the slow subsystem are developed using the integral manifold and the dynamics of the fast mode are presented by the fast subsystem. The adaptive controller uses the effects of unmodeled dynamics, identification errors, and parameter variations. Distributed control strategy was used in [21] to track desired trajectories in the workspace for a two-flexible-link manipulator. The redefinition output technique was used to select a non-collocated output, ensuring stability of internal dynamics. The control strategy consists in starting by stabilizing the last link while considering the remaining links stable. Then, the same strategy is applied backward until the first link. Only local stability was proved for this control strategy. The distributed control strategy was applied in [22, 23] to track workspace trajectories for rigid manipulators.

In this paper, the distributed control strategy is modified to take into account the flexibility of the links. In contrast to rigid manipulators, flexible manipulators are under-actuated systems, i.e. the deflection variables are not actuated. In this case, a subsystem has two parts: in addition to joints as in a rigid manipulator, it must also include the corresponding flexible link. The dynamical model is reorganized, in the first step, to take the form of n interconnected subsystems using a non-singular transformation matrix. In this form, each subsystem contains its own parameters and the parameters of upper level subsystems. Then, distributed control strategy is used from the last subsystem proceeding backwards until the first one. Each subsystem is controlled by assuming that the remaining subsystems are stable and follow their desired trajectories. The unknown parameters of the last subsystem are estimated and used for the lower level $(n-1)^{th}$ subsystem. The control law of each subsystem is developed using its own estimated parameters and the parameters which were estimated in the previous steps. Lyapunov theory is used to conclude the global stability. A real-time

implementation of a two-flexible-link manipulator is given as an example of the proposed control strategy and to show the effectiveness of this controller.

The paper is organized as follows: section 5.2 presents the modeling and problem formulation. The distributed adaptive control strategy of a multi-flexible-link manipulator is presented in section 5.3. Section 5.4 presents the stability analysis of the errors dynamics. In section 5.5, the proposed control strategy is applied to two-flexible-link manipulator and experimental results are shown. Finally, conclusions are given in section 5.6.

5.2 Modeling and problem formulation

The n-flexible-link manipulator is shown in Figure 5.1. The links are presented in a cascade form and actuated with individual motors. An inertial payload is clamped to the end effectors. The motion of each link is assumed to be in the horizontal plane and has a very small deflection. Using Lagrange equations, the dynamical model of an n DOF flexible manipulator is given by (De Luca et Siciliano, 1991):

$$M(q)\ddot{q} + C(q, \dot{q})\dot{q} + D\dot{q} + Kq = L\tau \quad (5.1)$$

where M is the inertia and mass matrix, $C(q, \dot{q})\dot{q}$ is the Coriolis and centrifugal forces vector, D is the friction matrix and K is the rigidity matrix. q represents the vector of the generalized coordinates and τ is the vector of the applied torques. For n rigid coordinates and n flexible links, the deformation of the i^{th} flexible link is given as follows:

$$v_i(x, t) = \sum_{j=1}^{z_i} \phi_{ij}(x) q_{fij}(t) \quad i = 1, \dots, n \quad (5.2)$$

where q_{fij} is the j^{th} generalized flexible coordinate, $\phi_{ij}(x)$ is its j^{th} shape function and z_i is the number of the retained flexible modes of the i^{th} flexible link. The total number of the flexible modes is $z = \sum_{i=1}^n z_i$ and the number of the rigid modes is n .

Usually, the dynamical model (5.1) is written as couples of rigid and flexible parts as follows:

$$\begin{bmatrix} M_r & M_{rf} \\ M_{rf}^T & M_f \end{bmatrix} \begin{bmatrix} \ddot{q}_r \\ \ddot{q}_f \end{bmatrix} + \begin{bmatrix} C_r & C_{rf} \\ C_{rf}^T & C_f \end{bmatrix} \begin{bmatrix} \dot{q}_r \\ \dot{q}_f \end{bmatrix} + \begin{bmatrix} 0 & 0 \\ 0 & D_f \end{bmatrix} \begin{bmatrix} \dot{q}_r \\ \dot{q}_f \end{bmatrix} + \begin{bmatrix} 0 & 0 \\ 0 & K_f \end{bmatrix} \begin{bmatrix} q_r \\ q_f \end{bmatrix} = \begin{bmatrix} \tau \\ 0 \end{bmatrix} \quad (5.3)$$

where M_r and M_f are the mass and inertia matrices for the rigid and the flexible parts respectively. M_{rf} is a coupled element. The same decomposition is used for the Coriolis matrix $C(q, \dot{q})$. K_f is the stiffness diagonal matrix and D_f is the damping diagonal matrix of the flexible part. The subscripts r and f denote the rigid and flexible modes. In this work we consider only the first flexible mode of each link, then: $z_i = 1$ and $z=n$.

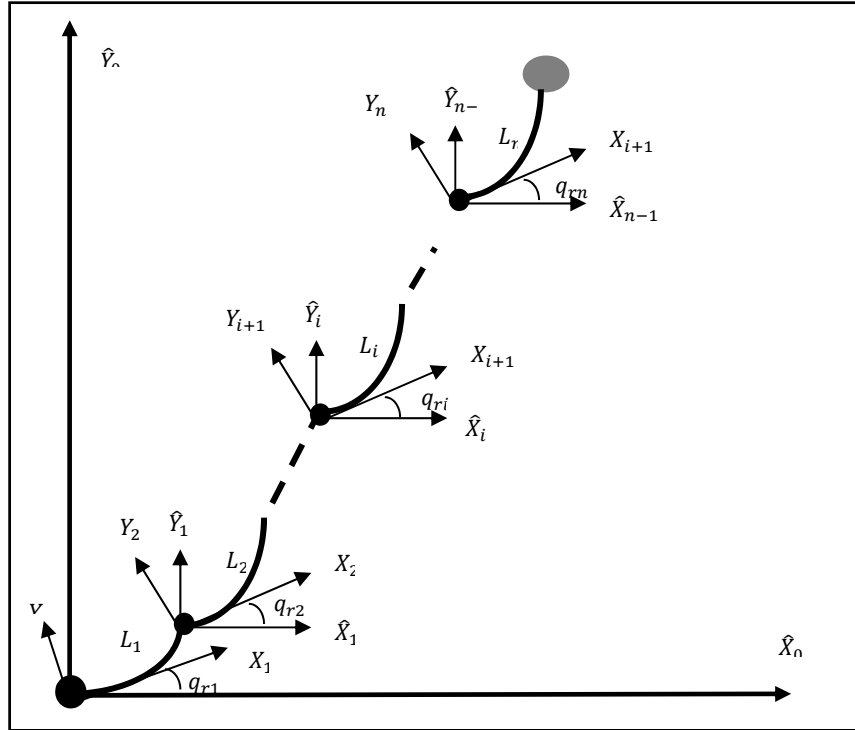


Figure 5.1 Flexible-link manipulator.

In general, the dynamical model is written as rigid and flexible parts as given in (5.3). The generalized coordinate ($q = [q_r \ q_f]^T$) includes the rigid coordinates in the first n elements and the remaining elements are the flexible coordinates. In this paper, to develop the distributed control law, we need to reorganise the elements given in the generalized coordinates and the dynamical model to take the form of n -interconnected subsystems. Each

subsystem has a pair of a joint and a link ($q_i = [q_{ri} \ q_{fi}]^T$). Then, there exists a non-singular matrix of transformation T_r such as:

$$\bar{q} = T_r q \quad (5.4)$$

where $q = [q_r \ q_f]^T = [q_{r1} \ \dots \ q_{rn} \ q_{f1} \ \dots \ q_{fn}]^T$ is the old generalized coordinate, $\bar{q} = [q_1 \ \dots \ q_i \ \dots \ q_n]^T = [q_{r1} \ q_{f1} \ \dots \ q_{ri} \ q_{fi} \ \dots \ q_{rn} \ q_{fn}]^T$ is the new one, $q_i = [q_{ri} \ q_{fi}]^T$ is the generalized coordinate associated with the i^{th} subsystem (i^{th} joint and link) and the matrix of transformation T_r is given by:

$$T_r = q_i \begin{bmatrix} 1 & 2 & \dots & i & \dots & n & n+1 & \dots & n+i & \dots & 2n \\ \hline 1 & 0 & \dots & 0 & 0 & 0 & 0 & 0 & 0 & \dots & 0 & 0 & 0 \\ 0 & 0 & \dots & 0 & 0 & 0 & 0 & 0 & 0 & \dots & 0 & 0 & 0 \\ & & & & & & & & & \vdots & & & \\ & & & & & & & & & & & & \\ 0 & 0 & \dots & 0 & 1 & 0 & \dots & 0 & 0 & 0 & 0 & 0 & 0 \\ 0 & 0 & \dots & 0 & 0 & 0 & \dots & 0 & 0 & 0 & 0 & 1 & 0 \\ & & & & & & & & & & & & \\ & & & & & & & & & & & & \\ 0 & 0 & \dots & 0 & 0 & 0 & \dots & 0 & 0 & 1 & 0 & 0 & 0 \\ 0 & 0 & \dots & 0 & 0 & 0 & \dots & 0 & 0 & 0 & 0 & 0 & 1 \end{bmatrix} \quad (5.5)$$

Using (5.4), the dynamical model (5.1) can be written as follows:

$$M(q)T_r^{-1}\ddot{\bar{q}} + C(q, \dot{q})T_r^{-1}\dot{\bar{q}} + DT_r^{-1}\dot{\bar{q}} + KT_r^{-1}\bar{q} = L\tau \quad (5.6)$$

where $\ddot{\bar{q}} = T_r\ddot{q}$ and $\dot{\bar{q}} = T_r\dot{q}$.

Equation (5.6) is equivalent to the following expression:

$$\bar{M}(q)\ddot{\bar{q}} + \bar{C}(q, \dot{q})\dot{\bar{q}} + \bar{D}\dot{\bar{q}} + \bar{K}\bar{q} = \bar{L}\tau \quad (5.7)$$

where $\bar{M}(q) = T_r M(q) T_r^{-1}$; $\bar{C}(q, \dot{q}) = T_r C(q, \dot{q}) T_r^{-1}$; $\bar{D} = T_r D T_r^{-1}$; $\bar{K} = T_r K T_r^{-1}$, $\bar{L} = T_r L$.

$$\bar{q} = \left[\underbrace{q_{r1} \ q_{f1}}_{q_1} \ \dots \ \underbrace{q_{ri} \ q_{fi}}_{q_i} \ \dots \ \underbrace{q_{rn} \ q_{fn}}_{q_n} \right]^T.$$

The obtained dynamical model (5.7) takes the form of n interconnected subsystems given as follows:

$$\begin{bmatrix} \bar{M}_1^T(q) \\ \vdots \\ \bar{M}_n^T(q) \end{bmatrix} \begin{bmatrix} \ddot{q}_1 \\ \vdots \\ \ddot{q}_n \end{bmatrix} + \begin{bmatrix} \bar{C}_1^T(q, \dot{q}) \\ \vdots \\ \bar{C}_n^T(q, \dot{q}) \end{bmatrix} \begin{bmatrix} \dot{q}_1 \\ \vdots \\ \dot{q}_n \end{bmatrix} + \begin{bmatrix} \bar{D}_1^T \\ \vdots \\ \bar{D}_n^T \end{bmatrix} \begin{bmatrix} \dot{q}_1 \\ \vdots \\ \dot{q}_n \end{bmatrix} + \begin{bmatrix} \bar{K}_1^T \\ \vdots \\ \bar{K}_n^T \end{bmatrix} \begin{bmatrix} q_1 \\ \vdots \\ q_n \end{bmatrix} = \begin{bmatrix} \bar{L}_1 \\ \vdots \\ \bar{L}_n \end{bmatrix} \tau \quad (5.8)$$

where $q_i = [q_{ri} \ q_{fi}]^T$; $\bar{M}_i^T = [\bar{M}_{i1} \ \dots \ \bar{M}_{ii} \ \dots \ \bar{M}_{in}]_{2 \times 2n}$;

$\bar{C}_i^T = [\bar{C}_{i1} \ \dots \ \bar{C}_{ii} \ \dots \ \bar{C}_{in}]_{2 \times 2n}$; $\bar{D}_i^T = [0 \ \dots \ 0 \ \bar{D}_{ii} \ 0 \ \dots \ 0]_{2 \times 2n}$;

$$\bar{K}_i^T = [0 \ \dots \ 0 \ \bar{K}_{ii} \ 0 \ \dots \ 0]_{2 \times 2n}, \bar{M}_{ij} = \begin{bmatrix} M_{r\bar{M}_{ij}} & M_{rf\bar{M}_{ij}} \\ M_{rf\bar{M}_{ij}} & M_{f\bar{M}_{ij}} \end{bmatrix}_{2 \times 2}; \bar{C}_{ij} = \begin{bmatrix} C_{r\bar{C}_{ij}} & C_{rf\bar{C}_{ij}} \\ C_{rf\bar{C}_{ij}} & C_{f\bar{C}_{ij}} \end{bmatrix}; \bar{D}_{ii} = \begin{bmatrix} 0 & 0 \\ 0 & D_{fi} \end{bmatrix}; \bar{K}_{ii} = \begin{bmatrix} 0 & 0 \\ 0 & K_{fi} \end{bmatrix}; \bar{L}_i = \begin{bmatrix} 0 & \dots & 0 & 1 & 0 & \dots & 0 \\ 0 & \dots & 0 & 0 & 0 & \dots & 0 \end{bmatrix}_{2 \times n}.$$

Let us define the sliding surface as follows:

$$s = \begin{bmatrix} s_r \\ s_f \end{bmatrix} = \begin{bmatrix} \dot{\tilde{q}}_r + \lambda_r \tilde{q}_r \\ \dot{\tilde{q}}_f + \lambda_f \tilde{q}_f \end{bmatrix} = \begin{bmatrix} \dot{q}_{rd} - \dot{q}_r + \lambda_r \tilde{q}_r \\ \dot{q}_{fd} - \dot{q}_f + \lambda_f \tilde{q}_f \end{bmatrix} = \begin{bmatrix} \dot{u}_r - \dot{q}_r \\ \dot{u}_f - \dot{q}_f \end{bmatrix} = \dot{u} - \dot{q} \quad (5.9)$$

We can also write: $s = [s_r \ s_f]^T = [s_{r1} \ \dots \ s_{rn} \ s_{f1} \ \dots \ s_{fn}]^T$

Using the transformation matrix, a new form of the sliding surface can be written as follows:

$$\bar{s} = T_r s = [s_1 \ \dots \ s_i \ \dots \ s_n]^T = [s_{r1} \ s_{f1} \ \dots \ s_{ri} \ s_{fi} \ \dots \ s_{rn} \ s_{fn}]^T \quad (5.10)$$

The same idea is used for u , then $\dot{u} = [\dot{u}_r \ \dot{u}_f]^T = [\dot{u}_{r1} \ \dots \ \dot{u}_{rn} \ \dot{u}_{f1} \ \dots \ \dot{u}_{fn}]^T$ and

$$\begin{aligned} \dot{\bar{u}} &= T_r \dot{u} = [\dot{u}_1 \ \dots \ \dot{u}_i \ \dots \ \dot{u}_n]^T \\ &= [\dot{u}_{r1} \ \dot{u}_{f1} \ \dots \ \dot{u}_{ri} \ \dot{u}_{fi} \ \dots \ \dot{u}_{rn} \ \dot{u}_{fn}]^T \end{aligned} \quad (5.11)$$

The properties that will be used in the control law development can be deduced from the dynamical model as follows:

P1: $M, M_{rr}, M_{ff}, D_{ff}$ and K_{ff} are symmetric positive definite matrices.

P2: The inertia-mass matrix $M(q)$ and the Coriolis matrix $C(q, \dot{q})$ satisfy the following skew-symmetric property:

$$X^T(\dot{M}(q, \dot{q}) - 2C(q, \dot{q}))X = 0 \quad \forall X \in \mathcal{R}^{n+z} \quad (5.12)$$

Let the desired trajectory associated to the rigid part of the i^{th} subsystem, its first and second-order derivatives be $q_{\text{rdi}}(t), \dot{q}_{\text{rdi}}(t)$ and $\ddot{q}_{\text{rdi}}(t)$ respectively, and $q_{\text{fdi}}(t), \dot{q}_{\text{fdi}}(t)$ and $\ddot{q}_{\text{fdi}}(t)$ are those associated to the flexible part of this subsystem. The objective is to track the desired trajectories in the joint space and cancel the vibrations of the links. The desired positions of the flexible modes are then set to zero.

5.3 Adaptive distributed control strategy

This section presents the development of a distributed adaptive control strategy for n -flexible-link manipulator to track desired trajectories in the joint space while reducing links vibrations. The distributed control strategy consists in controlling the flexible manipulator starting by the last subsystem and then working backward until the first one. Each subsystem is controlled by assuming that the remaining ones are stable. For the n^{th} subsystem, the equation of motion is derived from (5.8) as follows:

$$\bar{M}_n^T(q)\ddot{\bar{q}} + \bar{C}_n^T(q, \dot{q})\dot{\bar{q}} + \bar{D}_n^T\dot{\bar{q}} + \bar{K}_n^T\bar{q} = \bar{L}_n\tau \quad (5.13)$$

where $\bar{M}_n^T = [\bar{M}_{n1} \dots \bar{M}_{ni} \dots \bar{M}_{nn}]_{2 \times 2n}$; $\bar{C}_n^T = [\bar{C}_{n1} \dots \bar{C}_{ni} \dots \bar{C}_{nn}]_{2 \times 2n}$;

$\bar{D}_n^T = [0_{2 \times 2} \dots 0_{2 \times 2} \bar{D}_{nn}]_{2 \times 2n}$; $\bar{K}_n^T = [0_{2 \times 2} \dots 0_{2 \times 2} \bar{K}_{nn}]_{2 \times 2n}$ and $\bar{L}_n = \begin{bmatrix} 0 & 0 & \dots & 1 \\ 0 & 0 & \dots & 0 \end{bmatrix}_{2 \times n}$.

The generalized coordinate associate to the n^{th} subsystem is given by:

$$\begin{aligned}\bar{Q}_n &= [q_{rd1} \quad q_{fd1} \quad \cdots \quad q_{rd(n-1)} \quad q_{fd(n-1)} \quad q_{rn} \quad q_{fn}]^T \\ &= [q_{d1} \quad \cdots \quad q_{d(n-1)} \quad q_n]^T\end{aligned}\tag{5.14}$$

Note that the rigid and flexible coordinates of the n^{th} subsystem are the controlled ones while the rigid and flexible coordinates of the remaining subsystems are the desired ones. Using the new coordinate, the corresponding equation of motion becomes:

$$\bar{M}_n^T(\bar{Q}_n)\ddot{\bar{Q}}_n + \bar{C}_n^T(\bar{Q}_n, \dot{\bar{Q}}_n)\dot{\bar{Q}}_n + \bar{D}_n^T\dot{\bar{Q}}_n + \bar{K}_n^T\bar{Q}_n = \bar{L}_n\tau\tag{5.15}$$

where the velocity $\dot{\bar{Q}}_n$ is the time derivative of \bar{Q}_n and the acceleration $\ddot{\bar{Q}}_n$ is the time derivative of $\dot{\bar{Q}}_n$.

There exists a vector $p_n = \begin{bmatrix} p_{nr} \\ p_{nf} \end{bmatrix} \in \Re^{b_{nr}+b_{nf}}$ with components depending on manipulators' parameters (masses, moments in inertia, etc.), such as:

$$W_n(\bar{Q}_n, \dot{\bar{Q}}_n, t)p_n + RM_n = \bar{M}_n^T(\bar{Q}_n)\ddot{\bar{u}} + \bar{C}_n^T(\bar{Q}_n, \dot{\bar{Q}}_n)\dot{\bar{u}} + \bar{D}_n^T\bar{u}\tag{5.16}$$

where $\dot{\bar{u}}$ is given in (5.11) and $W_n = \begin{bmatrix} W_{nr} & 0 \\ 0 & W_{nf} \end{bmatrix}$ is the regressor matrix which contains all known functions, $W_{nr}^T \in \Re^{b_{nr}}$ and $W_{nf}^T \in \Re^{b_{nf}}$. RM_n is the remaining term which is independent of the parameters p_n .

The control law of the last subsystem can be proposed as follows:

$$\tau_n = K_{dnr}s_{nr} + T_n + W_{nr}\hat{p}_{nr} + RM_{nr} - \delta\tau_{nr}\tag{5.17}$$

where

$$T_n = \begin{cases} \frac{s_{nf}(K_{dnf}s_{nf} + K_{fn}\tilde{q}_{fn} + W_{nf}\hat{p}_{nf} + RM_{nf} + \delta\tau_{nf})}{s_{nr}} & ; s_{nr} \neq 0 \\ 0 & ; s_{nr} = 0 \end{cases}\tag{5.18}$$

$$W_n\hat{p}_n = \begin{bmatrix} W_{nr}\hat{p}_{nr} \\ W_{nf}\hat{p}_{nf} \end{bmatrix} = \widehat{M}_n^T(\bar{Q}_n)\ddot{\bar{u}} + \widehat{C}_n^T(\bar{Q}_n, \dot{\bar{Q}}_n)\dot{\bar{u}} + \widehat{D}_n^T\bar{u}\tag{5.19}$$

$$\delta\tau_n = \begin{bmatrix} \delta\tau_{nr} \\ \delta\tau_{nf} \end{bmatrix} = (\delta\bar{M}_n^T)\ddot{\tilde{u}} + (\delta\bar{C}_n^T)\dot{\tilde{u}} \quad (5.20)$$

and $K_{dn} = \begin{bmatrix} K_{dnr} & 0 \\ 0 & K_{dnf} \end{bmatrix}$; $\delta M_{nj} = \sum_{j=1}^{n-1} \frac{\partial M_{nj}(q)}{\partial q_j} \Big|_{q_{jd}} \tilde{q}_j + \mathcal{O}_{M_{nj}}(\tilde{q}_j)$

$$\delta C_{nj} = \sum_{j=1}^{n-1} \frac{\partial C_{nj}(q, \dot{q})}{\partial q_j} \Big|_{q_{jd}} \tilde{q}_j + \sum_{j=1}^{n-1} \frac{\partial C_{nj}(q, \dot{q})}{\partial \dot{q}_j} \Big|_{q_{jd}} \tilde{\dot{q}}_j + \mathcal{O}_{C_{nj}}(\tilde{q}_j, \tilde{\dot{q}}_j)$$

$\mathcal{O}_{M_{ij}}$ and $\mathcal{O}_{C_{ij}}$ are the high order terms of the Taylor series for $M_{ij}(q)$ and $C_{ij}(q)$, respectively.

The adaptive laws for rigid and flexible parts are given as follows:

$$\begin{aligned} \dot{\hat{p}}_{nr} &= K_{vn} W_{nr}^T s_{nr} \\ \dot{\hat{p}}_{nf} &= K_{vn} W_{nf}^T s_{nf} \end{aligned} \quad (5.21)$$

where K_{vn} and K_{vn} are some positive definite gains.

The same strategy is used backward for the remaining subsystems. Taking for example the i^{th} subsystem, the equation of motion using the new associated coordinate is given as follows:

$$\bar{M}_i^T(\bar{Q}_i)\ddot{\bar{Q}}_i + \bar{C}_i^T(\bar{Q}_i, \dot{\bar{Q}}_i)\dot{\bar{Q}}_i + \bar{D}_i^T\dot{\bar{Q}}_i + \bar{K}_i^T\bar{Q}_i = \bar{L}_i \quad (5.22)$$

where $\bar{M}_i^T = [\bar{M}_{i1} \dots \bar{M}_{ii} \dots \bar{M}_{in}]^T$; $\bar{C}_i^T = [\bar{C}_{i1} \dots \bar{C}_{ii} \dots \bar{C}_{in}]^T$; $\bar{L}_i =$

$$\begin{bmatrix} 0 & \dots & 0 & 1 & 0 & \dots & 0 \\ 0 & \dots & 0 & 0 & 0 & \dots & 0 \end{bmatrix}_{2 \times n}; \quad \bar{D}_i^T = [\bar{D}_{i1} \dots \bar{D}_{ii} \dots \bar{D}_{in}]^T; \quad \bar{K}_i^T = [\bar{K}_{i1} \dots \bar{K}_{ii} \dots \bar{K}_{in}]^T$$

$$\bar{M}_{ii} = \begin{bmatrix} M_{r\bar{M}_{ii}} & M_{rf\bar{M}_{ii}} \\ M_{rf\bar{M}_{ii}} & M_{f\bar{M}_{ii}} \end{bmatrix}_{2 \times 2}; \quad \bar{C}_{ii} = \begin{bmatrix} C_{r\bar{C}_{ii}} & C_{rf\bar{C}_{ii}} \\ C_{rf\bar{C}_{ii}} & C_{f\bar{C}_{ii}} \end{bmatrix}_{2 \times 2}; \quad \bar{D}_{ii} = \begin{bmatrix} 0 & 0 \\ 0 & D_{fi} \end{bmatrix}_{2 \times 2} \text{ and } \quad \bar{K}_{ii} =$$

$\begin{bmatrix} 0 & 0 \\ 0 & K_{fi} \end{bmatrix}_{2 \times 2}$ and the corresponding coordinate is:

$$\bar{Q}_i = [q_{d1} \dots q_{d(i-1)} \ q_i \ q_{d(i+1)} \ q_{dn}]^T \quad (5.23)$$

$$q_{dj} = [q_{rdj} \ q_{fdj}]^T, j = 1, \dots, n \text{ and } j \neq i, \text{ and } q_i = [q_{ri} \ q_{fi}]^T.$$

There exists a vector $p_i = [p_{ir} \ p_{if}]^T \in \Re^{b_{ir}+b_{if}}$ with components depending on manipulators' parameters and the regressor matrix $W_i = \begin{bmatrix} W_{ir} & 0 \\ 0 & W_{if} \end{bmatrix}$ which contains all known functions such as:

$$W_i (\bar{Q}_i, \dot{\bar{Q}}_i, t) p_i + RM_i = \bar{M}_i^T (\bar{Q}_i) \ddot{u} + \bar{C}_i^T (\bar{Q}_i, \dot{\bar{Q}}_i) \dot{u} + \bar{D}_i^T \dot{u} \quad (5.24)$$

where RM_i are the terms independent of p_i .

The proposed control law is given as follows:

$$\tau_i = K_{dir} s_{ir} + T_i + W_{ir} \hat{p}_{ir} + RM_{ir} - \delta \tau_{ir} \quad (5.25)$$

where

$$T_i = \begin{cases} \frac{s_{if}(K_{dif}s_{if} + K_{fi}\tilde{q}_{fi} + W_{if}\hat{p}_{if} + RM_{if} + \delta\tau_{if})}{s_{ir}} & ; s_{ir} \neq 0 \\ 0 & ; s_{ir} = 0 \end{cases} \quad (5.26)$$

$$W_i \hat{p}_i = \begin{bmatrix} W_{ir} \hat{p}_{ir} \\ W_{if} \hat{p}_{if} \end{bmatrix} = \widehat{M}_i^T (\bar{Q}_i) \ddot{u} + \widehat{C}_i^T (\bar{Q}_i, \dot{\bar{Q}}_i) \dot{u} + \widehat{D}_i^T \dot{u} \quad (5.27)$$

$$\delta \tau_i = \begin{bmatrix} \delta \tau_{ir} \\ \delta \tau_{if} \end{bmatrix} = \delta \bar{M}_i^T \ddot{u} + \delta \bar{C}_i^T \dot{u} \quad (5.28)$$

$$\text{and } \delta \bar{M}_{ij} = \sum_{j=1}^n \left. \frac{\partial \bar{M}_{ij}(q)}{\partial q_j} \right|_{q_{jd}} \tilde{q}_j + \mathcal{O}_{\bar{M}_{ij}}(\tilde{q}_j); K_{di} = \begin{bmatrix} K_{dir} & 0 \\ 0 & K_{dif} \end{bmatrix}$$

$$\delta \bar{C}_{ij} = \sum_{j=1}^n \left. \frac{\partial \bar{C}_{ij}(q, \dot{q})}{\partial q_j} \right|_{q_{jd}} \tilde{q}_j + \sum_{j=1}^n \left. \frac{\partial \bar{C}_{ij}(q, \dot{q})}{\partial \dot{q}_j} \right|_{q_{jd}} \tilde{\dot{q}}_j + \mathcal{O}_{\bar{C}_{ij}}(\tilde{q}_j, \tilde{\dot{q}}_j)$$

$\mathcal{O}_{\bar{M}_{ij}}$ and $\mathcal{O}_{\bar{C}_{ij}}$ are the high order terms of the Taylor series for $M_{ij}(q)$ and $C_{ij}(q)$, respectively.

The corresponding adaptive laws are given as follows:

$$\dot{\hat{p}}_{ir} = K_{vir} W_{ir}^T s_{ir} \quad (5.29)$$

$$\dot{\hat{p}}_{if} = K_{vif} W_{if}^T s_{if}$$

The i^{th} control law is presented in Figure 5.2.

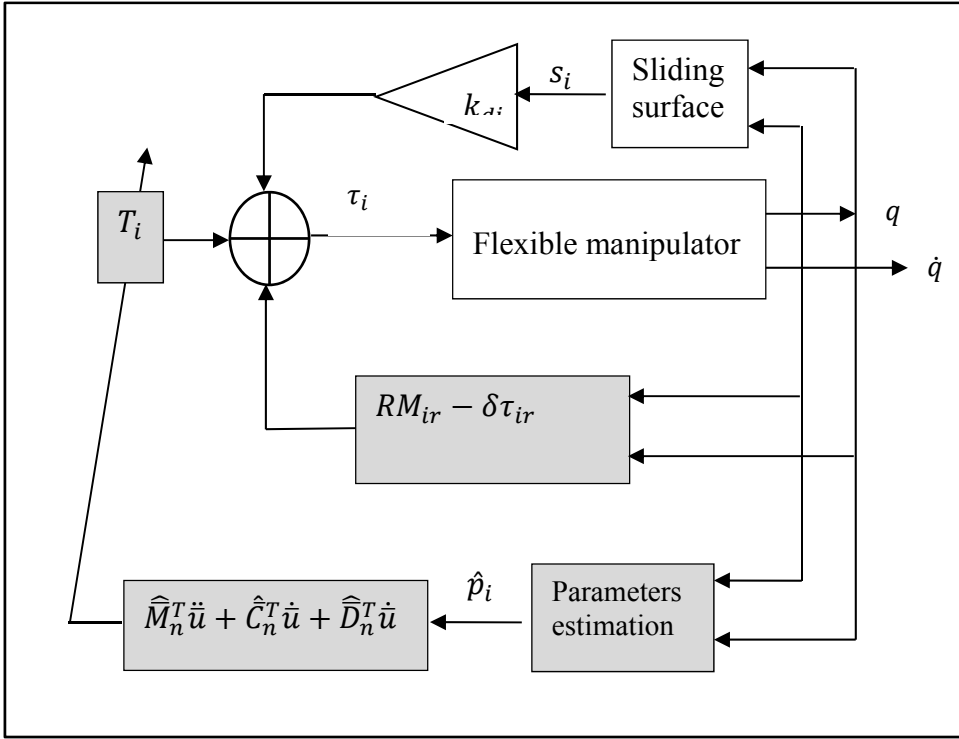


Figure 5.2 The i^{th} control law.

The n control laws can be written as follows:

$$\tau = K_{dr} s_r + T + W_r \hat{p}_r + RM - \delta \tau_r \quad (5.30)$$

where $W_r \hat{p}_r = [W_{1r} \hat{p}_{1r} \dots W_{nr} \hat{p}_{nr}]^T$, $T = [T_1 \dots T_n]^T$, $\delta \tau_r = [\delta \tau_{r1} \dots \delta \tau_{rn}]^T$,

$s_r = [s_{r1} \dots s_{rn}]^T$ and $K_{dr} = \text{diag}(K_{dri})$

The adaptive laws are given as follows:

$$\begin{aligned} \dot{\hat{p}}_r &= K_{vr} W_r^T s_r \\ \dot{\hat{p}}_f &= K_{vf} W_f^T s_f \end{aligned} \quad (5.31)$$

where $K_{vr} = \text{diag}(K_{vri})$ and $K_{vf} = \text{diag}(K_{vfi})$ are some positive definite gain matrices.

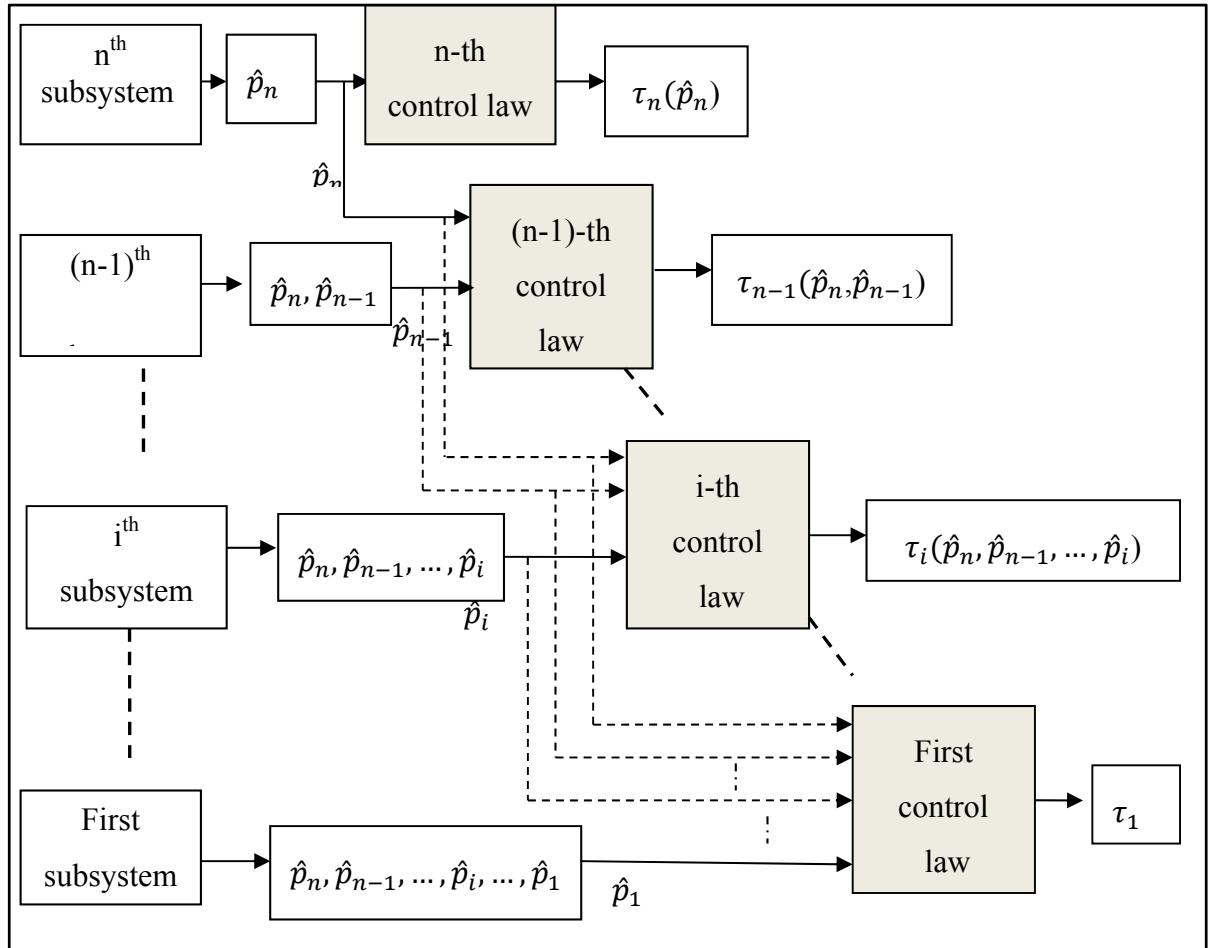


Figure 5.3 Distributed adaptive control strategy.

Figure 5.3 shows the distributed adaptive control strategy. Starting with the last subsystem and using its own estimated parameters, the n^{th} control law is developed. Then going backward to the $(n-1)^{\text{th}}$ subsystem, the control law is computed using its own estimated parameters and the estimated parameters of the n^{th} (upper level) subsystem. For an i^{th} subsystem, the controller depends on its own estimated parameters and the estimated parameters of all upper level subsystems ($n^{\text{th}}, \dots, (i+1)^{\text{th}}$). The same strategy is used for each subsequent subsystem until the first one.

5.4 Stability analysis

The global stability is studied by inserting the control law (5.30) in the initial dynamical model (5.1). From (5.9), the velocity \dot{q} and the acceleration \ddot{q} can be written as follows:

$$\begin{aligned}\dot{q} &= \dot{u} - s \\ \ddot{q} &= \ddot{u} - \dot{s}\end{aligned}\tag{5.32}$$

Using (5.32) and (5.1), the error dynamics can be deduced as follows:

$$M(q)\dot{s} + C(q, \dot{q})s + Ds + K_d s = M(q)\ddot{u} + C(q, \dot{q})\dot{u} + D\dot{u} + K_d s + Kq - L\tau\tag{5.33}$$

Proposition 1: The error dynamics (5.33) is equivalent to the following expression:

$$M(q)\dot{s} + C(q, \dot{q})s + Ds + K_d s = \begin{bmatrix} -T + W_r \tilde{p}_r \\ W_f p_f + RM_f + \delta \tau_f + K_{df} s_f + K_{ff} \tilde{q}_f \end{bmatrix}\tag{5.34}$$

Proof: See Appendix.

For the stability analysis, let us define the following positive Lyapunov function:

$$V = \frac{1}{2} s^T M(q) s + \frac{1}{2} \tilde{p}^T K_v^{-1} \tilde{p}\tag{5.35}$$

where $\tilde{p} = \begin{bmatrix} \tilde{p}_r \\ \tilde{p}_f \end{bmatrix}$; $K_v = \text{diag}(K_{vr}, K_{vf})$, $\tilde{p}^T K_v^{-1} \tilde{p} = \tilde{p}_r^T K_{vr}^{-1} \tilde{p}_r + \tilde{p}_f^T K_{vf}^{-1} \tilde{p}_f$

Take the time derivative of $V(t)$ to get

$$\begin{aligned}\dot{V}(t) &= \frac{1}{2} s^T M(q) \dot{s} + \frac{1}{2} s^T \dot{M}(q) s + \tilde{p}^T K_v^{-1} \tilde{p} \\ &= s^T \left(-C(q, \dot{q})s - Ds - K_d s + \begin{bmatrix} -T + W_r \tilde{p}_r \\ W_f p_f + RM_f + \delta \tau_f + K_{df} s_f + K_{ff} e_f \end{bmatrix} \right) + \frac{1}{2} s^T \dot{M}(q) s + \\ &\quad \tilde{p}^T K_v^{-1} \tilde{p}\end{aligned}$$

$$\begin{aligned}
&= -s^T(D + K_d)s + s^T \left(\begin{bmatrix} -T + W_r \tilde{p}_r \\ W_f p_f + RM_f + \delta \tau_f + K_{df} s_f + K_{ff} e_f \end{bmatrix} \right) + \dot{\tilde{p}}^T K_v^{-1} \tilde{p} \\
&= -s^T(D + K_d)s + R_s
\end{aligned}$$

where

$$R_s = s^T \left(\begin{bmatrix} -T + W_r \tilde{p}_r \\ W_f p_f + RM_f + \delta \tau_f + K_{df} s_f + K_{ff} e_f \end{bmatrix} \right) + \dot{\tilde{p}}^T K_v^{-1} \tilde{p} = s^T \tau_s + \dot{\tilde{p}}^T K_v^{-1} \tilde{p} \quad (5.36)$$

Proposition 2

Using the dynamical model (5.1) and the control law (5.30), the error dynamics is globally asymptotically stable and the time derivative of $V(t)$ is equivalent to the following expression:

$$\dot{V}(t) = -s^T(D + K_d)s \quad (5.37)$$

Proof: See Appendix

5.5 Experimental results

The system considered in this work is the two-flexible-link manipulator manufactured by Quanser, shown in Figure 5.4. It consists of two motors, two flexible links, and a payload. It moves in the horizontal plane and is connected by rigid revolute joints. Two motors actuate the system and generate the torques. Each flexible link is supposed uniform, has a mass m_i and length L_i . (\hat{X}_0, \hat{Y}_0) is the fixed reference frame. (X_1, Y_1) moves with the first link while (X_2, Y_2) moves with the second link. The flexible links are modeled as Euler-Bernoulli beams and the deformations of the links are assumed to be small.

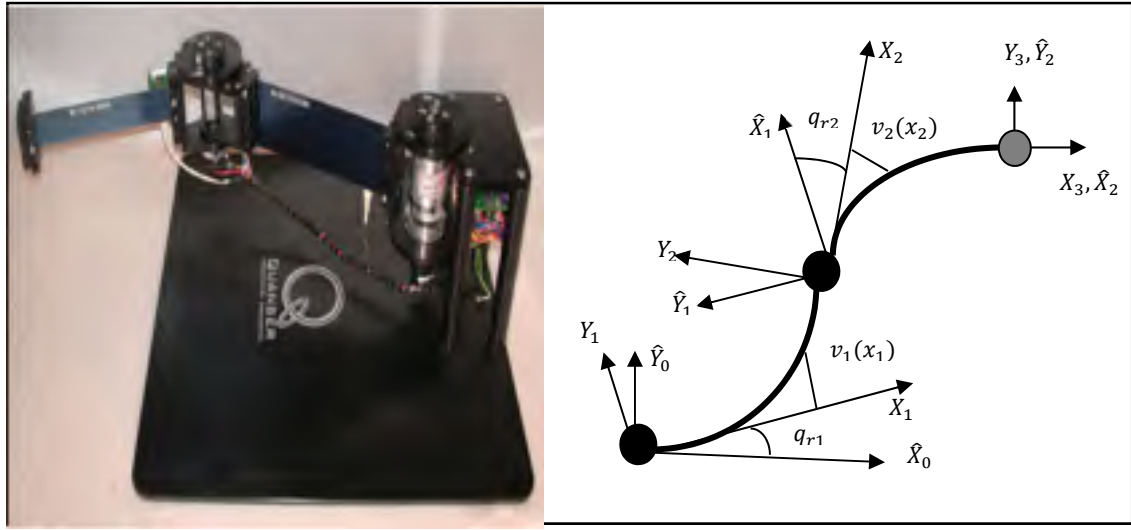


Figure 5.4 Two-flexible-link manipulator.

The model of the two-flexible-link system given in (De Luca et Siciliano, 1990; 1991) is modified in this work by only considering the first flexible mode of each link (Fareh, Saad et Saad, 2013a). Then, we have $n = 2$, $z = 2$ and $z_1 = z_2 = 1$. The dynamical model of the two-flexible-link manipulator is given in (5.3), where:

$$M_{rr} = \begin{bmatrix} M_{11} & M_{12} \\ M_{21} & M_{22} \end{bmatrix}; \quad M_{rf} = \begin{bmatrix} M_{13} & M_{14} \\ M_{23} & M_{24} \end{bmatrix}; \quad M_{ff} = \begin{bmatrix} M_{33} & M_{34} \\ M_{43} & M_{44} \end{bmatrix}; \quad C_{rr} = \begin{bmatrix} C_{11} & C_{12} \\ C_{21} & C_{22} \end{bmatrix}; \quad C_{rf} = \begin{bmatrix} C_{13} & C_{14} \\ C_{23} & C_{24} \end{bmatrix}; \quad C_{ff} = \begin{bmatrix} C_{33} & C_{34} \\ C_{43} & C_{44} \end{bmatrix}; \quad D_{ff} = \begin{bmatrix} D_{f1} & 0 \\ 0 & D_{f2} \end{bmatrix} \text{ and } K_{ff} = \begin{bmatrix} K_{f1} & 0 \\ 0 & K_{f2} \end{bmatrix}$$

The control strategies presented in the previous sections are applied and implemented on the two-degree-of-freedom (dof) Serial Flexible Link robot (Figure 5.4) manufactured by Quanser. The system consists of two hubs with two serial flexible links actuated by two motors. The tips deflection is measured using two strain gauges clamped at the base of each flexible beam. Table 5.1 shows the system parameters.

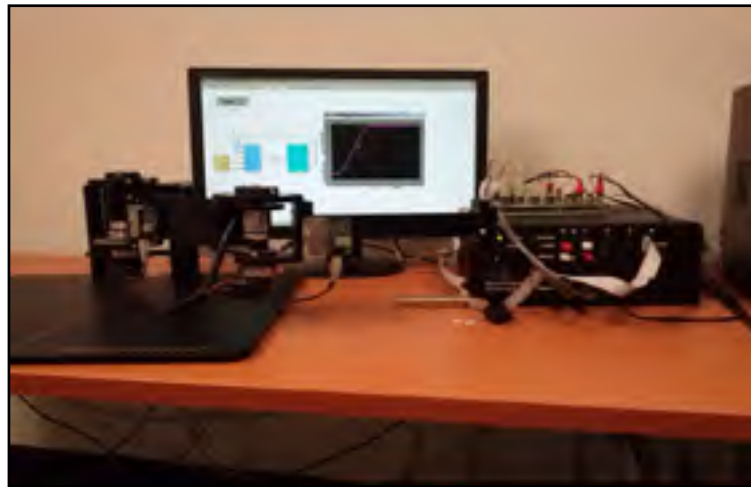


Figure 5.5 Quanser two-link flexible robot.

Table 5.1 System parameters

Parameter	Link 1	Link 2
Link length (L_i)	0.202 m	0.2 m
Link moment of inertia	0.17 kg.m ²	0.0064 10 ⁻⁶ kg.m ²
Elasticity	2.068 10 ¹¹ N/m ²	2.068 10 ¹¹ N/m ²
Gear ratio	100	50
Drive Torque constant	0.119 Nm/A	0.0234 N.m/A
Drive moment of inertia	7.63 10 ⁻⁴ kg.m ²	44.55 10 ⁻⁶ kg.m ²
Rotor moment of inertia	6.28 10 ⁻⁶ kg.m ²	1.03 10 ⁻⁶ kg.m ²
Maximum Rotation	+/- 90 deg	+/- 90 deg

The experimental setup of the serial two flexible links robot manipulator is shown in Figure 5.5. It consists of a Q8 terminal board, DAQ system, sensors such as strain gauges, encoder and limit switches. The proposed controllers are tested on Real-Time using Workshop (RTW) of Mathworks®.

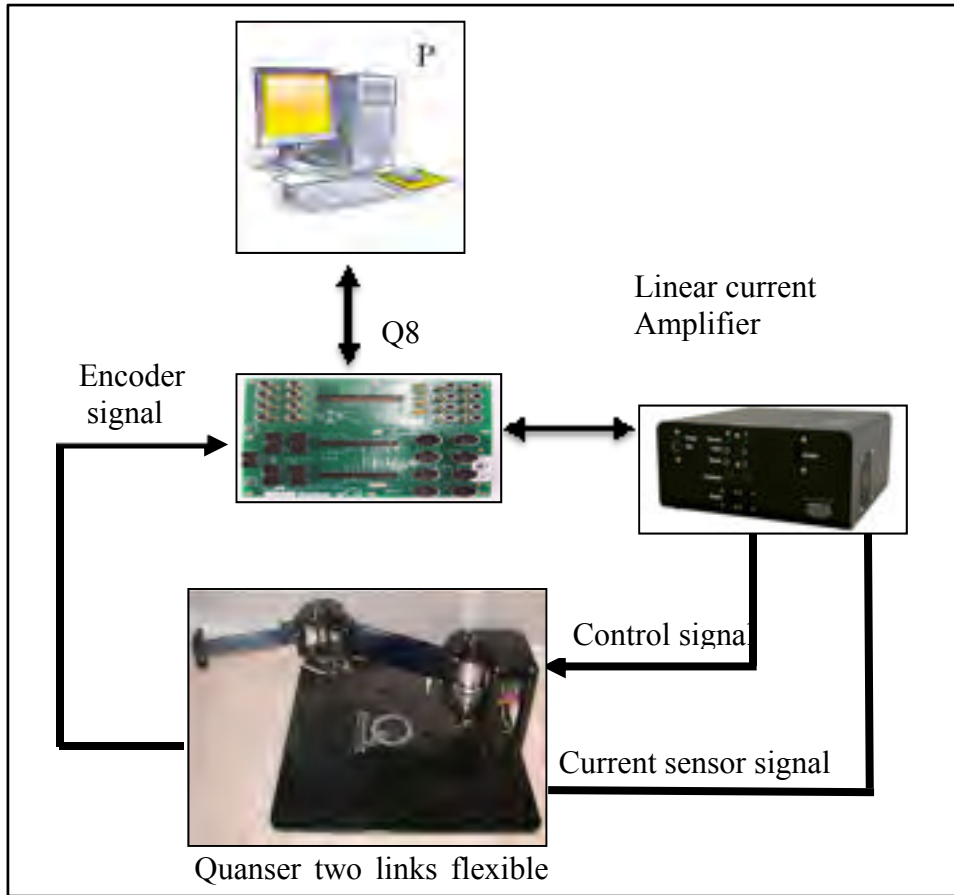


Figure 5.6. Real time setup.

The desired trajectory of the joint can be represented by a polynomial function given by the following expressions (Craig, 2005) (see figure 5.7):

$$q_{rd1}(t) = a_{10} + a_{11}t + a_{12}t^2 + a_{13}t^3 + a_{14}t^4 + a_{15}t^5 \quad (5.38)$$

$$q_{rd2}(t) = a_{20} + a_{21}t + a_{22}t^2 + a_{23}t^3 + a_{24}t^4 + a_{25}t^5 \quad (5.39)$$

for $0 \leq t \leq T_f = 5s$. For $t \geq T_f$, $q_{rd1}(t) = \frac{\pi}{4}$ and $q_{rd2}(t) = \frac{\pi}{8}$. For the flexible mode:

$$q_{fd1}(t) = q_{fd2}(t) = 0 \quad (5.40)$$

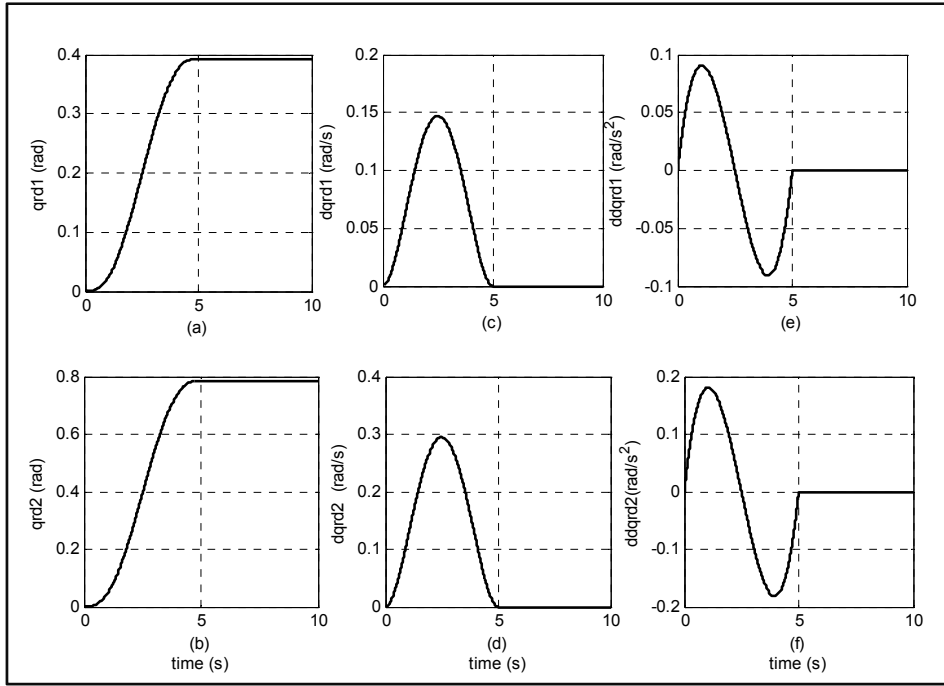


Figure 5.7. Desired trajectories: (a)-(b) position, (c)-(d) velocity, (e)-(f) acceleration of rigid part.

Using a trial and error method, the controller's gains are chosen as follows: for the distributed adaptive control strategy, the selected gains are: $K_{d1r} = 15$; $K_{d1f} = 10$, $K_{d2r} = 25$ and $K_{d2f} = 10$.

For an i -th subsystem, the previous theoretical development of the control law is given in the general case. For the sake of simplicity and the real-time implementation, a finite order Taylor series is fixed. The Taylor series is limited to the first order. Then, $\mathcal{O}_{M_{ij}} = \mathcal{O}_{C_{ij}} = 0$.

The uncertain parameters are chosen as follows:

For the second subsystem $p_2 = [p_{2r} \ p_{2f}]^T$:

$p_{2r} = [b_{121} \ b_{123} \ b_{251}]^T$ and $p_{2f} = [b_{153} \ b_{551}]^T$. Then τ_2 is developed using \hat{p}_2 .

For the first subsystem: $p_1 = [p_{1r} \ p_{1f}]^T$:

$p_{1r} = [p_2 \ J_{eq1}]^T$ and $p_{1f} = [p_{1r} \ b_{331}]^T$; τ_1 is developed using \hat{p}_2, \hat{J}_{eq1} and \hat{b}_{331} .

where b_{ijk} is given in (De Luca et Siciliano, 1991) and $J_{eq1} = J_{h1} + J_{o1} + m_{h2}l_1^2 + m_2l_1^2 + m_p l_1^2$.

The experimental results of the distributed control are shown in Figures 5.8-5.10.

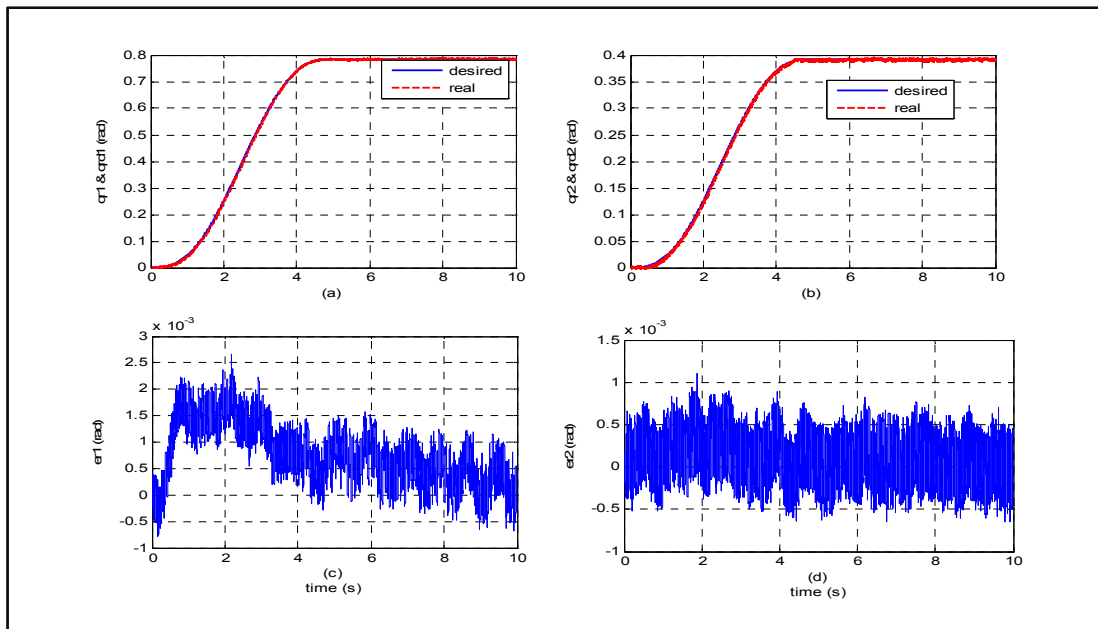


Figure 5.8 Adaptive control: (a)-(b) joints' tracking trajectories,
(c)-(d) joints' tracking errors.

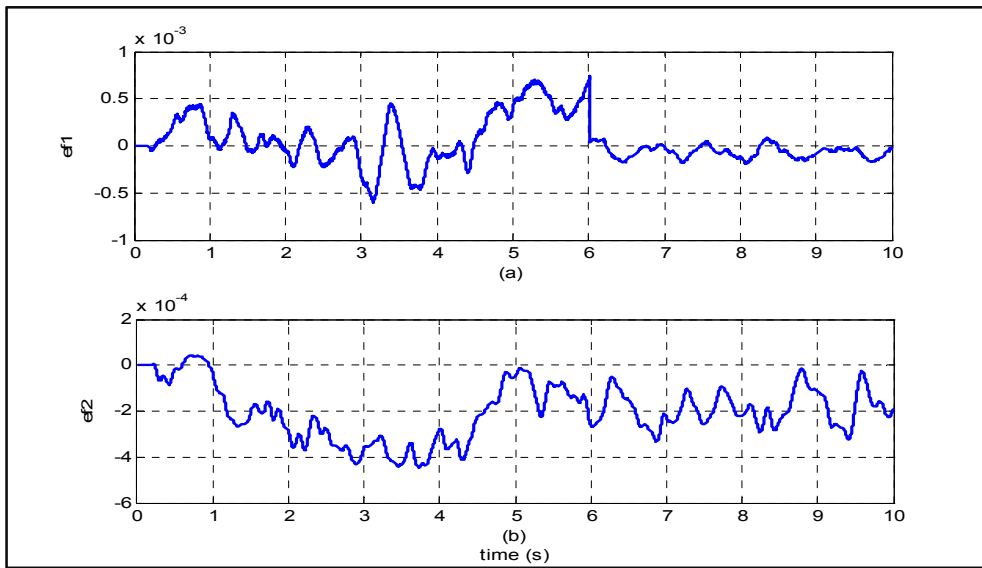


Figure 5.9. Adaptive control: errors of flexible part.

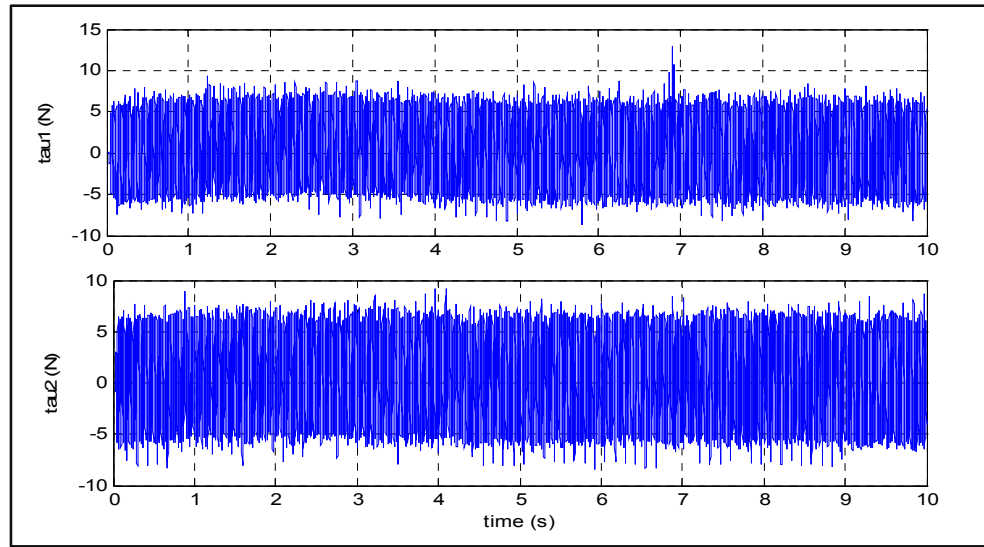


Figure 5.10 Adaptive control: control input.

To show the contribution of the developed adaptive distributed control method, the results were compared with a non-adaptive control version. The experimental results of the non-adaptive controller are given in Figures 5.10-5.13.

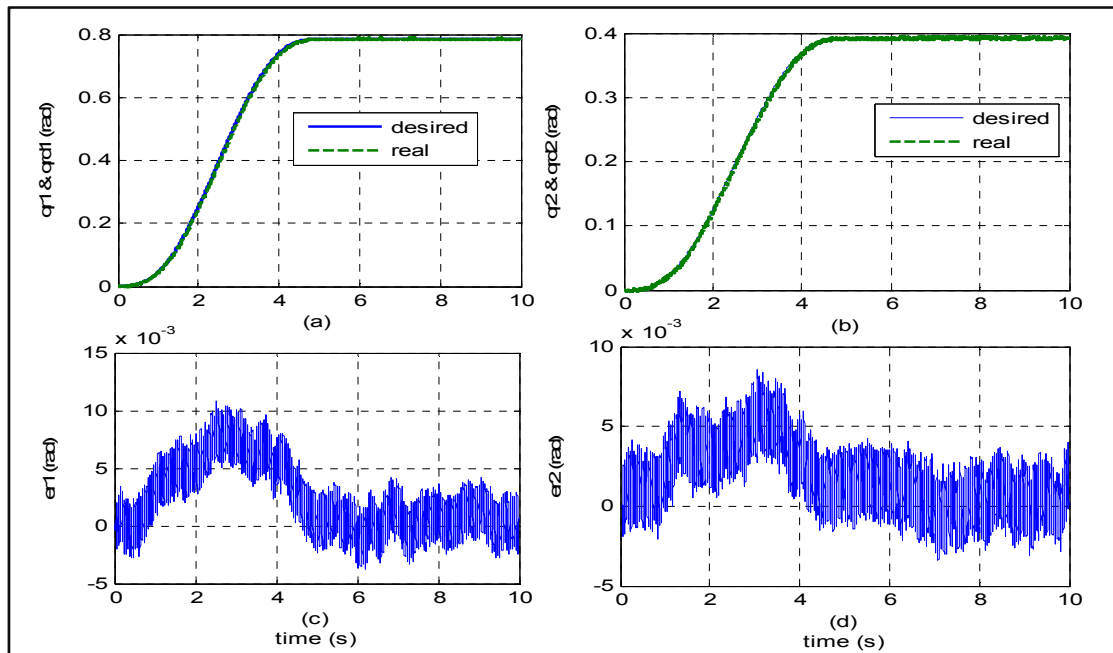


Figure 5.11 Distributed control: (a)-(b) joints' tracking trajectories,
(c)-(d) joints' tracking errors.

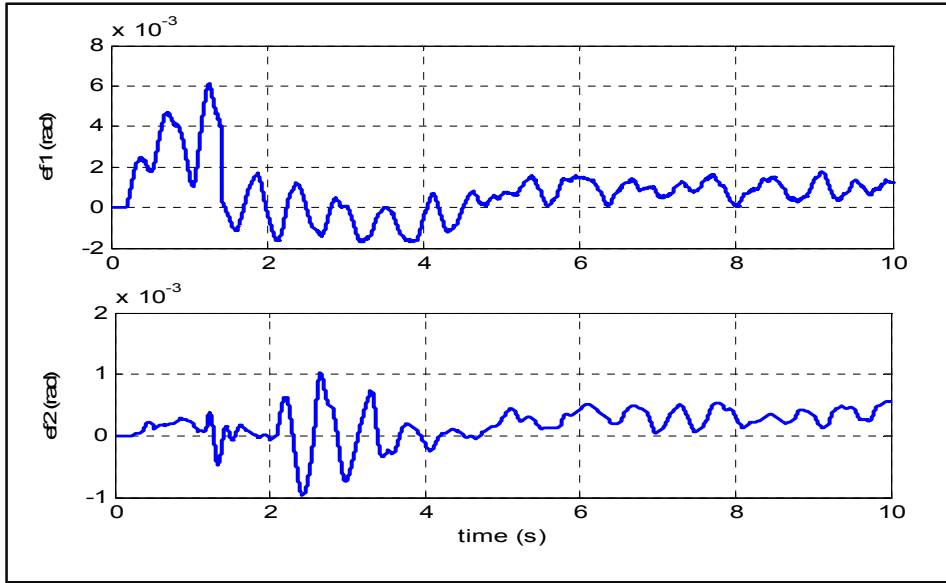


Figure 5.12 Distributed control: errors of the flexible parts.

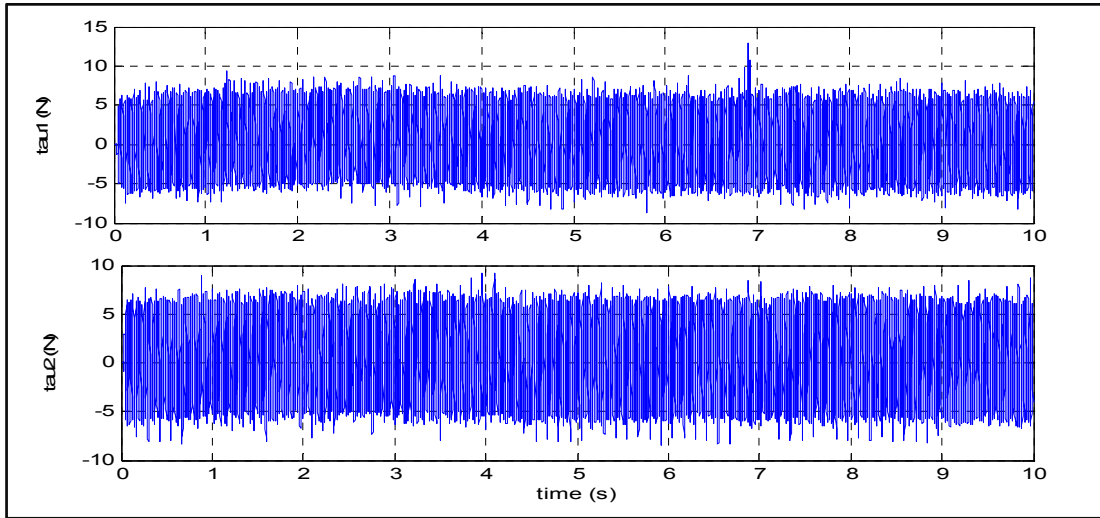


Figure 5.13 Distributed control: control input.

According to the experimental results, a good tracking is obtained in the joint space for the distributed adaptive control strategy. The tracking of the desired trajectory of joint 1 is shown in Figure 5.8-a and that of joint 2 is given in Figure 5.8-b. The tracking errors of joints 1 and 2 are given in Figures 5.8-c and 5.8-d, respectively. The good quality of the tracking obtained is confirmed by the tracking errors which do not exceed 0.0025 rad for joint 1 and 0.001 rad for joint 2. For flexible part, the desired trajectories are set to zero to minimize vibration in

the links. The errors, shown in Figure 5.9, are less than 0.0005. The control input for joints 1 and 2 are given in Figure 5.10. The non-adaptive version was tested on the two-flexible-link manipulator using the same desired trajectories. Figure 5.11 shows the tracking of joints 1, 2 and the corresponding tracking errors. The tracking errors of the flexible part are given in Figure 5.12, while the input torque signals are given in Figure 5.13. For the adaptive distributed control method, the tracking errors of the joints and the links' vibrations are smaller than those resulting from the non-adaptive control. Therefore, we can conclude that the adaptive controller reduce the vibrations and gives a good tracking of the desired trajectories.

5.6 Conclusion

This paper presents a distributed adaptive control strategy for flexible links manipulators. The control strategy consists in reorganizing the dynamical model into n subsystems. Each subsystem has a pair of joint and link. We start by controlling the last subsystem, then we progress backward until the first subsystem. The control law of a subsystem uses its own estimated parameters and the parameters already estimated in the upper level subsystems. The global stability is proved using Lyapunov theory. Experimental results compared with a non-adaptive controller show that the distributed adaptive control strategy gives good tracking and reduces the links' vibrations.

5.7 Appendix

Proof of proposition 1

From the error dynamics (5.33), let us define the second term as follows:

$$\tau_s = M(q)\ddot{u} + C(q, \dot{q})\dot{u} + D\dot{u} + K_d s + Kq - L\tau \quad (5.41)$$

Using the transformation matrix T_r and equations: (5.4), (5.9) and (5.11), we can write:
 $\ddot{u} = T_r^{-1}\ddot{\bar{u}}$; $\dot{u} = T_r^{-1}\dot{\bar{u}}$; $s = T_r^{-1}\bar{s}$ and $q = T_r^{-1}\bar{q}$. Equation (5.41) becomes:

$$\tau_s = M(q)T_r^{-1}\ddot{\bar{u}} + C(q, \dot{q})T_r^{-1}\dot{\bar{u}} + DT_r^{-1}\dot{\bar{u}} + K_d T_r^{-1}\bar{s} + KT_r^{-1}\bar{q} - L\tau \quad (5.42)$$

By multiplying (5.42) by the transformation matrix T_r , we obtain:

$$\bar{\tau}_s = \bar{M}(q)\ddot{\bar{u}} + \bar{C}(q, \dot{q})\dot{\bar{u}} + \bar{D}\dot{\bar{u}} + \bar{K}_d \bar{s} + \bar{K}\bar{q} - \bar{L}\tau \quad (5.43)$$

where $\bar{\tau}_s = T_r \tau_s$; $\bar{M}(q) = T_r M(q) T_r^{-1}$; $\bar{C}(q, \dot{q}) = T_r C(q, \dot{q}) T_r^{-1}$; $\bar{D} = T_r D T_r^{-1}$; $\bar{K} = T_r K T_r^{-1}$; $\bar{L} = T_r L$.

For the i^{th} subsystem, $\bar{\tau}_{si}$ is the i^{th} element of $\bar{\tau}_s$ and is given as follows:

$$\bar{\tau}_{si} = \bar{M}_i^T(q)\ddot{\bar{u}} + \bar{C}_i^T(q, \dot{q})\dot{\bar{u}} + \bar{D}_i^T\dot{\bar{u}} + \bar{K}_i^T\bar{q} + \bar{K}_{di}^T\bar{s} - \bar{L}_i\tau \quad (5.44)$$

where: $\bar{M}_i^T = [\bar{M}_{i1} \dots \bar{M}_{ii} \dots \bar{M}_{in}]_{2 \times 2n}$; $\bar{C}_i^T = [\bar{C}_{i1} \dots \bar{C}_{ii} \dots \bar{C}_{in}]_{2 \times 2n}$; $\bar{L}_i\tau = [\tau_i \ 0]^T$.

$\bar{D}_i^T = [0_{2 \times 2} \dots \bar{D}_{ii} \dots 0_{2 \times 2}]_{2 \times 2n}$; $\bar{K}_i^T = [0_{2 \times 2} \dots \bar{K}_{ii} \dots 0_{2 \times 2}]_{2 \times 2n}$,

$\bar{K}_{di}^T = [0_{2 \times 2} \dots \bar{K}_{dii} \dots 0_{2 \times 2}]^T$

Using Taylor series, we can write:

$$\bar{M}_{ij}(q) = \bar{M}_{ij}(Q_i) + D\bar{M}_{ij}(Q_i)^T(q - Q_i) + \frac{1}{2!}(q - Q_i)^T\{D^2\bar{M}_{ij}(Q_i)\}(q - Q_i) + \dots$$

where $D\bar{M}_{ij}(Q_i)$ is the gradient of \bar{M}_{ij} evaluated at $q = Q_i$ and $D^2\bar{M}_{ij}(Q_i)$ is a Hessian matrix. Then, we can write:

$$\begin{aligned}
\bar{M}_{ij}(q) &= \bar{M}_{ij}(Q_i) + \frac{\partial \bar{M}_{ij}(q)}{\partial [q_1 \dots q_{i-1} q_{i+1} \dots q_n]} \left| \begin{array}{c} q_{1d} \\ \vdots \\ q_{(i-1)d} \\ q_{(i+1)d} \\ \vdots \\ q_{nd} \end{array} \right| \left[\begin{array}{c} q_1 - q_{1d} \\ \vdots \\ q_{i-1} - q_{(i-1)d} \\ q_{i+1} - q_{(i+1)d} \\ \vdots \\ q_n - q_{nd} \end{array} \right] + \mathcal{O}_{M_{ij}}(\tilde{q}_j) \\
&= \bar{M}_{ij}(Q_i) - \sum_{\substack{j=1 \\ j \neq i}}^n \frac{\partial \bar{M}_{ij}(q)}{\partial q_j} \Big|_{q_{jd}} \tilde{q}_j + \mathcal{O}_{M_{ij}}(\tilde{q}_j) \\
\bar{M}_{ij}(q) &= \bar{M}_{ij}(Q_i) - \delta \bar{M}_{ij} \tag{5.45}
\end{aligned}$$

where $\delta \bar{M}_{ij} = \sum_{j=1}^n \frac{\partial \bar{M}_{ij}(q)}{\partial q_j} \Big|_{q_{jd}} \tilde{q}_j - \mathcal{O}_{M_{ij}}(\tilde{q}_j)$ and $\mathcal{O}_{M_{ij}}$ is the remaining terms given as

follows: $\mathcal{O}_{M_{ij}}(\tilde{q}_j) = \bar{M}_{ij}(q) - \bar{M}_{ij}(Q_i) + \sum_{j=1}^n \frac{\partial \bar{M}_{ij}(q)}{\partial q_j} \Big|_{q_{jd}} \tilde{q}_j$. The same idea is used for the Coriolis matrix C:

$$\bar{C}_{ij}(q, \dot{q}) = \bar{C}_{ij}(Q_i, \dot{Q}_i) - \delta \bar{C}_{ij} \tag{5.46}$$

Using (5.45) and (5.46), we can write:

$$\begin{aligned}
\bar{M}_i^T(q) &= \bar{M}_i^T(Q_i) - \delta \bar{M}_i^T \\
\bar{C}_i^T(q, \dot{q}) &= \bar{C}_i^T(Q_i, \dot{Q}_i) - \delta \bar{C}_i^T \tag{5.47}
\end{aligned}$$

and (5.44) becomes:

$$\bar{\tau}_{si} = \bar{M}_i^T(Q_i) \ddot{u} + \bar{C}_i^T(Q_i, \dot{Q}_i) \dot{u} - \delta \bar{M}_i^T \ddot{u} - \delta \bar{C}_i^T \dot{u} + \bar{D}_i^T \dot{u} + \bar{K}_i^T \bar{q} + \bar{K}_{di}^T \bar{s} - \bar{L}_i \tau \tag{5.48}$$

where: $\delta \tau_i = [\delta \tau_{ir} \quad \delta \tau_{if}]^T = \delta \bar{M}_i^T \ddot{u} + \delta \bar{C}_i^T \dot{u}; \bar{K}_i^T \bar{q} = [0 \quad K_{ff} q_{fi}]^T;$
 $\bar{K}_{di}^T \bar{s} = [K_{dir} s_{ir} \quad K_{dif} s_{if}]^T$

Using (5.24), the last equation (5.48) can be written as follows:

$$\bar{\tau}_{si} = \begin{bmatrix} W_{ir} p_{ir} + R M_{ir} + K_{dir} s_{ir} - \delta \tau_{ir} - \tau_i \\ W_{if} p_{if} + R M_{if} - \delta \tau_{if} + K_{dif} s_{if} + K_{ff} q_{fi} \end{bmatrix} \tag{5.49}$$

Using (5.25), we can deduce:

$$\bar{\tau}_{si} = \begin{bmatrix} -T_i + W_{ir}\tilde{p}_{ir} \\ W_{if}p_{if} + RM_{if} - \delta\tau_{if} + K_{dif}s_{if} + K_{ffi}\tilde{q}_{if} \end{bmatrix} \quad (5.50)$$

where $\tilde{p}_{ir} = p_{ir} - \hat{p}_{ir}$ and $\dot{\tilde{p}}_{ir} = -\dot{\hat{p}}_{ir}$ (the system parameters p_{ir} are assumed constant, then $\dot{p}_{ir} = 0$); $\tilde{q}_{if} = q_{fi} - q_{fai} = q_{fi}$.

The n elements of $\bar{\tau}_s$ can be written as follows:

$$\bar{\tau}_s = [\bar{\tau}_{s1} \quad \dots \quad \bar{\tau}_{sn}]^T \quad (5.51)$$

As done for q , \dot{u} and \dot{s} , τ_s can be reorganized as rigid and flexible parts using the matrix T_r :

$$\tau_s = T_r^{-1}\bar{\tau}_s = [\tau_{sr1} \quad \dots \quad \tau_{srn} \quad \tau_{sf1} \quad \dots \quad \tau_{sfm}]^T \quad (5.52)$$

where $\tau_{sir} = -T_i + W_{ir}\tilde{p}_{ir}$ and $\tau_{sif} = W_{if}p_{if} + RM_{if} - \delta\tau_{if} + K_{dif}s_{if} + K_{ffi}e_{fi}$

Then, (5.43) can be written as:

$$\tau_s = \begin{bmatrix} -T + W_r\tilde{p}_r \\ W_f p_f + RM_f - \delta\tau_f + K_{df}s_f + K_{ff}\tilde{q}_f \end{bmatrix} \quad (5.53)$$

where $T = [T_1 \quad \dots \quad T_n]^T$; $W_r\tilde{p}_r = [W_{1r}\tilde{p}_{1r} \quad \dots \quad W_{nr}\tilde{p}_{nr}]^T$;

$$W_f p_f = [W_{1f}p_{1f} \quad \dots \quad W_{nf}p_{nf}]^T$$

$$\delta\tau_f = [\delta\tau_{f1} \quad \dots \quad \delta\tau_{fn}]^T; K_{df} = diag(K_{dfi}); K_{ff} = diag(K_{ffi}); i = 1 \dots n.$$

The error dynamics (5.33) is equivalent to:

$$M(q)\dot{s} + C(q, \dot{q})s + Ds + K_d s = \begin{bmatrix} -T + W_r\tilde{p}_r \\ W_f p_f + RM_f - \delta\tau_f + K_{df}s_f + K_{ff}\tilde{q}_f \end{bmatrix} \quad (5.54)$$

Proof of proposition 2

As given in section 5.2, \bar{s} , $\bar{\tau}_s$, $\bar{K}_v^{-1}\bar{p}$ and $\bar{\tilde{p}}$ can be obtained by changing the order of elements of the vectors: s , τ_s , $K_v^{-1}\tilde{p}$ and \tilde{p} . Then, we can write:

$$M(q)\dot{s} + C(q, \dot{q})s + Ds + K_d s = \begin{bmatrix} -T + W_r \tilde{p}_r \\ W_f p_f + RM_f - \delta \tau_f + K_{df} s_f + K_{ff} \tilde{q}_f \end{bmatrix} \quad (5.55)$$

$$\dot{\tilde{p}}^T K_v^{-1} \tilde{p} = \dot{\tilde{p}}^T \bar{K}_v^{-1} \tilde{p} = \sum_{i=1}^n \dot{\tilde{p}}_i^T \bar{K}_{vi}^{-1} \tilde{p}_i = \sum_{i=1}^n \dot{\tilde{p}}_i^T K_{vi}^{-1} \tilde{p}_i \quad (5.56)$$

and

$$R_s = \sum_{i=1}^n \bar{s}_i^T \bar{\tau}_{si} + \dot{\tilde{p}}_i^T \bar{K}_{vi}^{-1} \tilde{p}_i = \sum_{i=1}^n s_i^T \tau_{si} + \dot{\tilde{p}}_i^T K_{vi}^{-1} \tilde{p}_i = \sum_{i=1}^n R_{si} \quad (5.57)$$

where

$$R_{si} = s_i^T \tau_{si} + \dot{\tilde{p}}_i^T K_{vi}^{-1} \tilde{p}_i; \quad \bar{\tau}_{si} = \begin{bmatrix} -T_i + W_{ir} \tilde{p}_{ir} \\ W_{if} p_{if} + RM_{if} + \delta \tau_{fi} + K_{dfi} s_{fi} + K_{fi} \tilde{q}_{if} \end{bmatrix};$$

$$\tilde{p}_i = [\tilde{p}_{ir} \quad \tilde{p}_{if}]^T$$

We can write:

$$\dot{\tilde{p}}_i^T K_{vi}^{-1} \tilde{p}_i = [\dot{\tilde{p}}_{ir}^T \quad \dot{\tilde{p}}_{if}^T] \begin{bmatrix} K_{vir}^{-1} & 0 \\ 0 & K_{vif}^{-1} \end{bmatrix} [\tilde{p}_{ri} \quad \tilde{p}_{fi}] = \dot{\tilde{p}}_{ir}^T K_{vir}^{-1} \tilde{p}_{ir} + \dot{\tilde{p}}_{if}^T K_{vif}^{-1} \tilde{p}_{if} \quad (5.58)$$

Then:

$$\begin{aligned} R_{si} &= [s_{ir} \quad s_{if}] \begin{bmatrix} -T_i + W_{ir} \tilde{p}_{ir} \\ W_{if} p_{if} + RM_{if} + \delta \tau_{fi} + K_{dfi} s_{fi} + K_{fi} \tilde{q}_{if} \end{bmatrix} + \dot{\tilde{p}}_{ir}^T K_{vir}^{-1} \tilde{p}_{ir} + \dot{\tilde{p}}_{if}^T K_{vif}^{-1} \tilde{p}_{if} \\ &= -s_{ir} T_i + s_{ir} W_{ir} \tilde{p}_{ir} + s_{if} (W_{if} p_{if} + RM_{if} + \delta \tau_{fi} + K_{dfi} s_{fi} + K_{fi} \tilde{q}_{if}) + \dot{\tilde{p}}_{ir}^T K_{vir}^{-1} \tilde{p}_{ir} \\ &\quad + \dot{\tilde{p}}_{if}^T K_{vif}^{-1} \tilde{p}_{if} \\ &= -s_{ir} T_i + (s_{ir} W_{ir} + \dot{\tilde{p}}_{ir}^T K_{vir}^{-1}) \tilde{p}_{ir} + s_{if} (W_{if} p_{if} + RM_{if} + \delta \tau_{fi} + K_{dfi} s_{fi} + K_{fi} \tilde{q}_{if}) \\ &\quad + \dot{\tilde{p}}_{if}^T K_{vif}^{-1} (p_{if} - \hat{p}_{if}) \\ &= (s_{ir} W_{ir} + \dot{\tilde{p}}_{ir}^T K_{vir}^{-1}) \tilde{p}_{ir} + (s_{if} W_{if} + \dot{\tilde{p}}_{if}^T K_{vif}^{-1}) p_{if} - s_{ir} T_i \\ &\quad + s_{if} (RM_{if} + \delta \tau_{fi} + K_{dfi} s_{fi} + K_{fi} \tilde{q}_{if}) - \dot{\tilde{p}}_{if}^T K_{vif}^{-1} \hat{p}_{if} \end{aligned}$$

The parameters system p_{ir} and p_{if} are assumed constant, then: $\tilde{p}_{ir} = p_{ir} - \hat{p}_{ir}$; $\tilde{p}_{if} = p_{if} - \hat{p}_{if}$; $\dot{\tilde{p}}_{ir} = -\dot{\hat{p}}_{ir}$ and $\dot{\tilde{p}}_{if} = -\dot{\hat{p}}_{if}$. Then :

$$\begin{aligned} R_{si} &= (s_{ir} W_{ir} - \dot{\hat{p}}_{ir}^T K_{vir}^{-1}) \tilde{p}_{ir} + (s_{if} W_{if} - \dot{\hat{p}}_{if}^T K_{vif}^{-1}) p_{if} - s_{ir} T_i \\ &\quad + s_{if} (RM_{if} + \delta \tau_{fi} + K_{dfi} s_{fi} + K_{fi} \tilde{q}_{if}) + \dot{\hat{p}}_{if}^T K_{vif}^{-1} \hat{p}_{if} \end{aligned}$$

Using the adaptive laws of the i^{th} subsystem:

$$\dot{\hat{p}}_{ir} = K_{vir} W_{ir}^T s_{ir} \quad (5.59)$$

$$\dot{\hat{p}}_{if} = K_{vif} W_{if}^T s_{if} \quad (5.60)$$

then:

$$R_{si} = -s_{ir} T_i + s_{if} (RM_{if} + \delta\tau_{fi} + K_{dfi} s_{fi} + K_{fi} \tilde{q}_{if}) + \dot{\hat{p}}_{if}^T K_{vif}^{-1} \hat{p}_{if} \quad (5.61)$$

Using (5.26), the equation (5.61) becomes:

$$\begin{aligned} R_{si} &= -s_{ir} \left[\frac{s_{if} (K_{dif} s_{if} + K_{fi} \tilde{q}_{fi} + W_{if} \hat{p}_{if} + RM_{if} + \delta\tau_{if})}{s_{ir}} \right] + \dot{\hat{p}}_{if}^T K_{vif}^{-1} \hat{p}_{if} \\ &\quad + s_{if} (RM_{if} + \delta\tau_{fi} + K_{dfi} s_{fi} + K_{fi} \tilde{q}_{if}) \\ &= -s_{if} (K_{dif} s_{if} + K_{fi} \tilde{q}_{fi} + W_{if} \hat{p}_{if} + RM_{if} + \delta\tau_{if}) + s_{if} (K_{dif} s_{if} + K_{fi} \tilde{q}_{fi} + RM_{if} + \delta\tau_{if}) \\ &\quad + \dot{\hat{p}}_{if}^T K_{vif}^{-1} \hat{p}_{if} \\ &= -s_{if} (K_{dif} s_{if} + K_{fi} \tilde{q}_{fi} + RM_{if} + \delta\tau_{if}) + s_{if} (K_{dif} s_{if} + K_{fi} \tilde{q}_{fi} + RM_{if} + \delta\tau_{if}) \\ &\quad + (\dot{\hat{p}}_{if}^T K_{vif}^{-1} - s_{if} W_{if}) \hat{p}_{if} \end{aligned}$$

Using the adaptive law (5.60), we can conclude that $R_{si} = 0$. Then $R_s = 0$ and the time derivative of V becomes:

$$\dot{V}(t) = -s^T (D + K_d) s \quad (5.62)$$

Since D and K_d are positive matrices, then $\dot{V}(t) \leq 0$. $V(t)$ is a continuous function of \tilde{p} . Using (5.62), $V(t)$ is nonincreasing in t . Then we can conclude that $s, \tilde{p} \in L_\infty$. From the definition of s given in (5.9), $\tilde{q} \in L_\infty$ and from the definition of T , $T \in L_\infty$. Using the error dynamics (5.34), $\dot{s} \in L_\infty$. On the other hand, we have $-\int_0^\infty \dot{V} dt = V(0) - V(\infty) < \infty$ or equivalently, $\int_0^\infty \|s\|^2 dt < \infty$, i.e. $s \in L_2$. Using Barbalat Lemma (Slotine et Li, 1991) we can conclude that $s \rightarrow 0$ as $t \rightarrow \infty$, i.e., $\tilde{q}, \dot{\tilde{q}} \rightarrow 0$ asymptotically as $t \rightarrow \infty$.

CHAPITRE 6

ARTICLE 5: WORKSPACE TRAJECTORY TRACKING CONTROL FOR TWO-FLEXIBLE-LINK MANIPULATOR THROUGH OUTPUT REDEFINITION

Fareh Raouf¹ Saad Mohamad² and Saad Maarouf¹

¹Electrical Engineering Department, Université du Québec, École de technologie supérieure,
1100, rue Notre-Dame ouest, Montréal (Québec), H3C 1K3, Canada

²School of Engineering, Université du Québec en Abitibi-Témiscamingue, 445, boul. de
l'Université, Rouyn-Noranda (Québec), J9X 5E4

Article publié à la revue «International Journal of Modelling, Identification and Control » en
Février 2013.

Abstract

In this paper, a control strategy and a stability analysis for a two-flexible-link manipulator are presented to track a desired trajectory in the workspace. The inverse dynamics problem is solved using a virtual space and the quasi-static approach. Flexible manipulators are non-minimum phase systems when the controlled output is the tip position. To overcome this problem, an output redefinition technique is used. Two steps are presented to control the manipulator's tip position. First, assuming that the first link is stable, we develop a control law for the last link to stabilize the error dynamics using the feedback linearization approach. The weighted parameter defining the non-collocated output is selected to guarantee bounded internal dynamics such that the output is as close as possible to the tip. Second, the same strategy is followed for the first link. Simulation results are presented to show good tracking of the desired trajectory in the workspace.

Keywords: Flexible manipulators, dynamic inversion, output redefinition, feedback linearization, passivity.

6.1 Introduction

Control of flexible manipulators has been the focus of much research in recent years. This is due to the many advantages of flexible manipulators as compared to rigid manipulators. For instance, flexible manipulators are faster, less massive and consume less energy. Since the tasks are defined in the workspace, many studies were interested in controlling the tip of such manipulators (De Luca et al., 1998; Matsuno and Hatayama, 1999; Wang and Yu, 2010; Wang et al., 2009; Zhao-Hui, 2002; 2008). For flexible manipulators, the workspace and the joint space are linked by kinematic and dynamic relationships. The inverse kinematic is then not sufficient to transform the desired trajectory, defined in the workspace, to the joint space.

To solve this problem, an intermediate space, called virtual space (Bigras et al., 2003; de Luca and Siciliano, 1989; Lucibello and Di Benedetto, 1993) is defined. The virtual space is linked to the workspace by a simple kinematic relation and has the same number of degrees-of-freedom (DOF) as the joint space. There are two steps to transform the desired trajectory from the workspace to the joint space. The first one represents the transformation from the workspace to the virtual space by using an inverse kinematic. In (de Luca and Siciliano, 1989), the virtual space coordinates for a one flexible link manipulator is used and in (Bigras et al., 2003), it is used for a class of manipulators where the last link is flexible. In the second step, the transformation from the virtual space to the joint space is achieved by solving nonlinear equations characterizing the flexible part. In (Pfeiffer, 1989), the quasi-static approach is used to adjust the desired trajectory of the joints by taking into account link deformations. In (Kwon and Book, 1994), an iterative solution using a causal-anticausal integration method is proposed to solve the inverse dynamic problem. When controlling the position of the end-effector, flexible link manipulators are non-minimum phase systems (Cannon and Schmitz, 1984). To overcome this problem, the output redefinition technique is used in (Lucibello and Di Benedetto, 1993; Moallem et al., 2001; Saad et al., 2000) to guarantee stable internal dynamics. The redefined output is usually chosen as the motor's angle augmented by a weighted value of the tip angle. The weighting parameter is chosen such that the selected output is the closest to the extremity with stable zero-dynamics.

Multi-link flexible manipulators can be seen either as a one MIMO system or as interconnected SISO subsystems. In the first case, many control schemes use a single controller for all joints and links. The feedback linearization technique is used in (Atashzar et al., 2010; Bigras et al., 2003; Modi et al., 1993; Woosoon, 1994) to control flexible manipulators in the joint space. In this case, the input torques and the joints' position outputs are collocated; the internal dynamics are then bounded (Woosoon, 1994). The non-minimum phase characteristic limits the application of the feedback linearization approach to control the end-effector position. This problem can be solved by the output redefinition technique. Adaptive control is also used for flexible link control in (Bai, 1998; Hoseini, 2010; Yang and Jung Hua, 1997). A sliding mode approach is used in (Cheung, 1995; Elkaranshway, 2011) for flexible link manipulators.

In the previous nonlinear control strategies, a single controller is used for all joints and links of flexible manipulators which are regarded as one MIMO system. Unfortunately, due to the complexity of the control structures, it is not easy to use this configuration on the real-time implementation in industrial control systems (Fu et al., 1987). For this reason, many industrial controls are viewed as interconnected subsystems (joints and links). Many advantages exist in this case such as reduction of computational effort, simplicity of implementation, etc. For this configuration, many control strategies are used. The decentralised control approach is used in (Bona and Li, 1992; Feiyue et al., 1993) for flexible link manipulators. An independent joint control method is also used in (Hillsley, 1993). A hierarchical control strategy is used in (Fareh et al., 2012) to solve the tracking control problem in the workspace for a 7-DOF hyper redundant articulated nimble adaptable trunks (ANAT) rigid manipulator. The hierarchical control strategy consists in controlling the last joint while assuming that the remaining joints are stable and follow their desired trajectories. Then, going backward, the same strategy is applied to control the (n-1)-th joint while assuming the remaining joints stable and follow their desired trajectories, and so on until the first joint. The feedback linearization approach was used to develop the control law and asymptotical stability is proved using Lyapunov theory. This algorithm was experimented on

the 7-DOF ANAT manipulator and gave effective results and good tracking of a desired trajectory defined in the workspace.

In this paper, a nonlinear control strategy ensuring trajectory tracking in the workspace is proposed for two-flexible-link manipulators. To solve the non-minimum phase problem, the output redefinition method is used to select a non-collocated output ensuring stability of internal dynamics. First, to solve the inverse dynamic problem, a trajectory transformation from the workspace to the joint space through a virtual space is used. Secondly, a nonlinear control strategy for the flexible manipulator is presented. This strategy is valid for n flexible links and is based on a hierarchical form. In fact, we begin by stabilizing the last link by considering the remaining links stable. Thereafter, we go backward until the first link. The stabilization of an i-th link is ensured using the feedback linearization approach. The non-collocated output is parameterized with a real parameter that is selected to guarantee bounded internal dynamics. In this paper, we use passivity and the circle criterion to analyze stability of the tracking error dynamics and to determine the new weighted outputs for two-flexible-link manipulators. The simulations show the effectiveness of the proposed method.

The paper is organized as follows: section 6.2 presents a description and modeling of the two-flexible-link manipulator. Section 6.3 proposes a transformation of the desired trajectory from the workspace to the joint space. The nonlinear control strategy is given in section 6.4. Section 5 presents the application and simulation of the proposed control strategy to the system at hand. Finally, conclusions are given in section 6.6.

6.2 Modeling

The system considered in this work is shown in Figure 1. It is a two-link flexible manipulator moving in the horizontal plane and connected by rigid revolute joints. It consists of two motors, two flexible links, and a payload. Two torques generated by the motors are acting on the system. The angle of the i-th motor is $\theta_i(t)$, its inertia coefficient is I_{mi} ($i=1,2$). The i-th flexible arm, supposed uniform, has a mass m_i and length L_i , linear density ρ_i , and rigidity

EI_i . The payload has a mass m_p . The first link is attached to the first motor and the second link is clamped to the rotor of the second motor. $(\hat{\mathbf{X}}_0, \hat{\mathbf{Y}}_0)$ is the fixed reference frame, while $(\mathbf{X}_1, \mathbf{Y}_1)$, and $(\mathbf{X}_2, \mathbf{Y}_2)$ are the links neutral axes and are moving with the first and the second link, respectively. $(\hat{\mathbf{X}}_1, \hat{\mathbf{Y}}_1)$ is linked to the second base. The flexible links are modeled as Euler-Bernoulli beams and the deformations are assumed to be small.

Using the Lagrangian formulation, the equation of motion of an n DOF manipulator can be written as:

$$M(q)\ddot{q} + C(q, \dot{q}) + D\dot{q} + Kq = \tau \quad (6.1)$$

where M is the mass matrix, D is the friction matrix, K is the rigidity matrix, and $C(q, \dot{q})$ is the Coriolis and centrifugal forces vector. q represents the vector of the generalized coordinates, and τ is the vector of the applied torques. Assume that there are a total of n rigid coordinates and n flexible links, the deformation of the i-th flexible link can be expressed as follows:

$$v_i(x, t) = \sum_{j=1}^{m_i} \phi_{ij}(x) q_{fij}(t) \quad i = 1, \dots, n \quad (6.2)$$

where q_{fij} is the j-th generalized flexible coordinate of the i-th flexible link, $\phi_{ij}(x)$ is its j-th shape function and m_i is the number of the retained flexible modes. The total number of the flexible modes is $m = \sum_{i=1}^n m_i$. In (Saad et al., 2006), a detailed comparison between assumed based models and finite element ones has been carried on a single flexible link system for one to eight flexible modes. This comparison shows that clamped beam shape functions for the AMM and cubic spline finite elements for the FEM describe best the shape functions of flexible link manipulators.

In our case, we have modified the model of the two flexible links presented in (De Luca et Siciliano, 1990; 1991) by only considering the first flexible mode of each link (see Appendix B).

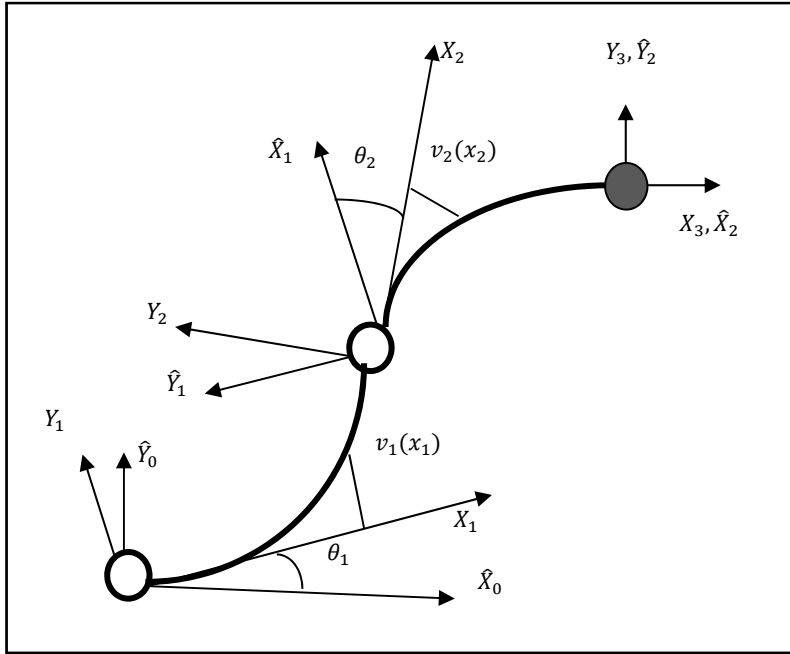


Figure 6.1 Two-flexible-link manipulator.

Then, we have $n = 2$, and $m_1 = m_2 = 1$. Equation (6.1) can be written as:

$$\begin{bmatrix} M_{rr} & M_{rf} \\ M_{fr} & M_{ff} \end{bmatrix} \begin{bmatrix} \ddot{q}_r \\ \ddot{q}_f \end{bmatrix} + \begin{bmatrix} C_r(q, \dot{q}) \\ C_f(q, \dot{q}) \end{bmatrix} + \begin{bmatrix} 0 & 0 \\ 0 & D_{ff} \end{bmatrix} \begin{bmatrix} \dot{q}_r \\ \dot{q}_f \end{bmatrix} + \begin{bmatrix} 0 & 0 \\ 0 & K_{ff} \end{bmatrix} \begin{bmatrix} q_r \\ q_f \end{bmatrix} = \begin{bmatrix} I \\ 0 \end{bmatrix} \tau \quad (6.3)$$

where:

$$M_{rr} = \begin{bmatrix} M_{r1r1} & M_{r1r2} \\ M_{r2r1} & M_{r2r2} \end{bmatrix}; M_{rf} = \begin{bmatrix} M_{r1f1} & M_{r1f2} \\ M_{r2f1} & M_{r2f2} \end{bmatrix}; M_{fr} = M_{rf}^T; M_{ff} = \begin{bmatrix} M_{f1f1} & M_{f1f2} \\ M_{f2f1} & M_{f2f2} \end{bmatrix}$$

The subscripts r_i and f_i denotes the rigid and flexible modes for the i -th link. $q_r \in \Re^n$ are the generalized coordinates associated with the movement of the rigid part, and $q_f \in \Re^m$ are associated with the flexible part. The dynamical equation of motion of the flexible manipulators has the following properties:

P1: $M, M_{rr}, M_{ff}, D_{ff}$ and K_{ff} are symmetric positive definite matrices.

P2: The first and second links are characterized by two sub-matrices: $M_1 = \begin{bmatrix} M_{r1r1} & M_{r1f1} \\ M_{f1r1} & M_{f1f1} \end{bmatrix}$

and $M_2 = \begin{bmatrix} M_{r2r2} & M_{r2f2} \\ M_{f2r2} & M_{f2f2} \end{bmatrix}$ that are symmetric positive definite.

P3: There exist a matrix $H(q, \dot{q})$ such that $C(q, \dot{q}) = H(q, \dot{q}) \dot{q}$ and $\forall x \in \Re^{n+m}, x^T(M - 2H)x = 0$.

6.3 Trajectory transformation

In this section, we transform in the desired trajectory from the workspace to the manipulator's joint space. The flexible manipulator is a non-minimum phase system when the end-effector is considered as the output (Cannon et Schmitz, 1984). In the linear case, transfer functions have one or more zeros in the right half s-plane. For the nonlinear system, the zero dynamics are unstable.

The workspace and the joint space are linked by kinematic and dynamic relationships. In the first step, we use the kinematic relation to transform the desired trajectory from the workspace to a virtual space. In the second step, we transform the desired trajectory from the virtual space to the generalized flexible coordinates space. The flexible coordinates are calculated by solving a nonlinear equation for the flexible part using the quasi-static approach. The generalized rigid coordinates are deduced from the generalized flexible coordinates and the generalized coordinates defined in the virtual space. The transformation of the desired trajectories from the workspace to the joint space is shown in Figure 6.2.

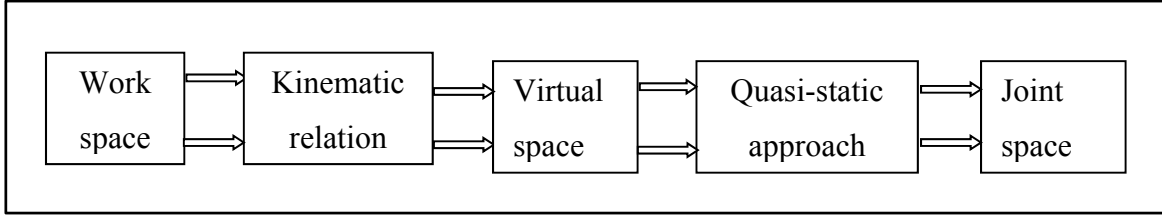


Figure 6.2 Transformation of the desired trajectories.

Then, it is easy to find the virtual generalized coordinates using an inverse kinematic as done for rigid manipulators. For an i -th link, the virtual coordinate Q_i is the link's angular position relative to \hat{X}_{i-1} as shown in Figure 6.3.

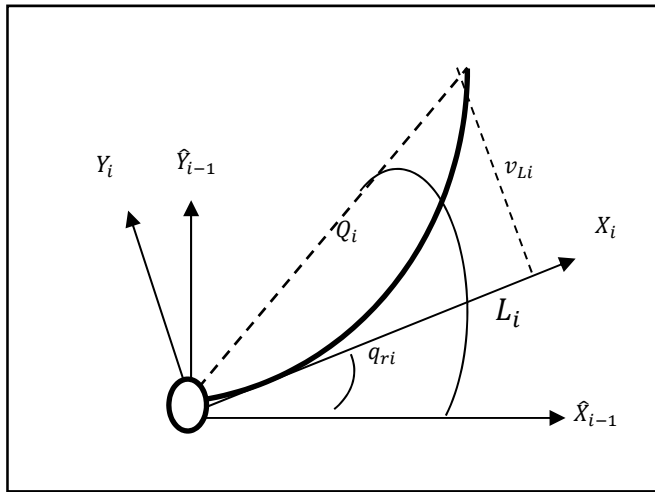


Figure 6.3 Virtual space.

The deformation is assumed to be small. According to Figure 6.3, we can write:

$$Q_i - q_{ri} = \arctan\left(\frac{v_{Li}}{L_i}\right) \approx \frac{v_{Li}}{L_i} \quad (6.4)$$

Then, the generalized coordinate in the virtual space is:

$$Q_i = q_{ri} + \beta_i^T q_{fi} \quad (6.5)$$

where $\beta_i^T = \frac{1}{L_i} [\emptyset_{i1}(L_i), \dots, \emptyset_{im_i}(L_i)]$, with L_i being the length of the i-th flexible link, and \emptyset_{ij} is the shape function of link i and mode j. The velocity and the acceleration in the virtual space can be found using the Jacobian matrix.

The quasi-static approach (Pfeiffer, 1989) can be used to compute the generalized flexible and rigid coordinates in the joint space. This approach neglects the velocity and acceleration of the flexible coordinates ($\dot{q}_f = \ddot{q}_f = 0$) when solving the inverse dynamics for the desired flexible trajectories. From (6.3), we get:

$$M_{fr}\ddot{q}_r + M_{ff}\ddot{q}_f + C_f(q, \dot{q}) + D_{ff}\dot{q}_f + K_{ff}q_f = 0$$

Neglecting \dot{q}_f and \ddot{q}_f and using (6.5), q_{fd} is found by solving the following nonlinear equation:

$$M_{fr}(q_d)\ddot{q}_{rd} + C_f(q_d, \dot{q}_d) + K_{ff}q_{fd} = 0 \quad (6.6)$$

where

$$q_{rdi} = Q_{di} - \beta_i^T q_{fdi}; \dot{q}_{rdi} = \dot{Q}_{di}; \ddot{q}_{rdi} = \ddot{Q}_{di} \quad (6.7)$$

In the final step, the generalized rigid coordinates are given by (6.7).

6.4 Control Strategy

6.4.1 Hierarchical control strategy for n flexible links

The control strategy presented in (Fareh, Saad et Saad, 2012) was applied and experimented on a 7-DOF rigid manipulator. This strategy is modified to take into account link flexibility. In fact, the control strategy consists in stabilizing the last joint and flexible link by assuming that the remaining joints and flexible links are stable. Then we go backward to the (n-1)-th joint and flexible link assuming the previous joints and links are stable, and so on until the first joint and flexible link. In each step we define a new non-collocated output and we use the feedback linearization approach to develop the control law. The weighted parameter characterizing the non-collocated output, that ensures bounded internal dynamics,

is found by studying the asymptotical stability of the resulting tracking error dynamics. The control strategy is shown in Figure 6.4.

For each link, we follow the following steps:

Step1. Set $i = n$; Assume that the first $(i-1)$ joints and links are stable, i.e. the generalized coordinates follow their desired trajectories.

Step2. Stabilize the i -th joint and flexible link by applying the following procedure:

Define a *new non collocated output* as the angle of the i -th motor augmented by a weighted value of the i -th link's extremity angle:

$$y_{inew} = q_{ri} + \alpha_i \beta_i^T q_{fi}, \quad 0 \leq \alpha_i < 1 \quad (6.8)$$

Redefine the dynamical model with the new generalized coordinates:

$$\bar{q}_i = [y_{inew} \ q_{fi}]^T \quad (6.9)$$

The *new model* is obtained by replacing in (6.3) the i -th rigid generalized coordinate q_{ri} by the new non-collocated output y_{inew} given in (6.8).

Develop the *control law* τ_i by applying the feedback linearization approach: first, separate the i -th acceleration of the flexible generalized coordinate \ddot{q}_{fi} from the flexible part of the new model. Second, insert this term in the rigid part to obtain the following form of the control law:

$$\tau_i = f(u_i, q_i, \dot{q}_i) \quad (6.10)$$

where u_i is a control law that ensures tracking of the new output. Finally, the linearized dynamics and the internal dynamics take the following form:

$$\begin{cases} \ddot{y}_{inew} = u_i \\ \ddot{q}_{fi} = g(u_i, q_i, \dot{q}_i) \end{cases} \quad (6.11)$$

Find the *critical value of the weighted parameter* α_i such that the output is the nearest to the i -th link's extremity while ensuring bounded internal dynamics. Then, study the asymptotical stability of the errors dynamics of the flexible part and choose the critical value which corresponds to its limit of stability. The passivity is used to analyze the stability.

Step3. Set $i = n - 1$ and go back to *Step1*.

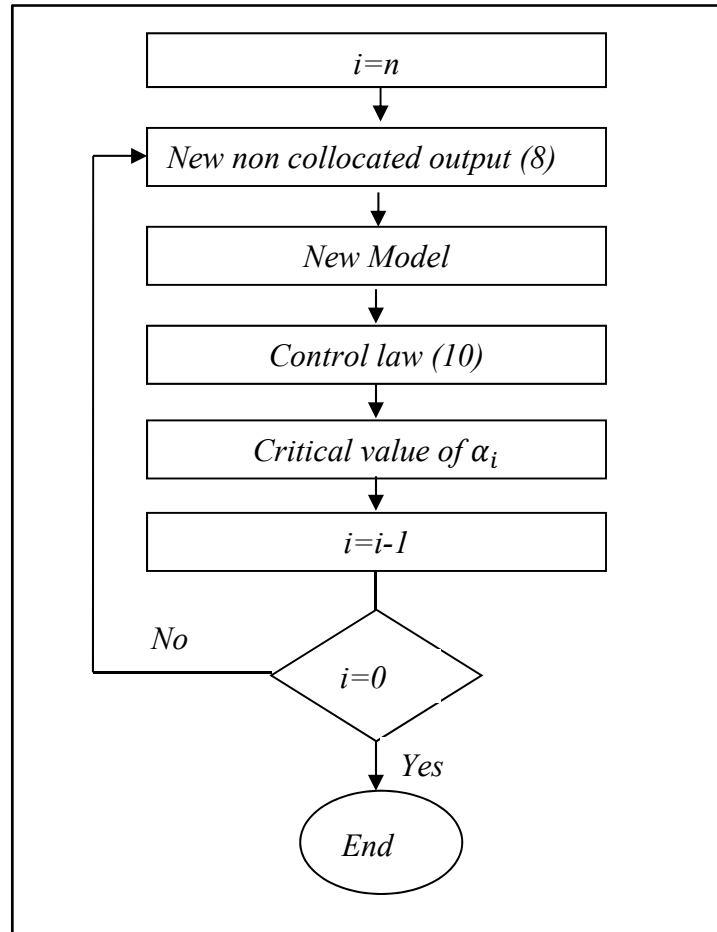


Figure 6.4 Control strategy.

6.4.2 Application to two flexible links manipulator

We now apply the previous strategy to a two-flexible-link manipulator as shown in Figure 6.1. From (6.3), the dynamical model is given by:

$$M_{11}\ddot{q}_{r1} + M_{12}\ddot{q}_{r2} + M_{13}\ddot{q}_{f1} + M_{14}\ddot{q}_{f2} + C_1 = \tau_1 \quad (6.12)$$

$$M_{21}\ddot{q}_{r1} + M_{22}\ddot{q}_{r2} + M_{23}\ddot{q}_{f1} + M_{24}\ddot{q}_{f2} + C_2 = \tau_2 \quad (6.13)$$

$$M_{31}\ddot{q}_{r1} + M_{32}\ddot{q}_{r2} + M_{33}\ddot{q}_{f1} + M_{34}\ddot{q}_{f2} + C_3 + D_{f1}\dot{q}_{f1} + K_{f1}q_{f1} = 0 \quad (6.14)$$

$$M_{41}\ddot{q}_{r1} + M_{42}\ddot{q}_{r2} + M_{43}\ddot{q}_{f1} + M_{44}\ddot{q}_{f2} + C_4 + D_{f2}\dot{q}_{f2} + K_{f2}q_{f2} = 0 \quad (6.15)$$

In the first step, we transform the desired trajectories in triangular form (Figure 6.5) from workspace to joint space. By following the same strategy given in section 6.3, the virtual space is defined as if it was a 2-DOF rigid manipulator as follows:

$$\begin{cases} Q_{d1} = q_{rd1} + \beta_1 q_{fd1} = \text{atan2}(y_d, x_d) - \text{atan2}(k_2, k_1) \\ Q_{d2} = q_{rd2} + \beta_2 q_{fd2} = \text{atan2}(s_2, c_2) \end{cases} \quad (6.16)$$

where $\beta_i = \frac{\phi_i(L_i)}{L_i}$, $i = 1, 2$; $c_2 = \frac{x^2 + y^2 - L_1^2 - L_2^2}{2L_1L_2}$; $s_2 = \pm\sqrt{1 - c_2^2}$; $k_1 = L_1 + L_2c_2$ and $k_2 = L_2s_2$; $s_i = \sin(Q_{di})$; and $c_i = \cos(Q_{di})$.

Using the Jacobian, the velocity and acceleration of the virtual coordinates are given by:

$$\begin{bmatrix} \dot{Q}_{d1} \\ \dot{Q}_{d2} \end{bmatrix} = J^{-1}(Q_d) \begin{bmatrix} \dot{x}_d \\ \dot{y}_d \end{bmatrix}; \begin{bmatrix} \ddot{Q}_{d1} \\ \ddot{Q}_{d2} \end{bmatrix} = J^{-1}(Q_d) \left\{ \begin{bmatrix} \ddot{x}_d \\ \ddot{y}_d \end{bmatrix} - J(Q_d) \begin{bmatrix} \dot{Q}_{d1} \\ \dot{Q}_{d2} \end{bmatrix} \right\} \quad (6.17)$$

$$\text{where } J(Q_d) = \begin{bmatrix} -l_1s_1 - l_2s_{12} & -l_2s_{12} \\ l_1c_1 + l_2c_{12} & l_2c_{12} \end{bmatrix}.$$

Using (6.16), the rigid coordinates and their time derivatives are replaced in (6.12)-(6.15) by the following expressions:

$$q_{rdi} = Q_{di} - \beta_i q_{fdi}; \dot{q}_{rdi} = \dot{Q}_{di}; \ddot{q}_{rdi} = \ddot{Q}_{di}; i = 1, 2 \quad (6.18)$$

The generalized flexible coordinates are calculated using the following nonlinear equations:

$$M_{31}\ddot{Q}_{d1} + M_{32}\ddot{Q}_{d2} + C_3(Q_d, \dot{Q}_d, q_{fd}) + K_{f1}q_{fd1} = 0 \quad (6.19)$$

$$M_{41}\ddot{Q}_{d1} + M_{42}\ddot{Q}_{d2} + C_4(Q_d, \dot{Q}_d, q_{fd}) + K_{f2}q_{fd2} = 0 \quad (6.20)$$

The generalized rigid coordinates are then given by (6.18).

6.4.2.1 Control and stability of the second link

We assume in this section that the first link is stable. Then its generalized coordinates, velocities, and accelerations follow their desired trajectories.

$$q_1 = [q_{rd1} \quad q_{fd1}]^T; \dot{q}_1 = [\dot{q}_{rd1} \quad 0]^T; \ddot{q}_1 = [\ddot{q}_{rd1} \quad 0]^T$$

The dynamical equations of the second link are given by (6.13) and (6.15):

The objective is to stabilize the second link and to track the desired trajectory in the workspace by selecting a non-collocated output close to the tip. The new output is given by:

$$y_{\alpha 2} = q_{r2} + \alpha_2 \beta_2 q_{f2}, \quad 0 \leq \alpha_2 < 1 \quad (6.21)$$

$$\text{where } \beta_2 = \frac{\emptyset_2(L_2)}{L_2}.$$

The generalized rigid coordinates of the second link and their derivatives can be expressed as follows:

$$q_{r2} = y_{\alpha 2} - \alpha_2 \beta_2 q_{f2}; \dot{q}_{r2} = \dot{y}_{\alpha 2} - \alpha_2 \beta_2 \dot{q}_{f2}; \ddot{q}_{r2} = \ddot{y}_{\alpha 2} - \alpha_2 \beta_2 \ddot{q}_{f2} \quad (6.22)$$

By substitution (6.22) in (6.13) and (6.15), the new dynamical model is given by:

$$M_{21}\ddot{q}_{rd1} + M_{22}\ddot{y}_{\alpha 2} + (M_{24} - \alpha_2 \beta_2 M_{22})\ddot{q}_{f2} + C_2 = \tau_2 \quad (6.23)$$

$$M_{41}\ddot{q}_{rd1} + M_{42}\ddot{y}_{\alpha 2} + (M_{44} - \alpha_2 \beta_2 M_{42})\ddot{q}_{f2} + C_4 + K_{f2}q_{f2} + D_{f2}\dot{q}_{f2} = 0 \quad (6.24)$$

By isolating \ddot{q}_{f2} in (6.24), the internal dynamics of the second link is given by:

$$\ddot{q}_{f2} = -\bar{M}_{41}\ddot{q}_{rd1} - \bar{M}_{42}\ddot{y}_{\alpha 2} - \bar{C}_4 - \bar{K}_{f2}q_{f2} - \bar{D}_{f2}\dot{q}_{f2} \quad (6.25)$$

where: $\bar{X} = (M_{44} - \alpha_2\beta_2 M_{42})^{-1} \cdot X$, and α_2 is chosen such that: $\alpha_2 \neq \frac{M_{44}}{\beta_2 M_{42}}$

Inserting (6.25) in (6.23), the control law is chosen as follows:

$$\tau_2 = M_{21}^* \ddot{q}_{rd1} + C_2^* + K_{f2}^* q_{f2} + D_{f2}^* \dot{q}_{f2} + M_{22}^* u_{\alpha 2} \quad (6.26)$$

where: $M_{21}^* = M_{21} - (M_{24} - \alpha_2\beta_2 M_{22})\bar{M}_{41}$; $M_{22}^* = M_{22} - (M_{24} - \alpha_2\beta_2 M_{22})\bar{M}_{42}$;

$C_2^* = C_2 - (M_{24} - \alpha_2\beta_2 M_{22})\bar{C}_4$; $K_{f2}^* = -(M_{24} - \alpha_2\beta_2 M_{22})\bar{K}_{f2}$;

$D_{f2}^* = -(M_{24} - \alpha_2\beta_2 M_{22})\bar{D}_{f2}$. $u_{\alpha 2}$ is the new control law.

Proposition 6.1

By considering the transformation matrix $T = \begin{bmatrix} 1 & \alpha_2\beta_2 \\ 0 & 1 \end{bmatrix}$ between the new generalized coordinates $\bar{q}_2 = [y_{\alpha 2} \quad q_{f2}]^T$ and the former generalized coordinates $q_2 = [q_{r2} \quad q_{f2}]^T$, M_{22}^* is then nonzero if $\alpha_2 \neq \frac{M_{44}}{\beta_2 M_{42}}$.

The proof of proposition is given in Appendix A.

To ensure the stability of the output tracking error, we choose the new control law as follows:

$$u_{\alpha 2} = \ddot{y}_{\alpha d2} + K_{d\alpha 2}\dot{\tilde{y}}_{\alpha 2} + K_{p\alpha 2}\tilde{y}_{\alpha 2} \quad (6.27)$$

where $\ddot{y}_{\alpha d2} = \ddot{q}_{rd2} + \alpha_2\beta_2\ddot{q}_{fd2}$ is the desired acceleration of the new weighted output, and $\tilde{y}_{\alpha 2} = y_{\alpha d2} - y_{\alpha 2}$ is its tracking error. $K_{p\alpha 2}, K_{d\alpha 2}$ are positive constants.

The tracking errors dynamics for the new output and internal dynamics are:

$$\ddot{\tilde{y}}_{\alpha 2} = \ddot{y}_{\alpha d 2} - u_{\alpha 2} = \delta u_2 \quad (6.28)$$

$$\begin{aligned} \ddot{\tilde{q}}_{f2} &= \ddot{q}_{fd 2} - \ddot{q}_{f2} = -(\bar{M}_{d41} - \bar{M}_{41})\ddot{q}_{rd 1} - (\bar{M}_{d42}\ddot{y}_{\alpha d 2} - \bar{M}_{42}u_{\alpha 2}) - (\bar{C}_{d4} - \bar{C}_4) \\ &\quad - (\bar{K}_{fd 2}q_{fd 2} - \bar{K}_{f2}q_{f2}) - (\bar{D}_{fd 2}\dot{q}_{fd 2} - \bar{D}_{f2}\dot{q}_{f2}) \end{aligned} \quad (6.29)$$

In state space form, (6.28)-(6.29) can be written as:

$$\begin{cases} \dot{\tilde{x}}_1 = \tilde{x}_2 \\ \dot{\tilde{x}}_2 = \ddot{y}_{\alpha d 2} - \ddot{y}_{\alpha 2} = \ddot{y}_{\alpha d 2} - u_{\alpha 2} = \delta u_2 \\ \dot{\tilde{x}}_3 = \tilde{x}_4 \\ \dot{\tilde{x}}_4 = \ddot{q}_{fd 2} - \ddot{q}_{f2} \end{cases} \quad (6.30)$$

Let $\tilde{x}_r = [\tilde{x}_1 \quad \tilde{x}_2]^T = [\tilde{y}_{\alpha 2} \quad \dot{\tilde{y}}_{\alpha 2}]^T$; $\tilde{x}_f = [\tilde{x}_3 \quad \tilde{x}_4]^T = [\tilde{q}_{f2} \quad \dot{\tilde{q}}_{f2}]^T$; $\tilde{x} = [\tilde{x}_r \quad \tilde{x}_f]^T$; $\tilde{q}_{f2} = q_{fd 2} - q_{f2}$.

The origin of (6.30) is asymptotically stable if the system is output passive and zero-state observable (Khalil, 1996).

Proposition 6.2

The system (6.30) is output passive and $\tilde{y}_{\alpha 2}, \dot{\tilde{y}}_{\alpha 2} \rightarrow 0$ as $t \rightarrow \infty$ if $\dot{\tilde{y}}_{\alpha 2}$ is chosen as the output and the input δv is given by:

$$\delta v = \delta u_2 + K_p \tilde{y}_{\alpha 2} + K_d \dot{\tilde{y}}_{\alpha 2} \quad (6.31)$$

Proof: see Appendix A.

It remains now to verify the second condition (zero-state observability) by cancelling the input and the output in the error dynamics of the flexible part. After that we study the asymptotical stability of the origin and find the critical value of α_2 , if it exists.

Proposition 6.3

The error dynamics of the flexible part given in (6.29) can be represented as a feedback connection of a linear system and a nonlinear memoryless element:

$$G: \begin{cases} \dot{\tilde{x}}_f = A_f \tilde{x}_f + B_f v \\ y = C_f^T \tilde{x}_f \end{cases} \quad (6.32)$$

$$v = -\psi(t, y)$$

where $A_f = \begin{bmatrix} 0 & 1 \\ -a_0(t) & -a_1(t) \end{bmatrix}$; $B_f = \begin{bmatrix} 0 \\ (M_{44} - \alpha_2 \beta_2 M_{42})^{-1} \end{bmatrix}$; $C_f^T = [-\alpha_2 \beta_2 \ 0]$ and $\psi(t, y)$ is a nonlinear element (see Appendix A for the demonstration).

Proposition 6.4

If the nonlinearity element $\psi(t, y)$ is passive and the linear system is input strictly passive, then the origin $\tilde{x}_f = 0$ of (6.32) is asymptotically stable (Khalil, 1996). There exists $\alpha_2 \leq \alpha_{2c}$ that ensures the asymptotical stability of the origin.

The proof of Proposition 6.4 is given in Appendix A.

The critical value of α_2 is selected such that A_f is Hurwitz and the Nyquist diagram of A_f lies in the right half-plan (Khalil, 1996).

6.4.2.2 Control and stability of the first link

After the stabilization and control of the second link, we follow the same strategy to control and stabilize the first link. The dynamical equations of the first link are given in (6.12) and (6.14).

We define the new weighted output, velocity and acceleration as follows:

$$y_{\alpha 1} = q_{r1} + \alpha_1 \beta_1 q_{f1}; \dot{y}_{\alpha 1} = \dot{q}_{r1} + \alpha_1 \beta_1 \dot{q}_{f1}; \ddot{y}_{\alpha 1} = \ddot{q}_{r1} + \alpha_1 \beta_1 \ddot{q}_{f1}.$$

Then,

$$q_{r1} = y_{\alpha 1} - \alpha_1 \beta_1 q_{f1} \quad (6.33)$$

Substituting (6.33) and its derivatives into (6.14), the internal dynamics is:

$$\ddot{q}_{f1} = -\bar{M}_{31}\ddot{y}_{\alpha 1} - \bar{M}_{32}\ddot{q}_{rd2} - \bar{C}_3 - \bar{K}_{f1}q_{f1} - \bar{D}_{f1}\dot{q}_{f1} \quad (6.34)$$

where: $\bar{X} = (M_{33} - \alpha_1 \beta_1 M_{31})^{-1}X$ and α_1 is chosen such that $\alpha_1 \neq \frac{M_{33}}{\beta_1 M_{31}}$.

The control law is chosen by inserting (6.34) in (6.12);

$$\tau_1 = M_{11}^* u_{\alpha 1} + M_{12}^* \dot{y}_{\alpha d1} + C_1^* + K_{f1}^* q_{f1} + D_{f1}^* \dot{q}_{f1} \quad (6.35)$$

where: $M_{11}^* = M_{11} - (M_{13} - \alpha_1 \beta_1 M_{11})\bar{M}_{31}$; $M_{12}^* = M_{12} - (M_{13} - \alpha_1 \beta_1 M_{11})\bar{M}_{32}$
 $C_1^* = C_1 - (M_{13} - \alpha_1 \beta_1 M_{11})\bar{C}_3$; $K_{f1}^* = -(M_{13} - \alpha_1 \beta_1 M_{11})\bar{K}_{f1}$; $D_{f1}^* = -(M_{13} - \alpha_1 \beta_1 M_{11})\bar{D}_{f1}$

M_{11}^* is nonzero using the Schur complement as in the previous section.

To track the desired new output trajectory, we choose the following control law:

$$u_{\alpha 1} = \ddot{y}_{\alpha d1} + K_{d\alpha 1}\dot{\tilde{y}}_{\alpha 1} + K_{p\alpha 1}\tilde{y}_{\alpha 1} \quad (6.36)$$

where $\ddot{y}_{\alpha d1}$ is the desired acceleration, $\tilde{y}_{\alpha 1} = y_{\alpha d1} - y_{\alpha 1}$ is the tracking error of the new output, $K_{d\alpha 1}$ and $K_{p\alpha 1}$ are positive constants.

The errors dynamics of the new output and the flexible coordinates are given by the following state space model:

$$\begin{cases} \dot{\tilde{x}}_1 = \dot{\tilde{y}}_{\alpha 1} = \tilde{x}_2 \\ \dot{\tilde{x}}_2 = \ddot{y}_{\alpha d1} - u_{\alpha 1} = \delta u_1 \\ \dot{\tilde{x}}_3 = \dot{\tilde{q}}_{f1} = \tilde{x}_4 \\ \dot{\tilde{x}}_4 = \ddot{\tilde{q}}_{f1} = \ddot{q}_{fd1} - \ddot{q}_{f1} \end{cases} \quad (6.37)$$

Let: $\tilde{x}_r = [\tilde{x}_1 \quad \tilde{x}_2]^T = [\tilde{y}_{\alpha 1} \quad \dot{\tilde{y}}_{\alpha 1}]^T$; $\tilde{x}_f = [\tilde{x}_3 \quad \tilde{x}_4]^T = [\tilde{q}_{f1} \quad \dot{\tilde{q}}_{f1}]^T$; $\tilde{x} = [\tilde{x}_r \quad \tilde{x}_f]^T$.

As already shown, the system is output passive and $\tilde{x}_r \rightarrow 0$ as $t \rightarrow \infty$ if we consider the following strictly passive control (Khalil, 1996).

$$\delta u_1 = -K_p \tilde{y}_{\alpha 1} - K_d \dot{\tilde{y}}_{\alpha 1} + \delta v \quad (6.38)$$

The error dynamics of the flexible part (6.34) can be expressed as:

$$\dot{\tilde{x}}_f = F(t, \tilde{x}_f, \delta u_1) \quad (6.39)$$

where $F(t, \tilde{x}_f, \delta u_1) = \begin{bmatrix} \tilde{x}_{f2} \\ f(t, \tilde{x}_f, \delta u_1) \end{bmatrix}$, $\tilde{x}_{f1} = \tilde{x}_3$, $\tilde{x}_{f2} = \tilde{x}_4$, and $f(t, \tilde{x}_f, \delta u_1)$ is given in Appendix A.

It remains to check the zero-state observability by setting the input and output to zero and studying the asymptotic stability of the origin of the errors dynamics.

Proposition 6.5

The asymptotical stability of the origin of (6.39) is equivalent to the asymptotical stability of the following system:

$$\dot{\tilde{x}}_f = \begin{bmatrix} 0 & 1 \\ -\bar{K}_{f1} & -\bar{D}_{f1} \end{bmatrix} \tilde{x}_f \quad (6.40)$$

where \bar{K}_{f1} and \bar{D}_{f1} are given in (6.34). The proof of proposition 6.5 is given in Appendix A.

The critical value of α_1 is given when the eigenvalues of (6.40) change their signs from negative to positive.

6.5 Simulation results

The parameters of the two flexible links manipulator are described in Table 1. The controllers parameters are chosen by using a trial and error method as follow: $K_{p1} = K_{d1} = 100$ and $K_{p2} = K_{d2} = 250$.

Table 6.1 System parameters

Parameter	Value
Hub inertia (Jh_i)	0.1 kg.m ²
Link length (L_i)	0.5 m
Link linear density (ρ)	1 kg/m
Link rigidity (EI_i)	10N.m ²
Link mass (m_i)	0.5 kg
Payload mass (m_p)	0.1 kg
Payload inertia (J_p)	0.0005 kg.m ²

The workspace desired trajectory in triangular form is shown by Figure 6.5.

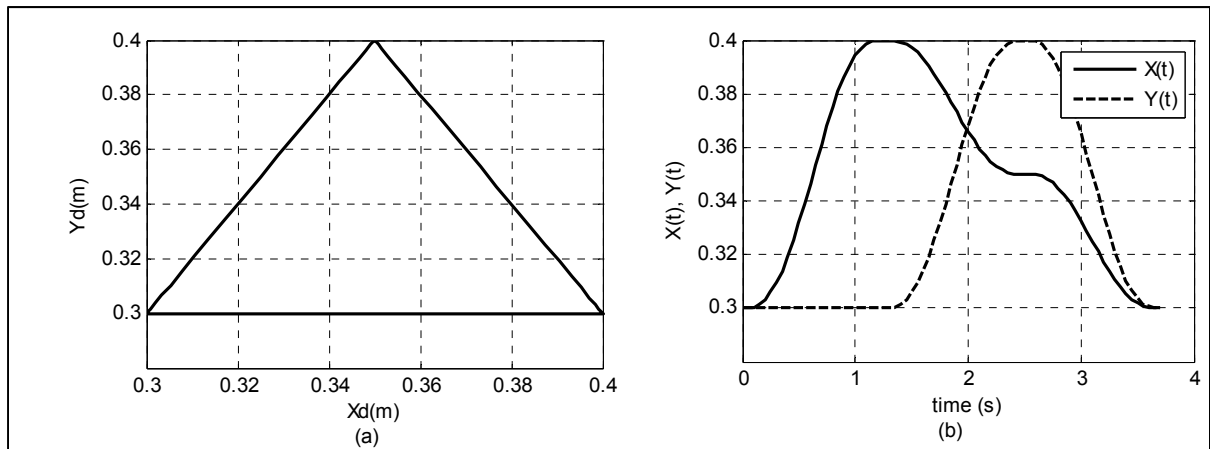


Figure 6.5 Workspace desired trajectory: (a) Y_d vs X_d and (b) $x_d(t)$, $y_d(t)$.

For the system parameters given in Table 6.1, the critical values of the weighted parameters of the second link and the first link are, respectively, $\alpha_{2c} = 0.92$ and $\alpha_{1c} = 0.85$ (Figures 6.6 and 6.7). Nyquist diagram is done for A_{f0} given in (6.53). Simulation results were done with $\alpha_2 = 0.9 < \alpha_{2c}$ and $\alpha_1 = 0.8 < \alpha_{1c}$. Note that these values respect the conditions given in equations (6.25) and (6.34).

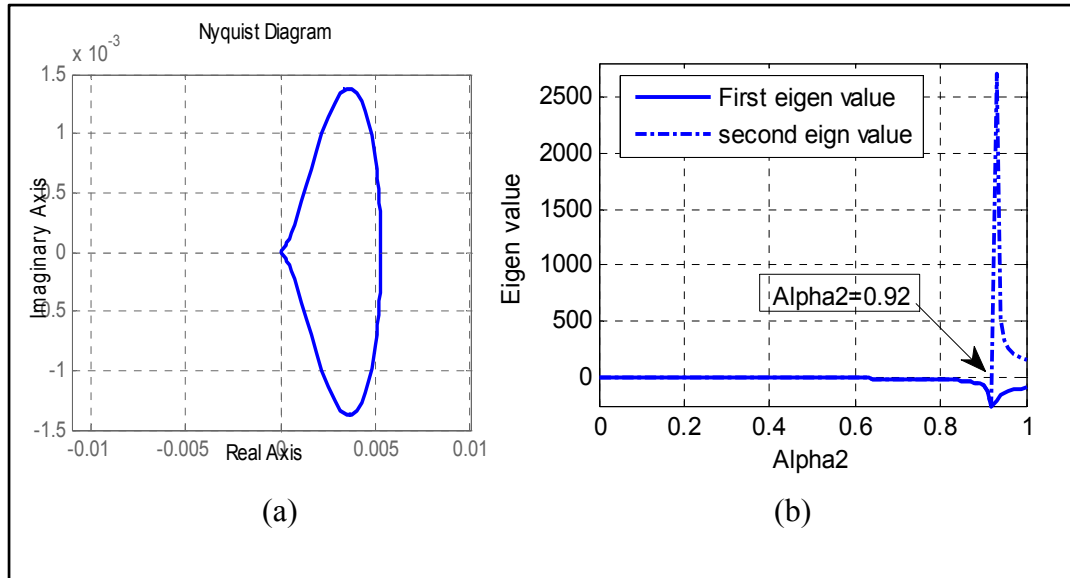


Figure 6.6 (a) Nyquist diagram, and (b) eigenvalues evolution.

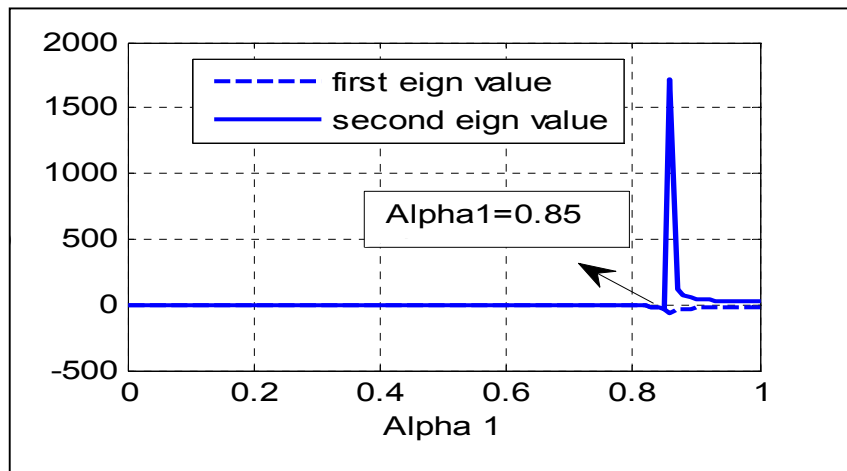


Figure 6.7 Eigenvalues vs. α_1 .

The workspace tracking is given in Figure 6.8. The virtual and joint space tracking are given in Figures 6.9 and 6.10, respectively. The joints tracking errors are given in Figure 6.11.

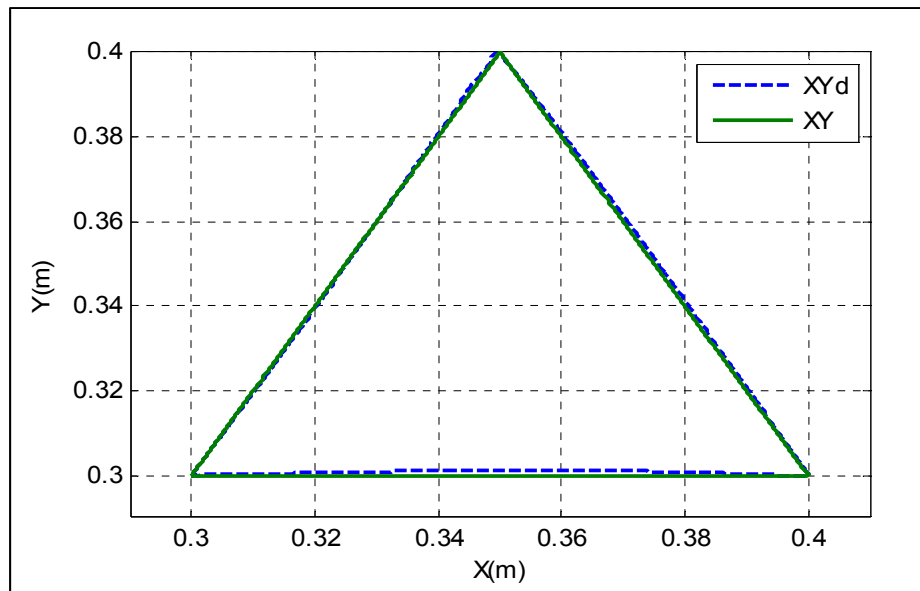


Figure 6.8 Tracking of X-Y trajectory.

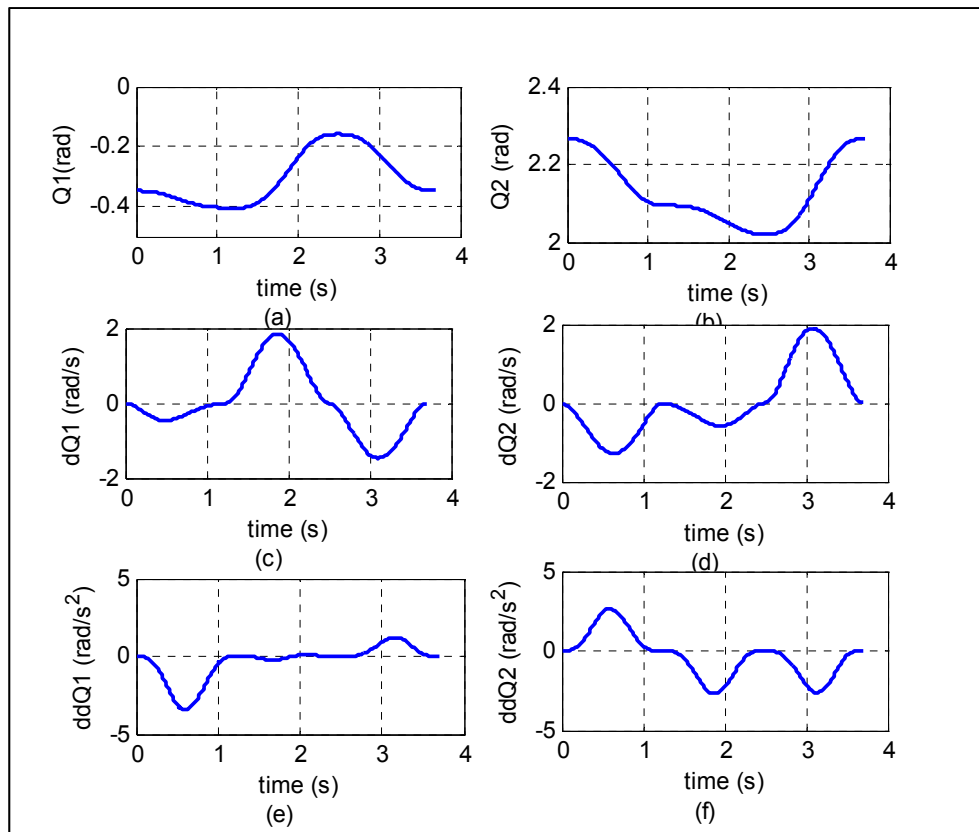


Figure 6.9 (a)-(b) Position of virtual joints, (c)-(d) velocity of virtual joints, (e)-(f) acceleration of virtual joints.

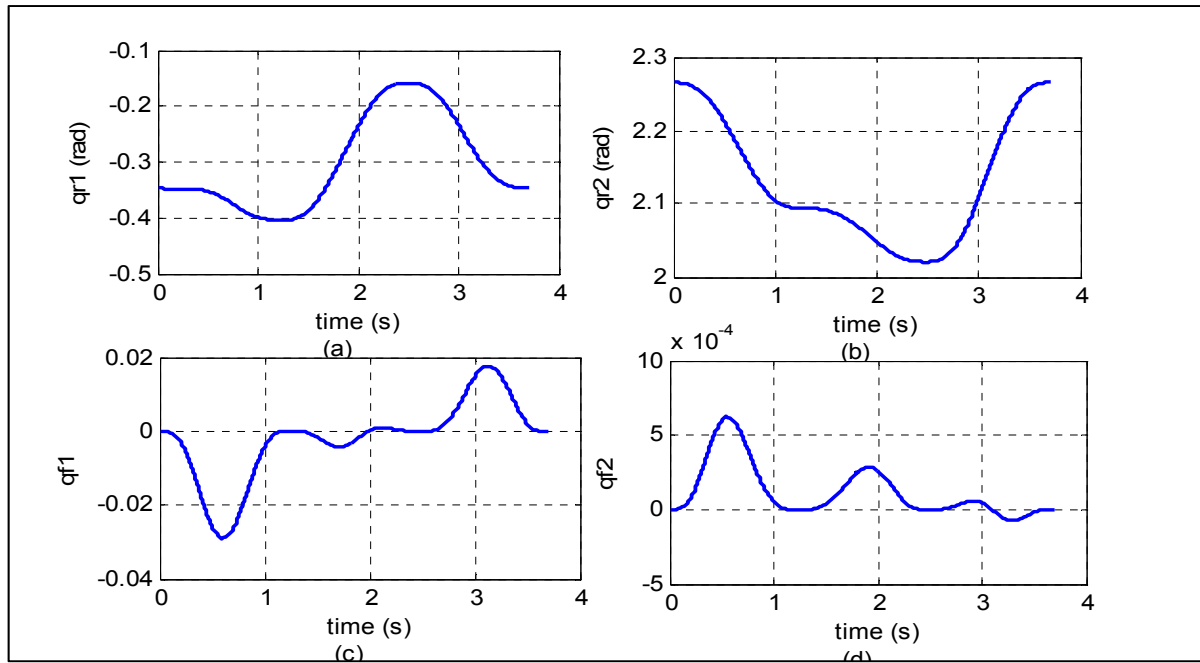


Figure 6.10 (a)-(b) Flexible coordinates; (c)-(d) Rigid coordinates.

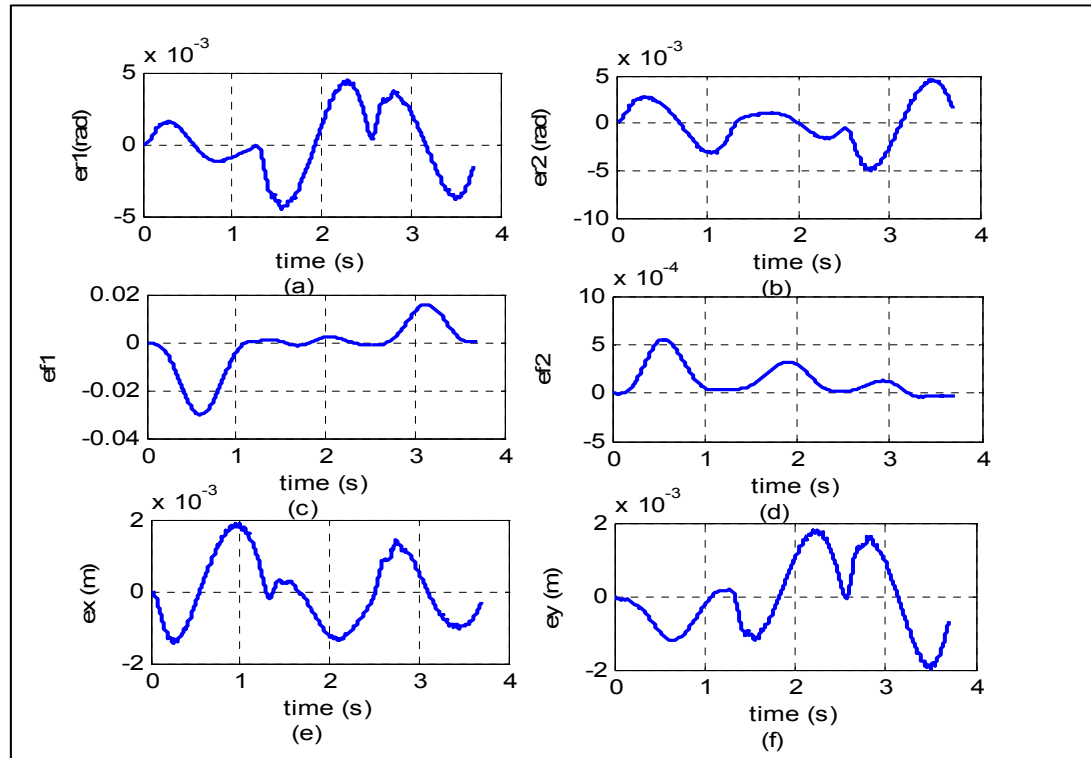


Figure 6.11 (a)-(b) Errors of joints 1 and 2; (c)-(d) errors of flexible coordinates 1, 2; (e)-(f) tracking errors of workspace trajectories $x(t)$ and $y(t)$.

According to the simulation results, we can conclude that the trajectory defined in the workspace was well transformed to the joint space by using the virtual space and the quasi-static approach. This good transformation is showed in Figure 6.9, which represents the position, velocity and acceleration in virtual space, and Figure 6.10 which represents the rigid and flexible coordinates in joint space. The control strategy was effective to ensure the tracking of the joints trajectories and reduce vibrations at the extremity. The good tracking in joint space is showed in Figure 6.11.a, b, c, and d which represent tracking errors in the joint space. In the workspace, the good tracking is showed in Figure 6.8 and the tracking errors are given in Figures 6.11-e and f. The new selected outputs are near links extremities. This explains the satisfactory results obtained using this approach. This control strategy has many advantages. Indeed, it is easier to study one arm at each step than to study the stability of the over whole system. In addition, this strategy takes a hierarchical form.

6.6 Conclusion and future work

In this paper, nonlinear control laws and stability analysis have been presented to stabilize the tracking errors of a two flexible links manipulator. A desired trajectory defined in the workspace has been transformed to the joint space using a virtual space transformation and the quasi-static approach. A desired trajectory (triangle) chosen in the workspace has been successfully transformed to the joint space using this transformation procedure. The control strategy used in this paper consists of stabilizing the system starting with the last flexible link and going backward until the first link. In each step, the output redefinition technique was used to select the nearest point to the extremity. This strategy shows good tracking trajectory in the workspace. Asymptotical stability of the tracking errors has been guaranteed using the passivity theory. In the present work, we were interested by the local stability of two flexible links manipulator. The global stability of the same control strategy is being investigated and will be considered in future work.

6.7 Appendix A

Proof of proposition 6.1

The new generalized coordinates $\bar{q}_2 = [y_{\alpha 2} \quad q_{f2}]^T$ are linked with the former generalized coordinates $q_2 = [q_{r2} \quad q_{f2}]^T$ by a nonsingular transformation matrix T :

$$\bar{q}_2 = \begin{bmatrix} q_{r2} + \alpha_2 \beta_2 q_{f2} \\ q_{f2} \end{bmatrix} = T q_2 \quad (6.41)$$

where: $T = \begin{bmatrix} 1 & \alpha_2 \beta_2 \\ 0 & 1 \end{bmatrix}$. Then we can write:

$$M_2^*(\bar{q}_2) = M_2(q_2)T^{-1} = M_2(T^{-1}\bar{q}_2)T^{-1} \quad (6.42)$$

where: $M_2^*(\bar{q}_2) = \begin{bmatrix} M_{22} & M_{24} - \alpha_2 \beta_2 M_{22} \\ M_{42} & M_{44} - \alpha_2 \beta_2 M_{42} \end{bmatrix}$ and $M_2(q_2) = \begin{bmatrix} M_{22} & M_{24} \\ M_{42} & M_{44} \end{bmatrix}$ is represented in section 6.2. Since $M_2(q_2)$ is a non-singular positive definite matrix and $(M_{44} - \alpha_2 \beta_2 M_{42})$ is a nonzero element, then the Schur complement M_{22}^* of $M_{44} - \alpha_2 \beta_2 M_{42}$ is a nonzero element (Zhang, 2005).

Proof of proposition 6.2

Let δu_2 be the input and $\dot{\tilde{y}}_{\alpha 2}$ the output. We consider the following energy function:

$$V(\tilde{x}) = \frac{1}{2} \tilde{x}_{r1}^2 \quad (6.43)$$

The time derivative of V is:

$$\dot{V}(\tilde{x}) = \tilde{x}_{r1} \dot{\tilde{x}}_{r1} = \delta u_2 \dot{\tilde{y}}_{\alpha 2}$$

The system (6.30) is then passive. This passivity is preserved with the following control law (Ortega, 1998; Saad, 2004):

$$\delta u_2 = -K_p \tilde{y}_{\alpha 2} + \delta v \quad (6.44)$$

where δv is a new control input. With δv as the input and $\dot{\tilde{y}}_{\alpha 2}$ as the output, the system is output strictly passive. The control law is given by:

$$\delta u_2 = -K_p \tilde{y}_{\alpha 2} - K_d \dot{\tilde{y}}_{\alpha 2} + \delta v \quad (6.45)$$

where K_p and $K_d > 0$. Then we can conclude that $\tilde{y}_{\alpha 2}, \dot{\tilde{y}}_{\alpha 2} \xrightarrow[t \rightarrow \infty]{} 0$ (Ortega, 1998).

Proof of proposition 6.3

Using the parameter system given in Appendix B, The errors dynamics of the flexible part (6.29-6.30) is written as:

$$\begin{cases} \dot{\tilde{x}}_{f1} = \tilde{x}_{f2} \\ \dot{\tilde{x}}_{f2} = -\bar{K}_{f2} \tilde{x}_{f1} - \bar{D}_{f2} \tilde{x}_{f2} - [M_{44} - \alpha_2 \beta_2 M_{42}]^{-1} \psi_1(t, y) \end{cases} \quad (6.46)$$

where $y = C_f^T \tilde{x}_f = [-\alpha_2 \beta_2 \ 0] \tilde{x}_f$, $\tilde{x}_{f1} = \tilde{q}_{f2}$, $\tilde{x}_{f2} = \dot{\tilde{q}}_{f2}$ and $\psi_1(t, y) = -(M_{d41} - M_{41}) \ddot{q}_{rd1} - (M_{d42} \ddot{y}_{\alpha d2} - M_{42} u_{\alpha 2}) - (C_{d4} - C_4)$. Using the system parameters (Appendix B), $\psi_1(t, y)$ can be written as follows:

$$\begin{aligned} \psi_1(t, y) = & (h_{501} \dot{q}_{rd1}^2 + b_{153} t_{11} q_{fd1}) [\sin(C_\alpha^T q_{d2}) - \sin(C_\alpha^T q_{d2} - y)] \\ & + b_{152} [\cos(C_\alpha^T q_{d2}) - \cos(C_\alpha^T q_{d2} - y)] \\ & + h_{504} t_{11} q_{fd1} \dot{q}_{rd1} [\dot{q}_{rd2} \cos(q_{rd2}) - \dot{q}_{r2} \cos(q_{r2})] \end{aligned}$$

and h_{ijk} , b_{ijk} and t_{ij} are constants and are given in Appendix B.

Using Taylor series, the last element can be written as:

$$\dot{q}_{rd2} \cos(q_{rd2}) - \dot{q}_{r2} \cos(q_{r2}) = \alpha_2 \beta_2 \dot{q}_{rd2} \sin(q_{rd2}) \tilde{q}_{f2} + \alpha_2 \beta_2 \cos(q_{rd2}) \dot{\tilde{q}}_{f2}$$

Then, the memoryless time-varying nonlinearity can be expressed as follows:

$$\psi_1(t, y) = \alpha_2 \beta_2 \dot{q}_{rd2} c(t) \sin(q_{rd2}) \tilde{q}_{f2} + \alpha_2 \beta_2 c(t) \cos(q_{rd2}) \dot{\tilde{q}}_{f2} + \psi(t, y) \quad (6.47)$$

where $c(t) = h_{504} t_{11} q_{fd1} \dot{Q}_{d1}$ and the new nonlinearity element is given by:

$$\begin{aligned} \psi(t, y) &= a(t) [\sin(C_\alpha^T q_{d2}) - \sin(C_\alpha^T q_{d2} - y)] \\ &\quad + b(t) [\cos(C_\alpha^T q_{d2}) - \cos(C_\alpha^T q_{d2} - y)] \end{aligned} \quad (6.48)$$

$$a(t) = h_{501} \dot{q}_{rd1}^2 + b_{153} t_{11} q_{fd1}; b(t) = b_{152}.$$

Thus, we can rewrite the errors dynamics of the flexible part (6.46) as follows:

$$\dot{\tilde{x}}_f = A_f(t) \tilde{x}_f - B_f \psi(t, y) \quad (6.49)$$

where:

$$A_f(t) = \begin{bmatrix} 0 & 1 \\ -a_0(t) & -a_1(t) \end{bmatrix}; B_f = \begin{bmatrix} 0 \\ (M_{44} - \alpha_2 \beta_2 M_{42})^{-1} \end{bmatrix}$$

$$a_0(t) = (M_{44} - \alpha_2 \beta_2 M_{42})^{-1} (K_{f2} - \alpha_2 \beta_2 \dot{q}_{rd2} c(t) \sin(q_{rd2}))$$

$$a_1(t) = (M_{44} - \alpha_2 \beta_2 M_{42})^{-1} (D_{f2} - \alpha_2 \beta_2 c(t) \cos(q_{rd2}))$$

The errors dynamics can be represented as a feedback connection of a linear system and a nonlinear memoryless system as follows:

$$G: \begin{cases} \dot{\tilde{x}}_f = A_f \tilde{x}_f + B_f v \\ y = C_f^T \tilde{x}_f \end{cases} \quad (6.50)$$

$$v = -\psi(t, y)$$

Proof of proposition 6.4

The origin of (6.32) is asymptotically stable if the nonlinear element $\psi(t, y)$ is passive and the linear system is input strictly passive (Ortega, 1998). For the nonlinear element, we can write:

$$\sin(C_\alpha^T q_{d2}) - \sin(C_\alpha^T q_{d2} - y) = 2 \cos(C_\alpha^T q_{d2} - y/2) \sin(y/2)$$

$$\cos(C_\alpha^T q_{d2}) - \cos(C_\alpha^T q_{d2} - y) = -2 \sin(C_\alpha^T q_{d2} - y/2) \sin(y/2)$$

Then, we can rewrite the memoryless nonlinearity as follows:

$$\psi(t, y) = 2a(t) \cos(C_\alpha^T q_{d2} - y/2) \sin(y/2) - 2b(t) \sin(C_\alpha^T q_{d2} - y/2) \sin(y/2) \quad (6.51)$$

where $a(t)$, $b(t)$, and $c(t)$ are given in (6.47-6.48) and are bounded. Then we can write:

$\underline{a} \leq a(t) \leq \bar{a}$; $b(t) = b_{152}$ is constant and the nonlinear term as:

$$-\underline{k}y^2 \leq y\psi(t, y) \leq \bar{k}y^2 \quad (6.52)$$

where $\underline{k} = b + \underline{a}$ and $\bar{k} = b + \bar{a}$

We can conclude that the nonlinear element $\psi(t, y)$ is passive (Khalil, 1996).

For the linear system, we can write:

$$A_f(t) = A_{f0} + \Delta(t) \quad (6.53)$$

where

$$A_{f0} = \begin{bmatrix} 0 & \frac{1}{\bar{D}_{f2}} \\ -\bar{K}_{f2} & -\bar{D}_{f2} \end{bmatrix}; \quad \Delta(t) = \begin{bmatrix} 0 & 0 \\ \delta_0(t) & \delta_1(t) \end{bmatrix}; \quad \delta_0(t) = \frac{\alpha_2 \beta_2 \dot{q}_{rd2} c(t) \sin(q_{rd2})}{b_{551} - \alpha_2 \beta_2 b_{251}}, \quad \delta_1(t) =$$

$$\frac{\alpha_2 \beta_2 c(t) \cos(q_{rd2})}{b_{551} - \alpha_2 \beta_2 b_{251}}$$

If A_{f0} is asymptotically stable then, the uniform asymptotical stability is preserved for any $\Delta(t) \xrightarrow[t \rightarrow \infty]{} 0$ (Khalil, 1996). However, $c(t) \rightarrow 0$ as $t \rightarrow \infty$. Then, $\Delta(t) \rightarrow 0$ as $t \rightarrow \infty$.

Finally, the passivity of the linear system depends only on A_{f0} . This can be easily done by an appropriate choice of α_2 .

Proof of proposition 6.5

The errors dynamic of the flexible part is:

$$\dot{\tilde{x}}_f = F(t, \tilde{x}_f, u) \quad (6.54)$$

where $u = \delta u_1$; $F(t, \tilde{x}_f, u) = \begin{bmatrix} \tilde{x}_{f2} \\ f(t, \tilde{x}_f, u) \end{bmatrix}$

$$f(t, \tilde{x}_f, 0) = a_1(t)\tilde{q}_{f1} + a_2(t)\dot{\tilde{q}}_{f1} + a_3(t)\dot{\tilde{q}}_{f1}^2 + c_0(t) \quad (6.55)$$

$$a_1(t) = -[M_{33} - \alpha_1\beta_1 M_{31}]^{-1}[K_{f1} + b_{234}s_2 t_{31}\ddot{q}_{rd2} + h_{319}\dot{q}_{rd2}^2 c_2 t_{31}]$$

$$\begin{aligned} a_2(t) = & -[M_{33} - \alpha_1\beta_1 M_{31}]^{-1}[D_{f1} + h_{307}\dot{q}_{rd2}s_2 + h_{311}s_2\dot{q}_{fd2} + h_{317}\dot{q}_{rd2}c_2 t_{21}q_{fd2} \\ & - \alpha_1\beta_1(h_{315}t_{21}q_{fd2}\dot{q}_{rd2}c_2 + h_{302}s_2\dot{q}_{rd2}) + 2\alpha_1\beta_1 h_{301}s_2\dot{q}_{rd1}] \end{aligned}$$

$$a_3(t) = -[M_{33} - \alpha_1\beta_1 M_{31}]^{-1}[2\alpha_1\beta_1 h_{301}s_2\dot{q}_{rd1}]$$

$$c_0(t) = -[M_{33} - \alpha_1\beta_1 M_{31}]^{-1}h_{301}s_2\dot{q}_{rd1}^2$$

To facilitate the stability analysis, equation (6.54) can be expressed as (Coppel, 1965):

$$\dot{\tilde{x}}_f = F(t, \tilde{x}_f) + G(t, \tilde{x}_f) \quad (6.56)$$

where: $F(t, \tilde{x}_f) = \begin{bmatrix} \tilde{x}_{f2} \\ a_1(t)\tilde{x}_{f1} + a_2(t)\tilde{x}_{f2} + c_0(t) \end{bmatrix}$; $G(t, \tilde{x}_f) = \begin{bmatrix} 0 \\ a_3(t)\tilde{x}_{f2} \end{bmatrix}$

It is clear that: $G(t, 0) = 0$ and $\|G(t, \tilde{x}_f)\| \leq \gamma \|\tilde{x}_f\|$ where $\gamma = \sup(a_3(t))$ a non negative constant. Then, the asymptotical stability of the origin of (6.56) is equivalent to:

$$\dot{\tilde{x}}_f = F(t, \tilde{x}_f) = A(t)\tilde{x}_f + C(t) \quad (6.57)$$

where: $A(t) = \begin{bmatrix} 0 & 1 \\ a_1(t) & a_2(t) \end{bmatrix}$; $C(t) = \begin{bmatrix} 0 \\ c_0(t) \end{bmatrix} \rightarrow \begin{bmatrix} 0 \\ 0 \end{bmatrix}$ as $t \rightarrow \infty$

The asymptotical stability of the origin of (6.57) depends only on the subsystem:

$$\dot{x}_f = A(t)\tilde{x}_f \quad (6.58)$$

Now, we analyze the asymptotical stability of the previous subsystem to choose the critical value of α_1 . $A(t)$ can be written as:

$$A(t) = A_0(t) + \Delta(t) \quad (6.59)$$

Where: $A_0(t) = \begin{bmatrix} 0 & 1 \\ a_{10} & a_{20} \end{bmatrix}$; $\Delta(t) = \begin{bmatrix} 0 & 0 \\ \delta_1(t) & \delta_2(t) \end{bmatrix}$; $a_{10} = -\bar{K}_{f1}$; $a_{20} = -\bar{D}_{f1}$

$$\delta_1(t) = -[M_{33} - \alpha_1 \beta_1 M_{31}]^{-1} [b_{234} s_2 t_{31} \ddot{q}_{rd2} + h_{319} \dot{q}_{rd2}^2 c_2 t_{31}]$$

$$\begin{aligned} \delta_2(t) = -[M_{33} - \alpha_1 \beta_1 M_{31}]^{-1} & [h_{307} \dot{q}_{rd2} s_2 + h_{311} s_2 \dot{q}_{fd2} + h_{317} \dot{q}_{rd2} c_2 t_{21} q_{fd2} \\ & - \alpha_1 \beta_1 (h_{315} t_{21} q_{fd2} \dot{q}_{rd2} c_2 + h_{302} s_2 \dot{q}_{rd2}) + 2 \alpha_1 \beta_1 h_{301} s_2 \dot{q}_{rd1}] \end{aligned}$$

We know that: $\dot{q}_{rd1}, \dot{q}_{rd2}, \ddot{q}_{rd2}, q_{fd2}, \dot{q}_{fd2} \rightarrow 0$ as $t \rightarrow \infty$, then $\delta_1(t), \delta_2(t) \rightarrow 0$, $(\Delta(t) \rightarrow 0)$.

Then the asymptotical stability of the origin of (6.59) is equivalent to the asymptotical stability of the origin of the following system:

$$\dot{\tilde{x}}_f = \begin{bmatrix} 0 & 1 \\ -\bar{K}_{f1} & -\bar{D}_{f1} \end{bmatrix} \tilde{x}_f \quad (6.60)$$

where \bar{K}_{f1} and \bar{D}_{f1} are given in (6.34). The critical value of α_1 is given when the eigenvalues of (6.60) change their signs from negative to positive.

Appendix B : Dynamical Model of two flexible links with one mode

The following dynamical model is deduced from (Khalil, 1996) by considering only one flexible mode to alleviate the computation.

$$\begin{bmatrix} M_{11} & M_{12} & M_{13} & M_{14} \\ M_{21} & M_{22} & M_{23} & M_{24} \\ M_{31} & M_{32} & M_{33} & M_{34} \\ M_{41} & M_{42} & M_{43} & M_{44} \end{bmatrix} \begin{bmatrix} \ddot{q}_{r1} \\ \ddot{q}_{r2} \\ \ddot{q}_{f1} \\ \ddot{q}_{f2} \end{bmatrix} + \begin{bmatrix} C_1(q, \dot{q}) \\ C_2(q, \dot{q}) \\ C_3(q, \dot{q}) \\ C_4(q, \dot{q}) \end{bmatrix} + \begin{bmatrix} 0 \\ 0 \\ K_{f1} q_{f1} \\ K_{f2} q_{f2} \end{bmatrix} + \begin{bmatrix} 0 \\ 0 \\ D_{f1} \dot{q}_{f1} \\ D_{f2} \dot{q}_{f2} \end{bmatrix} = \begin{bmatrix} \tau_1 \\ \tau_2 \\ 0 \\ 0 \end{bmatrix}$$

where:

$$\begin{aligned}
M_{11} &= b_{111} + b_{112}c_2 + (b_{113}t_1 + b_{114}t_2)s_2 \\
M_{12} &= b_{121} + b_{122}c_2 + (b_{123}t_1 + b_{124}t_2)s_2 \\
M_{13} &= b_{131} + b_{132}c_2 + b_{133}t_2s_2 \\
M_{15} &= b_{151} + b_{152}c_2 + b_{153}t_1s_2 \\
M_{22} &= b_{221} \\
M_{23} &= b_{231} + b_{232}c_2 + (b_{233}t_2 + b_{234}t_3)s_2 \\
M_{25} &= b_{251} \\
M_{33} &= b_{331} + b_{332}c_2 + b_{333}t_2s_2 \\
M_{35} &= b_{351} + b_{352}c_2 + b_{353}t_3s_2 \\
M_{55} &= b_{551} \\
t_1 &= t_{11}q_{f1}; t_2 = t_{21}q_{f2}; t_3 = t_{31}q_{f1}
\end{aligned}$$

The b_{ijk} coefficients are given as follow:

$$\begin{aligned}
b_{111} &= J_{h1} + J_{o1} + J_{h2} + m_{h2}l_1^2 + J_{o2} + m_2l_1^2 + J_p + m_p(l_1^2 + l_2^2) \\
b_{112} &= 2(m_2d_2 + m_pl_2)l_1 \\
b_{113} &= 2(m_2d_2 + m_pl_2) \\
b_{114} &= -2l_1 \\
b_{121} &= J_{h2} + J_{o2} + J_p + m_pl_2^2 \\
b_{122} &= (m_2d_2 + m_pl_2)l_1 \\
b_{123} &= m_2d_2 + m_pl_2 \\
b_{124} &= -l_1 \\
b_{131} &= w_{11} + (J_{h2} + J_{o2} + J_p + m_pl_2^2)\emptyset'_{1,e} + (m_{h2} + m_2 + m_p)l_1\emptyset_{1,e} \\
b_{132} &= (m_2d_2 + m_pl_2)(\emptyset_{1,e} + l_1\emptyset'_{1,e}) \\
b_{133} &= -(\emptyset_{1,e} + l_1\emptyset'_{1,e}) \\
b_{151} &= w_2 + J_p\emptyset'_{2,e} + m_pl_2\emptyset_{2,e} \\
b_{152} &= (v_2 + m_p\emptyset_{2,e})l_1 \\
b_{153} &= v_2 + m_p\emptyset_{2,e} \\
b_{221} &= J_{h2} + J_{o2} + J_p + m_pl_2^2 \\
b_{231} &= (J_{h2} + J_{o2} + J_p + m_pl_2^2)\emptyset'_{1,e} \\
b_{232} &= (m_2d_2 + m_pl_2)\emptyset_{1,e} \\
b_{233} &= -\emptyset_{1,e} \\
b_{234} &= -(m_2d_2 + m_pl_2)\emptyset_{1,e} \\
b_{251} &= w_2 + J_p\emptyset'_{2,e} + m_pl_2\emptyset_{2,e} \\
b_{331} &= m_1 \\
b_{332} &= 2(m_2d_2 + m_pl_2)\emptyset_{1,e}\emptyset'_{1,e} \\
b_{333} &= -2\emptyset_{1,e}\emptyset'_{1,e} \\
b_{351} &= (w_2 + J_p\emptyset'_{2,e} + m_pl_2\emptyset_{2,e})\emptyset'_{1,e} \\
b_{352} &= (v_2 + m_p\emptyset_{2,e})\emptyset_{1,e} \\
b_{353} &= -(v_2 + m_p\emptyset_{2,e})\emptyset_{1,e} \\
b_{551} &= m_2 \\
t_{11} &= \emptyset_{1,e} - l_1\emptyset'_{1,e}
\end{aligned}$$

$$\begin{aligned}t_{21} &= v_2 - m_p \emptyset_{2,e} \\t_{31} &= \emptyset'_{1,e}\end{aligned}$$

The Coriolis and centrifugal forces vector coefficients are:

$$\begin{aligned}C_1 &= [(h_{101}\dot{\theta}_2 + h_{102}\dot{q}_{f1} + h_{104}\dot{q}_{f2})\dot{\theta}_1 + (h_{106}\dot{\theta}_2 + h_{107}\dot{q}_{f1} + h_{109}\dot{q}_{f2})\dot{\theta}_1 \\&\quad + h_{111}\dot{q}_{f2}\dot{q}_{f1}]s_2 \\&\quad + [(h_{115}\dot{\theta}_1 + h_{116}\dot{\theta}_2 + h_{117}\dot{q}_{f2})t_1 + (h_{119}\dot{\theta}_1 + h_{120}\dot{\theta}_2 + h_{121}\dot{q}_{f1})t_2]\dot{\theta}_2c_2 \\C_2 &= (h_{201}\dot{\theta}_1 + h_{202}\dot{q}_{f1})\dot{\theta}_1s_2 \\&\quad + \{(h_{204}\dot{\theta}_1 + h_{205}\dot{q}_{f2})t_1 + (h_{207}\dot{\theta}_1 + h_{208}\dot{q}_{f1})t_2\}\dot{\theta}_1 \\&\quad + [h_{211}\dot{q}_{f1}t_2 + h_{214}\dot{q}_{f2}t_3]\dot{q}_{f1}c_2 \\C_3 &= [(h_{301}\dot{\theta}_1 + h_{302}\dot{\theta}_2 + h_{304}\dot{q}_{f2})\dot{\theta}_1 + (h_{306}\dot{\theta}_2 + h_{307}\dot{q}_{f1} + h_{309}\dot{q}_{f2})\dot{\theta}_2 \\&\quad + h_{311}\dot{q}_{f2}\dot{q}_{f11}]s_2 \\&\quad + [(h_{315}\dot{\theta}_1 + h_{316}\dot{\theta}_2 + h_{317}\dot{q}_{f1})t_2 + (h_{319}\dot{\theta}_2 + h_{320}\dot{q}_{f2})t_3]\dot{\theta}_2c_2 \\C_4 &= (h_{501}\dot{\theta}_1 + h_{502}\dot{q}_{f1})\dot{\theta}_1c_2 + [h_{504}t_1\dot{\theta}_1 + h_{505}\dot{q}_{f1}t_3]\dot{\theta}_2c_2\end{aligned}$$

The h_{ijk} coefficients are given as follow:

$$\begin{aligned}h_{101} &= -2(m_2d_2 + m_pl_2)l_1 \\h_{102} &= 2(m_2d_2 + m_pl_2)(\emptyset_{1,e} - l_1\emptyset'_{1,e}) \\h_{104} &= -2(v_2 + m_p\emptyset_{2,e})l_1 \\h_{106} &= -(m_2d_2 + m_pl_2)l_1 \\h_{107} &= -(m_2d_2 + m_pl_2)(l_1\emptyset'_{1,e}) \\h_{109} &= -2(v_2 + m_p\emptyset_{2,e})l_1 \\h_{111} &= -2(v_2 + m_p\emptyset_{2,e})l_1\emptyset'_{1,e} \\h_{115} &= 2(m_2d_2 + m_pl_2) \\h_{116} &= m_2d_2 + m_pl_2 \\h_{117} &= -(v_{21} + m_p\emptyset_{2,e}) \\h_{119} &= -2l_1 \\h_{120} &= -l_1 \\h_{121} &= -(\emptyset_{1,e} - l_1\emptyset'_{1,e}) \\h_{201} &= (m_2d_2 + m_pl_2)l_1 \\h_{202} &= 2(m_2d_2 + m_pl_2)\emptyset_{1,e} \\h_{204} &= -(m_2d_2 + m_pl_2) \\h_{205} &= -(v_2 + m_p\emptyset_{2,e}) \\h_{207} &= l_1 \\h_{208} &= \emptyset_{1,e} + l_1\emptyset'_{1,e} \\h_{212} &= \emptyset_{1,e}\emptyset'_{1,e} \\h_{214} &= (v_2 + m_p\emptyset_{2,e})\emptyset_{1,e} \\h_{301} &= -(m_2d_2 + m_pl_2)(\emptyset_{1,e} - l_1\emptyset'_{1,e}) \\h_{302} &= -2(m_2d_2 + m_pl_2)\emptyset_{1,e} \\h_{304} &= -2(v_2 + m_p\emptyset_{2,e})\emptyset_{1,e}\end{aligned}$$

$$\begin{aligned}
h_{306} &= -(m_2 d_2 + m_p l_2) \emptyset_{1,e} \\
h_{307} &= -2(m_2 d_2 + m_p l_2) \emptyset_{1,e} \emptyset'_{1,e} \\
h_{309} &= -2(v_2 + m_p \emptyset_{2,e}) \emptyset_{1,e} \\
h_{311} &= -2(v_2 + m_p \emptyset_{2,e}) \emptyset_{1,e} \emptyset'_{1,e} \\
h_{315} &= -(\emptyset_{1,e} + l_1 \emptyset'_{1,e}) \\
h_{316} &= -\emptyset_{1,e} \\
h_{317} &= -2\emptyset_{1,e} \emptyset'_{1,e} \\
h_{319} &= -(m_2 d_2 + m_p l_2) \emptyset_{1,e} \\
h_{320} &= -2(v_2 + m_p \emptyset_{2,e}) \emptyset_{1,e} \\
h_{501} &= (v_2 + m_p \emptyset_{2,e}) l_1 \\
h_{502} &= 2(v_2 + m_p \emptyset_{2,e}) \emptyset_{1,e} \\
h_{504} &= v_2 + m_p \emptyset_{2,e} \\
h_{505} &= -(v_2 + m_p \emptyset_{2,e}) \emptyset_{1,e}
\end{aligned}$$

CHAPITRE 7

ARTICLE 6: WORKSPACE TRAKING CONTROL OF TWO-FLEXIBLE-LINK MANIPULATOR USING DISTRIBUTED CONTROL STRATEGY

Fareh Raouf¹ Saad Mohamad² and Saad Maarouf¹

¹Electrical Engineering Department, Université du Québec, École de technologie supérieure,
1100, rue Notre-Dame ouest, Montréal (Québec), H3C 1K3, Canada

²School of Engineering, Université du Québec en Abitibi-Témiscamingue, 445, boul. de
l'Université, Rouyn-Noranda (Québec), J9X 5E4

Article soumis à la revue « Journal of Dynamical and Control Systems » en Février 2013.

Abstract : In this paper, a distributed nonlinear control strategy for two-flexible-link manipulators is presented to track a desired trajectory in the robot's workspace. The inverse dynamics problem is solved by transforming the desired trajectory from the workspace to the joint space using an intermediate space, called virtual space, and then using the quasi-static approach. To solve the non-minimum phase problem, an output redefinition technique is used. This output consists of the motor's angle augmented with a weighted value of the link's extremity. The distributed control strategy consists in controlling the last link by assuming that the first link is stable and follows its desired trajectories. The control law is developed to stabilize the error dynamics and to guarantee bounded internal dynamics such that the new output is as close as possible to the tip. The weighted parameter defining the non-collocated output is then selected. The same procedure is applied to control and stabilize the first link. The asymptotical stability is proved using Lyapunov theory. This algorithm is applied to a two-flexible-link manipulator in the horizontal plane and simulations showed a good tracking of the desired trajectory in the workspace.

Key Words: Flexible manipulators, inverse dynamics, output redefinition, internal dynamics, stability analysis.

7.1 Introduction

Many control strategies for manipulators have been the focus of several studies in recent years. The robot manipulators consist of a sequence of links and joints in various combinations. In industrial applications, most of the existing manipulators use rigid links and joints, and are known as rigid manipulators. Rigid manipulators are generally slow, extremely rigid and massive, and the useful load is very low compared to their weight. To improve the performance of the robot manipulators, their links must be lighter and therefore they become more flexible. Flexible manipulators present more advantages when compared to rigid manipulators: they are faster, less massive, and consume less energy. Some flexible manipulators are used in different areas e.g. the aerospace applications (Hirzinger et al., 2003) and medical applications (Hagn, 2008).

For flexible manipulators, the problem of workspace tracking trajectory is less covered so far than joint space tracking. There are few solutions to the workspace tracking problem, particularly for manipulators with many flexible links. The workspace tracking trajectory is very important since most of the tasks are defined in the operational space, such as painting, welding, and assembly. The flexible link manipulators are a non-minimum phase system when controlling the position of the end-effector (Cannon et Schmitz, 1984). Unlike rigid manipulators, the inverse kinematics of flexible manipulators is not sufficient to transform the desired trajectory from workspace to joint space because they are linked by kinematics and dynamics relationships. To solve this problem, many studies focused on the output redefinition technique (Bigras, 2003; Cuvillon, 2012; de Luca et Siciliano, 1989; Mosayebi, 2012). This technique consists in selecting a new output as close as possible to the tip such that internal dynamics become bounded. In (Bigras, 2003), this approach was used for a class of manipulators where the last link is flexible. An intermediate space between the joint space and the workspace called virtual space is used to transform the desired trajectory from the workspace to the joint space. The virtual space is linked with the workspace by a simple kinematics relation as in rigid manipulators. In (de Luca et Siciliano, 1989), the output

redefinition technique was used for one flexible link manipulator. This output consists of the motor's angle augmented with a weighted value of the angle of links extremity.

The nonlinear dynamics of flexible link manipulators combined with their under-actuated nature (the deflection variables are not actuated) present a challenging control problem. Multi-flexible-link manipulators can be controlled as one MIMO system so a single controller is used for all joints and links or as a set of interconnected subsystems so each pair of joint and link is controlled by its own controller. For the first case, many control schemes were used. Several studies used linearization around a nominal configuration of flexible manipulators model (De Wit, 1996; Siciliano et Khatib, 2008). Some nonlinear effects such as the variation of inertia matrix around an operating point were taken into account in the control design methodology. In (Moallem, Patel et Khorasani, 2001b), a control method based on the input-output linearization was developed to track a desired trajectory in the workspace for a class of flexible link manipulators when the last link is flexible. To select an output near the tip that guarantees the stability of the zero dynamics, authors used the output redefinition technique. A robust adaptive controller was developed in (Bigras, Saad et O'Shea, 2001) for a class of flexible link manipulators where the last link is flexible. This controller is based on feedback linearization and uses the virtual joint space that is kinematically related to workspace. For trajectory tracking control problems, many other techniques were covered in the literature such as: singular perturbation technique(Siciliano et Book, 1988), sliding mode control (Zhang, 2009), inversion-based nonlinear control (De Luca, 1993), etc.

All the above mentioned control methods use a single controller for all joints and links as one MIMO system. Unfortunately, due to the complexity of the control structures, the real time implementation in industrial applications is not easy (Fu, Gonzalez et Lee, 1987). A solution to this problem can be followed by considering the dynamics of the robot manipulators as interconnected subsystems (joint and link). Many control schemes consider this configuration. In (Khorrami, 1993), a decentralized control method for flexible link manipulators was used. The authors used a simple proportional derivative (PD) controller for

the joints and a linear quadratic regulator (LQR) with output feedback for each link. In (Sun, 2002), a PD controller was used for each joint and the measurement of linear velocity of the tip position was used for controlling each link. A distributed control strategy was introduced in (Fareh, Saad et Saad, 2012b) for rigid link manipulators. The distributed control strategy consists in controlling one joint at a time starting with the last joint and going backward until the first one. Lyapunov theory was used to prove the global stability of the error dynamics and this controller was successfully applied on a 7 DOF manipulator. This control strategy was modified in (Fareh, Saad et Saad, 2013a) to take into account links' flexibility. A good tracking performance in the workspace of a two-flexible-link manipulator was obtained. However, the control law, based on the feedback linearization approach, ensures only local stability. In this paper, a nonlinear distributed control strategy is presented for a two-flexible-link manipulator that ensures global stability. This strategy consists of controlling the second joint and link by assuming that the remaining joint and link are stable and follow their desired trajectories. Then, going backward, the first joint and link are controlled by following the same strategy. For the inversion dynamics problem, the virtual space and the quasi-static approach are used. The output redefinition technique is used to obtain the nearest point to the tip that ensures bounded internal dynamics. The Lyapunov approach is used to analyze stability of the tracking errors.

The paper is organized as follows: Section 7.2 presents the modeling of the two-flexible-link manipulator and presents its main proprieties that will be used in the control law design. Section 7.3 presents the distributed control strategy. The stability analysis is given in Section 7.4. The control method is applied on a two-flexible-link manipulator and the simulations are given in Section 7.5. Finally, a conclusion is given in Section 7.6.

7.2 Modeling

7.2.1 System description

Figure 7.1 shows a two-flexible-link manipulator. This system moves in the horizontal plane and consists of two motors that generate two torques, two flexible links with mass m_i , length L_i , linear density ρ_i , and rigidity EI_i ($i=1, 2$), and a payload that has a mass m_p . The first link is attached to the first motor, and the second link is clamped to the rotor of the second motor. The flexible links are supposed uniform and are modeled as Euler-Bernoulli beams and the deformations are assumed to be small.

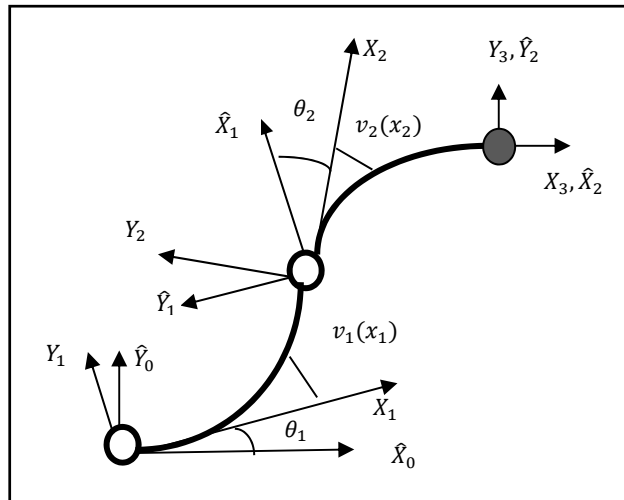


Figure 7.1 Two-flexible-link manipulator.

Using Lagrange equations, the dynamical model of an n DOF flexible manipulator is given by (De Luca et Siciliano, 1991):

$$M(q)\ddot{q} + H(q, \dot{q}) + D\dot{q} + Kq = \tau \quad (7.1)$$

where M is the inertia and mass matrix, $H(q, \dot{q})$ is the Coriolis and centrifugal forces vector, D is the friction matrix and K is the rigidity matrix. q represents the vector of the generalized coordinates and τ is the vector of the applied torques. For the n rigid coordinates and n flexible links, the deformation of the i-th flexible link is given by the following equation:

$$v_i(x, t) = \sum_{j=1}^{z_i} \emptyset_{ij}(x) q_{fij}(t) \quad i = 1, \dots, n \quad (7.2)$$

where q_{fij} is the j-th generalized flexible coordinate, $\emptyset_{ij}(x)$ is its j-th shape function and z_i is the number of the retained flexible modes of the i-th flexible link. Note that the total number of the flexible modes is $z = \sum_{i=1}^n z_i$ and the number of the rigid modes is n. The dynamical model (7.1) can be written as follows:

$$\begin{bmatrix} M_{rr} & M_{rf} \\ M_{rf}^T & M_{ff} \end{bmatrix} \begin{bmatrix} \ddot{q}_r \\ \ddot{q}_f \end{bmatrix} + \begin{bmatrix} H_r(q, \dot{q}) \\ H_f(q, \dot{q}) \end{bmatrix} + \begin{bmatrix} 0 & 0 \\ 0 & D_{ff} \end{bmatrix} \begin{bmatrix} \dot{q}_r \\ \dot{q}_f \end{bmatrix} + \begin{bmatrix} 0 & 0 \\ 0 & K_{ff} \end{bmatrix} \begin{bmatrix} q_r \\ q_f \end{bmatrix} = \begin{bmatrix} I \\ 0 \end{bmatrix} \tau \quad (7.3)$$

where $M_{rr} \in \Re^{n \times n}$ and $M_{ff} \in \Re^{z \times z}$ are mass and inertia matrices for rigid and flexible part respectively. $M_{rf} \in \Re^{n \times z}$ is a coupled element. K_{ff} is the stiffness diagonal matrix and D_{ff} is the damping diagonal matrix of the flexible part. The subscripts r and f denotes the rigid and flexible modes.

7.2.2 Proprieties and problem formulation

The dynamical model of the flexible link manipulators has the following properties that will be used in the control law development:

P1: $M, M_{rr}, M_{ff}, D_{ff}$ and K_{ff} are symmetric positive definite matrices (De Luca et Siciliano, 1991).

P2. From **P1**, we can deduce that the diagonal elements of M are positive (Bhatia, 2007):

$$M_{ii}(q) > 0; \text{ for } i = 1 \dots n \quad (7.4)$$

P3: There exists a matrix $C(q, \dot{q})$ such that:

$$H(q, \dot{q}) = C(q, \dot{q}) \dot{q} \quad (7.5)$$

P4: The inertia-mass matrix $M(q)$ and the Coriolis matrix $C(q, \dot{q})$ satisfy the following skew-symmetric property:

$$X^T (\dot{M}(q, \dot{q}) - 2C(q, \dot{q})) X = 0 \quad \forall X \in \mathcal{R}^{n+z} \quad (7.6)$$

P5. The propriety **P4** is preserved for the diagonal elements of $M(q)$ and $C(q, \dot{q})$. Then, we can write:

$$\dot{M}_{ii}(q) - 2C_{ii}(q, \dot{q}) = 0; \text{ for } i = 1 \dots n \quad (7.7)$$

The new non-collocated output of the i -th link defined by the motor's angle augmented with a weighted value α_i of the end point angular position is given as follows:

$$y_i = q_{ri} + \alpha_i \beta_i^T q_{fi}, \quad 0 \leq \alpha_i < 1 \quad (7.8)$$

where $\beta_i^T = \frac{1}{L_i} [\emptyset_{i1}(L_i), \dots, \emptyset_{iz_i}(L_i)]$, with L_i being the length of the i -th flexible link, and \emptyset_{ij} is the shape function of link i and mode j . In this paper, we consider only the first flexible mode of each link (i.e. $z_i = 1$). Thus, we have $z = n$.

In the distributed control strategy, when controlling the i -th link, we assume that the other links follow their desired trajectories. For the i -th link, a new generalized coordinate Q_i is defined such that the i -th coordinate is the controlled one and the other links follow their desired trajectories such that:

$$Q_i = [q_{rd1} \dots q_{rd(i-1)} \ q_{ri} \ q_{rd(i+1)} \dots q_{rdn} \ q_{fd1} \dots q_{fd(i-1)} \ q_{fi} \ q_{fd(i+1)} \dots q_{fdn}]^T \quad (7.9)$$

where (q_{ri}, q_{fi}) are the rigid and flexible modes associated with the i -th motor and link, respectively. The objective of this work is to track a desired trajectory defined in the workspace of a two-flexible-link manipulator using distributed control. Three steps are followed to achieve this objective:

Step 1. Transform the desired trajectory from the workspace to the joint space using inverse kinematics and quasi-static approach.

Step 2. Develop the control law for the second and first links to stabilize the errors dynamics and to guarantee bounded internal dynamics such that the output is as close as possible to the tip.

Step 3. Study the global stability.

7.3 Distributed control strategy

7.3.1 Inverse dynamics

To achieve the objective of workspace tracking trajectories, we need to transform the desired trajectories from the workspace to the joint space. The flexible manipulator is a non-minimum phase system when the end-effector is used as the output. In this case, kinematic and dynamic relationships link the workspace and the joint space. To overcome this problem, an intermediate space called virtual space can be used. Then the desired workspace trajectory is transformed to the virtual space using an inverse kinematics relation as in rigid manipulators. To transform the desired trajectories from the virtual space to the joint pace, the quasi-static approach can be used to solve a nonlinear equation for the flexible part.

Using inverse kinematics as in rigid manipulators, the generalized coordinates in virtual space can be easily found. The deformation is assumed to be small. According to Figure 7.2, we can write:

$$q_{vi} - q_{rdi} = \arctan\left(\frac{v_{Li}}{L_i}\right) \approx \frac{v_{Li}}{L_i} \quad (7.10)$$

In the virtual space, the generalized coordinate is given as follows:

$$q_{vi} = q_{rdi} + \beta_i q_{fdi} \quad (7.11)$$

where $\beta_i = \frac{\phi_i(L_i)}{L_i}$, ϕ_i is the shape function of link i.

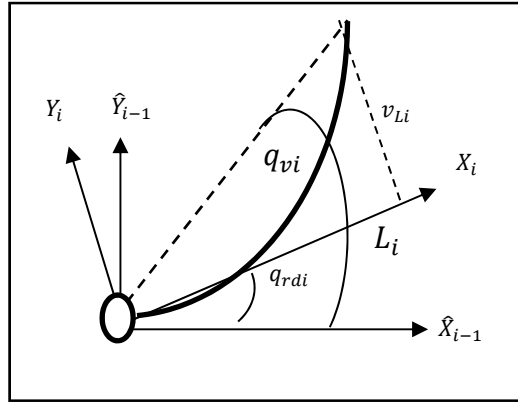


Figure 7.2 Virtual space.

Using the Jacobian matrix as in rigid manipulators, the velocity and acceleration in the virtual space can be deduced. Then, for a two DOF manipulator, the inverse kinematics is given by the following equation:

$$q_v = \begin{bmatrix} q_{v1} \\ q_{v2} \end{bmatrix} = \begin{bmatrix} \arctan 2(y, x) - \arctan 2(L_2 s_2, L_1 + L_2 c_2) \\ \arctan 2(s_2, c_2) \end{bmatrix} \quad (7.12)$$

$$\dot{q}_v = \begin{bmatrix} \dot{q}_{v1} \\ \dot{q}_{v2} \end{bmatrix} = J^{-1}(q_v) \begin{bmatrix} \dot{x} \\ \dot{y} \end{bmatrix} \quad (7.13)$$

$$\ddot{q}_v = \begin{bmatrix} \ddot{q}_{v1} \\ \ddot{q}_{v2} \end{bmatrix} = J^{-1}(q_v) \begin{bmatrix} \ddot{x} \\ \ddot{y} \end{bmatrix} - J^{-1}(q_v) \dot{J}(q_v) \dot{q}_v \quad (7.14)$$

where x and y are the workspace desired positions,

$c_2 = \frac{x^2 + y^2 - L_1^2 - L_2^2}{2L_1 L_2}$; $s_2 = \pm\sqrt{1 - c_2^2}$ and $J(q_v) = \begin{bmatrix} -L_1 s_1 - L_2 s_{12} & -L_2 s_{12} \\ L_1 c_1 + L_2 c_{12} & L_2 c_{12} \end{bmatrix}$ is the Jacobian matrix.

$s_1 = \sin(q_{v1})$; $c_1 = \cos(q_{v1})$; $s_{12} = \sin(q_{v1} + q_{v2})$; $c_{12} = \cos(q_{v1} + q_{v2})$; L_1 is length of link 1 and L_2 is length of link 2. The rigid and flexible coordinates are derived via quasi-static approach and using the generalized coordinates in the virtual space.

The dynamical model (7.3) can be written as a function of the desired coordinates as follows:

$$M_{rr}(q_d)\ddot{q}_{rd} + M_{rf}(q_d)\ddot{q}_{fd} + H_r(q_d, \dot{q}_d) = \tau \quad (7.15)$$

$$M_{rf}^T(q_d)\ddot{q}_{rd} + M_{ff}(q_d)\ddot{q}_{fd} + H_f(q_d, \dot{q}_d) + D_{ff}\dot{q}_{fd} + K_{ff}q_{fd} = 0 \quad (7.16)$$

The generalized flexible and rigid coordinates in the joint space are deduced using the quasi-static approach. In the first step, the nonlinear equation of the flexible part (7.16) is solved to find the generalized flexible coordinates. The quasi-static approach neglects the desired velocity and acceleration of the flexible coordinates ($\dot{q}_{fd} = \ddot{q}_{fd} = 0$). Then, the equation of the flexible part (7.16) can be written as follows:

$$M_{rf}^T(q_d)\ddot{q}_{rd} + H_f(q_d, \dot{q}_d) + K_{ff}q_{fd} = 0 \quad (7.17)$$

where:

$$q_{rdi} = q_{vi} - \beta_i^T q_{fdi}; \dot{q}_{rdi} = \dot{q}_{vi}; \ddot{q}_{rdi} = \ddot{q}_{vi} \quad (7.18)$$

Using (7.18), the generalized flexible coordinates q_{fd} are found by solving (7.17). Then the generalized rigid coordinates are given by (7.18).

7.4 Control strategy

For two-flexible-link manipulator, the distributed control strategy consists of controlling and stabilizing the last joint and flexible link by assuming that the first joint and flexible link are stable and follow their desired trajectories. Then, we move backward and apply the same procedure to the first joint and link. For each step, a new non-collocated output and a control law are developed. The weighting parameter characterizing the non-collocated output is calculated such as the tracking error is asymptotically stable. Thus, the system becomes minimum phase with the selected new weighted outputs.

In this paper, the two-flexible-link model given in (De Luca et Siciliano, 1990; 1991) is modified by considering only the first flexible mode of each link (Fareh, Saad et Saad, 2013a). Thus, we have: $n = z = 2$, and $z_1 = z_2 = 1$.

Using P3, the dynamical model of the two-flexible-link manipulator can be written as:

$$M(q)\ddot{q} + C(q, \dot{q})\dot{q} + D\dot{q} + Kq = L\tau \quad (7.19)$$

$$\text{where } M = \begin{bmatrix} M_{11} & M_{12} & M_{13} & M_{14} \\ M_{21} & M_{22} & M_{23} & M_{24} \\ M_{31} & M_{32} & M_{33} & M_{34} \\ M_{41} & M_{42} & M_{43} & M_{44} \end{bmatrix}; C = \begin{bmatrix} C_{11} & C_{12} & C_{13} & C_{14} \\ C_{21} & C_{22} & C_{23} & C_{24} \\ C_{31} & C_{32} & C_{33} & C_{34} \\ C_{41} & C_{42} & C_{43} & C_{44} \end{bmatrix};$$

$$D = \begin{bmatrix} 0 & 0 & 0 & 0 \\ 0 & 0 & 0 & 0 \\ 0 & 0 & D_{f1} & 0 \\ 0 & 0 & 0 & D_{f2} \end{bmatrix}; K = \begin{bmatrix} 0 & 0 & 0 & 0 \\ 0 & 0 & 0 & 0 \\ 0 & 0 & K_{f1} & 0 \\ 0 & 0 & 0 & K_{f2} \end{bmatrix}, q = \begin{bmatrix} q_{r1} \\ q_{r2} \\ q_{f1} \\ q_{f2} \end{bmatrix}, L = \begin{bmatrix} 1 & 0 \\ 0 & 1 \\ 0 & 0 \\ 0 & 0 \end{bmatrix} \text{ and } \tau = \begin{bmatrix} \tau_1 \\ \tau_2 \end{bmatrix}.$$

In rigid and flexible part decomposition, the dynamical model (7.19) can be written as:

$$\begin{bmatrix} M_r & M_{rf} \\ M_{rf}^T & M_f \end{bmatrix} \begin{bmatrix} \ddot{q}_r \\ \ddot{q}_f \end{bmatrix} + \begin{bmatrix} C_r & C_{rf} \\ C_{rf}^T & C_f \end{bmatrix} \begin{bmatrix} \dot{q}_r \\ \dot{q}_f \end{bmatrix} + \begin{bmatrix} 0 & 0 \\ 0 & D_f \end{bmatrix} \begin{bmatrix} \dot{q}_r \\ \dot{q}_f \end{bmatrix} + \begin{bmatrix} 0 & 0 \\ 0 & K_f \end{bmatrix} \begin{bmatrix} q_r \\ q_f \end{bmatrix} = \begin{bmatrix} I \\ 0 \end{bmatrix} \tau \quad (7.20)$$

$$\text{where } M_r = \begin{bmatrix} M_{11} & M_{12} \\ M_{21} & M_{22} \end{bmatrix}, \quad M_{rf} = \begin{bmatrix} M_{13} & M_{14} \\ M_{23} & M_{24} \end{bmatrix}, \quad M_f = \begin{bmatrix} M_{33} & M_{34} \\ M_{43} & M_{44} \end{bmatrix}, \quad C_{rr} = \begin{bmatrix} C_{11} & C_{12} \\ C_{21} & C_{22} \end{bmatrix},$$

$$C_{rf} = \begin{bmatrix} C_{13} & C_{14} \\ C_{23} & C_{24} \end{bmatrix}, \quad C_{ff} = \begin{bmatrix} C_{33} & C_{34} \\ C_{43} & C_{44} \end{bmatrix}, \quad D_f = \begin{bmatrix} D_{f1} & 0 \\ 0 & D_{f2} \end{bmatrix} \text{ and } K_f = \begin{bmatrix} K_{f1} & 0 \\ 0 & K_{f2} \end{bmatrix}.$$

To develop a control law, the dynamical model (7.19) is written as two interconnected subsystems. Each subsystem has a pair of joint and link. There exists a non-singular matrix of transformation T_r such as:

$$\bar{q} = T_r q \quad (7.21)$$

where $q = [q_r \ q_f]^T = [q_{r1} \ q_{r2} \ q_{f1} \ q_{f2}]^T$ is the original generalized coordinate, $\bar{q} = [q_1 \ q_2]^T = [q_{r1} \ q_{f1} \ q_{r2} \ q_{f2}]^T$ is the transformed one and the matrix of transformation T_r is given by:

$$T_r = \begin{bmatrix} 1 & 0 & 0 & 0 \\ 0 & 0 & 1 & 0 \\ 0 & 1 & 0 & 0 \\ 0 & 0 & 0 & 1 \end{bmatrix} \quad (7.22)$$

Using the previous transformation, the dynamical model (7.19) can be written as follows:

$$M(q)T_r^{-1}\ddot{\bar{q}} + C(q, \dot{q})T_r^{-1}\dot{\bar{q}} + DT_r^{-1}\dot{\bar{q}} + KT_r^{-1}\bar{q} = L\tau \quad (7.23)$$

where $\ddot{\bar{q}} = T_r\ddot{q}$ and $\dot{\bar{q}} = T_r\dot{q}$.

Equation (7.23) is equivalent to the following expression:

$$\bar{M}(q)\ddot{\bar{q}} + \bar{C}(q, \dot{q})\dot{\bar{q}} + \bar{D}\dot{\bar{q}} + \bar{K}\bar{q} = \bar{L}\tau \quad (7.24)$$

where $\bar{M} = T_r M(q) T_r^{-1}$; $\bar{C} = T_r C(q, \dot{q}) T_r^{-1}$; $\bar{D} = T_r D T_r^{-1}$; $\bar{K} = T_r K T_r^{-1}$; $\bar{q} = [q_1 \ q_2]^T = [q_{r1} \ q_{f1} \ q_{r2} \ q_{f2}]^T$; $\bar{L} = T_r L = \begin{bmatrix} 1 & 0 & 0 & 0 \\ 0 & 0 & 1 & 0 \end{bmatrix}^T$ and $\tau = [\tau_1 \ \tau_2]^T$.

The modified dynamical model (7.24) can be written as follows:

$$\begin{aligned} & \begin{bmatrix} \bar{M}_{11} & \bar{M}_{12} \\ \bar{M}_{21} & \bar{M}_{22} \end{bmatrix} \begin{bmatrix} \ddot{\bar{q}}_1 \\ \ddot{\bar{q}}_2 \end{bmatrix} + \begin{bmatrix} \bar{C}_{11} & \bar{C}_{12} \\ \bar{C}_{21} & \bar{C}_{22} \end{bmatrix} \begin{bmatrix} \dot{\bar{q}}_1 \\ \dot{\bar{q}}_2 \end{bmatrix} + \begin{bmatrix} \bar{D}_{11} & \bar{D}_{12} \\ \bar{D}_{21} & \bar{D}_{22} \end{bmatrix} \begin{bmatrix} \dot{\bar{q}}_1 \\ \dot{\bar{q}}_2 \end{bmatrix} + \begin{bmatrix} \bar{K}_{11} & \bar{K}_{12} \\ \bar{K}_{21} & \bar{K}_{22} \end{bmatrix} \begin{bmatrix} \bar{q}_1 \\ \bar{q}_2 \end{bmatrix} \\ &= \begin{bmatrix} \bar{L}_1 \tau \\ \bar{L}_2 \tau \end{bmatrix} \end{aligned} \quad (7.25)$$

where $\bar{M}_{11} = \begin{bmatrix} M_{11} & M_{13} \\ M_{31} & M_{33} \end{bmatrix}$, $\bar{M}_{12} = \begin{bmatrix} M_{12} & M_{14} \\ M_{32} & M_{34} \end{bmatrix}$, $\bar{C}_{11} = \begin{bmatrix} C_{11} & C_{13} \\ C_{31} & C_{33} \end{bmatrix}$, $\bar{C}_{12} = \begin{bmatrix} C_{12} & C_{14} \\ C_{32} & C_{34} \end{bmatrix}$, $\bar{D}_{11} = \begin{bmatrix} 0 & 0 \\ 0 & D_{f1} \end{bmatrix}$; $\bar{D}_{12} = \begin{bmatrix} 0 & 0 \\ 0 & 0 \end{bmatrix}$; $\bar{K}_{11} = \begin{bmatrix} 0 & 0 \\ 0 & K_{f1} \end{bmatrix}$; $\bar{K}_{12} = \begin{bmatrix} 0 & 0 \\ 0 & 0 \end{bmatrix}$; $\bar{M}_{21} = \begin{bmatrix} M_{21} & M_{23} \\ M_{41} & M_{43} \end{bmatrix}$;

$$\bar{M}_{22} = \begin{bmatrix} M_{22} & M_{24} \\ M_{42} & M_{44} \end{bmatrix}; \quad \bar{C}_{21} = \begin{bmatrix} C_{21} & C_{23} \\ C_{41} & C_{43} \end{bmatrix}; \quad \bar{C}_{22} = \begin{bmatrix} C_{22} & C_{24} \\ C_{42} & C_{44} \end{bmatrix}; \quad \bar{D}_{21} = \begin{bmatrix} 0 & 0 \\ 0 & 0 \end{bmatrix}; \quad \bar{D}_{22} = \begin{bmatrix} 0 & 0 \\ 0 & D_{f2} \end{bmatrix}; \quad \bar{K}_{21} = \begin{bmatrix} 0 & 0 \\ 0 & 0 \end{bmatrix}; \quad \bar{K}_{22} = \begin{bmatrix} 0 & 0 \\ 0 & K_{f2} \end{bmatrix}; \quad q_1 = \begin{bmatrix} q_{r1} \\ q_{f1} \end{bmatrix}; \quad q_2 = \begin{bmatrix} q_{r2} \\ q_{f2} \end{bmatrix}; \quad \bar{L}_1 = \begin{bmatrix} 1 & 0 \\ 0 & 0 \end{bmatrix}; \quad \bar{L}_2 = \begin{bmatrix} 0 & 1 \\ 0 & 0 \end{bmatrix}.$$

Equation (7.25) can be written in the following form that will be used for control law:

$$\begin{bmatrix} \bar{M}_1^T \\ \bar{M}_2^T \end{bmatrix} \ddot{\bar{q}} + \begin{bmatrix} \bar{C}_1^T \\ \bar{C}_2^T \end{bmatrix} \dot{\bar{q}} + \begin{bmatrix} \bar{D}_1^T \\ \bar{D}_2^T \end{bmatrix} \dot{\bar{q}} + \begin{bmatrix} \bar{K}_1^T \\ \bar{K}_2^T \end{bmatrix} \bar{q} = \begin{bmatrix} \bar{L}_1 \\ \bar{L}_2 \end{bmatrix} \tau \quad (7.26)$$

where $\bar{M}_1^T = [\bar{M}_{11} \quad \bar{M}_{12}]$; $\bar{C}_1^T = [\bar{C}_{11} \quad \bar{C}_{12}]$; $\bar{D}_1^T = [\bar{D}_{11} \quad \bar{D}_{12}]$; $\bar{K}_1^T = [\bar{K}_{11} \quad \bar{K}_{12}]$; $\bar{M}_2^T = [\bar{M}_{21} \quad \bar{M}_{22}]$; $\bar{C}_2^T = [\bar{C}_{21} \quad \bar{C}_{22}]$; $\bar{D}_2^T = [\bar{D}_{21} \quad \bar{D}_{22}]$; $\bar{K}_2^T = [\bar{K}_{21} \quad \bar{K}_{22}]$.

The first and the second subsystems can be characterized by two mass and inertia symmetric positive definite matrices: $\bar{M}_{11} = \begin{bmatrix} M_{11} & M_{13} \\ M_{31} & M_{33} \end{bmatrix}$ and $\bar{M}_{22} = \begin{bmatrix} M_{22} & M_{24} \\ M_{42} & M_{44} \end{bmatrix}$.

The new generalized coordinate, used for the second joint and link while the first joint and link are assumed stable, is given as follows:

$$\bar{Q}_2 = [q_{d1} \quad q_2]^T = [q_{rd1} \quad q_{fd1} \quad q_{r2} \quad q_{f2}]^T \quad (7.27)$$

Note that the coordinates of the first subsystem are the desired ones, and the coordinates of the second subsystem are the controlled ones. Using (7.26), the equation of motion of the second joint and link can be written as:

$$\bar{M}_2^T(\bar{Q}_2)\ddot{\bar{Q}}_2 + \bar{C}_2^T(\bar{Q}_2, \dot{\bar{Q}}_2)\dot{\bar{Q}}_2 + \bar{D}_2^T\dot{\bar{Q}}_2 + \bar{K}_2^T\bar{Q}_2 = \bar{L}_2\tau_2 \quad (7.28)$$

The velocity $\dot{\bar{Q}}_2$ is the time derivative of \bar{Q}_2 and the acceleration $\ddot{\bar{Q}}_2$ is the time derivative of $\dot{\bar{Q}}_2$.

According to (7.8), the new non-collocated output is given as follows:

$$y_2 = q_{r2} + \alpha_2 \beta_2^T q_{f2}, \quad 0 \leq \alpha_2 < 1 \quad (7.29)$$

where $\beta_2^T = \beta_2 = \frac{\phi_{21}(L_2)}{L_2}$ when considering just one mode. α_2 is the weighted parameter characterizing the second non-collocated output.

Using (7.29), the equation of motion of the second subsystem is given as follows:

$$\begin{aligned} M_{21} \ddot{q}_{rd1} + M_{22} \ddot{y}_2 + M_{23} \ddot{q}_{fd1} + (M_{24} - \alpha_2 \beta_2 M_{22}) \ddot{q}_{f2} + C_{21} \dot{q}_{rd1} + C_{22} \dot{y}_2 \\ + C_{23} \dot{q}_{fd1} + C_{24} \dot{q}_{f2} = \tau_2 \end{aligned} \quad (7.30)$$

$$\begin{aligned} M_{41} \ddot{q}_{rd1} + M_{42} \ddot{y}_2 + M_{43} \ddot{q}_{fd1} + (M_{44} - \alpha_2 \beta_2 M_{42}) \ddot{q}_{f2} + C_{41} \dot{q}_{rd1} + C_{42} \dot{y}_2 \\ + C_{43} \dot{q}_{fd1} + C_{44} \dot{q}_{f2} + D_{f2} \dot{q}_{f2} + K_{f2} q_{f2} = 0 \end{aligned} \quad (7.31)$$

where $C_{24} = C_{24} - \alpha_2 \beta_2 C_{22}$ and $C_{44} = C_{44} - \alpha_2 \beta_2 C_{42}$

The internal dynamics of the second link is deduced from (7.31) as follows:

$$\begin{aligned} \ddot{q}_{f2} = -\mathcal{M}_{41} \ddot{q}_{rd1} - \mathcal{M}_{43} \ddot{q}_{fd1} - \mathcal{M}_{42} \ddot{y}_2 - C_{41} \dot{q}_{rd1} - C_{42} \dot{y}_2 - C_{43} \dot{q}_{fd1} - C_{44} \dot{q}_{f2} \\ - \mathcal{K}_{f2} q_{f2} - \mathcal{D}_{f2} \dot{q}_{f2} \end{aligned} \quad (7.32)$$

where: $\mathcal{M}_{41} = (M_{44} - \alpha_2 \beta_2 M_{42})^{-1} M_{41}$; $\mathcal{M}_{42} = (M_{44} - \alpha_2 \beta_2 M_{42})^{-1} M_{42}$; $\mathcal{M}_{43} = (M_{44} - \alpha_2 \beta_2 M_{42})^{-1} M_{43}$; $C_{41} = (M_{44} - \alpha_2 \beta_2 M_{42})^{-1} C_{41}$; $C_{42} = (M_{44} - \alpha_2 \beta_2 M_{42})^{-1} C_{42}$; $C_{44} = (M_{44} - \alpha_2 \beta_2 M_{42})^{-1} C_{44}$; $\mathcal{K}_{f2} = (M_{44} - \alpha_2 \beta_2 M_{42})^{-1} K_{f2}$; $\mathcal{D}_{f2} = (M_{44} - \alpha_2 \beta_2 M_{42})^{-1} D_{f2}$ and α_2 is chosen such as: $\alpha_2 \neq \frac{M_{44}}{\beta_2 M_{42}}$.

Inserting (7.32) in (7.30), we get:

$$\begin{aligned} M_{21}^* \ddot{q}_{rd1} + M_{22}^* \ddot{y}_2 + M_{23}^* \ddot{q}_{fd1} + C_{21}^* \dot{q}_{rd1} + C_{22}^* \dot{y}_2 + C_{23}^* \dot{q}_{fd1} + C_{24}^* \dot{q}_{f2} + K_{f2}^* q_{f2} \\ + D_{f2}^* \dot{q}_{f2} = \tau_2 \end{aligned} \quad (7.33)$$

where: $M_{21}^* = M_{21} - (M_{24} - \alpha_2 \beta_2 M_{22})\mathcal{M}_{41}$; $M_{22}^* = M_{22} - (M_{24} - \alpha_2 \beta_2 M_{22})\mathcal{M}_{42}$; $M_{23}^* = M_{23} - (M_{24} - \alpha_2 \beta_2 M_{22})\mathcal{M}_{43}$; $C_{21}^* = C_{21} - (M_{24} - \alpha_2 \beta_2 M_{22})C_{41}$; $C_{22}^* = C_{22} - (M_{24} - \alpha_2 \beta_2 M_{22})C_{42}$; $C_{23}^* = C_{23} - (M_{24} - \alpha_2 \beta_2 M_{22})C_{43}$; $C_{24}^* = \bar{C}_{24} - (M_{24} - \alpha_2 \beta_2 M_{22})C_{44}$; $K_{f2}^* = -(M_{24} - \alpha_2 \beta_2 M_{22})\mathcal{K}_{f2}$ and $D_{f2}^* = -(M_{24} - \alpha_2 \beta_2 M_{22})\mathcal{D}_{f2}$.

To control the second link, we propose the following control law:

$$\tau_2 = \tau_{r2} + \tau_{f2} + \delta\tau_2 \quad (7.34)$$

where τ_{r2} is used for the rigid part, τ_{f2} is for the flexible part and $\delta\tau_2$ is the setting term.

$$\tau_{r2} = K_{p2}\tilde{y}_2 + K_{d2}\dot{\tilde{y}}_2 + M_{22}^*\ddot{y}_2^* + M_{21}^*\ddot{q}_{rd1} + C_{21}^*\dot{q}_{rd1} + C_{22}^*\dot{y}_{d2} \quad (7.35)$$

$$\tau_{f2} = C_{23}^*\dot{q}_{fd1} + C_{24}^*\dot{q}_{f2} + \alpha_2 \beta_2 (M_{21}^*\ddot{q}_{fd1} + C_{21}^*\dot{q}_{fd1}) + K_{f2}^*q_{f2} + D_{f2}^*\dot{q}_{f2} \quad (7.36)$$

$$\delta\tau_2 = \delta M_{22}^*\ddot{y}_2^* + \delta M_{21}^*\ddot{y}_{d1} + \delta C_{21}^*\dot{y}_{d1} + \delta C_{22}^*\dot{y}_{d2} + \delta C_{23}^*\dot{q}_{fd1} + \delta C_{24}^*\dot{q}_{f2} \quad (7.37)$$

where $\tilde{y}_2 = y_{d2} - y_2$; $\dot{\tilde{y}}_2 = \dot{y}_{d2} - \dot{y}_2$ and $\ddot{y}_2^* = \ddot{y}_{d2} + \lambda_2 \dot{\tilde{y}}_2$, $\lambda_2 > 0$. The terms of $\delta\tau_2$ are given in Appendix.

Now going backward for the first subsystem and assuming that the second subsystem is stable. The new generalized coordinate associate to the second subsystem becomes:

$$\bar{Q}_1 = [q_1 \quad q_{d2}]^T = [q_{r1} \quad q_{f1} \quad q_{rd2} \quad q_{fd2}]^T \quad (7.38)$$

Using (7.26), the equation of motion of the first subsystem (i.e. first link and joint) is given as follows:

$$\bar{M}_1^T(\bar{Q}_1)\ddot{\bar{Q}}_1 + \bar{C}_1^T(\bar{Q}_1, \dot{\bar{Q}}_1)\dot{\bar{Q}}_1 + D_1^T\dot{\bar{Q}}_1 + \bar{K}_1^T\bar{Q}_1 = \bar{L}_1\tau_1 \quad (7.39)$$

The new non-collocated output, defined as the angle of the first motor augmented by a weighted value of the link's extremity angle, is given as follows:

$$y_1 = q_{r1} + \alpha_1 \beta_1^T q_{f1}, \quad 0 \leq \alpha_1 < 1 \quad (7.40)$$

where $\beta_1^T = \beta_1 = \frac{\phi_{11}(L_1)}{L_1}$ for one mode.

Using (7.39) and (7.40), the equation of motion of the first joint and link is given as follows:

$$\begin{aligned} M_{11}\ddot{y}_1 + M_{12}\ddot{q}_{rd2} + (M_{13} - \alpha_1 \beta_1 M_{11})\ddot{q}_{f1} + M_{14}\ddot{q}_{fd2} + C_{11}\dot{y}_1 + C_{12}\dot{q}_{rd2} \\ + C_{13}\dot{q}_{f1} + C_{14}\dot{q}_{fd2} = \tau_1 \end{aligned} \quad (7.41)$$

$$\begin{aligned} M_{31}\ddot{y}_1 + M_{32}\ddot{q}_{rd2} + (M_{33} - \alpha_1 \beta_1 M_{31})\ddot{q}_{f1} + M_{34}\ddot{q}_{fd2} + C_{31}\dot{y}_1 + C_{32}\dot{q}_{rd2} \\ + C_{33}\dot{q}_{f1} + C_{34}\dot{q}_{fd2} + D_{f1}\dot{q}_{f1} + K_{f1}q_{f1} = 0 \end{aligned} \quad (7.42)$$

Let us define $C_{13} = C_{13} - \alpha_1 \beta_1 C_{11}$ and $C_{33} = C_{33} - \alpha_1 \beta_1 C_{31}$.

To find the internal dynamics of the first link, \ddot{q}_{f1} is given from (7.42) as follows:

$$\begin{aligned} \ddot{q}_{f1} = -\mathcal{M}_{31}\ddot{y}_1 - \mathcal{M}_{32}\ddot{q}_{rd2} - \mathcal{M}_{34}\ddot{q}_{fd2} - C_{31}\dot{y}_1 - C_{32}\dot{q}_{rd2} - C_{33}\dot{q}_{f1} - C_{34}\dot{q}_{fd2} \\ - \mathcal{K}_{f1}q_{f1} - \mathcal{D}_{f1}\dot{q}_{f1} \end{aligned} \quad (7.43)$$

where: $\mathcal{M}_{31} = (M_{33} - \alpha_1 \beta_1 M_{31})^{-1}M_{31}$; $\mathcal{M}_{32} = (M_{33} - \alpha_1 \beta_1 M_{31})^{-1}M_{32}$; $\mathcal{M}_{34} = (M_{33} - \alpha_1 \beta_1 M_{31})^{-1}M_{34}$; $C_{31} = (M_{33} - \alpha_1 \beta_1 M_{31})^{-1}C_{31}$; $C_{33} = (M_{33} - \alpha_1 \beta_1 M_{31})^{-1}C_{33}$; $C_{34} = (M_{33} - \alpha_1 \beta_1 M_{31})^{-1}C_{34}$; $\mathcal{K}_{f1} = (M_{33} - \alpha_1 \beta_1 M_{31})^{-1}K_{f1}$; $\mathcal{D}_{f1} = (M_{33} - \alpha_1 \beta_1 M_{31})^{-1}D_{f1}$ and α_1 is selected such as: $\alpha_1 \neq \frac{M_{33}}{\beta_1 M_{31}}$. Using the same strategy, the control law of the first subsystem is given as follows:

$$\tau_1 = \tau_{r1} + \tau_{f1} + \delta\tau_1 \quad (7.44)$$

where:

$$\tau_{r1} = K_{p1}\tilde{y}_1 + K_{d1}\hat{y}_1 + M_{11}^*\ddot{y}_1^* + M_{12}^*\ddot{q}_{rd2} + C_{11}^*\dot{y}_{d1} + C_{12}^*\dot{q}_{rd2} \quad (7.45)$$

$$\tau_{f1} = C_{13}^*\dot{q}_{f1} + C_{14}^*\dot{q}_{fd2} + \alpha_1\beta_1(M_{12}^*\ddot{q}_{fd2} + C_{12}^*\dot{q}_{fd2}) + K_{f1}^*q_{f1} + D_{f1}^*\dot{q}_{f1} \quad (7.46)$$

$$\delta\tau_1 = \delta M_{11}^*\ddot{y}_1^* + \delta M_{12}^*\ddot{y}_{d2} + \delta C_{11}^*\dot{y}_{d1} + \delta C_{12}^*\dot{y}_{d2} + \delta C_{13}^*\dot{q}_{f1} + \delta C_{14}^*\dot{q}_{fd2} \quad (7.47)$$

where $\tilde{y}_1 = y_{d1} - y_1$; $\ddot{y}_2^* = \ddot{y}_{d2} + \lambda_2\dot{\tilde{y}}_2$ and $\dot{\tilde{y}}_2 = \dot{y}_{d2} - \dot{y}_2$; $\lambda_2 > 0$.

$M_{1j}^* = M_{1j} - (M_{13} - \alpha_1\beta_1 M_{11})\mathcal{M}_{3j}$; $j = 1, 2, 4$; $C_{1j}^* = C_{1j} - (M_{13} - \alpha_1\beta_1 M_{11})\mathcal{C}_{3j}$; $j = 1, 2, 3, 4$; $K_{f1}^* = -(M_{13} - \alpha_1\beta_1 M_{11})\mathcal{K}_{f1}$; $D_{f1}^* = -(M_{13} - \alpha_1\beta_1 M_{11})\mathcal{D}_{f1}$. The terms of $\delta\tau_1$ are given in Appendix.

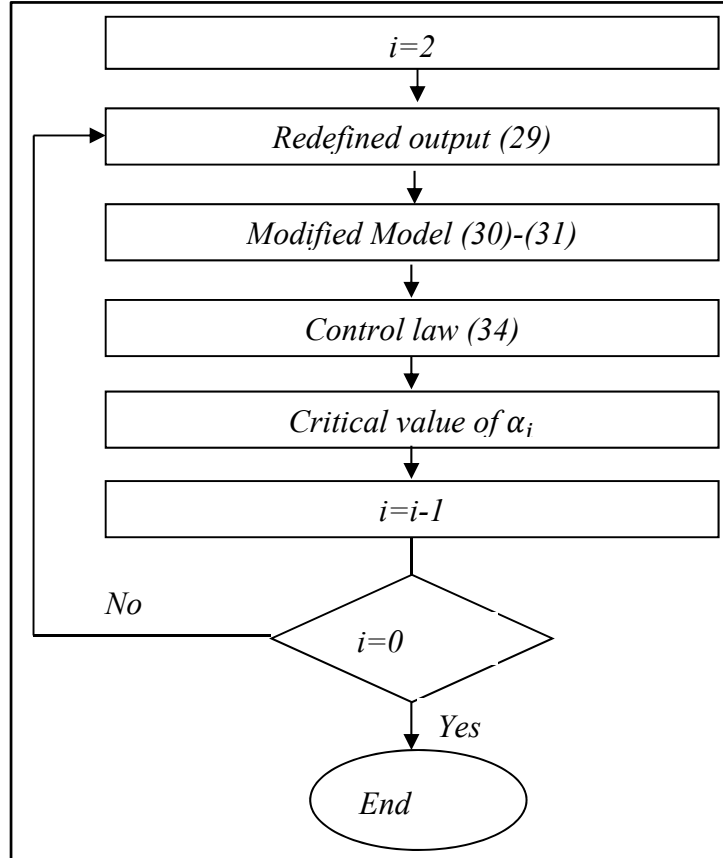


Figure 7.3 Distributed control strategy.

7.5 Stability analysis

This section presents the stability analysis of the tracking errors of the rigid and the flexible parts. First, we study the global stability of the rigid part by inserting the two control laws in the initial dynamical model. Second, the stability of the flexible part is studied to select the weighted parameters and guarantee bounded internal dynamics such that the new output is as close as possible to the tip.

7.5.1 Stability of rigid part

In compact form, the first (7.34) and second (7.44) control laws can be written as follows:

$$\tau = \tau_r + \tau_f + \delta\tau \quad (7.48)$$

where:

$$\tau_r = K_p \tilde{y} + K_d \dot{\tilde{y}} + M_{rd}^* \ddot{y}^* + M_{rnd}^* \ddot{q}_{rd} + C_{rd}^* \dot{y}_d + C_{rnd}^* \dot{q}_{rd} \quad (7.49)$$

$$\tau_f = C_{rf}^* \dot{q}_f + \alpha\beta(M_{rnd}^* \ddot{q}_{fd} + C_{rnd}^* \dot{q}_{fd}) + K_f^* q_f + D_f^* \dot{q}_f \quad (7.50)$$

$$\delta\tau = \delta M_{rd}^* \ddot{y}^* + \delta M_{rnd}^* \ddot{y}_d + \delta C_r^* \dot{y}_d + \delta C_{rf}^* \dot{q}_f \quad (7.51)$$

$$K_p = \begin{bmatrix} K_{p1} & 0 \\ 0 & K_{p2} \end{bmatrix}; \quad K_d = \begin{bmatrix} K_{d1} & 0 \\ 0 & K_{d2} \end{bmatrix}; \quad M_{rd}^* = \begin{bmatrix} M_{11}^* & 0 \\ 0 & M_{22}^* \end{bmatrix}; \quad M_{rnd}^* = \begin{bmatrix} 0 & M_{12}^* \\ M_{21}^* & 0 \end{bmatrix}; \quad C_{rd}^* = \begin{bmatrix} C_{11}^* & 0 \\ 0 & C_{22}^* \end{bmatrix}; \quad C_{rnd}^* = \begin{bmatrix} 0 & C_{12}^* \\ C_{21}^* & 0 \end{bmatrix}; \quad C_{rf}^* = \begin{bmatrix} C_{13}^* & C_{14}^* \\ C_{23}^* & C_{24}^* \end{bmatrix}; \quad \delta M_{rd}^* = \begin{bmatrix} \delta M_{11}^* & 0 \\ 0 & \delta M_{22}^* \end{bmatrix}; \quad \delta M_{rnd}^* = \begin{bmatrix} 0 & \delta M_{12}^* \\ \delta M_{21}^* & 0 \end{bmatrix}; \quad \delta C_r^* = \begin{bmatrix} \delta C_{11}^* & \delta C_{12}^* \\ \delta C_{21}^* & \delta C_{22}^* \end{bmatrix}; \quad \delta C_{rf}^* = \begin{bmatrix} \delta C_{13}^* & \delta C_{14}^* \\ \delta C_{23}^* & \delta C_{24}^* \end{bmatrix}; \quad \delta M_{ij}^* \text{ are given in (7.88).}$$

To study the global stability, we insert the control law given in (7.48) in the dynamical model given in (7.1).

Proposition 1

The equation of motion of the two-flexible-link manipulator (7.19) is equivalent to the following model:

$$M_r^*(q_\alpha)\ddot{y} + C_r^*(q_\alpha, \dot{q}_\alpha)\dot{y} + C_{rf}^*(q_\alpha, \dot{q}_\alpha)\dot{q}_f + K_f^*q_f + D_f^*\dot{q}_f = \tau \quad (7.52)$$

where $q_\alpha = [y_1 \ y_2 \ q_{f1} \ q_{f2}]^T$; $M_r^* = \begin{bmatrix} M_{11}^* & M_{12}^* \\ M_{21}^* & M_{22}^* \end{bmatrix}$ is positive definite matrix; $C_r^* = \begin{bmatrix} C_{11}^* & C_{12}^* \\ C_{21}^* & C_{22}^* \end{bmatrix}$, and $C_{rf}^* = \begin{bmatrix} C_{13}^* & C_{14}^* \\ C_{23}^* & C_{24}^* \end{bmatrix}$; M_r^* and C_r^* satisfy the following skew-symmetric property:

$$X^T(\dot{M}_r^* - 2C_r^*)X = 0 \quad \forall X \in \mathcal{R}^n \quad (7.53)$$

Proof: see Appendix.

M_r^* can be written as:

$$M_r^* = M_{rd}^* + M_{rnd}^* \quad (7.54)$$

where M_{rd}^* is the diagonal elements and M_{rnd}^* is the non-diagonal elements of M_{rd}^* . Then, the dynamical model (7.52) can be written as follows:

$$M_{rd}^*(q_\alpha)\ddot{y} + M_{rnd}^*(q_\alpha)\ddot{y} + C_r^*(q_\alpha, \dot{q}_\alpha)\dot{y} + C_{rf}^*(q_\alpha, \dot{q}_\alpha)\dot{q}_f + K_f^*q_f + D_f^*\dot{q}_f = \tau \quad (7.55)$$

Using (7.54), the control law (7.48) is equivalent to :

$$\begin{aligned} \tau = & K_p\tilde{y} + K_d\dot{\tilde{y}} + M_{rd}^*(Q)\ddot{y}^* + M_{rnd}^*(Q)\ddot{y}_d + C_r^*(Q, \dot{Q})\dot{y}_d + C_{rf}^*(Q, \dot{Q})\dot{q}_f \\ & + K_f^*q_f + D_f^*\dot{q}_f + \delta\tau \end{aligned} \quad (7.56)$$

Now, the global stability is studied by inserting the control law (7.56) in the dynamical model (7.55). Then, the error dynamics are given by the following equation:

$$\begin{aligned} K_p \tilde{y} + K_d \dot{\tilde{y}} + [M_{rd}^*(Q) \ddot{y}^* - M_{rd}^*(q_\alpha) \ddot{y}] + [M_{rnd}^*(Q) \ddot{y}_d - M_{rnd}^*(q_\alpha) \ddot{y}] \\ + [C_r^*(Q, \dot{Q}) \dot{y}_d - C_r^*(q_\alpha, \dot{q}_\alpha) \dot{y}] + [C_{rf}^*(Q, \dot{Q}) \dot{q}_f - C_{rf}^*(q_\alpha, \dot{q}_\alpha) \dot{q}_f] \\ + \delta\tau = 0 \end{aligned} \quad (7.57)$$

Proposition 2

When using the control law (7.56) and the dynamical model (7.55), the error dynamics given by (7.57) are equivalent to:

$$K_p \tilde{y} + K_d \dot{\tilde{y}} + M_r^*(q_\alpha) \ddot{\tilde{y}} + C_r^*(q_\alpha, \dot{q}_\alpha) \dot{\tilde{y}} + \lambda M_{rd}^*(q_\alpha) \dot{\tilde{y}} = 0 \quad (7.58)$$

Proof: see Appendix.

To prove the asymptotical stability of the error dynamics, we propose the following Lyapunov function:

$$V = \frac{1}{2} \dot{\tilde{y}}^T M_r^* \dot{\tilde{y}} + \frac{1}{2} \tilde{y}^T K_d \tilde{y} \quad (7.59)$$

The time derivative of V is:

$$\begin{aligned} \dot{V}(t) &= \dot{\tilde{y}}^T M_r^* \ddot{\tilde{y}} + \frac{1}{2} \dot{\tilde{y}}^T \dot{M}_r^* \dot{\tilde{y}} + \tilde{y}^T K_p \dot{\tilde{y}} \\ &= \dot{\tilde{y}}^T (-C_r^* \dot{\tilde{y}} - \lambda M_{rd}^* \dot{\tilde{y}} - K_p \tilde{y} - K_d \dot{\tilde{y}}) + \frac{1}{2} \dot{\tilde{y}}^T \dot{M}_r^* \dot{\tilde{y}} + \tilde{y}^T K_p \dot{\tilde{y}} \end{aligned}$$

Using proposition 1, we can conclude that:

$$\dot{V}(t) = -\dot{\tilde{y}}^T (K_d + \lambda M_{rd}^*) \dot{\tilde{y}} \quad (7.60)$$

K_d , λ and M_{rd}^* are positive definite diagonal matrices. Then, using LaSalle theorem (Spong et Vidyasagar, 1989), the error dynamics are globally asymptotically stable.

7.5.2 Stability of the flexible part

In this section, asymptotical stability of the flexible part is studied using the internal dynamics. From the dynamical model given in (7.1) and (7.3), the equation of motion of the flexible part of the second link is given by:

$$M_{41}\ddot{q}_{r1} + M_{42}\ddot{q}_{r2} + M_{43}\ddot{q}_{f1} + M_{44}\ddot{q}_{f2} + H_4 + D_{f2}\dot{q}_{f2} + K_{f2}q_{f2} = 0 \quad (7.61)$$

Using the new generalized coordinate (7.27) and the new non-collocated output (7.29), the equation (7.61) is equivalent to:

$$\begin{aligned} M_{41}\ddot{q}_{rd1} + M_{42}\ddot{y}_2 + M_{43}\ddot{q}_{fd1} + (M_{44} - \alpha_2\beta_2 M_{42})\ddot{q}_{f2} + H_4 + D_{f2}\dot{q}_{f2} + K_{f2}q_{f2} \\ = 0 \end{aligned} \quad (7.62)$$

The internal dynamics of the second link are given by subtracting \ddot{q}_{f2} from (7.62) as follows:

$$\ddot{q}_{f2} = -\mathcal{M}_{41}\ddot{q}_{rd1} - \mathcal{M}_{42}\ddot{y}_2 - \mathcal{M}_{43}\ddot{q}_{fd1} - \mathcal{H}_4 - \mathcal{K}_{f2}q_{f2} - \mathcal{D}_{f2}\dot{q}_{f2} \quad (7.63)$$

where $\mathcal{M}_{41} = (M_{44} - \alpha_2\beta_2 M_{42})^{-1}M_{41}$; $\mathcal{M}_{42} = (M_{44} - \alpha_2\beta_2 M_{42})^{-1}M_{42}$; $\mathcal{M}_{43} = (M_{44} - \alpha_2\beta_2 M_{42})^{-1}M_{43}$; $\mathcal{H}_4 = (M_{44} - \alpha_2\beta_2 M_{42})^{-1}H_4$; $\mathcal{D}_{f2} = (M_{44} - \alpha_2\beta_2 M_{42})^{-1}D_{f2}$; $\mathcal{K}_{f2} = (M_{44} - \alpha_2\beta_2 M_{42})^{-1}K_{f2}$ and α_2 is chosen such as $\alpha_2 \neq \frac{M_{44}}{\beta_2 M_{42}}$.

The quasi-static approach, using the inverse dynamics, neglects \dot{q}_{fd1} and \ddot{q}_{fd1} . Then, the tracking errors of the rigid and flexible part of the second link are given by the following expressions:

$$\begin{aligned}\ddot{\tilde{q}}_{f2} &= \ddot{q}_{fd2} - \ddot{q}_{f2} = -(\mathcal{M}_{d41} - \mathcal{M}_{41})\ddot{q}_{rd1} - \mathcal{M}_{d42}\ddot{\tilde{y}}_2 - (\mathcal{H}_{d4} - \mathcal{H}_4) \\ &\quad - (\mathcal{K}_{fd2}q_{fd2} - \mathcal{K}_{f2}q_{f2}) - (\mathcal{D}_{fd2}\dot{q}_{fd2} - \mathcal{D}_{f2}\dot{q}_{f2})\end{aligned}\tag{7.64}$$

In the above section, the tracking error of the rigid part was proved to be asymptotically stable, then $\tilde{y}_2, \dot{\tilde{y}}_2, \ddot{\tilde{y}}_2 \rightarrow 0$ as $t \rightarrow \infty$. Then, the tracking error of the flexible part can be written as:

$$\ddot{\tilde{q}}_{f2} = -(\mathcal{M}_{d41} - \mathcal{M}_{41})\ddot{q}_{rd1} - (\mathcal{H}_{d4} - \mathcal{H}_4) - \mathcal{K}_{f2}\tilde{q}_{f2} - \mathcal{D}_{f2}\dot{\tilde{q}}_{f2}\tag{7.65}$$

In state space form, the tracking error of the flexible part takes the same form than the one obtained in (Fareh, Saad et Saad, 2013a) and is given by the following expression:

$$\begin{cases} \dot{\tilde{x}}_1 = \tilde{x}_2 \\ \dot{\tilde{x}}_2 = \ddot{\tilde{q}}_{f2} - \ddot{q}_{f2} \end{cases}\tag{7.66}$$

Let $\tilde{x}_f = [\tilde{x}_1 \quad \tilde{x}_2]^T = [\tilde{q}_{f2} \quad \dot{\tilde{q}}_{f2}]^T$; $\tilde{q}_{f2} = q_{fd2} - q_{f2}$.

The critical value of α_2 is selected such that A_{f2} is Hurwitz and the Nyquist diagram of A_{f2} is in the right half-plan (Fareh, Saad et Saad, 2013a), where $A_{f2} = \begin{bmatrix} 0 & 1 \\ -\mathcal{K}_{f2} & -\mathcal{D}_{f2} \end{bmatrix}$. \mathcal{K}_{f2} and \mathcal{D}_{f2} are given in (7.63).

The same procedure is now applied, proceeding to the first joint-link subsystem. Using (7.1) and (7.3), the equation of motion of the flexible part of the first link is given by:

$$M_{31}\ddot{q}_{r1} + M_{32}\ddot{q}_{r2} + M_{33}\ddot{q}_{f1} + M_{34}\ddot{q}_{f2} + H_3 + D_{f1}\dot{q}_{f1} + K_{f1}q_{f1} = 0\tag{7.67}$$

Using the new generalized coordinate (7.38) and the new non-collocated output (7.40), the equation of motion becomes:

$$\begin{aligned}M_{31}\ddot{y}_1 + M_{32}\ddot{q}_{rd2} + (M_{33} - \alpha_1\beta_1 M_{31})\ddot{q}_{f1} + M_{34}\ddot{q}_{fd2} + H_3 + D_{f1}\dot{q}_{f1} + K_{f1}q_{f1} \\ = 0\end{aligned}\tag{7.68}$$

Subtracting \ddot{q}_{f1} from (7.68), the internal dynamics is given as follows:

$$\ddot{q}_{f1} = -\mathcal{M}_{31}\ddot{y}_1 - \mathcal{M}_{32}\ddot{q}_{rd2} - \mathcal{M}_{34}\ddot{q}_{fd2} - \mathcal{H}_3 - \mathcal{K}_{f1}q_{f1} - \mathcal{D}_{f1}\dot{q}_{f1} \quad (7.69)$$

where: $\mathcal{M}_{31} = (M_{33} - \alpha_1\beta_1 M_{31})^{-1}M_{31}$; $\mathcal{M}_{32} = (M_{33} - \alpha_1\beta_1 M_{31})^{-1}M_{32}$; $\mathcal{M}_{34} = (M_{33} - \alpha_1\beta_1 M_{31})^{-1}M_{34}$; $\mathcal{H}_3 = (M_{33} - \alpha_1\beta_1 M_{31})^{-1}H_3$; $\mathcal{K}_{f1} = (M_{33} - \alpha_1\beta_1 M_{31})^{-1}K_{f1}$; $\mathcal{D}_{f1} = (M_{33} - \alpha_1\beta_1 M_{31})^{-1}D_{f1}$ and α_1 is chosen such as $\alpha_1 \neq \frac{M_{33}}{\beta_1 M_{31}}$.

In the state space form, the tracking error of the flexible part of the first link can be written as follows:

$$\begin{cases} \dot{\tilde{x}}_{f1} = \dot{\tilde{q}}_{f1} = \tilde{x}_{f2} \\ \dot{\tilde{x}}_{f2} = \ddot{\tilde{q}}_{f1} = \ddot{q}_{fd1} - \ddot{q}_{f1} \end{cases} \quad (7.70)$$

Let: $\tilde{x}_f = [\tilde{x}_{f1} \quad \tilde{x}_{f2}]^T = [\tilde{q}_{f1} \quad \dot{\tilde{q}}_{f1}]^T$.

As already shown in the stability analysis of the rigid part, $\tilde{y}_1, \dot{\tilde{y}}_1$ and $\ddot{\tilde{y}}_1 \rightarrow 0$ as $t \rightarrow \infty$. The error dynamics of the flexible part (7.70) take the same form as the one obtained one in (Fareh, Saad et Saad, 2013a).

The critical value of α_1 is selected when the eigenvalues of A_{f1} change their signs from negative to positive, i.e. the internal dynamics become instable (Fareh, Saad et Saad, 2013a),

where: $A_{f1} = \begin{bmatrix} 0 & 1 \\ -\overline{K}_{f1} & -\overline{D}_{f1} \end{bmatrix}$.

7.6 Simulation results

The two-flexible-link manipulator shown in Figure 7.2 is used to test the control strategy performance. Using the trial and error method, the controllers' gains are chosen as: $K_{p1} = 12, K_{p2} = 10, K_{d1} = 15, K_{d2} = 18$. In sections 7.3 and 7.4, the theoretical development of the control law and stability analysis are given in the general case i.e. for any higher order. In the simulation case, a finite order of Taylor series is fixed. In this section, and for simplicity, the Taylor series is limited to the first order. Then, $R_{M_{nj}} = R_{C_{nj}} = R_{G_n} = 0$.

Table 7.1 presents the parameters of the two-flexible-link manipulator.

Table 7.1 System parameters

Parameter	Value
Hub inertia (J_{hi})	0.1 kg.m ²
Link length (L_i)	0.5 m
Link linear density (ρ)	1 kg/m
Link rigidity (EI_i)	10N.m ²
Link mass (m_i)	0.5 kg
Payload mass (m_p)	0.1 kg
Payload inertia (J_p)	0.0005 kg.m ²

Simulation results are given in the following figures.

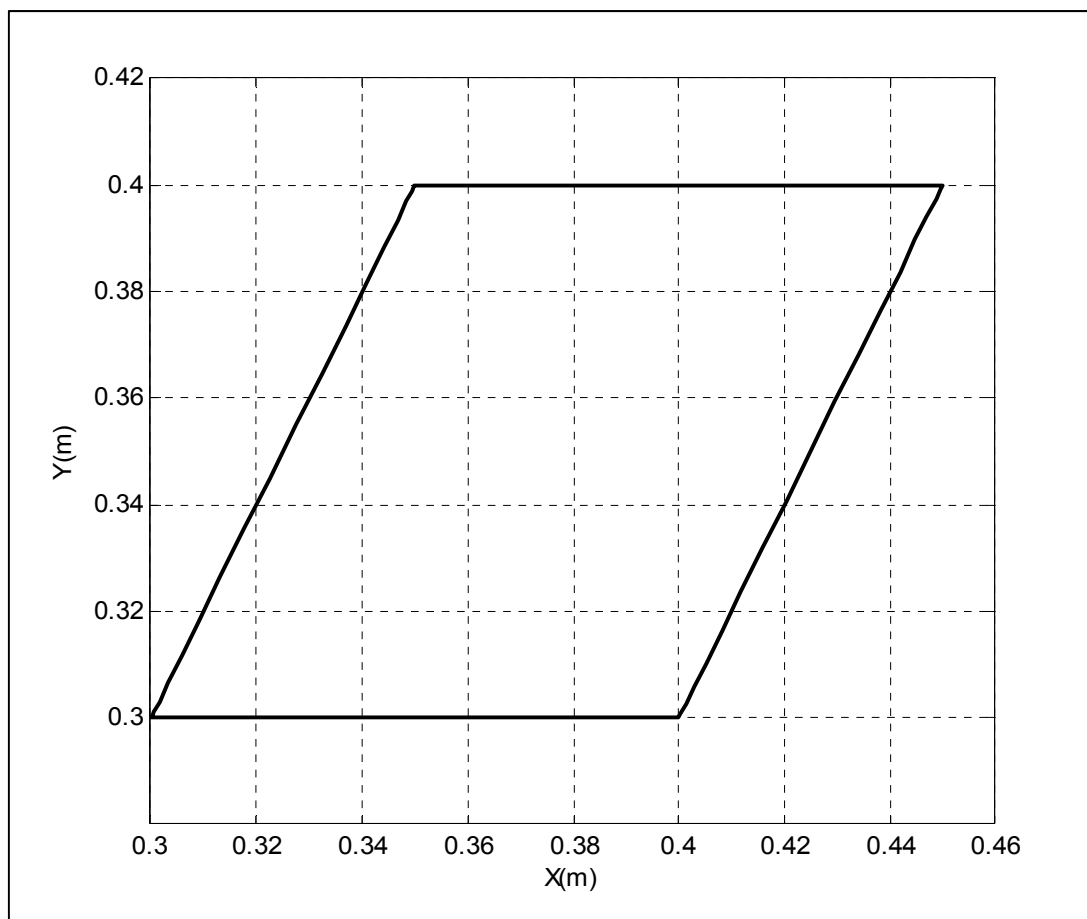


Figure 7.4 X-Y desired workspace trajectory.

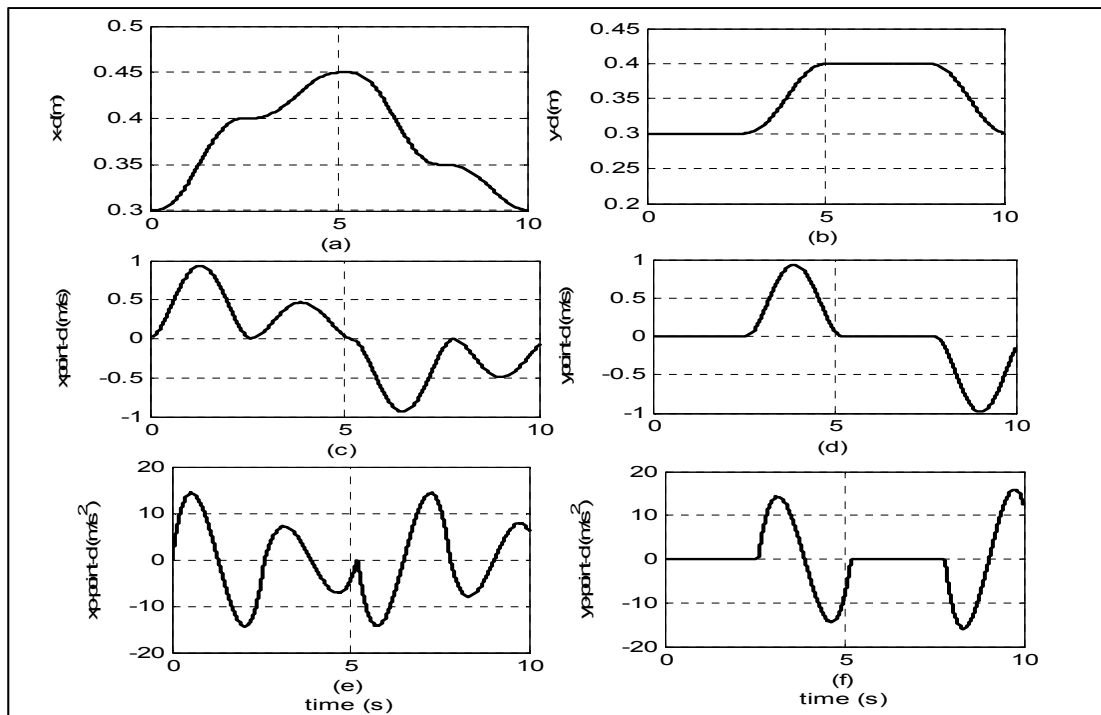


Figure 7.5 Desired workspace trajectory: (a)-(b) position trajectory, (c)-(d) velocity trajectories and (e)-(f) acceleration trajectories.

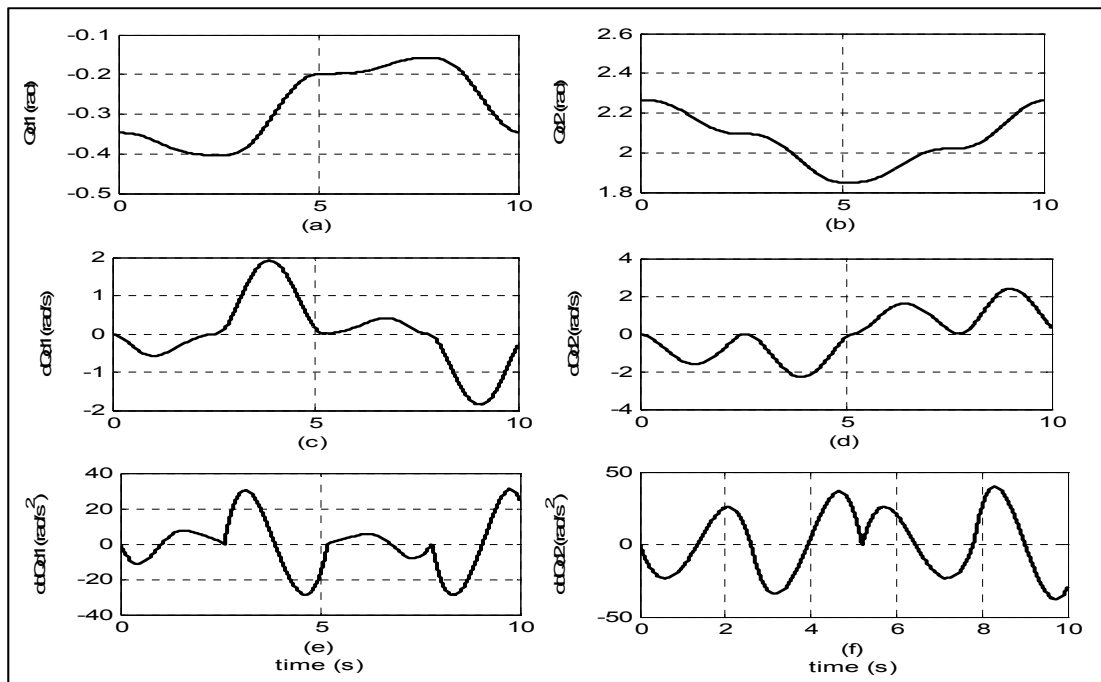


Figure 7.6 Desired virtual space trajectories: (a)-(b) position trajectories, (c)-(d) velocity trajectories and (e)-(f) acceleration trajectories.

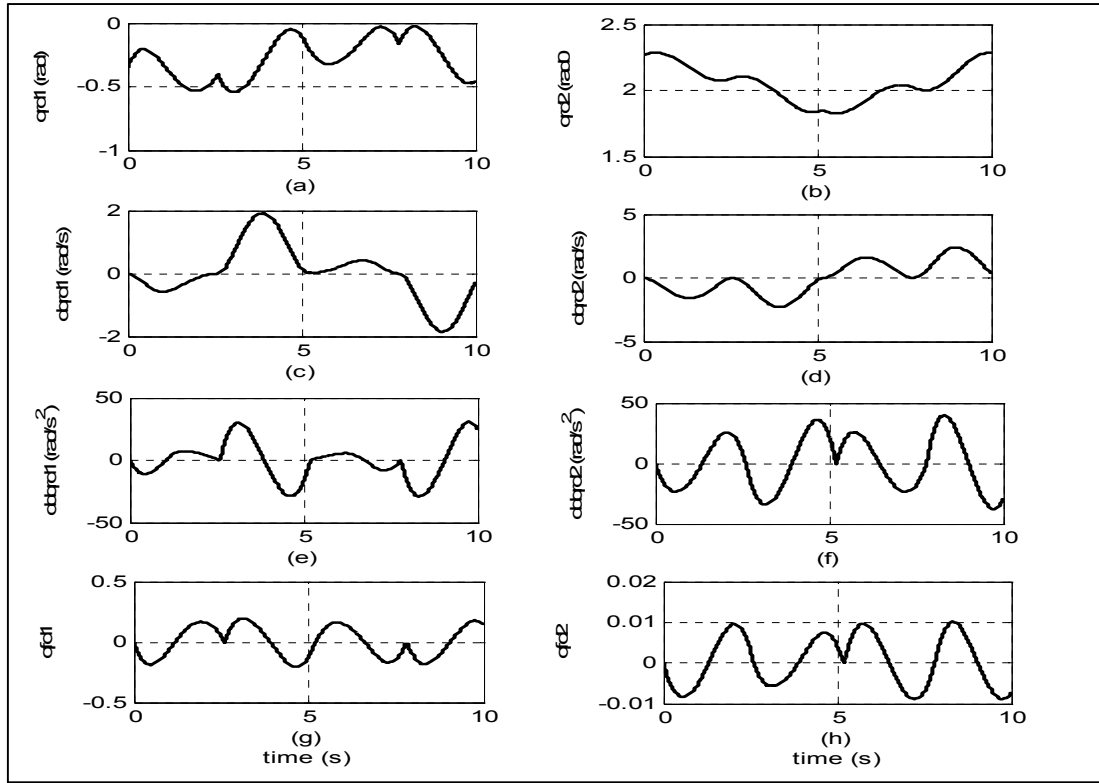


Figure 7.7 Desired joint space trajectories: (a)-(b) positiontrajectories of rigid coordinates, (c)-(d) velocity trajectories of rigidcoordinates, (e)-(f) acceleration trajectories of rigid coordinatesand (g)-(h) position trajectories of flexible coordinates.

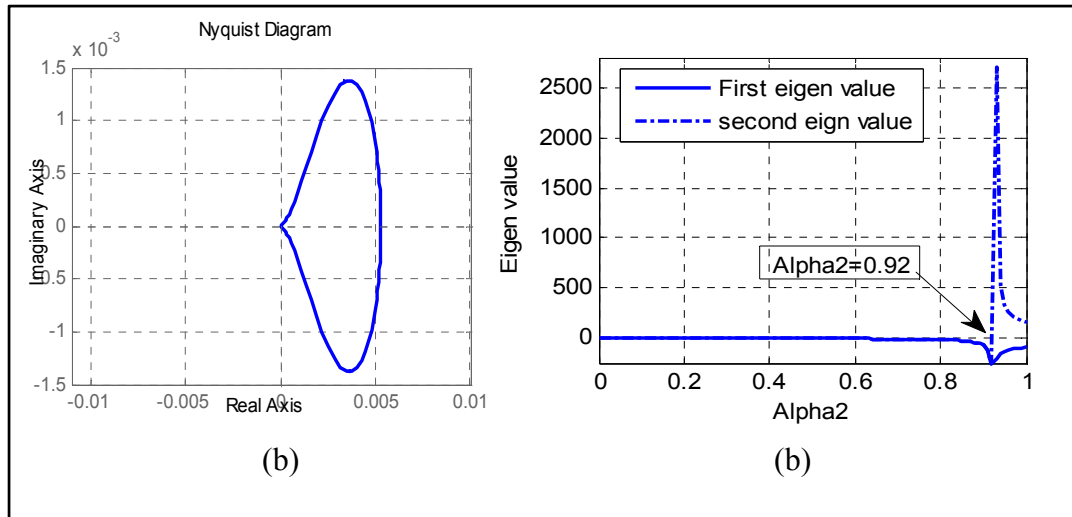
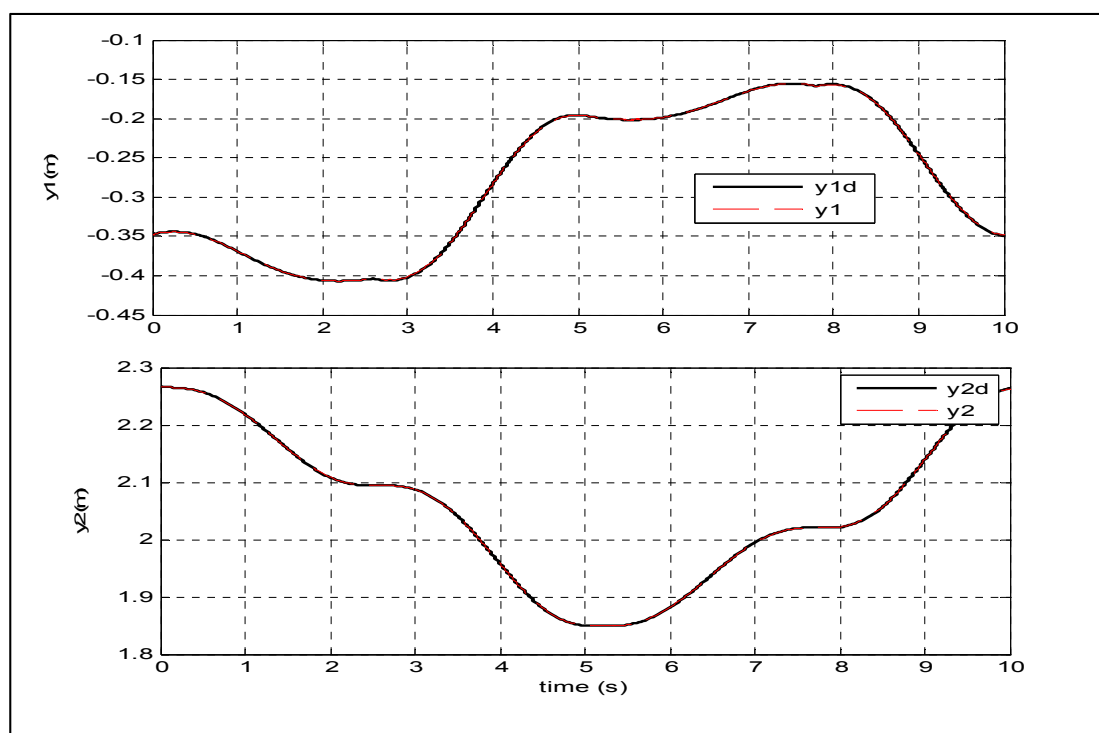
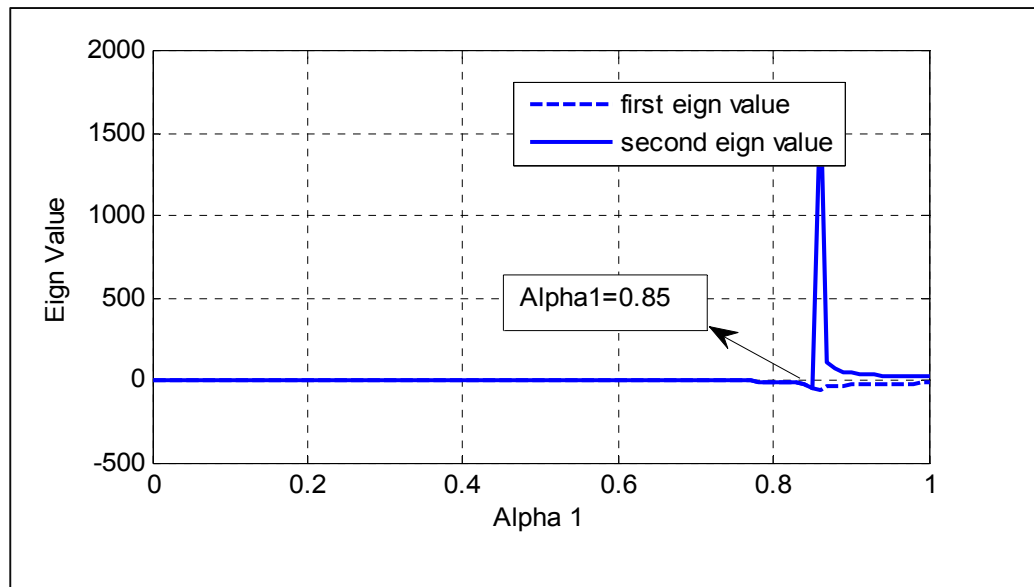


Figure 7.8 Stability of second link. (a) Nyquist diagram, and (b) eigenvalues evolution.
Tirée de (Fareh, Saad et Saad, 2013a)



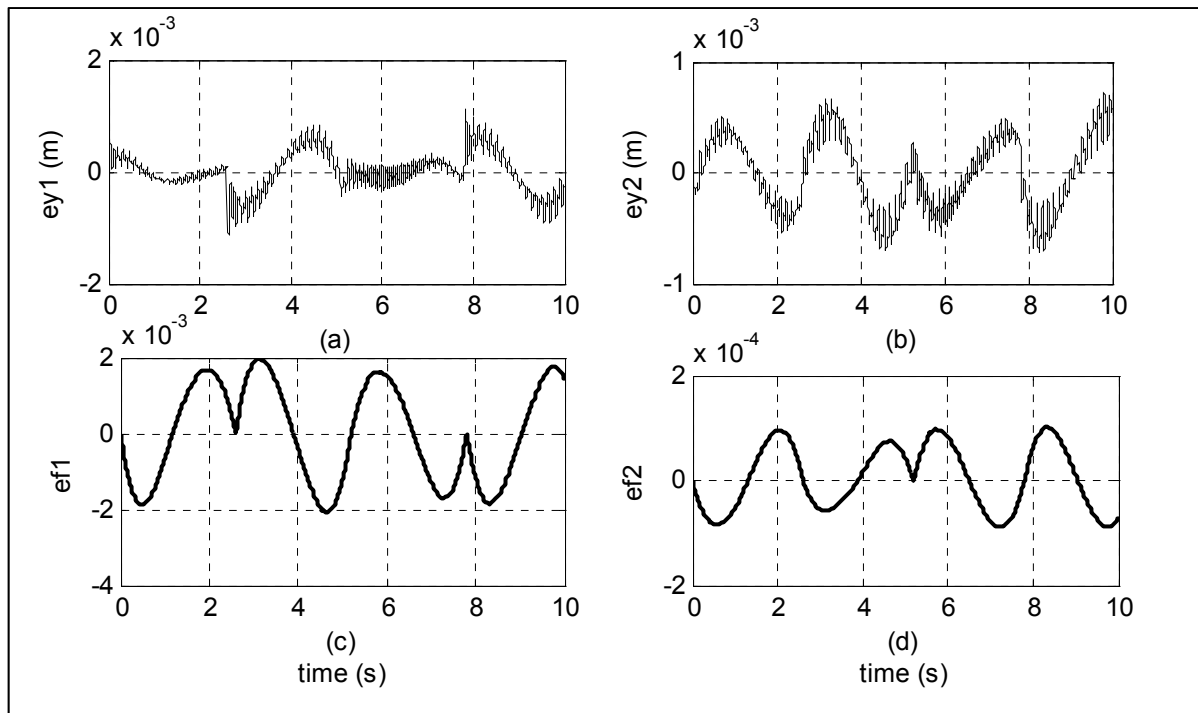


Figure 7.11. Tracking errors in joint space. (a)-(b) tracking errors of non-collocated outputs and (c)-(d) tracking errors of the flexible coordinates.

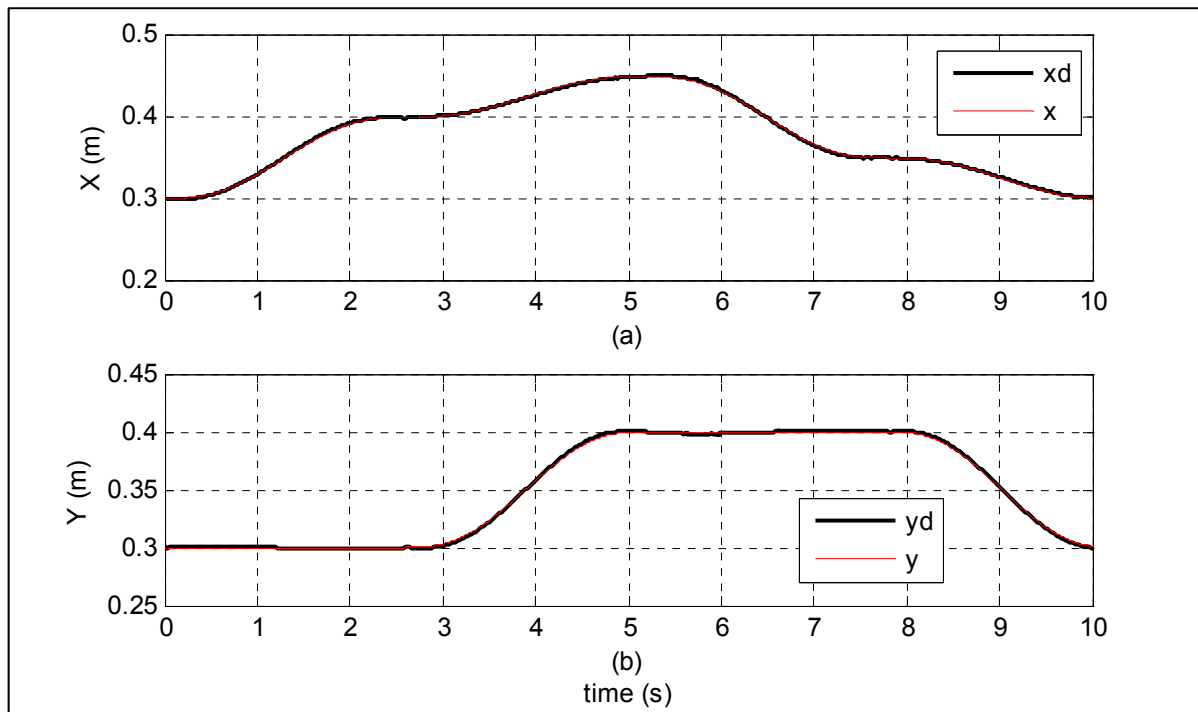


Figure 7.12. Tracking in the workspace. (a) x-position tracking and (b) y-position tracking.

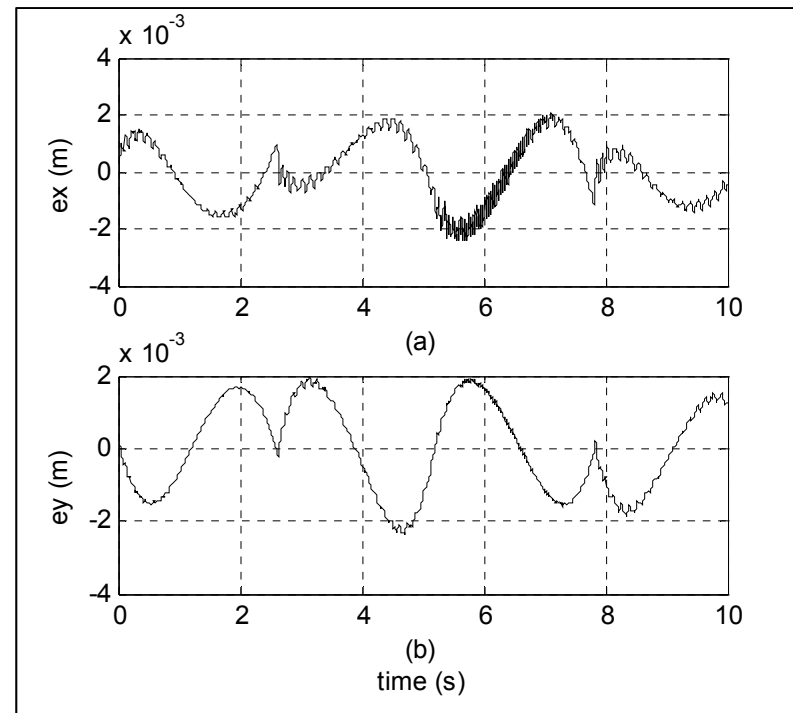


Figure 7.13. Workspace tracking errors. (a) x-position tracking errors and
(b) y-position tracking errors.

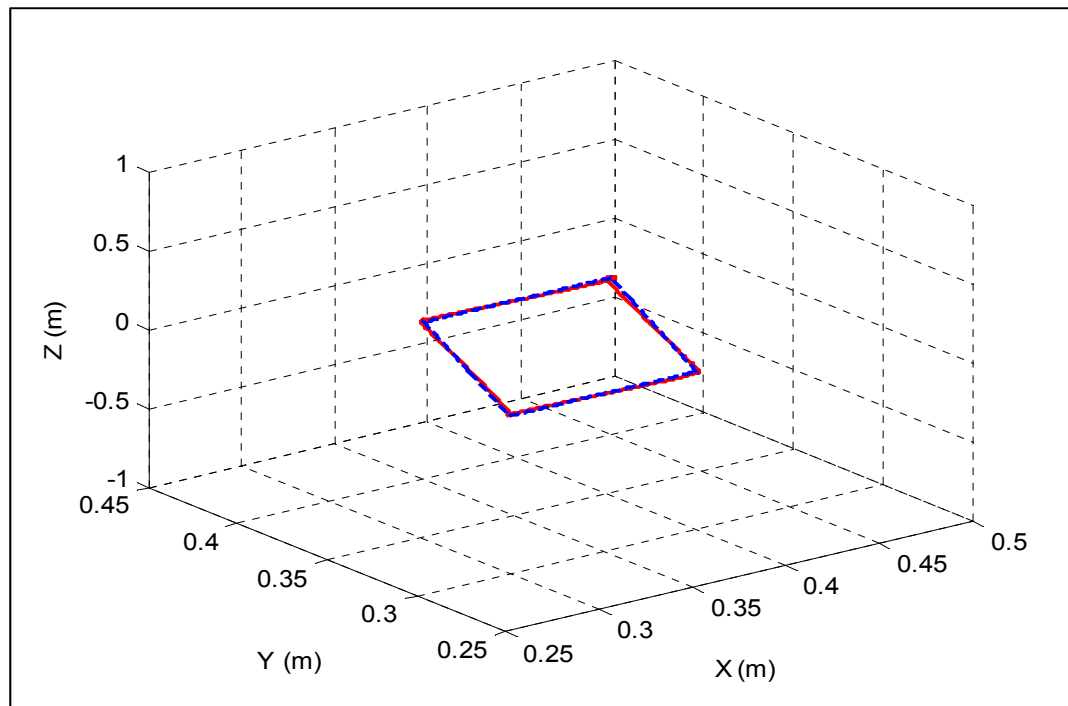


Figure 7.14. X-Y workspace tracking.

For two-flexible-link manipulators, the desired workspace trajectory is chosen as lozenge form. The results of the inverse kinematics problem are given in Figures 7.4-7.7. Workspace trajectory is shown in Figures 7.4-7.5, virtual space trajectories are given in Figure 7.6 and joint space trajectories are shown in Figure 7.7. According to simulation results, the workspace desired trajectory was well transformed to the joint space using the virtual space and the quasi-static approach. For the second subsystem, the Nyquist diagram and the evolution of eigenvalues of A_{f2} are given in Figure 7.8. For the first subsystem, the eigenvalues evolution of A_{f1} is given in Figure 7.9. Using the system parameters given in Table 7.1, the critical value of the second and first links are $\alpha_{2c} = 0.92$. and $\alpha_{1c} = 0.85$, respectively. The simulation results were obtained with $\alpha_2 = 0.9 < \alpha_{2c}$ and $\alpha_1 = 0.8 < \alpha_{1c}$. Note that these values satisfy the conditions given in equations (7.28) and (7.38). A good tracking performance of the new non-collocated output was obtained as shown in Figure 7.10. This tracking is confirmed by Figure 7.11 which shows the tracking error. In the workspace, a good tracking performance is shown in Figure 7.12 and the tracking error shown in Figure 7.13 doesn't exceed 2mm in x-position and y-position. The good tracking in the workspace is confirmed in Figure 7.14 that shows the tracking of the desired lozenge. Thus, we can conclude that the control strategy was effective to ensure the tracking of the non-collocated output and to reduce vibrations at the extremity; this explains the satisfactory results obtained using this approach.

7.7 Conclusion

This paper presents a nonlinear distributed control for two-flexible-link manipulator. For the inverse dynamics, a virtual space, linked with the workspace by a simple kinematics relation as in rigid manipulators, and a quasi-static approach were used. Using this transformation procedure, a workspace desired trajectory (lozenge) has been successfully transformed to the joint space. The distributed control strategy presented in this paper use the output redefinition technique and consists of stabilizing the flexible manipulators starting with the last joint and flexible link and going backward until the first joint and link. Lyapunov theory was used to

prove the asymptotical stability. An adaptive version of this control strategy will be investigated in future work.

7.8 Appendix

Proof of proposition 1

Using (7.3) and (7.5), the dynamical model can be written as follows:

$$\begin{bmatrix} M_{rr} & M_{rf} \\ M_{rf}^T & M_{ff} \end{bmatrix} \begin{bmatrix} \ddot{q}_r \\ \ddot{q}_f \end{bmatrix} + \begin{bmatrix} C_{rr} & C_{rf} \\ C_{rf}^T & C_{ff} \end{bmatrix} \begin{bmatrix} \dot{q}_r \\ \dot{q}_f \end{bmatrix} + \begin{bmatrix} 0 & 0 \\ 0 & D_{ff} \end{bmatrix} \begin{bmatrix} \dot{q}_r \\ \dot{q}_f \end{bmatrix} + \begin{bmatrix} 0 & 0 \\ 0 & K_{ff} \end{bmatrix} \begin{bmatrix} q_r \\ q_f \end{bmatrix} = \begin{bmatrix} I \\ 0 \end{bmatrix} \tau \quad (7.71)$$

Equation (7.71) can be written as:

$$M_{rr}\ddot{q}_r + M_{rf}\ddot{q}_f + C_{rr}\dot{q}_r + C_{rf}\dot{q}_f = \tau \quad (7.72)$$

$$M_{rf}^T\ddot{q}_r + M_{ff}\ddot{q}_f + C_{rf}^T\dot{q}_r + C_{ff}\dot{q}_f + D_{ff}\dot{q}_f + K_{ff}q_f = 0 \quad (7.73)$$

Using the outputs redefinition (7.29) and (7.40), we can write:

$$q_r = y - \alpha\beta q_f \quad (7.74)$$

where $q_r = [q_{r1} \quad q_{r2}]^T$; $q_f = [q_{f1} \quad q_{f2}]^T$; $y = [y_1 \quad y_2]^T$ and $\alpha\beta = \begin{bmatrix} \alpha_1\beta_1 & 0 \\ 0 & \alpha_2\beta_2 \end{bmatrix}$. Then,

the dynamical model becomes:

$$M_{rr}\ddot{y} + M_{rf}\ddot{q}_f + C_{rr}\dot{y} + C_{rf}\dot{q}_f = \tau \quad (7.75)$$

$$M_{rf}^T\ddot{y} + M_{ff}\ddot{q}_f + C_{rf}^T\dot{y} + C_{ff}\dot{q}_f + D_{ff}\dot{q}_f + K_{ff}q_f = 0 \quad (7.76)$$

where $\mathcal{M}_{rf} = M_{rf} - \alpha\beta M_{rr}$; $\mathcal{C}_{rf} = C_{rf} - \alpha\beta C_{rr}$; $\mathcal{M}_{ff} = M_{ff} - \alpha\beta M_{rf}^T$; $\mathcal{C}_{ff} = C_{ff} - \alpha\beta C_{rf}^T$;

Deducing \ddot{q}_f from (7.76), we get the following internal dynamics:

$$\ddot{q}_f = -\mathcal{M}_{ff}^{-1}(M_{rf}^T \ddot{y} + C_{rf}^T \dot{y} + \mathcal{C}_{ff} \dot{q}_f + D_{ff} \dot{q}_f + K_{ff} q_f) \quad (7.77)$$

Inserting (7.77) in (7.75), we obtain:

$$M_r^* \ddot{y} + C_r^* \dot{y} + \mathcal{C}_{rf}^* \dot{q}_f + D_f^* \dot{q}_f + K_f^* q_f = \tau \quad (7.78)$$

where $M_r^* = M_{rr} - \mathcal{M}_{rf} \mathcal{M}_{ff}^{-1} M_{rf}^T$; $C_r^* = C_{rr} - \mathcal{M}_{rf} \mathcal{M}_{ff}^{-1} C_{rf}^T$; $\mathcal{C}_{rf}^* = \mathcal{C}_{rf} - \mathcal{M}_{rf} \mathcal{M}_{ff}^{-1} \mathcal{C}_{ff}$; $D_f^* = -\mathcal{M}_{rf} \mathcal{M}_{ff}^{-1} D_{ff}$ and $K_f^* = -\mathcal{M}_{rf} \mathcal{M}_{ff}^{-1} K_{ff}$.

The models using the collocated output (7.3) and the new output (7.75)-(7.76) are linked by a non-singular positive transformation matrix as follows:

$$q_\alpha = \begin{bmatrix} q_r + \alpha\beta q_f \\ q_f \end{bmatrix} = Tq \quad (7.79)$$

where $q_\alpha = [y \quad q_f]^T$ and $T = \begin{bmatrix} 1 & \alpha\beta \\ 0 & 1 \end{bmatrix}$.

Using the transformation T, the mass matrix becomes:

$$M(q) = \begin{bmatrix} M_{rr}(q) & M_{rf}(q) \\ M_{rf}^T(q) & M_{ff}(q) \end{bmatrix} \xrightarrow{q_\alpha=Tq} \mathcal{M}(q_\alpha) = \begin{bmatrix} M_{rr}(q_\alpha) & \mathcal{M}_{rf}(q_\alpha) \\ M_{rf}^T(q_\alpha) & \mathcal{M}_{ff}(q_\alpha) \end{bmatrix} \quad (7.80)$$

where; $\mathcal{M}_{rf}(q_\alpha) = M_{rf}(q_\alpha) - \alpha\beta M_{rr}(q_\alpha)$ and $\mathcal{M}_{ff}(q_\alpha) = M_{ff}(q_\alpha) - \alpha\beta M_{rf}^T(q_\alpha)$, or in a matrix form:

$$\mathcal{M}(q_\alpha) = M(T^{-1}q_\alpha)T^{-1} \quad (7.81)$$

The parameter α is selected such that \mathcal{M} is positive definite matrix. Then, using **P1** and **P2**, \mathcal{M}_{rr} , \mathcal{M}_{ff} and \mathcal{M}_{ii} are positive definite matrices. The same transformation matrix can be used for the Coriolis matrix as follows:

$$\mathcal{C}(q_\alpha, \dot{q}_\alpha) = \mathcal{C}(T^{-1}q_\alpha, T^{-1}\dot{q}_\alpha)T^{-1} \quad (7.82)$$

$$\text{where } \mathcal{C}(q_\alpha) = \begin{bmatrix} \mathcal{C}_{rr} & \bar{\mathcal{C}}_{rf} \\ \mathcal{C}_{rf}^T & \bar{\mathcal{C}}_{ff} \end{bmatrix}; \mathcal{C}_{rf} = \mathcal{C}_{rf} - \alpha\beta\mathcal{C}_{rr} \text{ and } \mathcal{C}_{ff} = \mathcal{C}_{ff} - \alpha\beta\mathcal{C}_{rf}^T.$$

From **P4**, by multiplying (7.6) by a constant matrix T^{-1} , we can write:

$$X^T(\dot{\mathcal{M}}(q_\alpha) - 2\mathcal{C}(q_\alpha, \dot{q}_\alpha))X = 0 \quad \forall X \in \mathcal{R}^n \quad (7.83)$$

The Schur complement of the positive definite matrix \mathcal{M}_{ff} given by:

$$M_r^* = M_{rr} - \mathcal{M}_{rf}\mathcal{M}_{ff}^{-1}\mathcal{M}_{rf}^T \quad (7.84)$$

is positive (Bhatia, 2007). Then, from **P2**, the diagonal elements of M_r^* are also positive.

The Schur complement of \mathcal{C}_{ff} is given by the following equation:

$$C_r^* = \mathcal{C}_{rr} - \mathcal{C}_{rf}\mathcal{C}_{ff}^{-1}\mathcal{C}_{rf}^T \quad (7.85)$$

Using the dynamical model of the two-flexible-link manipulator (Fareh, Saad et Saad, 2013a), we can write:

$$X^T(\dot{M}_r^* - 2C_r^*)X = 0 \quad \forall X \in \mathcal{R}^n \quad (7.86)$$

Proof of proposition 2

In the following section, we study the error dynamics given by (7.57). In the first step, we investigate the following elements of the error dynamics: $[M_{rd}^*(Q)\ddot{y}^* - M_{rd}^*(q_\alpha)\ddot{y}]$, $[M_{rnd}^*(Q)\ddot{y}_d - M_{rnd}^*(q_\alpha)\ddot{y}]$, $[\mathcal{C}_r^*(Q, \dot{Q})\dot{y}_d - \mathcal{C}_r^*(q_\alpha, \dot{q}_\alpha)\dot{y}]$ and $[\mathcal{C}_{rf}^*(Q, \dot{Q})\dot{q}_f - \mathcal{C}_{rf}^*(q_\alpha, \dot{q}_\alpha)\dot{q}_f]$.

The first element is developed as:

$$\begin{aligned}
 & [M_{rd}^*(Q)\ddot{y}^* - M_{rd}^*(q_\alpha)\ddot{y}] \\
 &= \begin{bmatrix} M_{11}^*(Q_1) & 0 \\ 0 & M_{22}^*(Q_2) \end{bmatrix} \begin{bmatrix} \ddot{y}_1^* \\ \ddot{y}_2^* \end{bmatrix} - \begin{bmatrix} M_{11}^*(q_\alpha) & 0 \\ 0 & M_{22}^*(q_\alpha) \end{bmatrix} \begin{bmatrix} \ddot{y}_1 \\ \ddot{y}_2 \end{bmatrix} \\
 &= \begin{bmatrix} M_{11}^*(Q_1)\ddot{y}_1^* - M_{11}^*(q_\alpha)\ddot{y}_1 \\ M_{22}^*(Q_2)\ddot{y}_2^* - M_{22}^*(q_\alpha)\ddot{y}_2 \end{bmatrix}
 \end{aligned} \tag{7.87}$$

where $q_\alpha = [y_1 \ y_2 \ q_{f1} \ q_{f2}]^T$, $Q_1 = [y_1 \ q_{rd2} \ q_{f1} \ q_{fd2}]^T$,

$Q_2 = [q_{rd1} \ y_2 \ q_{fd1} \ q_{f2}]^T$ and $q_2 = [q_{r2} \ q_{f2}]^T$.

Using Taylor series, we can write:

$$\begin{aligned}
 M_{11}^*(q_\alpha) &= M_{11}^*(Q_1) + \frac{\partial M_{11}(q_\alpha)}{\partial q_2} \Big|_{q_{d2}} (q_2 - q_{d2}) + R_{M_{11}}(\tilde{q}_2) \\
 &= M_{11}^*(Q_1) - \frac{\partial M_{11}(q_\alpha)}{\partial q_{r2}} \Big|_{q_{rd2}} \tilde{q}_{r2} - \frac{\partial M_{11}(q_\alpha)}{\partial q_{f2}} \Big|_{q_{fd2}} \tilde{q}_{f2} + R_{M_{11}}(\tilde{q}_2) \\
 &= M_{11}^*(Q_1) - \delta M_{11}
 \end{aligned}$$

where

$$\delta M_{11} = \frac{\partial M_{11}(q_\alpha)}{\partial q_{r2}} \Big|_{q_{rd2}} \tilde{q}_{r2} + \frac{\partial M_{11}(q_\alpha)}{\partial q_{f2}} \Big|_{q_{fd2}} \tilde{q}_{f2} - R_{M_{11}}(\tilde{q}_2) \tag{7.88}$$

$R_{M_{11}}$ are the high order terms of the Taylor series for $M_{11}^*(q_\alpha)$. Then,

$$M_{11}^*(Q_1) = M_{11}^*(q_\alpha) + \delta M_{11} \tag{7.89}$$

The Taylor series is also applied to the following elements to obtain:

$$M_{rd}^*(Q) = M_{rd}^*(q_\alpha) + \delta M_{rd}^*$$

$$M_{rnd}^*(Q) = M_{rnd}^*(q_\alpha) + \delta M_{rnd}^*$$

$$C_r^*(Q, \dot{Q}) = C_r^*(q_\alpha, \dot{q}_\alpha) + \delta C_r^*$$

$$C_{rf}^*(Q, \dot{Q}) = C_{rf}^*(q_\alpha, \dot{q}_\alpha) + \delta C_{rf}^*$$

Then the previous elements in the error dynamics become:

$$M_{rd}^*(Q)\ddot{y}^* - M_{rd}^*(q_\alpha)\ddot{y} = M_{rd}^*(q_\alpha)[\ddot{y}^* - \ddot{y}] + \delta M_{rd}^*\ddot{y}^*$$

$$= M_{rd}^*(q_\alpha) \ddot{\tilde{y}} + \lambda M_{rd}^*(q_\alpha) \dot{\tilde{y}} + \delta M_{rd}^* \ddot{y}^*$$

$$[M_{rnd}^*(Q) \ddot{y}_d - M_{rnd}^*(q_\alpha) \ddot{y}] = M_{rnd}^*(q_\alpha) \ddot{\tilde{y}} + \delta M_{rnd}^* \ddot{y}_d$$

$$[C_r^*(Q, \dot{Q}) \dot{y}_d - C_r^*(q_\alpha, \dot{q}_\alpha) \dot{y}] = C_r^*(q_\alpha, \dot{q}_\alpha) \dot{\tilde{y}} + \delta C_r^* \dot{y}_d$$

Inserting these expressions into the error dynamics (7.57), they become:

$$\begin{aligned} K_p \tilde{y} + K_d \dot{\tilde{y}} + M_{rd}^*(q_\alpha) \ddot{\tilde{y}} + \lambda M_{rd}^*(q_\alpha) \dot{\tilde{y}} + M_{rnd}^*(q_\alpha) \ddot{\tilde{y}} + C_r^*(q_\alpha, \dot{q}_\alpha) \dot{\tilde{y}} + \delta M_{rd}^* \ddot{y}^* \\ + \delta M_{rnd}^* \ddot{y}_d + \delta C_r^* \dot{y}_d + \delta C_{rf}^* + \delta \tau = 0 \end{aligned} \quad (7.90)$$

Using the expression of $\delta \tau$ given in (7.51), the error dynamics become:

$$K_p \tilde{y} + K_d \dot{\tilde{y}} + M_r^*(q_\alpha) \ddot{\tilde{y}} + C_r^*(q_\alpha, \dot{q}_\alpha) \dot{\tilde{y}} + \lambda M_{rd}^*(q_\alpha) \dot{\tilde{y}} = 0 \quad (7.91)$$

CONCLUSIONS ET RECOMMANDATION

Cette thèse poursuivait les principaux objectifs suivants: i) proposer une stratégie de commande distribuée et robuste pour les manipulateurs rigides assurant la stabilité des erreurs de suivi; ii) modifier cette stratégie de commande pour tenir compte de la flexibilité des bras au niveau des manipulateurs flexibles en assurant la poursuite dans l'espace articulaire et cartésien.

Pour atteindre les objectifs visés, la modélisation des manipulateurs rigides et flexibles constitue une étape primordiale afin de déduire les principales propriétés à utiliser dans le développement des lois de commande. Premièrement, un modèle mathématique d'un manipulateur rigide à 7 ddl (ANAT) a été développé pour l'exploiter dans le développement de la commande distribuée et adaptative. Par la suite, nous avons développé un modèle mathématique d'un manipulateur à deux bras flexibles.

Pour développer une stratégie de commande distribuée assurant la stabilité de la dynamique des erreurs de suivi dans l'espace de travail des manipulateurs rigides, trois étapes ont été suivies; 1) utilisation de la cinématique inverse pour transformer la trajectoire désirée définie dans l'espace de travail vers l'espace articulaire; 2) développement d'une stratégie de commande distribuée pour assurer la stabilité de la dynamique des erreurs de suivi et 3) utilisation de la cinématique directe pour transformer la trajectoire obtenue dans l'espace articulaire vers l'espace de travail. Afin de faciliter l'implémentation en temps réel de la stratégie de commande, la dynamique du système a été mise sous forme d'un ensemble de sous-systèmes interconnectés, dont chacun représente une articulation. En commençant par la dernière articulation, une loi de commande est développée en supposant que le reste des articulations est stable. Cette démarche a été appliquée, au rebours, jusqu'au premier joint. La stabilité globale de tous les sous-systèmes a été prouvée par l'approche de Lyapunov. L'implémentation en temps réel de cette stratégie sur un manipulateur rigide à 7 ddl (ANAT) a montré un bon suivi de trajectoire désirée sous forme triangulaire. Cette stratégie a été

comparée avec celle du couple pré-calculé pour montrer son efficacité et son apport par rapport à une configuration classique.

Une version adaptative de la stratégie de commande distribuée, dite « hiérarchique », a ensuite été proposée pour assurer la robustesse de la loi de commande tout en suivant des trajectoires désirées dans l'espace de travail. Après la transformation de la trajectoire désirée de l'espace de travail vers l'espace articulaire via la cinématique inverse, la stratégie de commande adaptative a été ensuite développée à partir de la dernière articulation jusqu'au premier. Une seule commande par articulation est développée à chaque étape. La loi de commande du dernier sous système a été développée en utilisant juste les paramètres estimés existant dans l'équation de mouvement de la dernière articulation. La loi de commande de la $i^{\text{ème}}$ articulation dépend de ses propres paramètres estimés et celles de tous les sous-systèmes de niveau supérieur. Une implémentation à temps réel a été présentée pour un manipulateur à 7 ddl pour montrer l'efficacité et la performance de cette approche. Une comparaison avec la version non-adaptative a été également présentée.

La stratégie de commande déjà développée pour les manipulateurs rigides a été modifiée pour prendre en considération la flexibilité existant dans les manipulateurs à bras flexibles. Le premier objectif était le développement d'une commande distribuée pour assurer la stabilité de la dynamique des erreurs dans l'espace articulaire des manipulateurs flexibles. Le modèle dynamique a été réorganisé pour prendre la forme d'un ensemble de sous-systèmes interconnectés. Chaque sous-système est représenté par une articulation et son bras flexible associé. La stratégie de commande consiste à commander un seul sous-système à la fois en commençant par le dernier. En effet, le dernier sous-système est contrôlé en supposant que le reste des sous-systèmes sont stables. Puis, la même procédure est suivie au rebours jusqu'au premier sous-système. Cette stratégie de commande a été implantée en temps-réel sur un robot à deux bras flexibles. L'étude expérimentale a montré un bon suivi de trajectoire et une réduction des vibrations au niveau des bras flexibles. Une comparaison avec une commande PD a montré l'apport et l'efficacité de cette stratégie de commande par rapport à une configuration classique.

Pour assurer la robustesse de la loi de commande distribuée développée pour les manipulateurs flexibles, une commande adaptative indirecte a été développée pour suivre les trajectoires désirées dans l'espace articulaire et minimiser les vibrations au niveau des b. La loi de commande du dernier sous-système a été développée en utilisant les paramètres estimés existant dans l'équation de mouvement de ce système. En reculant vers l'arrière, la loi de commande du $i^{\text{ème}}$ sous-système est développée en fonction de ses propres paramètres estimés et les paramètres déjà estimés dans les sous-systèmes de niveaux supérieurs. La stabilité globale a été prouvée par l'approche de Lyapunov. Les résultats expérimentaux ont montré que cette commande adaptative assure un bon suivi de trajectoire dans l'espace articulaire et qu'elle est capable de minimiser les vibrations mieux que la version non-adaptative.

La stratégie de commande distribuée a été étendue pour assurer un suivi de trajectoire dans l'espace de travail pour un manipulateur à deux bras flexibles. Lors du contrôle de l'extrémité d'un manipulateur flexible, le système devient à non-minimum de phase et la dynamique interne n'est plus bornée. La technique de redéfinition de sortie a été utilisée pour sélectionner la sortie la plus proche possible de l'extrémité assurant une dynamique interne bornée. L'espace de travail et articulaire ne sont plus liés par une seule relation cinématique, comme le cas des manipulateurs rigides. Donc, la cinématique inverse n'est plus suffisante pour transformer les trajectoires désirées de l'espace de travail vers l'espace articulaire des manipulateurs flexibles. Un espace intermédiaire nommé « espace virtuel » a été défini pour résoudre le problème de l'inversion de la dynamique. Le modèle dynamique du manipulateur à deux bras flexibles a été organisé, dans un premier temps, pour prendre la forme de deux sous-systèmes interconnectés. Chaque sous-système contient une articulation et le bras flexible associé. En commençant par le deuxième sous-système, nous avons supposé que le premier sous-système est stable et une loi de commande basée sur l'approche de linéarisation par retour d'état a été développée. La loi de commande pour le premier sous-système a été développée en utilisant la même démarche.

Pour étudier la stabilité de la dynamique interne, le théorème de passivité est utilisé. En effet, la dynamique interne est divisée en deux parties: une partie linéaire en contre réaction une partie non linéaire. Avec ce genre des systèmes, la théorie de passivité permet d'étudier la stabilité généralisée du système et de démontrer sa convergence asymptotique, voir exponentielle et globale. La valeur critique du paramètre caractérisant la sortie paramétrisée a été déduite en utilisant la passivité de la dynamique interne. Juste la stabilité locale a été prouvée par cette stratégie de commande. Les résultats de simulation montrent un bon suivi de trajectoire dans l'espace de travail sous forme triangulaire. Afin d'assurer la stabilité globale des erreurs de suivi, la loi de commande distribuée développée pour les manipulateurs rigides a été modifiée et appliquée sur un robot à deux bras flexibles. La technique de redéfinition de sortie, l'espace virtuel et l'approche quasi-statique ont été utilisés pour résoudre les problèmes de déphasage non-minimal et de l'inversion de la dynamique. La théorie de Lyapunov a été utilisée pour démontrer la stabilité globale de la partie rigide et flexible. Un bon suivi de trajectoire sous forme d'un losange a été obtenu avec cette loi de commande.

Finalement nous pouvons conclure que la stratégie de commande développée, que ce soit pour les manipulateurs rigides ou flexibles, assure toujours la stabilité des erreurs de suivi et minimise les vibrations dans les bras flexibles.

Des limitations et des problèmes peuvent être soulevés dans cette thèse. Dans le cas des manipulateurs flexibles, le nombre de modes flexibles a été limité à un seul mode. Il est clair cependant que plus le nombre de modes flexibles augmente plus le modèle dynamique du manipulateur à bras flexible devient plus précis. L'augmentation du nombre de modes flexibles est fortement recommandable pour voir son effet sur la précision en utilisant la même stratégie de commande.

La stratégie de commande, assurant le suivi de trajectoire dans l'espace de travail, a été appliquée à un robot à deux bras flexibles. Une généralisation à plusieurs bras flexibles est toujours possible.

L'inversion de la dynamique du manipulateur flexible utilise l'approche quasi-statique qui néglige la vitesse et l'accélération de la dynamique flexible. Le développement d'autres approches, qui tiennent en compte la dynamique flexible, peut donner plus de précision lors de l'inversion de la dynamique.

Afin de rendre cette stratégie de commande plus utile pour l'industrie ou pour les robots de service, elle peut être modifiée pour l'appliquer à des manipulateurs mobiles. En effet, une nouvelle stratégie consiste à contrôler une plate-forme pour suivre une trajectoire bien définie afin d'amener le manipulateur à l'endroit de l'exécution de la tâche. Puis, la stratégie de commande distribuée peut être appliquée pendant la phase de manipulation tout en faisant une attention particulière au problème de la coordination de la plate-forme et du bras.

LISTE DE RÉFÉRENCES BIBLIOGRAPHIQUES

- Abiko, S., et K. Yoshida. 2005. « An adaptive control of a space manipulator for vibration suppression ». In *2005 IEEE/RSJ International Conference on Intelligent Robots and Systems*, 2-6 Aug. 2005. p. 2167-72. Piscataway, NJ, USA: IEEE.
- Aoustin, Y. 1994. « Experimental results for the end-effector control of a single flexible robotic arm ». *IEEE Transactions on Control Systems Technology*, vol. 2, n° 4, p. 371-381.
- Arnautovic, S. H., et A. J. Koivo. 1990. « Parameter adaptive control for redundant manipulators ». In *IEEE International Conference on Systems Engineering*. p. 304-307. New York, NY, USA.
- Asada, Haruhiko, et Jean-Jacques E. Slotine. 1986. *Robot analysis and control*. New York: J. Wiley, 266 p.
- Bartle, Robert Gardner, et Donald R. Sherbert. 2000. *Introduction to real analysis*, 3rd. New York: Wiley, 388 p.
- Bartolini, G., A. Ferrara et E. Usani. 1998. « Chattering avoidance by second-order sliding mode control ». *IEEE Transactions on Automatic Control*, vol. 43, n° 2, p. 241-246.
- Bhatia, Rajendra. 2007. *Positive definite matrices*. Coll. « Princeton series in applied mathematics ». Princeton, N.J.: Princeton University Press, 254 p.
- Bigras, P. 2003. « Convergence Analysis of an Inverse Flexible Manipulator Model Algorithm ». *Journal of Vibration and Control*, vol. 9, n° 10, p. 1141-1158.
- Bigras, P., M. Saad et J. O'Shea. 2001. « Robust trajectory control in the workspace of a class of flexible robots ». *Journal of Robotic Systems*, vol. 18, n° 6, p. 275-288.
- Bigras, Pascal. 1997. « Suivi de trajectoires dans l'espace de travail d'une classe de manipulateurs flexibles ». 224 p.
- Cannon, R. H., Jr., et E. Schmitz. 1984. « Initial experiments on the end-point control of a flexible one-link robot ». *International Journal of Robotics Research*, vol. 3, n° 3, p. 62-75.
- Canudas de Wit, Carlos A., Bruno Siciliano et G. Bastin. 1996. *Theory of robot control*. Coll. « Communications and control engineering ». Berlin ; New York: Springer, 392 p.
- Chan, T. M. 1995. « Point-to-point motion commands that eliminate residual vibration ». In *American Control Conference*. p. 909-915. Seattle, WA.

- Chen, Fang-Shiung, et Jung-Shan Lin. 2004. « Nonlinear backstepping design of robot manipulators with velocity estimation feedback ». In *2004 5th Asian Control Conference, July 20-23*. Vol. 1, p. 351-356. Melbourne, Australia.
- Cheong, Joono, Wankyun Chung et Youngil Youm. 2000. « Bandwidth modulation of rigid subsystem for the class of flexible robots ». In *IEEE International Conference on Robotics and Automation, April 24-28*. p. 1478-1483. San Francisco, CA, USA.
- Christoforou, E. G. 2000. « The control of flexible-link robots manipulating large payloads: Theory and experiments ». *Journal of Robotic Systems*, vol. 17, n° 5, p. 255-271.
- Colbaugh, R., et K. Glass. 1995. « Robust adaptive control of redundant manipulators ». *Journal of Intelligent and Robotic Systems: Theory and Applications*, vol. 14, n° 1, p. 69-88.
- Colbaugh, R., et K. Glass. 1996. « Decentralized adaptive control of electrically-driven manipulators ». *Computers & Electrical Engineering*, vol. 22, n° 6, p. 383-401.
- Colbaugh, R., H. Seraji et K. Glass. 1994. « Decentralized adaptive control of manipulators ». *Journal of Robotic Systems*, vol. 11, n° 5, p. 425-440.
- Coppel, W. A. 1965. *Stability and asymptotic behavior of differential equations*. Boston.
- Craig, John J. 2005. *Introduction to robotics : mechanics and control*, 3rd. Upper Saddle River, N.J.: Pearson/Prentice Hall, 400 p.
- Cuvillon, L. 2012. « A Mutivariable Methodology for Fast Visual Servoing of Flexible Manipulators Moving in a Restricted Workspace ». *Advanced robotics*, vol. 26, n° 15, p. 1771-1797.
- Dawson, D., M. Grabbe et F. L. Lewis. 1991. « Optimal control of a modified computed-torque controller for a robot manipulator ». *International Journal of Robotics & Automation*, vol. 6, n° 3, p. 161-165.
- De Luca, A. 1993. « Inversion-based nonlinear control of robot arms with flexible links ». *Journal of guidance, control, and dynamics*, vol. 16, n° 6, p. 1169-1176.
- De Luca, A., et G. Di Giovanni. 2001. « Rest-to-rest motion of a two-link robot with a flexible forearm ». In *IEEE/ASME International Conference on Advanced Intelligent Mechatronics, July 8-12* p. 929-935. Piscataway, NJ, USA.
- de Luca, A., et B. Siciliano. 1989. « Trajectory control of a nonlinear one-link flexible arm ». *International Journal of Control*, vol. 50, n° 5, p. 1699-1715.

- De Luca, A., et B. Siciliano. 1990. « Explicit dynamic modeling of a planar two-link flexible manipulator ». In *Proceedings of the 29th IEEE Conference on Decision and Control Part 6, December 5-7*. p. 528-530. Honolulu, HI, USA.
- De Luca, A., et B. Siciliano. 1991. « Closed-form dynamic model of planar multilink lightweight robots ». *IEEE Transactions on Systems, Man and Cybernetics*, vol. 21, n° 4, p. 826-839.
- De Luca, A., et B. Siciliano. 1993. « Regulation of flexible arms under gravity ». *IEEE Transactions on Robotics and Automation*, vol. 9, n° 4, p. 463-497.
- De Wit, C. C. 1996. *Theory of robot control*. New York, USA: Springer-Verlag.
- Fallaha, C.J., M. Saad, H.Y Kanaan et K. Haddad. 2011. « Sliding-mode robot control with exponential reaching law ». *IEEE Transactions on Industrial Electronics*, vol. 58, n° 2, p. 600-610.
- Fareh, R, M.R. Saad et M. Saad. 2012a. « Workspace distributed real-time control of rigid manipulators ». *Journal of Vibration and Control*.
- Fareh, R, M.R. Saad et M. Saad. 2012b. « Workspace tracking trajectory for 7-DOF ANAT robot using a hierarchical control strategy ». In *20th Mediterranean Conference on Control and Automation, July 3-6*. p. 122-127. Barcelona, Spain
- Fareh, R, M.R. Saad et M. Saad. 2012 «Hierarchical Adaptive Control for 3 DOF Manipulator Using Sliding Mode Technique, June 24-28 ». In *International Symposium on Intelligent Automation and Control*. p. 1-6. Puerto Vallarta, Mexico.
- Fareh, R, M.R. Saad et M. Saad. 2012 «Real time hierarchical control for 5 DOF redundant robot using sliding mode technique ». In *25th Annual Canadian Conference on Electrical & Computer Engineering*. p. 1-6. Montreal, Canada.
- Fareh, R, M.R. Saad et M. Saad. 2013a. « Workspace trajectory tracking control for two-flexible-link manipulator through output redefinition ». *Int. J. Modelling, Identification and Control* vol. 18, n° 2, p. 119-135.
- Fareh, R., M.R. Saad et M. Saad. 2009. « Adaptive control for a single flexible link manipulator using sliding mode technique ». In *6th International Multi-Conference on Systems, Signals and Devices, March 23-26* p. 1-6. Djerba, Tunisia.
- Fareh, R., M.R. Saad et M. Saad. 2012c. « Design and experimental validation of a hierarchical control strategy for 7 DOF manipulators ». In *38th Annual Conference of the IEEE Industrial Electronics Society (IECON), oct. 25-28*. p. 2680 - 2685 Montreal, Canada.

- Fareh, R., M.R. Saad et M. Saad. 2013b. « Tracking control of two-flexible-link manipulators using distributed control strategy, May 6-8 ». In *International Conference on Control, Decision and Information Technologies*. Hammamet, Tunisia (Accepted).
- Fareh, R., M.R. Saad, M. Saad et A. Brahmi. 2011. « Real time tracking trajectory in workspace for ANAT robot manipulator using hierarchical control, Dec. 11-14 ». In *18th IEEE International Conference on Electronics, Circuits and Systems*. p. 639-642. Beirut, Lebanon.
- Fei, Yue-nong, et Q. H. Wu. 2005. « Tracking control of robot manipulators via output feedback linearization ». *Journal of Shenzhen University Science & Engineering*, vol. 22, n° 3, p. 329-335.
- Fu, King Sun, Rafael C. Gonzalez et C. S. George Lee. 1987. *Robotics : control, sensing, vision, and intelligence*. New York: McGraw-Hill, 580 p.
- Galicki, M. 2006. « Adaptive control of kinematically redundant manipulator along a prescribed geometric path ». In *Robot Motion and Control*. p. 129-139. Berlin, Germany: Springer-Verlag.
- Hagn, U. 2008. « The DLR MIRO: a versatile lightweight robot for surgical applications ». *Industrial robot*, vol. 35, n° 4, p. 324-336.
- Harashima, Fumio, Hideki Hashimoto et Seiji Kondo. 1985. « Mosofet converter-fed position servo system with sliding mode control ». *IEEE transactions on industrial electronics and control instrumentation*, vol. 32, n° 3, p. 238-244.
- Hashimoto, H., K. Maruyama, Y. Arai et F. Harashima. 1986. « Practical realization of VSS controller for robotic arm ». In *International Conference on Industrial Electronics, Control and Instrumentation. I29 Sept.-3 Oct. .* p. 34-40. New York, NY, USA.
- Hirzinger, G., N. Sporer, M. Schedl, J. Butterfaß et M. Grebenstein. 2003. « Torque-controlled Light Weight Arms and Articulated Hands—Do We Reach Technological Limits Now? ». vol. 5, n° 2, p. 331-340.
- Hsia, T. C. S., T. A. Lasky et Z. Guo. 1991. « Robust independent joint controller design for industrial robot manipulators ». *IEEE Transactions on Industrial Electronics*, vol. 38, n° 1, p. 21-35.
- Hsu, S.H, et L.C Fu. 2003. « Globally adaptive decentralized control of time-varying robot manipulators ». In *IEEE International Conference on Robotics and Automation*. p. 1458-1463. Taipei, Taiwan.

- Hung, N. V. Q. 2008. « Adaptive control for nonlinearly parameterized uncertainties in robot manipulators ». *IEEE Transactions on Control Systems Technology*, vol. 16, n° 3, p. 458-468.
- Indrawanto, J. Swevers et H. Van Brussel. 1998. « Robust decentralized adaptive control of robot manipulators ». In *Proceedings of Symposium on Robot Control, Sept 3-5*. p. 215-220. Kidlington, UK.
- Irani, A. N., et H. A. Talebi. 2011. « Tip tracking of a rigid-flexible manipulator based on deflection estimation using neural network observer: A backstepping approach ». In *37th Annual Conference of the IEEE Industrial Electronics Society, IECON 2011, November 7-10*. p. 313-318. Melbourne, VIC, Australia.
- Isidori, Alberto. 1995. *Nonlinear control systems*, 3rd. Coll. « Communications and control engineering series ». Berlin: Springer-Verlag, 549 p.
- Jian-Qi, Wang, et H. D. Wend. 1999. « Robust decentralized control of robot manipulators ». *International Journal of Systems Science*, vol. 30, n° 3, p. 323-330.
- Katic, D., et M. Vukobratovic. 1994. « Contribution to the indirect decentralized adaptive control of manipulation robots ». *Journal of Intelligent and Robotic Systems: Theory and Applications*, vol. 9, n° 3, p. 235-251.
- Kelkar, A. G., et S. M. Joshi. 2004. « Control of elastic systems via passivity-based methods ». *Journal of Vibration and Control*, vol. 10, n° 11, p. 1699-735.
- Khalil, Hassan K. 1996. *Nonlinear systems*, 2nd. Upper Saddle River, N.J.: Prentice-Hall, 734 p.
- Khalil, Hassan K. 2002. *Nonlinear systems*, 3rd. Upper Saddle River, N.J.: Prentice Hall, 750 p.
- Khalil, Wisama, et E. Dombre. 1999. *Modélisation, identification et commande des robots*, 2e éd. revue et augm. Coll. « Robotique ». Paris: Hermès Science Publications, 503 p.
- Khorrami, F. 1993. « Experimental results on active control of flexible-link manipulators with embedded piezoceramics ». In *Proceedings IEEE International Conference on Robotics and Automation*. p. 222-227.
- Krstic, M. 2004. « Feedback linearizability and explicit integrator forwarding controllers for classes of feedforward systems ». *IEEE Transactions on Automatic Control*, vol. 49, n° 10, p. 1668-1682.

- Kwon, S. J. 2006. « Robust Kalman filtering with perturbation estimation process for uncertain systems ». *IEE Proceedings-Control Theory and Applications*, vol. 153, n° 5, p. 600-606.
- Lanari, L. 1992. « Asymptotically stable set point control laws for flexible robots ». *Systems & control letters*, vol. 19, n° 2, p. 119-129.
- Le Boudec, B., M. Saad et V. Nerguizian. 2006. « Modeling and adaptive control of redundant robots ». *Mathematics and Computers in Simulation*, vol. 71, n° 4, p. 395-403.
- Li, Q., S. K. Tso et A. N. Poo. 1998. « Enhanced computed-torque control algorithm for robot manipulators ». *Proceedings of the Institution of Mechanical Engineers. Part I, Journal of systems and control engineering*, vol. 212, n° 1, p. 11-15.
- Lih-Chang, Lin, et Yeh Sy-Lin. 1996. « A composite adaptive control with flexible quantity feedback for flexible-link manipulators ». *Journal of Robotic Systems*, vol. 13, n° 5, p. 289-302.
- Lotfazar, A., et M. Eghtesad. 2007a. « Application and comparison of passivity-based and integrator backstepping control methods for trajectory tracking of rigid-link robot manipulators incorporating motor dynamics ». *International Journal of Robotics and Automation*, vol. 22, n° 3, p. 196-205.
- Lotfazar, A., et M. Eghtesad. 2007b. « Passivity-based and integrator backstepping control methods for trajectory tracking of rigid-link robot manipulators incorporating motor dynamics ». *International Journal of Robotics & Automation*, vol. 22, n° 3, p. 196-205.
- Man, Z., S. Khoo, X. Yu, C. Miao, J. Jin et F. Tay. 2011. « A new design of sliding mode control systems ». *Lecture Notes in Control and Information Sciences*, vol. 412, p. 151-167.
- Meckl, P. H. 1994. « Robust motion control of flexible systems using feedforward forcing functions ». *IEEE Transactions on Control Systems Technology*, vol. 2, n° 3, p. 245-254.
- Middleton, R. H. 1988. « Adaptive computed torque control for rigid link manipulations ». *Systems & control letters*, vol. 10, n° 1, p. 9-16.
- Moallem, M., R. V. Patel et K. Khorasani. 2001a. « Nonlinear tip-position tracking control of a flexible-link manipulator: theory and experiments ». *Automatica*, vol. 37, n° 11, p. 1825-34.

- Moallem, M., R. V. Patel et K. Khorasani. 2001b. « Nonlinear tip-position tracking control of a flexible-link manipulator: theory and experiments ». *Automatica*, vol. 37, n° 11, p. 1825-1834.
- Mosayebi, M. 2012. « A Nonlinear High Gain Observer Based Input-Output Control of Flexible Link Manipulator ». *Mechanics research communications*, vol. 45, p. 34-41.
- Mu, Xiaojiang. 2011. « Sliding mode control based on self-organized fuzzy neural networks for multi-link robots ». In *2nd International Conference on Intelligent Control and Information Processing*. p. 415-419. Harbin, China.
- Ortega, R. 1989. « Adaptive motion control of rigid robots: A tutorial ». *Automatica*, vol. 25, n° 6, p. 1575-1584.
- Ortega, Romeo. 1998. *Passivity-based control of Euler-Lagrange systems : mechanical, electrical and electromechanical applications*. Coll. « Communications and control engineering ». New York, : Springer-Verlag., 543 p.
- Osman, J. H. S., et P. D. Roberts. 1994. « Decentralized and hierarchical control of a class of robot manipulators ». *Proceedings of the Institution of Mechanical Engineers*, vol. 208, n° 13, p. 139-148.
- Parra-Vega, V., et G. Hirzinger. 2001. « Chattering-free sliding mode control for a class of nonlinear mechanical systems ». *International journal of robust and nonlinear control*, vol. 11, n° 12, p. 1161-1178.
- Pfeiffer, F. 1989. « A feedforward decoupling concept for the control of elastic robots ». *Journal of Robotic Systems*, vol. 6, n° 4, p. 407-416.
- Pfeiffer, F., et B. Gebler. 1988. « A multistage-approach to the dynamics and control of elastic robots ». In *Proceedings of the 1988 IEEE International Conference on Robotics and Automation, April 24-29*. p. 2-8. Washington, DC, USA.
- Saad, M., L. Saydy et O. Akhrif. 2000a. « Noncollocated passive transfer functions for a flexible link robot ». In *IEEE International Conference on Control Applications, sept. 25-27*. p. 971-975. Piscataway, NJ, USA.
- Saad, M., L. Saydy et O. Akhril. 2000. « Robust noncollocated passive models of a flexible link with uncertain payload and joint inertia ». In *7th IEEE International Conference on Electronics, Circuits and Systems, Dec 17-20*. p. 713-716. Piscataway, NJ, USA.
- Saad, M.R., J. Piedbuf, O. Akhrif et L. Saydy. 2006. « Modal analysis of assumed-mode models of flexible slewing beam ». *International Journal of Modelling, Identification and Control*, vol. 1, n° 4, p. 325-337.

- Saad, Mohamad. 2004. « Modelisation et passivite d'un systeme a un bras flexible ». Canada, Ecole Polytechnique, Montreal (Canada), 200 p.
- Saad, Mohamad, Lahcen Saydy et Ouassima Akhrif. 2000b. « Passivity-based control of a flexible link robot ». In *CCECE 2000-Canadian Conference on Electrical and Computer Egineering, May 7-10*. p. 118-123. Nova Scotia, NS, Can.
- Sadati, N., et E. Elhamifar. 2005. « Adaptive fuzzy decentralized control of robot manipulators ». In *International Conference on Industrial Electronics and Control Applications*. p. 1-6. Quito, Ecuador.
- Salehi, M., et G. Vossoughi. 2008. « Impedance control of flexible base mobile manipulator using singular perturbation method and sliding mode control law ». *International Journal of Control, Automation, and Systems*, vol. 6, n° 5, p. 677-688.
- Sciavicco, L., et Bruno Siciliano. 2000. *Modelling and control of robot manipulators*, 2nd. Coll. « Advanced textbooks in control and signal processing ». London ; New York: Springer, 377 p.
- Seraji, H. 1988. « Adaptive independent joint control of manipulators: theory and experiment ». In *IEEE International Conference on Robotics and Automation, April 24-29*. p. 854-861. Washington, DC, USA.
- Siciliano, B., et W. J. Book. 1988. « A singular perturbation approach to control of lightweight flexible manipulators ». *International Journal of Robotics Research*, vol. 7, n° 4, p. 79-90.
- Siciliano, Bruno, et Oussama Khatib (1611). 2008. *Springer Handbook of Robotics*.
- Slotine, J. J. E., et J. A. Coetsee. 1986. « Adaptive sliding controller synthesis for non-linear systems ». *International Journal of Control*, vol. 43, n° 6, p. 1631-1651.
- Slotine, J. J. E., et Weiping Li. 1991. *Applied nonlinear control*. Englewood Cliffs, N.J.: Prentice-Hall, 459 p.
- Slotine, J. J. E., et Li Weiping. 1987. « On the adaptive control of robot manipulators ». *International Journal of Robotics Research*, vol. 6, n° 3, p. 49-59.
- Spong, Mark W., et M. Vidyasagar. 1989. *Robot dynamics and control*. New York: J. Wiley, 336 p.
- Subudhi, B. 2005. « On the singular perturbation approach to trajectory control of a multilink manipulator with flexible links and joints ». *Proceedings of the Institution of Mechanical Engineers. Part I, Journal of systems and control engineering*, vol. 215, n° 6, p. 587-598.

- Sun, D. 2002. « Control of a rotating cantilever beam using a torque actuator and a distributed piezoelectric polymer actuator ». *Applied acoustics*, vol. 63, n° 8, p. 885-899.
- Talebi, H. A., K. Khorasani et R. V. Patel. 1999. « Experimental results on tracking control of a flexible-link manipulator: a new output re-definition approach ». *IEEE International Conference on Robotics and Automation*, p. 1090-1095.
- Tatlicioglu, E., D. Braganza, T. C. Burg et D. M. Dawson. 2009. « Adaptive control of redundant robot manipulators with sub-task objectives ». *Robotica*, vol. 27, n° 6, p. 873-881.
- Truckenbrodt, A. 1982. « Truncation problems in the dynamics and control of flexible mechanical systems ». In *Proceedings of the Eighth Triennial World Congress of the International Federation of Automatic Control, Aug 24-28* p. 1909-1914. Oxford, UK.
- Utkin, Vadim I. 1993. « Sliding mode control design principles and applications to electric drives ». *IEEE Transactions on Industrial Electronics*, vol. 40, n° 1, p. 23-36.
- Vukobratovic, M., et B. Karan. 1996. « Experiments with fuzzy logic robot control with model-based dynamic compensation in nonadaptive decentralized control scheme ». *International Journal of Robotics & Automation*, vol. 11, n° 3, p. 118-131.
- Wang, D. 1991. « Transfer functions for a single flexible link ». *The international journal of robotics research*, vol. 10, n° 5, p. 540-549.
- Wang, D. 1992. « Passive control of a stiff flexible link ». *The international journal of robotics research*, vol. 11, n° 6, p. 572-578.
- Wang, D., et M. Vidyasagar. 1991. « Control of a class of manipulators with a single flexible link. II. Observer-controller stabilization ». *Transactions of the ASME. Journal of Dynamic Systems, Measurement and Control*, vol. 113, n° 4, p. 662-668.
- Wang, Dalong, Youfang Lu, Yan Liu et Xiaoguang Li. 1996. « Dynamic model and tip trajectory tracking control for a two-link flexible robotic manipulator ». In *Proceedings of IEEE International Conference on Systems, Man and Cybernetics, 14-17 Oct. 1996*. Vol. vol.2, p. 1020-4. New York, NY, USA: IEEE.
- Xu, L.J., J. Wu et S. Liang. 2000. « Adaptive control of redundant variable geometry truss manipulators based on fuzzy neural network ». *Robot*, vol. 22, n° 6, p. 495-500.

- Yang, H., H. Krishnan et M. H. Ang Jr. 1999. « Tip-trajectory tracking control of single-link flexible robots via output redefinition ». *Proceedings - IEEE International Conference on Robotics and Automation*, vol. 2, p. 1102-1107.
- Yang, Z. J., K. Miyazaki, S. Kanae et K. Wada. 2004. « Robust position control of a magnetic levitation system via dynamic surface control technique ». *IEEE Transactions on Industrial Electronics*, vol. 51, n° 1, p. 26-34.
- Yim, W., et S. N. Singh. 1993. « Feedback linearization of differential-algebraic systems and force and position control of manipulators ». In *American Control Conference*. p. 2279-2283. Evanston.
- Zhang, Fuzhen. 2005. *The Schur complement and its applications / [ressource électronique]*. Coll. « Numerical methods and algorithms ». New York: Springer, 295 p.
- Zhang, Y. 2009. « Neuro-Sliding-Mode Control of Flexible-Link Manipulators Based on Singularly Perturbed Model ». *Tsinghua Science and Technology*, vol. 14, n° 4, p. 444-451.
- Zhenhua, Qin, et He Xiongxiong. 2011. « A robust terminal sliding mode adaptive control for robot manipulators ». *Advanced Materials Research*, vol. 204-210, p. 1978-83.

ANNEXE

Dans cette section, on présente quelques détails pour démontrer quelques propositions données dans le Chapitre 6.

Détails pour Proposition 6.2

Le système précédent est passif si on prend la sortie l'erreur de la vitesse $\dot{y}_{\alpha 2}$ et l'entrée δu_2 .

Pour démontrer cette passivité soit la fonction d'énergie suivante :

$$V(\tilde{x}) = \frac{1}{2} \tilde{x}_3^2 \Rightarrow \dot{V}(\tilde{x}) = \tilde{x}_3 \dot{\tilde{x}}_3 = \delta u_2 \dot{y}_{\alpha 2} \quad (1)$$

Donc : $\int \delta u_2 \dot{y}_{\alpha 2} = V(\tilde{x}) \geq 0$

La propriété de passivité est conservée avec la loi de commande suivant :

$$\delta u_2 = -K_p \tilde{y}_{\alpha 2} + \delta v = -K_p \tilde{x}_1 + \delta v \quad (2)$$

En choisissant la fonction d'énergie suivante :

$$V(\tilde{x}) = \frac{1}{2} \tilde{x}_3^2 + \frac{1}{2} K_p \tilde{x}_1^2 \quad (3)$$

La dérivée de cette fonction d'énergie est donnée par :

$$\begin{aligned} \dot{V}(\tilde{x}) &= \tilde{x}_3 \dot{\tilde{x}}_3 + K_p \tilde{x}_1 \dot{\tilde{x}}_1 \\ &= \tilde{x}_3 \dot{\tilde{x}}_3 + K_p \tilde{x}_1 \tilde{x}_3 \\ &= \tilde{x}_3 (\dot{\tilde{x}}_3 + K_p \tilde{x}_1) \\ &= \tilde{x}_3 (\delta u_2 + K_p \tilde{x}_1) \\ &= \tilde{x}_3 \delta v \\ &= \delta v \dot{y}_{\alpha 2} \end{aligned}$$

Donc :

$$\int \delta u_2 \dot{y}_{\alpha 2} = V(\tilde{x}) \geq 0 \quad (4)$$

Par la suite, le système $(\delta v, \tilde{x}_3)$ est toujours passif.

En choisissant, la loi de commande suivante :

$$u_2 = -K_p \tilde{y}_{\alpha 2} - K_d \dot{\tilde{y}}_{\alpha 2} + \delta v \quad (5)$$

où K_p et $K_d \geq 0$.

La relation entre l'entrée δv et la sortie $\dot{\tilde{y}}_{\alpha 2}$ devient strictement passive à la sortie. En effet, soit la fonction d'énergie suivante :

$$V(\tilde{x}) = \frac{1}{2} \tilde{x}_1^2 + \frac{1}{2} K_p \tilde{x}_1^2 + \frac{1}{2} \tilde{x}_3^2 \geq 0 \quad (6)$$

la dérivée de cette fonction est donnée par l'expression suivante :

$$\begin{aligned} \dot{V}(\tilde{x}) &= \tilde{x}_1 \dot{\tilde{x}}_1 + K_p \tilde{x}_1 \dot{\tilde{x}}_1 + \tilde{x}_3 \dot{\tilde{x}}_3 \\ &= \tilde{x}_1 \dot{\tilde{x}}_1 + K_p \tilde{x}_1 \tilde{x}_3 + \tilde{x}_3 \delta u_2 \\ &= \tilde{x}_1 \dot{\tilde{x}}_1 + K_p \tilde{x}_1 \tilde{x}_3 + \tilde{x}_3 (-K_p \tilde{x}_1 - K_d \tilde{x}_3 + \delta v) \\ &= \tilde{x}_1 \dot{\tilde{x}}_1 - K_d \tilde{x}_3^2 + \dot{\tilde{y}}_{\alpha 2} \delta v \end{aligned}$$

Donc :

$$\int \tilde{x}_1 \dot{\tilde{x}}_1 - \int K_d \tilde{x}_3^2 + \int \delta v \dot{\tilde{y}}_{\alpha 2} = V(\tilde{x}) \geq 0 \quad (7)$$

On peut écrire donc :

$$\int \delta v \dot{\tilde{y}}_{\alpha 2} \geq K_d \int \dot{\tilde{y}}_{\alpha 2}^2 + \beta \text{ avec } \beta = -\frac{1}{2} \tilde{x}_1^2 \in \mathcal{R} \quad (8)$$

D'où le système est strictement passif à la sortie.

Donc, d'après (Ortega 1998) les erreurs de la position $\tilde{y}_{\alpha 2}$ et la vitesse $\dot{\tilde{y}}_{\alpha 2} \rightarrow 0$ quand $t \rightarrow \infty$.

Détails pour Proposition 6.3

Après la stabilisation de la partie rigide, on choisit maintenant α_2 pour que la dynamique flexible devienne asymptotiquement stable.

Le point d'équilibre du système $\tilde{x} = 0$ est asymptotiquement stable si le système est (Khalil, 1996):

- i. Strictement passif à la sortie, et;
- ii. Déetectable.

La première condition est déjà vérifiée dans la section précédente et pour tester la détectabilité du système, on vérifie la stabilité asymptotique du point d'équilibre en annulant l'entrée et la sortie de la dynamique de la partie flexible suivante :

$$\tilde{x}_f = \begin{bmatrix} \tilde{x}_{f1} \\ \tilde{x}_{f2} \end{bmatrix} = \begin{bmatrix} \tilde{q}_{f1} \\ \dot{\tilde{q}}_{f2} \end{bmatrix} \Rightarrow \begin{cases} \dot{\tilde{x}}_{f1} = \tilde{x}_{f2} \\ \dot{\tilde{x}}_{f2} = -\bar{K}_{f2}\tilde{x}_{f1} - \bar{D}_{f2}\tilde{x}_{f2} - [b_{551} - \alpha_2\beta_2 b_{251}]^{-1}\psi(t, y) \end{cases} \quad (9)$$

Avec $y = C_f^T \tilde{x}_f = [-\alpha_2\beta_2 \quad 0] \begin{bmatrix} \tilde{q}_{f2} \\ \dot{\tilde{q}}_{f2} \end{bmatrix}$

$$\begin{aligned} \psi(t, y) = & (h_{501}\dot{q}_{rd1}^2 + b_{153}t_{11}q_{fd1})[\sin(C_\alpha^T q_{d2}) - \sin(C_\alpha^T q_{d2} - y)] \\ & + b_{152}[\cos(C_\alpha^T q_{d2}) - \cos(C_\alpha^T q_{d2} - y)] \\ & + h_{504}t_{11}q_{fd1}\dot{q}_{rd1}\{\dot{q}_{rd2} \cos(q_{rd2}) - \dot{q}_{r2} \cos(q_{r2})\} \end{aligned}$$

Soit :

$$a(t) = h_{501}\dot{q}_{rd1}^2 + b_{153}t_{11}q_{fd1}$$

$$b(t) = b_{152}$$

$$c(t) = h_{504}t_{11}q_{fd1}\dot{Q}_{d1}$$

En utilisant le développement de Taylor :

$$f(x, y) = f(a, b) + \frac{\partial f}{\partial x}(a, b)[x - a] + \frac{\partial f}{\partial y}(a, b)[y - b]$$

Soit $x = q_{r2}; y = \dot{q}_{r2}; a = q_{rd2}$ et $b = \dot{q}_{rd2}$

$$\begin{aligned} \dot{q}_{r2} \cos(q_{r2}) &= \dot{q}_{rd2} \cos(q_{rd2}) - \dot{q}_{rd2} \sin(q_{rd2})(q_{r2} - q_{rd2}) + \cos(q_{rd2})(\dot{q}_{r2} - \dot{q}_{rd2}) \\ &= \dot{q}_{rd2} \cos(q_{rd2}) + \dot{q}_{rd2} \sin(q_{rd2})\tilde{q}_{r2} + \cos(q_{rd2})\dot{\tilde{q}}_{r2} \end{aligned}$$

$$\begin{aligned}
&= \dot{q}_{rd2} \cos(q_{rd2}) + \dot{q}_{rd2} \sin(q_{rd2}) \tilde{y}_{\alpha 2} + \cos(q_{rd2}) \dot{\tilde{y}}_{\alpha 2} \\
&\quad - \alpha_2 \beta_2 \dot{q}_{rd2} \sin(q_{rd2}) \tilde{q}_{f2} - \alpha_2 \beta_2 \cos(q_{rd2}) \dot{\tilde{q}}_{f2}
\end{aligned}$$

En plus, on a :

$$\begin{aligned}
\tilde{q}_{r2} &= q_{rd2} - q_{r2} = (y_{ad2} - \alpha_2 \beta_2 q_{fd2}) - (y_{\alpha 2} - \alpha_2 \beta_2 q_{f2}) = \tilde{y}_{\alpha 2} - \alpha_2 \beta_2 \tilde{q}_{f2} \\
\dot{\tilde{q}}_{r2} &= \dot{q}_{rd2} - \dot{q}_{r2} = (\dot{y}_{ad2} - \alpha_2 \beta_2 \dot{q}_{fd2}) - (\dot{y}_{\alpha 2} - \alpha_2 \beta_2 \dot{q}_{f2}) = \dot{\tilde{y}}_{\alpha 2} - \alpha_2 \beta_2 \dot{\tilde{q}}_{f2}
\end{aligned}$$

Donc :

$$\begin{aligned}
&\dot{q}_{rd2} \cos(q_{rd2}) - \dot{q}_{r2} \cos(q_{r2}) \\
&= -\dot{q}_{rd2} \sin(q_{rd2}) \tilde{y}_{\alpha 2} - \cos(q_{rd2}) \dot{\tilde{y}}_{\alpha 2} + \alpha_2 \beta_2 \dot{q}_{rd2} \sin(q_{rd2}) \tilde{q}_{f2} \\
&\quad + \alpha_2 \beta_2 \cos(q_{rd2}) \dot{\tilde{q}}_{f2}
\end{aligned} \tag{9}$$

Or, à partir de la section précédente on a $\tilde{y}_{\alpha 2}, \dot{\tilde{y}}_{\alpha 2} \rightarrow 0$ quand $t \rightarrow \infty$.

Donc :

$$\begin{aligned}
\psi(t, y) &= a(t)[\sin(C_\alpha^T q_{d2}) - \sin(C_\alpha^T q_{d2} - y)] + b(t)[\cos(C_\alpha^T q_{d2}) - \cos(C_\alpha^T q_{d2} - y)] \\
&\quad + c(t)\{\alpha_2 \beta_2 \dot{q}_{rd2} \sin(q_{rd2}) \tilde{q}_{f2} + \alpha_2 \beta_2 \cos(q_{rd2}) \dot{\tilde{q}}_{f2}\} \\
&= \alpha_2 \beta_2 \dot{q}_{rd2} c(t) \sin(q_{rd2}) \tilde{q}_{f2} + \alpha_2 \beta_2 c(t) \cos(q_{rd2}) \dot{\tilde{q}}_{f2} + \psi_1(t, y)
\end{aligned}$$

Avec :

$$\begin{aligned}
\psi_1(t, y) &= a(t)[\sin(C_\alpha^T q_{d2}) - \sin(C_\alpha^T q_{d2} - y)] \\
&\quad + b(t)[\cos(C_\alpha^T q_{d2}) - \cos(C_\alpha^T q_{d2} - y)]
\end{aligned} \tag{10}$$

$$\psi_1(t, y) = a(t)[\sin(C_\alpha^T q_{d2}) - \sin(C_\alpha^T q_{d2} - y)] + b(t)[\cos(C_\alpha^T q_{d2}) - \cos(C_\alpha^T q_{d2} - y)]$$

Or, on a :

$$\sin(C_\alpha^T q_{d2}) - \sin(C_\alpha^T q_{d2} - y) = 2 \cos(C_\alpha^T q_{d2} - y/2) \sin(y/2)$$

$$\cos(C_\alpha^T q_{d2}) - \cos(C_\alpha^T q_{d2} - y) = -2 \sin(C_\alpha^T q_{d2} - y/2) \sin(y/2)$$

Donc :

$$\psi_1(t, y) = 2a(t) \cos(C_\alpha^T q_{d2} - y/2) \sin(y/2) - 2b(t) \sin(C_\alpha^T q_{d2} - y/2) \sin(y/2)$$

Cette dynamique peut être mise sous la forme suivante :

$$\begin{aligned}\dot{\tilde{x}}_f &= \begin{bmatrix} 0 & 1 \\ -a_0(t) & -a_1(t) \end{bmatrix} \tilde{x}_f - \left[[b_{551} - \alpha_2 \beta_2 b_{251}]^{-1} \right] \psi_1(t, y) \\ &= A_f(t) \tilde{x}_f - B_f \psi_1(t, y)\end{aligned}\quad (11)$$

$$\text{Avec : } a_0(t) = [b_{551} - \alpha_2 \beta_2 b_{251}]^{-1} (K_{f2} - \alpha_2 \beta_2 \dot{q}_{rd2} c(t) \sin(q_{rd2}))$$

$$a_1(t) = [b_{551} - \alpha_2 \beta_2 b_{251}]^{-1} (D_{f2} - \alpha_2 \beta_2 c(t) \cos(q_{rd2}))$$

Il existe une valeur critique de α_{c2} pour laquelle le point d'équilibre $\tilde{x}_f = 0$ soit asymptotiquement stable.

La dynamique précédente peut être mise sous forme d'un système linéaire en contre réaction d'une fonction linéaire comme le montre la figure suivante :

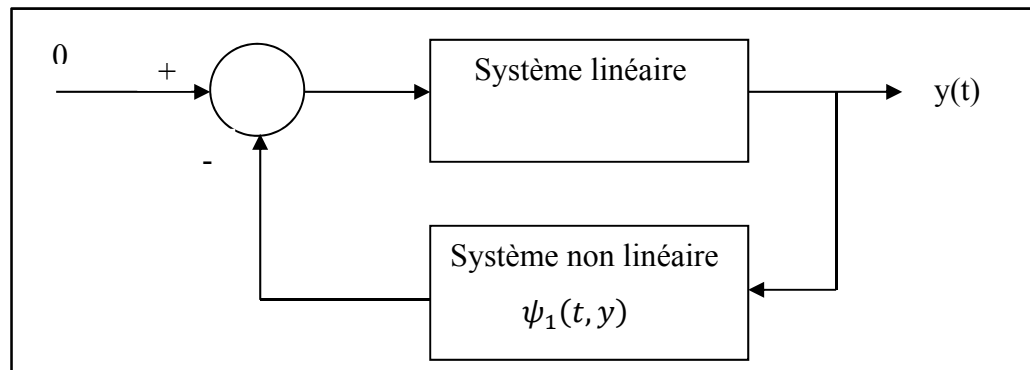


Figure 1. système à contre réaction.

Avec

$$G: \begin{cases} \dot{\tilde{x}}_f = A_f \tilde{x}_f + B_f v \\ y = C_f^T \tilde{x}_f \end{cases} \quad (12)$$

En contre réaction avec :

$$\nu = -\psi_1(t, y) \quad (13)$$

Le point d'équilibre du système précédent est globalement asymptotiquement stable si la partie non linéaire $\psi_1(t, y)$ est passive et le système linéaire est strictement passif à l'entrée (Khalil, 1996).